Probabilistic Assessment of Toe-Excavation Induced Hillslope Instability Involving Random Field Modeling of Spatial Variability

A Thesis

Submitted in partial fulfilment of the requirements for the degree of

DOCTOR OF PHILOSOPHY

by

RUBI CHAKRABORTY

DEPARTMENT OF CIVIL ENGINEERING

INDIAN INSTITUTE OF TECHNOLOGY GUWAHATI

Guwahati-781039, India

January 2022

STATEMENT

I do hereby declare that the matter embodied in this thesis is the result of investigations carried out by me and with the aid of the Department of Civil Engineering, Indian Institute of Technology Guwahati, Assam, India.

In keeping with the general practice of reporting scientific observations, due acknowledgements have been made wherever the work described is based on the findings of other investigators.

Date: 25.01.2022

Place: IIT Guwahati

Rubi Chakraborty

(Rubi Chakraborty)

CERTIFICATE

This is to certify that the thesis entitled **"Probabilistic Assessment of Toe-Excavation Induced Instability of Hill Slopes Involving Random Field Modeling of Spatial Variability"** submitted by **Rubi Chakraborty,** Roll No. 166104040, to the Indian Institute of Technology, Guwahati, for the award of the degree of Doctor of Philosophy in Civil Engineering, is a record of bonafide research work carried out by her under my supervision and guidance. The thesis work, in my opinion, has reached the requisite standard fulfilling the requirement for the degree of Doctor of Philosophy.

The results contained in this thesis have not been submitted in part or full to any other University or Institute for award of any degree.

Arindam Dey 25.01.2022

Date: 25.01.2022

Place: IIT Guwahati

Dr. Arindam Dey
Associate Professor
Indian Institute of Technology Guwahati
Guwahati - 781039, India

ACKNOWLEDGMENTS

Undertaking this PhD has been a truly life-changing experience for me, and I am indebted to many people without the support and guidance received from whom it would not have been possible to complete this journey. Firstly, I would like to thank and convey my deepest gratitude to my thesis supervisor Dr. Arindam Dey for his enthusiastic guidance, patience, motivation and continual support throughout this research work. He has been an ideal teacher, mentor, and thesis supervisor, offering advice and encouragement whenever needed. I'm proud of, and grateful for, my time working with him. I could not have imagined having a better advisor and mentor for my Ph.D study. I feel fortunate to have Dr. Rajan Choudhury, Dr. Ravi K and Dr. Deepak Sharma in my doctoral committee and would like to thank them for their constructive suggestions. I am also thankful to all the faculties of Civil Engineering Department of IIT Guwahati for their support throughout my PhD. I would also like to thank MHRD for sponsoring my PhD through NIT-IIT MoU "Trainee Teacher Scheme".

I would like to express my deepest gratitude to my parents, Late Ratan Chakraborty and Rina Chakraborty, who have been the constant source of my inspiration. I would also like to thank my sister Rakhi Chakraborty and brother-in-law Sujit Roy for all their love and blessings. I am really grateful to have Shibananda Choudhury as my life partner, whose unconditional love and encouragement made me believe in myself throughout this journey. Most importantly, I would like to express my love for my daughter Swanaya Choudhury for making me strong every day and to help me upgrade myself to a better version.

Last but not the least, I would like to thank my colleagues and friends Debasmita Pal, Jhuma Debnath, Dr. Sanasam Vipej Devi, Avilash Sahoo, Dr. Nur Alom, Sambit Majumder, Suman

Kumar, Supratim Kaushik, Ramyani Chakrabarty, Dr. Priyanka Talukdar, Dr. Rana Acharyya for their companionship and support.

Date: 25.01.2022

Rubi Chakraborty

RUBI CHAKRABORTY

ABSTRACT

In mountainous territory of India, roadways are the pre-eminent means of conveyance and communication. For last few years, rapid growth in the population has increased the requirement of urbanization, leading to an enhanced necessity of more highways along the hill slopes. Slope excavation in hilly regions is a traditional practice for construction of new roads or widening of the existing roads. Hill slope failures due to toe cutting and excavation need notable attention as it may cause high level of casualties in terms of loss of lives, property and economy. As immense accountability is associated with cut slope failures, geotechnical engineers and highway planners must perform rigorous investigation to predict the influence of toe cutting on hill slopes. Typically, the consequences of toe cut on the stability of hill slopes is reviewed based on the deterministic Limit Equilibrium Method (LEM) that predicts the failure of a cut slope by a single measure of factor of safety (FoS). Owing to the inevitable uncertainty in geotechnical properties, especially those related to soil strength and lack of representative in-situ data in hilly regions, deterministic LEM is incapable of appropriate assessment of slope failure. Hence, the analysis of influence of toe excavation on slope stability is highly persuadable to probabilistic treatments. To encounter the uncertainty related to geotechnical engineering practise, this dissertation presents the assessment of toe excavation induced slope instability in a probabilistic framework. To deal with uncertainty in soil shear strength, the shear strength parameters are considered as random variables and the cross-correlation between them, as well as their spatial variation in slope domain, is taken into account. Firstly, a stochastic model of spatially varying Standard Penetration Test (SPT)-*N* data is developed utilising the random field theory. Thereafter, a report is provided stating the influence of various parameters on probabilistic slope stability study using a simplistic LEM-based probabilistic approach. A schematic approach to incorporate the LEM based probabilistic method

for toe excavation induced slope stability study is presented. The study is further extended to investigate the performance of a sheet pile (SP) wall and a sheet pile anchor retention (SPAR) system as a retention measure against the cut slope failure through probabilistic analysis. Further, the study incorporated Random Finite Element Method (RFEM) for probabilistic cut slope analysis to assess the efficacy of the advanced RFEM over the traditional LEM based probabilistic approach for cut slope stability analysis. Finally, the response of the cut slope is also presented within a probabilistic framework under seismic condition. The outcomes of the study have been successful in illustrating the importance of a probabilistic approach over the conventional deterministic slope stability analysis, where the former clearly elucidates that slopes adjudged safe from deterministic yet might have high probabilities of failure, and that the same should be accounted for design of the slope stabilization measures. The study also reveals that identifying the variability in the in-situ soil properties is immensely important in arriving at a suitable probabilistic analysis and design, and this calls for a detailed site investigation for developing any successful understanding of the hillslope stability and slope stabilization practices.

Keywords: Hillslope instability; Deterministic and Probabilistic assessment; Toe-excavated hillslopes; Limit Equilibrium Method; Factor of safety; Random variable; Probability of failure; Spatial variability; Random field; Random Finite Element Method; Sheet pile anchor retention (SPAR); Seismic response.

TABLE OF CONTENTS

CHAPTER 4

ESTIMATION OF THE VERTICAL SCALE OF FLUCTUATION OF SPATIALLY VARYING SPT DATA

CHAPTER 5

PARAMETRIC INFLUENCE ON THE PROBABILISTIC SLOPE STABILITY ASSESSMENT

CHAPTER 6

HILLSLOPE INSTABILITY INDUCED BY TOE EXCAVATION: A COMPARATIVE STUDY OF LEM-BASED DETERMINISTIC AND PROBABILISTIC APPROACHES

CHAPTER 7

PROBABILISTIC ASSESSMENT OF TOE-EXCAVATED HILL SLOPE SUPPORTED BY SHEET PILE WALL OR SHEET-PILE-ANCHOR RETENTION SYSTEM

LIST OF FIGURES

LIST OF TABLES

LIST OF SYMBOLS

b_t	Possible horizontal width of vertical toe excavation of slope
c	Drained cohesion
c_u	Undrained cohesion
f_s(s)	Probability density function for undrained shear strength of soil
k_0	Coefficient of earth pressure at rest
E	Interslice normal force
E_s	Young's Modulus
Ff	Factor of safety satisfying force equilibrium
Fm	Factor of safety satisfying moment equilibrium
$F_s(s)$	Cumulative distribution function for undrained shear strength of soil
N	Standard Penetration Test data
X	Interslice shear force
G_{max}	Maximum Shear Modulus
G_{sec}	Secant Shear Modulus
G_{tan}	Tangent Shear Modulus
P_f	Probability of failure
S	Undrained shear strength of soil
φ_u	Undrained angle of internal friction
φ	Drained angle of internal friction
μ	Mean
σ	Standard deviation
β	Reliability Index

δ_v	Vertical scale of fluctuation
θ	Correlation length
ρ	Correlation coefficient
τ	Separation distance
$\gamma\ (T)$	Variance function
σ'_h	Horizontal effective stress
σ'_v	Vertical effective stresses
ν	Poisson's ratio
γ	Soil unit weight
ψ	Dilation angle
ξ	Damping ratio
λ	Reduction factor in GLE equation
$\Phi(.)$	Standard normal cumulative distribution function
Θ	Dimensionless correlation length

LIST OF ABBREVIATIONS

ACF	Auto-correlation function
ACM	Auto-correlation model
CDF	Cumulative distribution function
CMC	Coupled Markov Chain
CoV	Coefficient of variation
CPT	Cone Penetration Test
FEM	Finite element method
FE-SRM	Finite Element Strength Reduction Method
FORM	First Order Reliability Method
FoS	Factor of safety
GA	Genetic algorithm
GLE	General Limit Equilibrium
HTPM	Horizontal Transition Probability Matrix
LAS	Local average subdivision
LEM	Limit Equilibrium Method
MCS	Monte Carlo Simulation
MVFOSM	Mean Value First Order Second-Moment Reliability Method
PDF	Probability density function
PGA	Peak ground acceleration
RF	Random field
RI	Reliability Index
SoF	Scale of fluctuation
SORM	Second Order Reliability Method

SP	Sheet pile
SPAC	Spatial autocorrelation
SPAR	Sheet pile anchor retention
SPT	Standard Penetration Test
RFEM	Random Finite Element Method
RLEM	Random Limit Equilibrium Method
VTPM	Vertical Transition Probability Matrix

CHAPTER 1

INTRODUCTION

1.1. GENERAL

Uncertainty in slope stability practise fundamentally appears on account of geological anomalies, data scarcity, spatial variation in soil properties, uncertainty related to slope failure mechanism, simplifying assumptions considered in geotechnical modelling, and human errors in design and construction of geotechnical structures. In a conventional deterministic slope stability analysis, the stability is generally measured in terms of Factor of Safety (FoS). However, due to the uncertainties present in input parameters, it is hardly possible to assess the slope failure with a single FoS value. Among several deterministic methods available, the Limit Equilibrium Methods (LEM) are most popular among geotechnical engineers due to its simplicity. However, deterministic slope stability analysis, using LEM, presumes the potential failure surface and other geotechnical properties that may affect the overall failure behaviour of slope. Therefore, to overcome the limitations of traditional slope stability practise, collective knowledge from research and practise suggests incorporating uncertainty-based perspective in slope stability analysis within a probabilistic framework for better assessment of slope failure. Although the application of statistics in geotechnical engineering was introduced in the 1960s (Lumb, 1966, 1970), slope engineering adopted the probabilistic concepts in the 1970s (Tang et al., 1976; Alonso, 1976). The importance of incorporating spatial variability in soil properties has long been realised (DeGroot, 1996; Elkateb et al., 2003). Over the last few decades, the probabilistic concepts for slope stability analysis have developed (Chowdhury et al., 1988; Christian et al., 1994; Lacasse and Nadim, 1996; Griffiths and Fenton, 2000; Huang et al., 2017, 2021), and serves to be an emerging field of interest for many researchers.

In hilly regions of India, roadways are the primary means of transportation and communication which are often constructed by excavating the toe of the hills. For last few years, rapid growth in the population has increased the requirement of urbanization, leading to repeated excavation of slope toe in hilly regions, either for construction of new roads or for widening of the existing roads. Stability of the cut slopes along the hills are of major concern, as the failure of such cut slopes are of dire consequences, posing a high risk to human lives as well as monetary loss. Therefore, geotechnical engineers and highway planners must perform extensive investigation to assess the effect of toe cut on hill slope failure. Figure 1.1 shows some of the recent landslides occurred in different states of north-east India causing disruption in surface communication and casualties in terms of life and property.

(a)

(b)

(c)

(d)

(e)

Fig. 1.1 Recent landslides in different states of north-east India (a) Landslides in Arunachal Pradesh disrupt surface communication to districts (https://www.sentinelassam.com/north-east-

india-news/arunachal-news/landslides-in-arunachal-pradesh-disrupt-surface-communication-to-districts-478274) (b) Meghalaya's Shillong bypass closed due to landslide (https://nenow.in/north-east-news/meghalaya/meghalayas-shillong-bypass-closed-due-to-landslide.html) (c) Landslides in north Sikkim near border (https://www.telegraphindia.com/west-bengal/landslides-in-north-sikkim-near-border/cid/1784333) (d) Massive landslide on NH-2 in Manipur (https://www.nagalandpost.com/massive-landslide-on-nh-2-in-manipur/223695.html) (e) Slope failure at Gauripur, Guwahati due to toe-cutting and triggering intense rainfall (Photo Courtesy: Arindam Dey, IIT Guwahati)

1.2. BROAD OBJECTIVES OF THE DISSERTATION WORK

Although geotechnical profession shows an ample progress in subsuming probabilistic concepts to incorporate various geotechnical uncertainties, there is a lack of using such advance techniques in geotechnical practices such as to assess the safety of toe excavated hill slopes, owing to the improper guidelines and review of the current advance techniques. Moreover, in the case of limited representative empirical data, probabilistic study of slope is also a useful tool for risk assessment. Therefore, this thesis would attempt to make an effort towards developing a schematic approach to incorporate the LEM based probabilistic method for toe excavation induced slope stability study. It would also be intended to extend the study to ascertain the performance of sheet pile (SP) and sheet pile anchor retention (SPAR) system in mitigating the slope failure in static as well as in seismic conditions. Furthermore, Random Finite Element Method (RFEM) for probabilistic cut slope analysis would also be attempted to capture the two-dimensional variability in soil properties and explore the efficacy of the advanced RFEM over the traditional LEM based probabilistic approach for cut slope stability analysis.

1.3. OUTLINE OF THE DISSERTATION

To report the dissertation study, the thesis is divided into ten chapters. **Chapter 1** introduces the subject matter and states the motivation of the dissertation work, along with the broad objectives of the present work. **Chapter 2** presents the background study and comprehensive literature review. Based on the critical appraisal of the reviewed literature and gap areas, the precise objectives and the scope of the study are listed. **Chapter 3** provides the details of the methodologies of various numerical approaches adopted in the present study. **Chapter 4** provides a simplistic approach to model soil spatial variability as random field to incorporate uncertainty related to soil strength. **Chapter 5** elucidates the effect of various geotechnical and statistical parameters on slope failure probability or the reliability index. **Chapter 6** presents a comparative study between deterministic and LEM based probabilistic cut slope analysis. Further, a simplified procedure for assigning uncertainty related to soil shear strength in designing toe excavated cut slopes is presented. **Chapter 7** presents the probabilistic stability analysis for cut slopes using Sheet Pile (SP) and Sheet Pile Anchor Retention (SPAR) system. **Chapter 8** extends the cut slope stability study using more advanced RFEM and assesses the efficacies and advantages of RFEM over LEM based probabilistic method for cut slope design. **Chapter 9** investigates the cut slope stability using probability framework under seismic condition. **Chapter 10** lists out the important conclusions derived from the outcomes of the present study. The limitations of the present study and the scope of future research are also presented in this chapter.

CHAPTER 2

BACKGROUND STUDY AND LITERATURE REVIEW

2.1. GENERAL

The slope stability analysis is one of the most significant yet difficult geotechnical practice owing to the various uncertainties involved in the analysis. In a traditional deterministic slope stability analysis, the stability of the slope is usually represented in terms of Factor of Safety (FoS). However, owing to the presence of various uncertainties in input parameters, it is difficult to predict the slope stability with a single measure of FoS. Different issues of uncertainty in slope stability practise emerges primarily due to geological anomalies, data insufficiency, spatial variation in soil properties, uncertainty in slope failure mechanism, simplifying assumptions considered in geotechnical modelling, and human errors in design and construction of geotechnical structures. It is found in several studies that two nearly similar slopes, having nearly similar FoS obtained from a deterministic analysis, can have recognizably different failure probabilities due to the uncertainties involved in the geotechnical properties and failure mechanisms (Tang et al., 1976; El-Ramly et al., 2002; Griffiths and Fenton, 2004; Cho, 2009; Javankhoshdel and Bathurst, 2014). Different methods for deterministic slope stability analyses are prescribed, such as Limit Equilibrium Method (LEM) (Chakraborty and Dey, 2016a, b), Finite Element Method (FEM) (Griffiths and Lane, 1999) and Finite Difference Method (FDM) (Sjöberg, 1999). Even in the recent years, although computationally expensive, the application of smooth particle hydrodynamics (SPH) in assessing the stability analyses of slopes under large deformation scenario is gaining grounds (Rahman et al., 2021). Among these methods, the LEMs are still the most popular among engineers due to its simplicity in application and analyses methodology.

However, deterministic slope stability analysis, using LEM, presumes the potential failure surface and other geotechnical properties of the slope that might influence the overall failure behaviour of slope. Moreover, for simplification of the problem, additional approximations are made with respect to externally applied loads, whether static, seismic or climatic. Therefore, to overcome the limitations of traditional slope stability practise, probabilistic concepts are incorporated in slope stability analysis for better assessment of slope failure while incorporating the variability and uncertainty prevailing in any natural slope.

The application of statistics in geotechnical engineering and soil property characterization was introduced in the late 1960 (Lumb, 1966; 1970). In slope engineering, the probabilistic concept was first introduced in the 1970s (Tang et al., 1976; Wu and Kraft, 1970; Matsuo and Kuroda, 1974; Alonso, 1976). The advantages of probabilistic slope stability analyses and the importance of incorporating spatial variability in soil properties has long been realised by the researchers (Whitman, 1984; Mostyn and Soo, 1992; DeGroot, 1996; Elkateb et al., 2003). Over the last few decades, the probabilistic concepts for slope stability analysis have evolved and serves to be an emerging field of interest for many researchers (Li and Lumb, 1987; Chowdhury et al., 1988; Christian et al., 1994; Lacasse and Nadim, 1996; Paice, 1997; Griffiths and Fenton, 2000; Duncan, 2000; Whitman 2000; Huang et al., 2017; Chen et al., 2020; Lee and Ching, 2020). Moreover, in the case of limited representative empirical data, probabilistic study of slope is also a useful tool for risk assessment. However, there is a lack of usage of the current advanced probabilistic approaches by the practitioners owing to the inconsistent guidelines to apply the current advanced techniques.

Therefore, this chapter makes an effort to provide a detailed review of probabilistic concepts in different aspects of slope stability practise that has developed over the years. Starting with the basic probability and statistical concepts, various uncertainties involved in the slope stability modelling and the different approaches to incorporate these uncertainties in probabilistic slope stability practise are discussed. A brief review is also presented regarding stability analysis of reinforced soil slope, the slopes subjected to dynamic excitations and instability in hill slopes due to toe excavation within probabilistic framework.

2.2. DIFFERENT APPROACHES FOR PROBABILISTIC SLOPE STABILITY ANALYSIS

There are mainly two categorical approaches for probabilistic study of slope stability. First among them are the approximate methods that includes the first order reliability method (FORM) (Christian et al., 1994), the mean value first order second-moment reliability method (MVFOSM) (Hassan and Wolff, 1999) and the second order reliability method (SORM) (Mbarka et al., 2010); while the second categorical approach adopts the Monte Carlo Simulation (MCS) based methods (Griffiths et al., 2007; Hicks et al., 2014). In their primordial form, both the approximate and simulation-based methods make use of deterministic analysis (LEM or FEM based approach) to estimate the FoS, which is further used to assess the failure probability. The following subsections highlight the characteristics of each of the categorical approaches.

2.2.1. Approximate Methods based Estimation of Failure Probability

Among the approximate methods, FORM has been used extensively in several applications in civil and geotechnical engineering. In the field of structural reliability, the Hasofer–Lind reliability

index and the First Order Reliability index were developed for approximation of the probability of failure (Kitch, 1994; Tun et al., 2016). First, the reliability index (β) is estimated by solving an optimisation problem and, then, the failure probability is evaluated using $P_f = \Phi(-\beta)$, where $\Phi(.)$ denotes the standard normal cumulative distribution function. Several researchers have reported the significance of reliability indices (Chowdhury et al., 1988; Christian et al., 1994; Bhattacharya et al., 2003; Baecher and Christian, 2003). There are various methods for evaluation of reliability index by solving an optimisation problem, including methods such as genetic algorithms (GA) (Cui and Sheng, 2005; Tun et al., 2016). GAs have gained substantial acceptability as optimisation method due to their inherent capability of identifying the global optima and the ability to deal with multimodal problems to identify multiple potential failures. Other commonly used optimization techniques in geotechnical engineering, to name a few, are particle swarm optimisation (Reale et al., 2015), ant colony (Kahatadeniya et al., 2009), and other nature-inspired algorithms (Yang, 2014). Mbarka et al. (2010) coupled different methods of reliability analysis such as MCS, MVFOSM, FORM and SORM with various mechanical approaches (Caquot-Taylor formula that is a LE method of Bishop and a FE model based on the strength reduction method) for a slope stability assessment, considering the cohesion and friction angle of the soil as correlated random variables without any spatial variation of the properties. The study showed that the approximate methods need lesser performance function calls and, hence, are less time consuming than MCS. The study also revealed that if the mechanical model is accurate and the search procedure to find out the minimum reliability index is well defined; these methods result in good approximations of reliability of the slope system. Besides its simplicity of implementing in different applications, it is revealed that the results obtained using FORM have higher accuracy when applied to stability of slopes having smaller failure probability or higher reliability index (Phoon, 2008). However, in

the same period, Griffiths et al. (2007) has pointed out that FORM is incapable of considering inherent spatial variability in soil properties, thereby resulting in either over-estimation or under-estimation of the probability of slope failure under different conditions.

2.2.2. Monte Carlo Simulation based Estimation of Failure Probability

In the MCS-based probabilistic studies for the assessment of the failure of any geotechnical structure, the geotechnical properties are considered as random variables. The ease of computation and simplicity of direct Monte Carlo Simulation (MCS) technique makes it preferable over other methods. Based on specified ranges of input parameters treated as random variables, MCS generates a set of trial values of the random variable within a specified range, and for each trial value, the random variable estimates the *limit state function*. A *limit state function*, usually represented as $g(x)$, is a mathematical quantification of the failure of a system. The limit state function is invariably (though arbitrarily) described such that $g(x)>0$ specifies a safe state and $g(x)<0$ specifies a state of failure. The total number of failures occurring in all the trial values of random variable is counted, and the failure probability is expressed as

$$P_f = \frac{n_f}{N} \tag{2.1}$$

where, n_f is the number of failures that occurred in total N number of trials. This method is commonly adopted into different commercially available geotechnical software such as PLAXIS (https://www.bentley.com/en/products/brands/plaxis), FLAC (Sarma et al., 2014), SVSlope (Javankhoshdel and Bathurst, 2014), GeoStudio (DeWolfe et al., 2010) and GEO5 (https://www.finesoftware.eu/geotechnical-software/).

However, a disadvantage of this technique is that it largely depends on the substantial number of trials (iterations) to be undertaken to arrive at the reliable solution, thereby demanding excessive computation time. For reference, as per the US Army Corps of Engineers (1997), Table 2.1 shows the relationship between reliability index (β) and the probability of failure (P_f) of any geotechnical system and their desired performance levels.

Table 2.1. Relationships between probability of failure, P_f and reliability index, β (U.S. Army Corps of Engineers, 1997)

Reliability Index, β	Probability of failure, $P_f = \Phi(-\beta)$	Performance level
1	0.16	Hazardous
1.5	0.07	Unsatisfactory
2	0.023	Poor
2.5	0.006	Below average
3	0.001	Above average
4	3×10^{-5}	Good
5	3×10^{-7}	High

Note: $\Phi(.)$ is the standard normal cumulative distribution function.

The value of β generally ranges from 1 to 5, and the corresponding P_f value vary within 0.16 to 3×10^{-7}. Standard geotechnical designs prefer a β value of at least 2 (i.e., P_f <0.023) for desired performance level better than 'poor'. A relatively small P_f value is of great interest to geotechnical practitioners. To ensure accuracy in the value of failure probability, this direct MCS technique requires a sample number of at least 10 times greater than the reciprocal of the desired probability level (Roberts and Casella, 1999). Therefore, to obtain a P_f level of 0.001, corresponding to a desired performance level of 'Above average' (Table 2.1), the number of iterations required in

direct MCS is more than 10,000. Hence, the direct MCS demands a large amount of computational time as the deterministic slope stability analysis explicitly searches for a number of potential slip surfaces to obtain the minimum FoS. This shortcoming calls for further improvement in the computational efficiency of direct Monte Carlo based simulation procedures.

In recent years, an 'advanced subset simulation' method is introduced for improving the efficiency of the MCS at relatively small probability levels (Wang et al., 2010a, 2011). Subset simulation is a stochastic simulation technique for efficiently generating failure samples and computing probability of failure at relatively smaller level. It is based on the concept that a small probability of failure can be represented by a product of larger conditional failure probabilities for some intermediate failure events (Au and Beck, 2001, 2003). Moreover, direct MCS does not offer insight into the effect of different type of uncertainties in the probabilistic study. Therefore, Wang (2012) proposed an improvised approach to conduct sensitivity study of the uncertain parameters within the MCS framework. The variation of slip surface is also stated to be an important factor to be incorporated while considering the spatial variability in MCS-based probabilistic slope stability analysis (Wang et al., 2011). In addition, Li et al. (2013, 2014a) proposed that multiple representative slip surfaces can also be used together with MCS to consider multiple failure mode with significantly reduced computational effort. Moving further ahead, instead of adopting several MCS instances to reach a convergence on the FoS for the probabilistic slope stability analysis, Dyson and Tolooiyan (2019) presented a probabilistic slope stability approach using the random finite element method (RFEM) to predict the FoS of each MCS random field instances prior to FE-based simulation on random field similarity measures. This approach resulted in an exceptional reduction of the computational time. Fang et al. (2020) proposed a new probabilistic approach for

slope stability analysis based on slip-line field theory within MCS framework. The method significantly increases the computational efficiency as this method does not require to compute the FoS and critical failure surface for estimation of probability of failure.

2.3. UNCERTAINTY DUE TO SOIL HETEROGENEITY

Soil is originated from different geological, environmental and physico–chemical processes. Soil heterogeneity is categorised into two main classes, namely lithological heterogeneity and inherent spatial variability. The lithological heterogeneity is described as one layer of soil overlying another layer, or the presence of pockets of different lithology within a nearly uniform soil mass. Inherent spatial variability refers to the variation of soil properties within one particular soil layer, which originates due to different loading histories and deposition conditions. Earlier, the traditional way to deal with spatial variability was to rely upon a high safety factor, engineering judgement and local experience. However, Morgenstern (2000) presented some case studies for various geotechnical engineering applications, where it was clearly highlighted that a complete dependence on the engineering judgment led to noticeably erroneous assessments in 70% of the cases. Hence, it was realised that it is essential to develop more advanced, reliable and appropriate techniques to address geotechnical uncertainties in safety analysis. In the beginning, in order to address soil heterogeneity in geotechnical engineering studies, limit equilibrium analysis coupled with MCS technique was introduced (Ji et al., 2012, Tabbaroki et al., 2013, Javankhoshdel and Bathurst, 2014; Javankhoshdel et al., 2017). Later on, random finite element method (RFEM) coupled with MCS was introduced to incorporate soil spatial variability into a numerical analysis (Griffiths and Fenton, 2004; DeWolfe et al., 2010).

2.3.1. Inherent Spatial Variability of Shear Strength Parameters of Soil

Spatial variation in soil properties is considered to be a significant source of uncertainty in geotechnical engineering problems such as slope stability analyses. At present, incorporation of spatial variability of soil is primarily concentrated on inherent variation of soil property within one nominally homogeneous layer (Griffiths and Fenton, 2000; Ji et al., 2012; Hicks et al., 2014; Jiang et al., 2014; Le, 2014; Li et al., 2015a; Jamshidi and Alaie, 2015). Ji et al. (2012) stated that probability of failure is overvalued when spatial variation of soil is not considered, i.e., a slope may be much more stable than it is assessed by ignoring the spatial variability. Wang et al. (2011) also reported that ignoring spatial variability results in over-estimation of the variance of FoS, which may result in either over- or under-estimation of failure probability of a slope. However, Allahverdizadeh et al. (2015) reported the existence of a critical spatial correlation length value that leads to an underestimation of the probability of failure, thereby resulting in a non-conservative design. The critical correlation length resulting in the maximum probability of failure was reported to be of 0.5H-1.0H, where H represents the height of the slope. Similar observation about the critical spatial correlation length was reported by Griffiths and Fenton (2000), which is further discussed in a later section. Several researchers have studied the influence of spatial variation in soil shear strength parameters on the failure probability or reliability of slope structures (Griffiths and Fenton, 2004; Cho, 2009; Hicks and Samy, 2002; Hicks et al., 2008; Hicks and Spencer, 2008; Hicks and Spencer, 2010). Low et al. (2007) proposed a practical MS-Excel based programming procedure for assessing the reliability of a slope failure considering spatial variation in soil shear strength parameters. Srivastava and Babu (2009) quantified the spatial variability in soil shear strength parameters with the aid of field-test data and estimated the reliability of a soil slope (having spatial variability) against failure. The study revealed that although the deterministic

FoS value is acceptable, the estimated reliability index indicated the performance level of the given soil slope to be 'below average'. Griffiths et al. (2011) carried out a probabilistic study on infinite slopes to explore the effect of spatial variation of shear strength parameters on reliability-based slope stability analysis. It was highlighted that the first order reliability methods might result in non-conservative estimation because of ignoring the spatial variability in soil. Considering spatial variation in shear strength of soil, Ji et al. (2012) carried out a slope stability analysis by using the First Order Reliability Method (FORM), combined with a deterministic slope stability analysis, to search for the probabilistic critical slip surface. In this study, two methods, namely the method of auto-correlated slices and the method of interpolated autocorrelations, were adopted. This study was an extension of the method of interpolated autocorrelations of one-dimensional spatial variability of undrained shear strength (Low and Tang, 1997) of a soft foundation supporting an embankment, which has been further improvised to model a two-dimensional spatial variation in reliability-based slope stability analysis. The study revealed that as compared to the effect of spatial variation in horizontal direction, the effect of spatial variation in vertical direction has more significance on the probability of failure of slope structure. This fact has also been reported by the findings of other studies (Cho, 2009). Zhu et al. (2013) utilized the random field analysis approach to study the influence of material heterogeneity of slope considering the spatial variation of permeability function under steady state rainfall infiltration. The parametric study, considering the correlation length of log-permeability of the heterogeneous slope varying from 0.4 to 50 times of the slope height, shows a variation in the matric suction values ranging from 0.5-1.25 times of those of a homogeneous case.

2.3.1.1. *Incorporation of Spatial Variability through Probabilistic Approach*

To deal with spatial variability regarding soil properties, literature suggests considering the soil property as continuous random variable (Fenton and Griffiths, 2008). A continuous random variable can be characterised by a probability density function (pdf). In geotechnical engineering, the Normal or Gaussian distribution functions are most commonly used (Fenton and Griffiths, 2008). As an illustration, if the undrained shear strength (S) of soil be considered as a continuous random variable, the Normal pdf can be represented as $f_s(s)$ through the expression

$$f_s(s) = \frac{1}{\sqrt{2\pi\sigma_s}} e^{-(s-\mu_s)/2\sigma_s^2} \tag{2.2}$$

where, μ_s and σ_s are the mean and standard deviation of S, respectively. Figure 2.1a (Kitch, 1994) shows a typical probability density function for a normally distributed random variable (undrained shear strength, S). The Normal distribution is preferably used to characterise the properties in geotechnical engineering, since the sum of random variables tends to have a normally distributed pdf according to the Central Limit Theorem (Papoulis, 1991). However, the disadvantage of adopting a Normal distribution is that it incorporates negative values, which is infeasible for the soil shear strength and other physical parameters in geotechnical engineering. A prudent approach to avoid choosing the negative values for such cases is to characterise the geotechnical properties using a non-negative distribution such as the 'Lognormal distribution' (Cao and Wang, 2014; Burgess et al., 2019). The distribution of the random variable can also be represented in terms of the cumulative distribution function (cdf), as shown in Fig. 2.1b (Kitch, 1994). The cumulative distribution function (cdf), usually denoted as $F_s(s)$, represents the probability of the random variable S taking a value less than s, and is expressed as

$$P(S < s) = F_s(s) \tag{2.3}$$

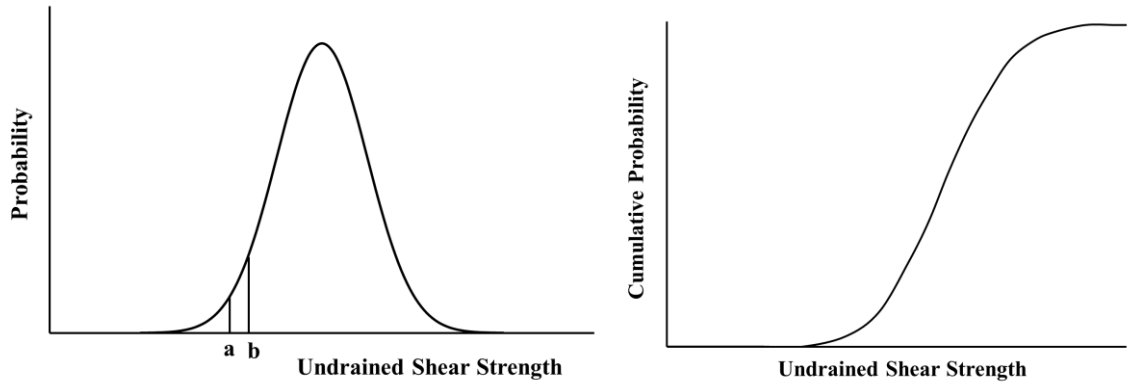

(a) (b)

Fig. 2.1 A typical representation of a (a) Probability Density Function (PDF) and (b) Cumulative Density Function (CDF)

Apart from the pdfs and cdfs used to characterize a random variable, it is also desirable to have some quantitative descriptors for the same purpose. The most common characteristic of a random variable (for example, undrained shear strength) is its 'mean' or the 'Expectation' value, which is denoted as:

$$\mu_s \text{ or } E[S] = \int_{-\infty}^{\infty} s f_s(s) ds \tag{2.4}$$

Variance is another important characteristic of a random variable that is indicative of the deviation of the random variable from its mean value. The average deviation value is known variance, σ_s^2, and the magnitude of its square root is referred as standard deviation (σ_s). The stated entities are expressed as

$$\sigma_s^{\,2} = E[(s-\mu_s)^2] = \int_{-\infty}^{\infty} (s-\mu_s)^2 f_s(s) ds$$
$$\sigma_s = \sqrt{\sigma_s^{\,2}} \tag{2.5}$$

Further, for comparing two random variables having different expectation, it is often convenient to normalize the standard deviation by its mean value, and the same is termed as the coefficient of variation (CoV), which is defined as:

$$\text{CoV} = \frac{\sigma_s}{\mu_s} \tag{2.6}$$

Typical ranges of CoV for cohesion and internal friction angles are 0.05-0.5 and 0.02-0.56 respectively (Griffiths and Fenton, 2007). A summary about the typical range of inherent variability of the undrained shear strength, effective-stress friction angle and its tangent is presented in Table 2.2; further details are available in Phoon et al. (1995).

Although it is well-recognized that the soil variability is highly site-specific, it is strenuous to acquire site-specific probability distribution for geotechnical properties. The basic probability principles for characterising geotechnical properties, so discussed in this section, are based on the assessment of soil variability from a huge number of data collected from different sites of a large region, or even from various parts of the world. For geotechnical engineering projects at a specific site, the designers are more interested in the variability of geotechnical properties within the particular site, and avoid the variability assessed from sites at other locations. In recent years, several researchers reported that soil property in a specific site does not necessarily follow Normal or Lognormal distributions. In this regard, in recent years, Bayesian methods have been adopted to obtain the site-specific probability distribution from limited site-specific test data (Wang et al., 2015, 2016a). The site-specific probability distribution of any geotechnical property can be considered as the weighted summation of a number of Normal or Lognormal distributions with different distribution parameters. Thus, based on the available data, estimating the site-specific

probability distribution of geotechnical properties is indicative of finding a suitable group of Normal or Lognormal distributions and their respective weights.

Table 2.2: A summary of inherent variation in soil strength properties (Phoon et al., 1995)

Soil property[a]	Type of soil	No. of group of data	Number of tests per group		Soil property value		CoV of Soil property (%)	
			Range	Mean	Range	Mean	Range	Mean
$\bar{\phi}$ (^{0})[#]	Sand	7	29-136	62	35-41	37.6	5-11	9
$\bar{\phi}$ (^{0})[#]	Clay, Silt	12	5-51	16	9-33	15.3	10-50	21
$\bar{\phi}$ (^{0})[#]	Clay, Silt	9	-------	------	17-41	33.3	4-12	9
s_u (kN/m^2) (UU)	Clay, Silt	13	14-82	33	15-363	276	11-49	22
s_u (kN/m^2) (UC)	Fine grained	38	2-538	101	6-412	100	6-56	33
s_u (kN/m^2) (CIUC)	Clay	10	12-86	47	130-713	405	18-42	32
s_u (kN/m^2)[#]	Clay	42	24-124	48	8-638	112	6-80	32
tan $\bar{\phi}$[#]	Sand	13	6-111	45	0.65-0.92	0.744	5-14	9
tan $\bar{\phi}$ (DS)	Clay, Silt	3	-------	------	-------	0.615	6-46	23
tan $\bar{\phi}$ (TC)	Clay, Silt	4	-------	------	0.24-0.69	0.509	6-46	20

s_u: undrained shear strength; $\bar{\phi}$: effective stress angle of internal friction; DS: direct shear test; TC: triaxial compression test; UU: unconsolidated–undrained triaxial compression test; CIUC: consolidated isotropic undrained triaxial compression test; UC: unconfined compression test.
[#] Laboratory test type are not reported.

Scale of fluctuation

The pattern of spatial variation in soil is expressed by the correlation length or the scale of fluctuation (Vanmarcke, 1977). The scale of fluctuation (SoF) indicates the spatial extent within which the soil property is significantly correlated. An approximate way of estimating the vertical SoF is presented by Vanmarcke (1977), expressed as:

$$\delta_v = 0.8\bar{d} \tag{2.7}$$

where, δ_v is the scale of fluctuation in the vertical direction and $\bar{d}$ is the average of the distance between the intersections of the fluctuating entity with its mean trend, as shown in Fig. 2.2 Vanmarcke (1977). The detailed description of the techniques for evaluation of the correlation are available in literature (Lacasse and Nadim, 1996; DeGroot, 1996). A larger correlation distance (θ) or higher SoF signifies a smooth variation of properties, whereas a smaller correlation distance signifies an erratic variation of properties within a soil domain, as shown in Fig. 2.3 (Fenton and Griffiths, 2008). A summary of typical SoF for different geotechnical properties is given in Table 2.3; further details are available in Phoon et al. (1995).

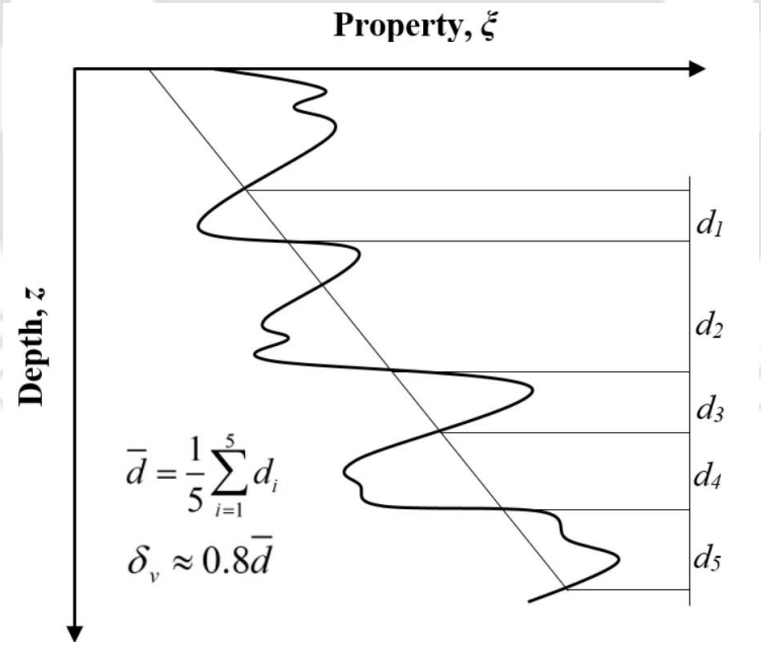

Fig. 2.2 A typical representation of the estimation of vertical scale of fluctuation

Table 2.3: Summary of SoF for various geotechnical properties (Phoon et al., 1995)

Property[a]	Soil type	No. of studies	Scale of fluctuation (m)	
			Range	Mean
Horizontal fluctuation				
s_u (VST)	Clay	3	46.0-60.0	50.7
q_c	Sand, clay	11	3.0-80.0	47.9
q_T	Clay	2	23.0-66.0	44.5
Vertical fluctuation				
s_u (VST)	Clay	6	2.0-6.2	3.8
s_u	Clay	5	0.8-6.1	2.5
q_c	Sand, Clay	7	0.1-2.2	0.9
q_T	Clay	10	0.2-0.5	0.3
N	Sand	1	----------	2.4
γ	Clay, loam	2	2.4-7.9	5.2

[a]s_u and s_u (VST): undrained shear strength from laboratory tests and vane shear tests, respectively; γ: unit weight; q_c: cone penetration test tip resistance value; q_T: corrected cone penetration test tip resistance; N: Standard Penetration Test value (number of blows per foot or per 305 mm).

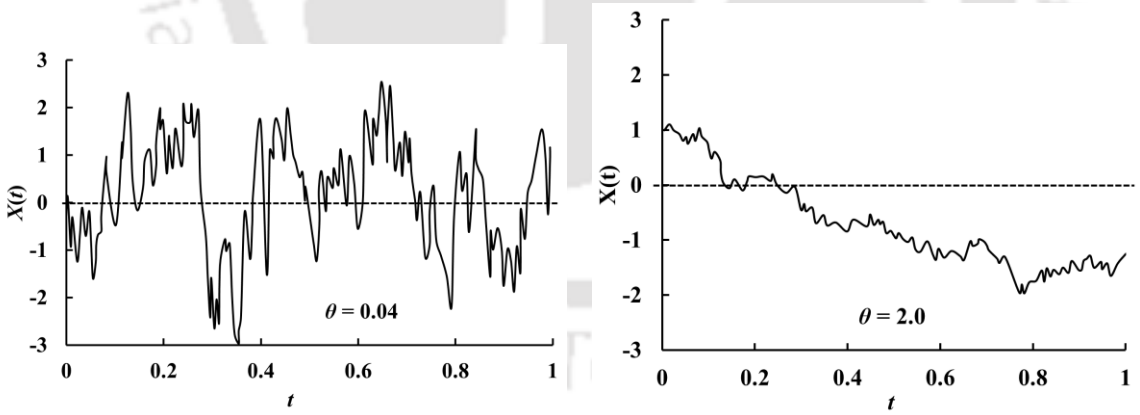

(a) **(b)**

Fig. 2.3 Sample realizations of a one-dimensional random field *X(t)* for two different SoF values

(a) θ = 0.04 (b) θ = 2.0

Coefficient of variation, auto-correlation function and cross-correlation between shear strength parameters

In most of the cases, geotechnical engineering problems are functions of more than one variable. For example, the drained shear strength of a soil is a function of both cohesion (c) and the angle of internal friction (φ). In such cases, the joint probability distribution is considered for a particular range of values of the governing parameters (Fenton and Griffiths, 2008). In most of the geotechnical engineering problems involving two variables, there is often a statistical relationship between the variables, which is quantified by their covariance $Cov[X, Y]$, and is represented as

$$Cov[X,Y] = E[(X - \mu_X)(Y - \mu_Y)] \tag{2.8}$$

The normalized covariance is called the correlation coefficient (ρ), and is expressed as

$$\rho_{X,Y} = \frac{Cov[X,Y]}{\sigma_X \sigma_Y} \tag{2.9}$$

where, X and Y are the two random variables, μ_X and μ_Y are the expectations of the two variables respectively, and σ_X and σ_Y are their standard deviations, respectively.

In random field theory, the spatial correlation between various soil properties, considered as random variables, is expressed by a spatial autocorrelation (SPAC) function (Christakos, 1992; Fenton and Griffiths, 2008). Table 2.4 presents different typical autocorrelation functions available in literature for various geotechnical engineering properties, in their one-dimensional (1D) and two-dimensional (2D) representations. The selection of a proper correlation function for a particular site is a challenging task, especially when the obtained site-specific test results are limited during geotechnical site characterization. Li et al. (2015a) compared the differences between various 2D theoretical autocorrelation functions and stated that Squared Exponential and

Second-Order Markov type autocorrelation functions might be the most appropriate ones to simulate the spatial correlation between different soil properties. Cao and Wang (2014) suggested that for probabilistic study of a specific slope, the autocorrelation model should be selected based on the data collected from the given site. In this regard, the development of 1D stochastic model to characterize inherent spatial variation in SPT data obtained from field test and subsequently estimating the correlation length is reported in the present study.

Table 2.4: Different autocorrelation functions for geotechnical engineering properties (Fenton and Griffiths, 2008)

Type	Autocorrelation function (1D)	Scale of fluctuation	Auto correlation function (2D)
Single exponential	$\rho(\tau)=\exp(-a\tau)$	$\delta=2/a$	$\rho(\tau_x,\tau_y)=\exp\left[-2\left(\frac{\tau_x}{\delta_h}+\frac{\tau_y}{\delta_v}\right)\right]$
Squared exponential	$\rho(\tau)=\exp[(-b\tau)^2]$	$\delta=\sqrt{\pi}/b$	$\rho(\tau_x,\tau_y)=\exp\left[-\pi\left(\frac{\tau_x^2}{\delta_h^2}+\frac{\tau_y^2}{\delta_v^2}\right)\right]$
Second order Markov	$\rho(\tau)=\exp(-c\tau)(1+c\tau)$	$\delta=4/c$	$\rho(\tau_x,\tau_y)=\exp\left[-4\left(\frac{\tau_x}{\delta_h}+\frac{\tau_y}{\delta_v}\right)\right]\left(1+\frac{4\tau_x}{\delta_h}\right)\left(1+\frac{4\tau_y}{\delta_v}\right)$
Cosine exponential	$\rho(\tau)=\exp(-d\tau)\cos(d\tau)$	$\delta=1/d$	$\rho(\tau_x,\tau_y)=\exp\left[-\left(\frac{\tau_x}{\delta_h}+\frac{\tau_y}{\delta_v}\right)\right]\cos\left(\frac{\tau_x}{\delta_h}\right)\cos\left(\frac{\tau_y}{\delta_v}\right)$

ρ: correlation coefficient; τ: separation distance; δ: scale of fluctuation

In geotechnical engineering, the influence of heterogeneity in cohesion (c) and angle of internal friction (φ), and the correlation between them, are very significant. Several authors have studied the correlation between various soil properties (Lumb, 1970; Mostyn and Soo, 1992; Hicks and Samy, 2002; Baecher and Christian, 2003; Babu and Mukesh, 2004; Griffiths and Fenton, 2004; Javankhoshdel and Bathurst, 2014). While some researchers ignored all possible cross-correlations

between the soil shear strength parameters for mathematical convenience (Lumb, 1970; Schultze, 1975; Alonso, 1977; Tobutt, 1982; Nguyen and Chowdhury, 1984; Huang et al., 2010), some studies considered the cross-correlation among geotechnical parameters in their numerical studies to be an important factor (Nguyen and Chowdhury, 1985; Tamimi et al., 1989; Fenton and Griffiths, 2003; Ferson and Hajagos, 2006; Youssef et al., 2008; Griffiths et al., 2009; Cho and Park, 2009; Lü and Low, 2011). The correlation coefficient between cohesion (c) and angle of internal friction (φ) has been proposed to be negative by several authors (Lumb, 1970; Yucemen et al. 1973; Wolff, 1985; Cherubini, 1997; Forrest and Orr 2010; Hata et al. 2012), which means that at any specific location, a higher magnitude of c is accompanied by a smaller magnitude of φ, or vice-versa. It was observed by several authors that the negative correlation between c and φ was found to improve the structural reliability as compared to assuming zero correlation coefficient (Griffiths et al., 2009; Griffiths et al., 2011; Javankhoshdel and Bathurst, 2014). Javankhoshdel and Bathurst (2015) reported that the failure probability of a slope decreases as the values of c and φ become more negatively correlated. At the same time, it is understood that a slope with zero or positive correlation between the shear strength parameters is likely to be associated with larger risk of failure, and should be rigorously studied as well. Very few studies have explored the influence of positive correlation between c and φ on slope stability (Griffiths et al., 2009; Griffiths et al., 2011; Le, 2014). Griffiths et al. (2009) conducted analysis on a drained slope having correlation between soil shear strength parameters (c' and φ') and reported that a positive correlation coefficient resulted in the decrement of the critical coefficient of variation (CoV) value, ignoring which would lead to a non-conservative estimate of the failure probability.

Local averaging and variance reduction

Generally, all engineering properties refer to some sort of local average property. Therefore, it is often significant to investigate the behaviour of the averages of random field, rather than the properties at discrete locations (Fenton and Vanmarcke, 1990). For example, there is higher possibility of slope failure when the applied shear stress exceeds the average shear strength along the critical slip surface, rather than because of the presence of some local weak zones within the soil mass. Therefore, uncertainty in the average shear strength along the critical failure surface is a more appropriate measure than estimating the uncertainty in shear strength at discrete location within the slope. The moving local average is defined as:

$$X_T(t) = \frac{1}{T}\int_{t-T/2}^{t+T/2} X(\xi)d\xi \tag{2.10}$$

where, T is the moving window length and $X_T(t)$ represents local average of $X(t)$ over a window of width T and centred at t, as illustrated in Fig. 2.4 (Griffiths and Fenton, 2007). Fig. 2.4 (a) shows a random process which is then averaged within a moving window of width T to get Fig. 2.4(b). It can be noticed that averaging smooths the process by reducing its variance. The point variance is reduced due to the local averaging process and the reduction is governed by a *variance function, $\gamma(T)$*, which is expressed as,

$$\gamma(T) = \frac{1}{T^2}\int_0^T\int_0^T \rho_x(\xi-\eta)d\xi d\eta \tag{2.11}$$

The variance function (Eq. 2.11) is an average of the correlation coefficient between two subsequent points on the interval [0, T]. If the correlation function diminishes with a steep gradient i.e., correlation between two points decreases substantially with separation distance, then $\gamma(T)$ will be small. In case all the points are perfectly correlated on the interval [0, T], having $\rho(\tau) = 1$

for all τ, then $\gamma(T)$ will be 1.0, thereby not exhibiting any reduction in variance due to local averaging.

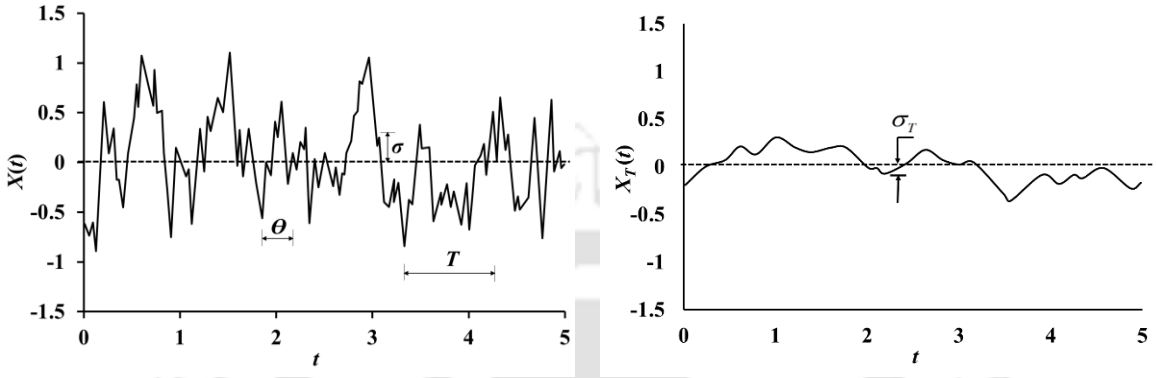

(a) (b)

Fig. 2.4 A typical effect of local averaging on the variance

Local averaging results in the decrease in the variance of the random process and also damps out the contribution from the high frequency components. Hence, the variance of any geotechnical property, spatially averaged over a particular soil domain, is lower than the variance at discrete locations. The variance decreases with an increase in the extent of the soil domain over which the property is averaged. In case an entity is represented by a Normal probability distribution function, local averaging reduces the variance while maintaining the mean unchanged. On the other hand, in case of a Lognormal probability distribution function, local averaging results in the reduction in both the mean and the standard deviation. This is due to the fact that the mean and variance of a Lognormal distribution is dependent on both the mean and variance of the underlying Normal distribution (Griffiths and Fenton, 2004; Fenton and Griffiths, 2008; Chok, 2009).

2.3.1.2. *Random Finite Element Method (RFEM)*

A more advanced and appropriate tool for probabilistic analysis in geotechnical engineering to incorporate spatial variation in soil was developed in 1990's, commonly known as 'Random Finite Element Method' (RFEM) (Paice, 1997; Griffiths and Fenton, 2000). A soil property is an uncertain quantity at any location within a soil domain and therefore, is considered as a random variable in RFEM. As an illustration of one-dimensional random field, Fig. 2.5 (Fenton and Griffiths, 2008) shows a typical variation of the cone tip resistance measured during a cone penetration test (CPT).

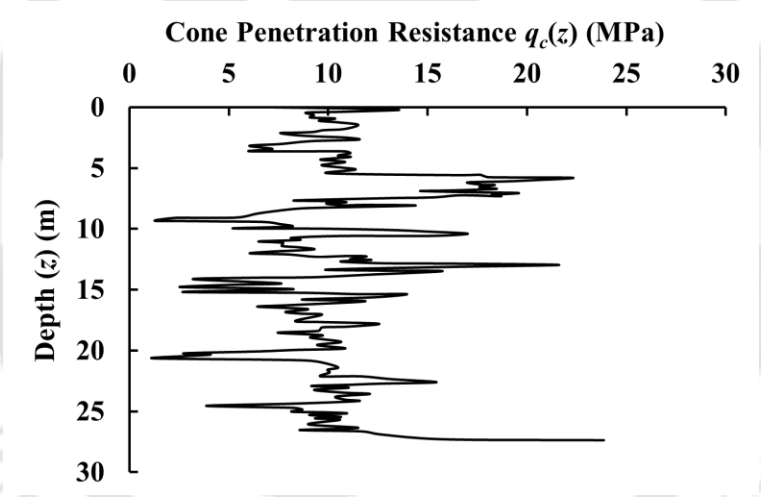

Fig. 2.5 A typical variation of cone tip resistance with depth

In the random finite element method, each random variable is characterised using a pdf and is correlated with other random variables at adjoint locations. The set of random variables is characterised by the joint probability distribution function and is represented as a random field. RFEM combines nonlinear finite element method (FEM) with random field theory. In RFEM, a random field is overlaid upon a finite element mesh and hence, each mesh behaves as a random

variable. This approach succeeds to gain much popularity among researchers and often used in probabilistic slope stability study as this method completely accounts for spatial correlation and local averaging (Griffiths and Fenton, 2007). Further, the method does not make any presumptions regarding the location and shape of the critical slip surface, which is automatically determined using FEM that can search for actual weakest path through the soil domain.

If the mean and covariance of a random field vary with the location, the characterising joint pdf is highly inconvenient to use in mathematical practice as well as to estimate from real field data. Therefore, simplifications of stationarity or statistically homogeneity of random field is essential. A statistically homogeneous or stationary random field indicates that the joint pdf characterising the random field is spatially invariant; i.e., the mean, variance and all the higher order moments are constant at any location within the random field. The correlation between any two random variables entirely depends on their separation distance, not on their absolute locations. In order to characterize a random field under the simplifying assumptions of stationary random field, the mean, variance and the pattern of soil spatial variability should be known. The pattern of spatial variability in soil can be characterized using autocorrelation function, variance function or spectral density function.

The most commonly used algorithms available in literature to generate multi-dimensional random fields in geotechnical engineering are the Moving average (MA) method, Discrete Fourier Transformation (DFT) method, Covariance Matrix Decomposition (Sarma et al., 2014), Turning Bands Method (TBM), Fast Fourier Transformation (FFT) method and Local Average Subdivision (LAS) method (Hicks and Spencer, 2010). The accuracy of probabilistic study highly depends on

the aptness of the algorithm under consideration for generation of random field realisations. Fenton and Griffiths (2007) compared different random field generator with respect to their accuracy, efficiency, ease of use and implementation. The FFT, TBM, and LAS methods were found to be much more efficient than the first three methods. It has been highlighted that every method has some advantages and disadvantages, and the selection of random field generator algorithm entirely depends on the particular problem under consideration; further details are furnished in Fenton and Griffiths (2007).

Over the years, several researchers have considered the theory of random fields in order to incorporate the spatial variability of soil properties in geotechnical engineering practise (Vanmarcke, 1977; Vanmarcke, 1983; Griffiths and Fenton, 2000; Griffiths and Fenton, 2004). However, in most of these studies, the spatial variation in soil shear strength was characterised as stationary random field, i.e., the mean of the shear strength parameters is invariant with depth of soil slope. However, it is well understood that the soil properties are non-stationary i.e., soil property progressively changes with depth from the surface (Phoon and Kulhawy, 1999). Several in-situ test data showed that soil properties of a homogeneous soil layer exhibit variable trends with depth (Elkateb et al., 2003; Hicks and Samy, 2002; Kulatilake and Um, 2003). Srivastava and Babu (2009) reported that for a data exhibiting no trend with depth, the reliability index (β) values underestimate the reliability of slope failure as compared to those obtained with linear trend in data. Further, Li et al. (2014b) stated that ignoring this increasing trend in shear strength parameters with depth results in overestimation of failure probability. Moreover, the chances of critical slip surface developing at the bottom of the slope decreases significantly when the increasing trend of mean shear strength parameters is considered. In this regard, to incorporate the progressive

increment of the various geotechnical parameters with depth, Griffiths et al. (2015) introduced the incorporation of non-stationary random fields in probabilistic slope stability studies. Further Huang et al. (2021) investigated the effect of rotated transverse anisotropy, occurring due to various geological processes, combined with non-stationary random field on reliability of the stability of an undrained soil slope. The study considered two different cases of non-stationary random field: the trend of soil strength increasing with depth and the trend increasing along the direction perpendicular to bedding. The study revealed that the reliability of the slope stability highly depends on the directions of the trend.

Further, it is worth mentioning that although the random field theory is well established in geotechnical slope stability literature, for small or medium sized projects, it is understandable that the data collected from the site is usually sparse. Therefore, random field parameters estimated from such sparse data may contain significant uncertainty resulting in inaccurate estimation of random field samples for slope stability analysis. To overcome such limitations, Wang et al. (2018a) recently proposed a random field generator based on Bayesian Compressive Sampling (BCS) and Karhunen-Loeve (KL) expansion, which can be suitable for generating random field samples based on sparse measurements obtained from a given site.

As mentioned earlier, lognormal pdf is often chosen in RFEM analysis to avoid negative values for soil properties considered as random variables. However, while using lognormal pdf the correlation length of the random soil property **Y** relates to **X = lnY** instead of **Y** itself. Few research (Fenton and Griffiths, 2004; Pieczy´nska-Kozłowska et al., 2015) stated that the differences between the correlation length in the lognormal random field **Y** and the underlying Gaussian

random field **X** should not crucially influence the results of RFEM estimations. Pula and Griffiths (2021) investigated the theoretical relationship between spatial correlation lengths in transformed lognormal and hyperbolic tangent random fields, and the underlying Gaussian random fields from which they are derived. The study shows that for CoV less than 0.3, the untransformed and transformed spatial correlation lengths are essentially the same. An application to a bearing capacity problem shows that the transformations result in more conservative design values as compared with the untransformed results, however, the differences are very modest.

2.3.1.3. *A Comparative of RFEM with Other Approaches*

In the evolution of different probabilistic techniques, RFEM has gained more popularity in the recent times. This section presents the contrast between the advanced RFEM approach to estimate probability of failure (or reliability) of slopes in comparison to the traditional FORM or LEM based probabilistic methods. All the three stated methods predict the probability of failure as opposed to more conventional FoS, however, they predict significantly different failure probability depending on the magnitude of correlation length (Griffiths et al., 2007). Griffiths et al. (2007) showed that based on RFEM analyses, the failure probability is essentially zero when the correlation lengths are small, beyond which it increases rapidly for intermediate values of correlation lengths, while for the larger correlation lengths, the failure probability becomes constant and equal in magnitude to that obtained by FORM analyses. A typical illustration of the same is shown in Fig. 2.6 (Griffiths et al., 2007) that depicts the similarity and differences of the outcomes from FORM and RFEM analyses for various correlation lengths. Therefore, it can be stated FORM results are convergent to RFEM based outcomes when the correlation lengths are sufficiently large. For smaller correlation lengths, failure probabilities estimated by FORM are

found to be conservative. Huang et al. (2010) stated that the RFEM can accurately estimate the failure probability of slopes considering a two layered medium. However, FORM was observed to provide less accurate prediction regarding the system reliability of slopes as it primarily targets the minimum reliability index related to a particular slip surface.

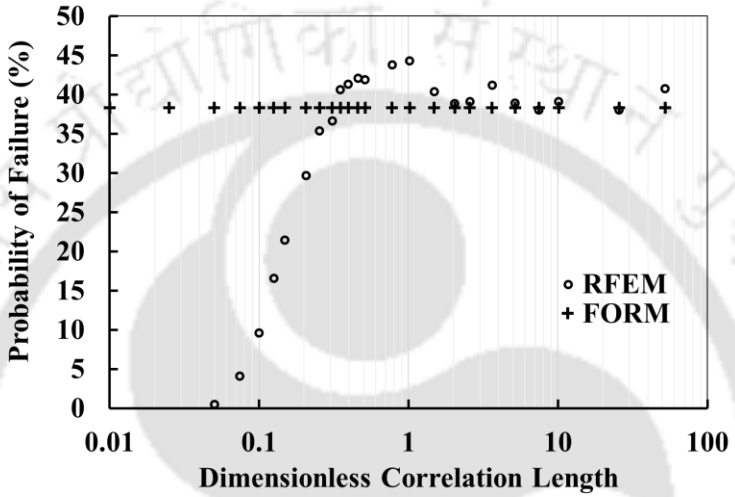

Fig. 2.6. Comparison of FORM and RFEM in terms of the probability of failure for various correlation length

Javankhoshdel et al. (2017) conducted a comparative study on Random Limit Equilibrium Method (RLEM) and RFEM to investigate the effect of spatial variability of soil shear strength parameters on the probability of failure of slopes. It is found that the results of 2D-RLEM and 2D-RFEM analyses considering isotropic random fields showed satisfactory agreement in case of slopes with smaller inclinations. However, noticeable differences are seen in case of analyses for large probabilities of failure and steeper slopes. Recently, Li et al. (2016a) developed a new probabilistic simulation method using subset simulation method in FEM to efficiently estimate the failure probability (P_f) of slope. This method significantly improves the computational efficiency in the

range of smaller failure probability (e.g., P_f <10^{-3}), thus making FEM-based probabilistic simulation techniques (e.g., RFEM) more feasible in probabilistic slope stability studies for smaller failure probability levels. However, it is noticed that subset simulation in RFEM requires calculation of FoS which could be a tedious task. Huang et al. (2017) proposed a new approach where the subset simulation is coupled with RFEM, thereby eliminating the requirement for the estimation of FoS. In this method, in order to measure the safety margin, the value of yield function from an elastoplastic finite element analysis was used instead of the FoS. Very recently, Chwala (2021) presented the kinematic failure mechanisms to analyse the stability of slope (comprising spatially variable strength parameters) based on upper bound approach. This approach is observed to be numerically efficient due to the use of rigid block failure mechanisms accompanied by an optimization technique based on the subset simulation.

2.3.2. Geological or Lithological Uncertainty

As mentioned earlier, the other type of soil heterogeneity originates from geological or lithological heterogeneity. This refers to the case of stratified soil layers or the presence of pockets of various type of soil within a more uniform soil mass. The literature suggests that very less attention has been drawn to address the effect of geological uncertainty on the probabilistic studies of heterogeneous soil. In order to deal with such heterogeneity, practising geotechnical engineers mostly depend on local experience and engineering judgment, which can possibly lead to erroneous results in slope stability assessments. Site investigation plays crucial role to interpret such uncertainties in geological and geotechnical practices. Among various site investigation methods borehole exploration is often used to assess the subsurface geological model. However, a limited number of borehole exploration is possible for small to medium projects due to project cost

and schedule. This leads to collection of geological and geotechnical information at sparse borehole locations. At other locations, the information are interpreted based on the limited borehole explorations.

Some of the early research reported for characterization of the geological uncertainty are by Evans (1982), Tang and Gilbert (1989), Halim (1991), Hansen et al. (2007) and De Marsily et al. (2005). Tang and Gilbert (1989) developed a renewal process to incorporate the probabilistic behaviour of a soil domain consisting of two different types of material. Halim (1991) modelled the geological anomalies by the means of a Poisson process for evaluating the reliability of geotechnical systems. However, both the processes could only deal with the modelling of the two simplest forms of geological uncertainty. These two processes could not handle soil layers having more than two types of material overlying each other. On the contrary, in real field, geological uncertainty always involves more complex soil formations, with more than two soil types overlying each other. Recently, to deal with the lithological uncertainty, probabilistic approaches including clustering method (Liao and Mayne, 2007), Bayesian method (Cao and Wang, 2013), wavelet transform modulus maxima method (Ching et al., 2015) and machine learning-based methods (Wang et al., 2018b) have been developed. The geological structures at the site can be interpreted from the spatial interpolation from the stratigraphic configuration obtained at borehole locations, (Patel and McMechan, 2003; Li et al., 2015b; Chen et al., 2018). The spatial interpolation methods including Kriging (Schloeder et al., 2001; Li et al., 2016d), inverse-distance weighting (Bartier and Keller, 1996) and compressive sampling (Wang and Zhao, 2016) may be utilized for interpretation of properties of the geological strata. Subsequently, the uncertainty in the geological configuration can be defined with the probabilistic methods using coupled Markov chain (Elfeki and Dekking,

2001; Hu and Huang, 2007; Qi et al., 2016), stochastic Markov random field (Norberg et al., 2002; Li et al., 2016b; Wang et al., 2016b and Wang et al., 2017) or using random variables or random fields (Li and Lumb, 1987; Christian et al., 1994; Phoon and Kulhawy, 1999; Duncan, 2000; Ching et al., 2016; Papaioannou and Straub, 2017, Griffiths and Fenton, 2004; Feng and Jimenez, 2014; Tian et al., 2016; Xiao et al., 2017; Gong et al., 2014 and 2018; Wang et al., 2018c).

Huang et al. (2010) estimated the system failure probability of two-layered slopes in the framework of Monte-Carlo simulations and showed that the RFEM can accurately predict the system reliability of slopes. Qi et al. (2016) proposed a more appropriate method of simulating geological uncertainty by the means of Coupled Markov Chain (CMC) model to assess probability of slope failure, considering the Horizontal Transition Probability Matrix (HTPM). Later on, Li et al. (2016c) extended the work to predict the failure probability of slopes simulating geological uncertainty by an efficient CMC model considering both Horizontal Transition Probability Matrix (HTPM) and Vertical Transition Probability Matrix (VTPM). Based on the simulated soil heterogeneity, MCS was conducted to estimate the FoS of slope by Finite Element Strength Reduction Method (FE-SRM). Li et al. (2016b) stated that the contribution of the stratigraphic dips to the sampled geological strata realizations is highly affected by the input statistical coefficients. In the mentioned probabilistic approaches, the complex Markov theory is embedded, thus making their use in the geotechnical practice a bit complicated. Recently, Crisp et al. (2019, 2020) presented a customised linear interpolation algorithm to characterize the strata boundaries, in which a random noise component is included for simulating the stratigraphic uncertainty. Gong et al. (2020) presented a random field approach to characterise the geological uncertainty, wherein an autocorrelation function is used to define the spatial correlation of the stratum existing between

different subsurface elements. In a non-borehole element, the probability of existence of a stratum is assessed from the derived spatial correlations and MCS is used for sampling the realizations of the geological configuration.

2.4. PROBABILISTIC SLOPE STABILITY STUDIES UNDER SEISMIC CONDITIONS

Earthquake is one of the most significant factors leading to catastrophic failure of slopes in a seismically active region. Hence, analyses for the stability of slopes under earthquake conditions are necessarily important in earthquake prone zones. In geotechnical engineering, the most commonly used seismic slope stability analyses techniques include the stress deformation analysis, permanent deformation analysis and pseudo-static analysis. The stress deformation analyses are conducted using FEM in combination with different constitutive models to incorporate nonlinear material behaviour under seismic motions (Chakraborty and Dey, 2016b). Permanent deformation analyses are based on the evaluation of permanent displacements in slope mass due to earthquake force, using the simple sliding block analogy proposed by Newmark (1965). The most common and popular approach of seismic slope stability analysis is the pseudo-static method, in which earthquake forces are considered as equivalent to horizontal and vertical inertia forces acting on the slope. The pseudo-static analyses are primarily improvisations on the LEMs of static slope stability analysis and, in this case as well, the stability of slope is expressed in terms of FoS. Apart from the inherent disadvantages of LEMs, the selection of the proper value of the seismic coefficients is a crucial factor in such analyses, which controls the inertial forces on the soil masses. This method is well known to give conservative results.

Limited literatures are available regarding the probabilistic seismic analysis of slopes. Tsompanakis et al. (2010) performed the probabilistic seismic fragility analysis of an embankment, which is a more realistic and efficient approach to accurately interpret the seismic performance and the vulnerability. Xiao et al. (2016) presented a probabilistic seismic slope stability analysis considering ground motion parameter in terms of the peak ground acceleration (PGA) in a specified exposure time at a given site as random variable. The spatial variability of the soil property is simulated using random field and the fluctuation of the groundwater level is simulated by random variable. The study demonstrated the effectiveness of the probabilistic seismic stability analysis of slope at a given site in a specified exposure time. Burgess et al. (2019) conducted a probabilistic seismic slope stability analysis by modelling the slope using RFEM. The investigation was conducted to find out the cost analysis and risk-based design, thereby revealing the probable savings if spatial variability is properly incorporated. Seismic slope stability charts were developed for c-φ soils by RFEM using *Rslope2d* computer model developed by Griffiths and Fenton (2000, 2004), providing practicing engineers an alternative to computer based modeling. Although earthquake records are random in nature, the studies mentioned earlier disregards the random nature of the earthquake by considering a constant pseudo-static earthquake coefficient. However, Malekpoor et al. (2020) showed that consideration of random variability in the earthquake coefficient results in conservative assessment of the probability of failure of the heterogeneous slope deposit.

However, these adopted approaches primarily do not deal with the actual dynamic response of the slope structure and their consequent deformations during earthquake. Therefore, these approaches are incapable of assessing the actual response of the slope during a seismic event. Therefore,

rigorous dynamic analysis needs to be carried out to assess the stability of the slope. To address the random nature of earthquake record, Youssef et al. (2008) and Johari et al. (2015) assigned a truncated exponential probability distribution function (pdf) for the earthquake acceleration coefficients. Malekpoor et al. (2020) also suggested to explore the random nature of earthquake for appropriate assessment of seismic response of slopes for future research in this regard. However, the work done by Xiao et al. (2016) and Burgess et al. (2019) can be stated as the first step towards a rigorous seismic slope stability analysis within a probabilistic framework.

2.5. PROBABILISTIC STUDY OF REINFORCED SLOPES

With the aim of constructing new roads or widening of an existing road in the hilly terrains, ensuring the stability of toe-excavated cut slope is of utmost importance. Failure of such slopes during and after the road construction can be catastrophic, resulting in loss of life and property, along with severe disruption of traffic operations. Landslides triggered due to toe excavation of slopes around the world has been studied by several researchers (Stark et al., 2005; Singh et al., 2008; Umrao et al., 2011; Kainthola et al., 2012; Kainthola et al., 2015; Mahanta et al., 2016). As toe excavation disturbs the natural stability of the hill slopes, it is imperative that a mitigation system is designed and installed for proper retention of the soil mass and prevent any sliding or translational movement.

Since the early 1980s, application of foreign reinforcements (natural or geosynthetic based) have gained popularity as a measure of slope stabilization and enhancing the stability of slopes. Some commonly used retention techniques for toe protection include installation of retaining walls and piles (Ausilio et al., 2001; Kourkoulis et al., 2012), soil nails (Chia and Jium, 2008), sheet pile

walls (Basma, 1990), stone columns (Vekli et al., 2012) and vegetation covers (Stokes et al., 2014). At the beginning, traditional deterministic limit equilibrium methods for unreinforced slopes had been improvised to incorporate the contribution of reinforcement layers in soil structures (Schneider and Holtz, 1986; Leshchinsky and Boedeker, 1989; Kitch et al., 2012). The stability of reinforced slope or embankments were investigated in terms of the modification and enhancement in the factor of safety. With the help of numerical analysis and supported by field-monitoring results for progressive stages of reinforcement application, Kang et al. (2009) investigated the stability of a large-scale cut slope reinforced by a combination of piles, soil nails and anchors. Rao et al. (2019) evaluated the stability of a heterogeneous and anisotropic soil slope reinforced with piles. The study showed that the increment in the factor of safety was governed by the increase in the heterogeneity factor and decrease in the anisotropic factor. In spite of many literatures available, the problem has been mostly addressed on a deterministic purview. However, due to uncertainties in the laboratory or field-investigated input parameters considered for such analyses, it is often difficult to capture the real picture of slope stability with a single measure of Factor of Safety (FoS).

Kitch (1994) conducted probabilistic analyses of two steep reinforced slope problems using commercially published guidelines based on deterministic LEMs, where the reliability of internal failure modes (passing within the reinforced zone) and composite failure modes (passing mostly outside of the reinforced zone) were computed and compared. Low and Tang (1997) presented a limit equilibrium model for reinforced embankments on soft ground allowing tension crack in the embankment, tensile reinforcement at the base of the embankment and a nonlinear undrained shear strength profile in the soft foundation. A practical reliability evaluation procedure was adopted for

the study. Cherubini (2000) designed an anchored sheet pile wall considering the spatial variability in soil. Li and Liang (2014) developed a reliability-based computational algorithm to stabilize an unstable slope with piles in the probabilistic framework using MCS based LE approach. Zhang et al. (2017) adapted an existing reliability analysis method for unreinforced slopes to estimate reliability of slopes reinforced with piles. However, it is worth noticing that both the mentioned studies ignored the inherent spatial variability of soil slope considering the soil shear strength parameters only as random variables. Other researchers (Luo et al., 2016; Luo and Bathurst, 2018a, 2018b) investigated the stability of geogrid reinforced slope while accounting for the soil spatial variability. Recently, Chen et al. (2020) presented a random LEM based approach for reinforced slope stability study using pile for spatially variable soil. However, in all the above studies, the adopted traditional limit equilibrium approach has the limitation of presuming the critical failure slip surface as well as the magnitude and distribution of incipient reinforcement tensile forces. Hence, there is an ardent need to assess the stability of such reinforced slopes using a more rational finite element based method including rigorous probabilistic approaches. It is also worth noting that probabilistic analysis of reinforced slopes under seismic conditions has not yet been taken into account in the research domain of probabilistic slope practise.

2.6. PROBABILISTIC STUDY OF TOE-EXCAVATED SLOPES

Road cuts are repeatedly carried out in hilly regions, either for construction of new roads or for widening of the existing roads. Stability of the cut slopes along the hills are of major concern, as the failure of such cut slopes are of dire consequences, posing a high risk to human lives as well as monetary loss (Huang and Chan, 2004; Borgatti and Soldati, 2005; Stark et al., 2005; Erginal et al., 2008; Ayalew et al., 2009; Lee and Hencher, 2009; Zhang et al., 2009, 2012). The foremost

reason of cut slope failure is the reduction of confining stress in the slope structure due to excavation. The primary design parameters for the excavated slope are the slope geometry, shear strength of soil and location of ground water table. In the case of cut slopes with granular soils, the stability of the slope is predominantly governed by the slope angle. In case of slopes comprising cohesive soils, the excavation height is recognized to be the key design parameter. In case of a saturated or partially saturated c-φ soil slope and saturated soils, both the slope height and angle of cut plays contributing role in slope stability and failure.

Stark et al. (2005) investigated the reason behind the distress to a single-family residence located atop a major cut slope of approximately 70 m height in east-west state highway of San Francisco, California. The study revealed that the distress occurred because of a landslide triggered by excavation of slope for widening of the existing highway. Umrao et al. (2011) investigated the instability occurred because of toe cutting in rock slopes at five different sites across the NH-109 in Himalayan territory of India, using continuous slope mass rating (CSMR) technique. Kainthola et al. (2012) studied the influence of toe cutting on the stability of Mahabaleshwar hill slope using distinct element modeling. The study revealed that the hill slope was marginally stable in dry condition, whereas it failed along well-defined joint planes under the saturated condition. Zhang et al. (2012) reported a case history of repeated failures on a high cut slope due to multi-excavation near highway G212, 15 km east from Lanzhou Basin in Gansu Province, China. The geological study revealed that the exposure of the weak bedding plane and unloading of the toe region in the cut slope are the reasons behind the repeated failures. Kainthola et al. (2015) studied the influence of large height toe cut on the natural stability of a basaltic and lateritic hill slope at Mahabaleshwar, India. Several critical parameters (mode of failure, factor of safety, shear strain rate, displacement

magnitudes) and their influence on the stability were deciphered. Mahanta et al. (2016) conducted Finite element method (FEM) based stability analysis of slopes in vulnerable areas (derived from hazard zonation studies) in the region of Luhri village (NH-305) in Kullu district of Himachal Pradesh, India. Chakraborty and Dey (2016c) inspected the influence of vertical toe cut on hill slope stability using deterministic LEM for various geotechnical, hydraulic and seismic parameters. The study recommended the critical horizontal extent of vertical toe cut of hill slopes as a function of the slope type and different geotechnical parameters. All the above-reported studies, conducted to elucidate the effect of toe cutting on hill slope stability, were carried out in a deterministic platform. Probabilistic studies in toe excavated slopes is significantly lacking. No such studies are yet incorporated in this field where spatial variability is incorporated with the aid of random field theory.

2.7. CRITICAL APPRAISAL OF THE LITERATURE

It is explicitly understood that different types of uncertainties associated to geotechnical properties substantially influence the assessment of slope stability. In many cases, it is experienced that conventional limit-equilibrium or finite element based analyses, incorporating deterministic soil parameters, fails to address the stability and failure of actual slopes. Under such circumstances, the incorporation of parametric uncertainty through probabilistic analysis of the slope stability becomes imperative. Although probabilistic study in slope engineering has started in early 1970's, it is yet developing with newer understanding and incorporation of realistic intricacies. It has been noted in the literature that depending on the variation of soil properties, the consideration of the uncertainties in soil properties can underestimate or overestimate the slope stability in terms of probability of failure or reliability of slope structure. In this regard, this chapter critically highlights

the salient works related to probabilistic slope stability analyses and their conceptual-cum-technical evolution over the decades. Further, the critical review also elucidates the present day understanding of the problem and future scope to address important slope stability problems.

The overview of the literature indicates that there exist two main approaches, namely 'approximate methods' and 'simulation-based methods', for incorporating uncertainty in soil properties in probabilistic slope stability analysis. Approximate method such as FORM is found to provide either overestimated or underestimated probability of slope failure, and is also found incapable of incorporating spatial variability. On the other hand, although the simulation-based methods, such as MCS, are capable of conveniently incorporating the soil spatial variability accurately, they are largely dependent on the number of iterations to achieve a desired level of failure probability, and is thus computationally expensive. To overcome such limitations, advanced simulation techniques such as subset-simulation are being suggested by researchers in the recent times. This limitation is overcome by employing the advanced subset simulation based MCS technique which proves to be capable of capturing slope failure with sufficient accuracy, even at relatively smaller probability levels. Rigorous researches are further required in this direction for improving the accuracy in detecting of slope failure at lower probability levels and reduce the computational time, which is coveted by the geotechnical engineers.

In probabilistic slope stability analysis, both LEM and FEM approaches can be adopted to estimate the probability of slope failure. To overrule the inherent limitations of deterministic approach, such as presuming the location as well as shape of failure surface and adopting presumed geotechnical properties for estimating the factor of safety against slope failure, Random Finite Element Method

(RFEM) is mostly adopted in recent times. RFEM considers the shear strength parameters of soil as random variable and a random field is used as a provision of their spatial variability, thus aiding the RFEM to seek out the critical slip surface and the associated failure mechanism as an outcome of the analysis. A comparison between the outcomes of FORM and RFEM indicates that the former gives conservative results for smaller correlation lengths, while the results from FORM and RFEM seems to agree well at larger correlation lengths. It is also found that the results of 2D RLEM and 2D RFEM analyses considering isotropic random fields showed satisfactory agreement in case of slopes with smaller inclinations. However, noticeable differences are seen in case of analyses for larger probabilities of failure and steeper slopes. The correlation lengths are mostly guided by the variation of the real-field properties. With respect to the shear strength parameters, although it is found that mostly they are negative correlated, there are specific cases of soil heterogeneity which leads to positive correlations as well. Although it is noticed that most of the literature deals with negative correlation between shear strength parameters, the positively correlated instances of spatial variability of soil did not fetch much attention, even though they can lead to a noticeable different understanding to the probabilistic failure of slopes. Further, most of the studies have considered stationary random fields to simulate the soil uncertainty using random field theory. Such studies are prescribed to provide overestimated failure probability. Very few recent studies have attempted to incorporate non-stationary random fields, although significant research is required in this direction in the future to address the slope failure probabilities in a more realistic manner. It is worth noting that soil heterogeneity, in terms of spatial variability, has drawn the attention of many researchers. Nonetheless, the ground uncertainty due to lithological heterogeneity remains to be widely ventured for efficient slope stability assessment, thereby demanding more rigorous studies in this direction.

The seismic response of slopes is even more complicated given the presence of variability of soil shear strength parameters. Very few literatures are available on seismic stability studies of slopes considering probabilistic concepts and principles. Furthermore, the probabilistic seismic studies done until date are only based on the pseudo-static earthquake condition which falls short in representing the actual dynamic response of slopes during and post-occurrence of an earthquake. Further rigorous research should be directed to understand the influence of uncertainty and spatial variability of the soil shear strength parameters on the rigorous dynamic analysis and seismic response of slopes. This would further help to develop better understanding and guidelines against such slope failure. The vulnerability of toe-excavated slopes increase manifold, and is generally suggested to be avoided. However, infrastructure development, especially roadways and railways construction through hilly terrains, calls for unavoidable excavation of the toe or berms. Such slopes need to be protected by proper and selective retention measures. Most of the studies regarding the stability analysis of cut slopes adopted deterministic LEM based approaches. Probabilistic studies in reinforced or retained slopes is significantly lacking. Further, probabilistic seismic studies for the analysis of cut-slope stability is yet to be ventured.

2.8. OBJECTIVES AND SCOPES OF THE DISSERTATION WORK

Based on the gap areas found during thorough survey of available literature and motivated to address the problem of hill-slope failures frequently incorporated during the road construction through hilly terrains, the following objectives and corresponding scopes are decided to address the problem through a realistic probabilistic framework:

- To develop a simplistic stochastic model to incorporate the prevailing uncertainty in soil properties.

- To meet the stated objective, a stochastic model of spatially varying Standard Penetration Test (SPT) N-value data is developed to estimate the vertical scale of fluctuation (SoF) for a specific region (addressed in **Chapter 4**).

- To assess the effect of various parameters on probabilistic slope stability analysis.
  - To meet the stated objective, the influence of various parameters on probabilistic slope stability study using a simplistic LEM based probabilistic approach is established (addressed in **Chapter 5**).
- To assess the influence of toe excavation induced slope instability using LEM based probabilistic slope stability analysis for static conditions.
  - To meet the stated objective, a schematic approach to incorporate the LEM based probabilistic method for toe excavation induced slope stability study is developed (addressed in **Chapter 6**).
- To investigate the retention systems in mitigating the slope failure due to toe excavation using a probabilistic framework for static conditions.
  - To meet the stated objective, the performance of a sheet pile wall (SP) and a sheet pile anchor retention (SPAR) system in mitigating the slope failure through probabilistic cut slope stability analysis is ascertained (addressed in **Chapter 7**).
- To investigate the advantages of Random Finite Element Method (RFEM) based probabilistic study over LEM based approach to assess the influence of toe excavation induced slope instability.
  - To meet the stated objective, RFEM for probabilistic cut slope analysis is incorporated and the efficacy of the advanced RFEM over the traditional LEM

based probabilistic approach for cut slope stability analysis is assessed (addressed in **Chapter 8**).

- To investigate toe excavation induced instability using a probabilistic framework under earthquake conditions.
    - To meet the stated objective, the seismic response of both unsupported and supported (with SPAR system) cut slopes within a probabilistic framework is investigated (addressed in **Chapter 9**).

CHAPTER 3

NUMERICAL MODELLING

3.1. GENERAL

A numerical modeling is exclusively mathematical and is very different than a full-scaled field modeling or a scaled physical modeling in the laboratory. Numerical modelling can be defined as a mathematical representation of a physical process, based on relevant hypothesis and simplifying assumptions. Some of the advantages of numerical modeling over physical modeling are that they can operate quicker, provides the user a higher conditional variability, and also accommodates many boundary conditions. In recent decades, the Finite Element Method (FEM) is used increasingly for the analysis of stress, deformation, structural forces, bearing capacity, stability and ground water flow in geotechnical engineering applications. The continuous evolution in mathematics and unprecedented computing power has led to the development of advanced software tools for engineering and scientific analysis. In the present study, the stability of excavated slopes is extensively studied within probabilistic framework using the commercially available Finite Element program GeoStudio v2018 and its corresponding modules of Slope/W, Sigma/W and Quake/W. The computer model *Rslope2d* is also utilised in present work for Random Finite Element Method (RFEM) based probabilistic study of toe excavated slope sections. Slope/W can effectively analyze both simple and complex stability related limit-equilibrium problems for a variety of slip surface shapes, pore-water pressure conditions, soil properties, and loading conditions. Sigma/W is a powerful finite element software product for modeling stress and deformation in earth and structural materials, and the analyses may range from simple linear elastic simulations to soil-structure interaction problems with nonlinear material models. The Quake/W

module is a finite element software product used for the dynamic analysis of earth structures subjected to earthquake shaking and other sudden impact loading, for example, dynamite explosions or pile driving. *Rslope2d* is a computer model developed by Griffiths and Fenton (2000; 2004) for random finite element based probabilistic analysis of slopes.

3.2. WORKING PRINCIPLES OF VARIOUS MODULES OF GEOSTUDIO AND RSLOPE2D

The theoretical background of each of the three modules of GeoStudio (Slope/W, Sigma/W and Quake/W) as well as *Rslope2d* are explored thoroughly to understand the mathematical formulation working behind the simulations carried out in the present study and the same is reported in this section.

3.2.1. Slope/W for Slope Stability Modeling

This section briefs the theoretical basis utilised in the development of Slope/W module. Slope/W basically solves for two factor of safety equations considering static equilibrium; one satisfying the force equilibrium (*Ff*) and the other satisfying the moment equilibrium (*Fm*), following the basic conventions of slope stability analysis. The commonly used methods of slices (for example, Bishop's Simplified method, Janbu's Simplified method, Spencer method, Morgenstern-Price method) are special cases of the General Limit Equilibrium (GLE) solution which allows a range of assumptions related to the interrelationship between the interslice shear forces and normal forces. Limit equilibrium types of analyses for assessing the stability of earth slopes have been in use in geotechnical engineering for many decades. The idea of discretizing a potential sliding mass into vertical slices was introduced early in the 20th century and is consequently the oldest numerical

analysis technique in geotechnical engineering. Many different solution techniques for the method of slices have been developed over the years. Basically, all of them are very similar. The differences between the methods depends on the equations of statics that are satisfied, the interslice forces that are considered in the equilibrium solution, and the assumed relationship between the interslice shear and normal forces.

The Ordinary, or Fellenius (1936), method was the first method developed. The method ignored all interslice forces and satisfied only moment equilibrium. Adopting these simplified assumptions made it possible to compute a factor of safety using hand calculations, which was important since there were no computers available. Later, Bishop (1955) devised a scheme that included interslice normal forces but ignored the interslice shear forces. Again, Bishop's Simplified method satisfies only moment equilibrium. Of interest and significance with this method is the fact that by including the normal interslice forces, the factor of safety equation became nonlinear, and an iterative procedure was required to calculate the factor of safety. The Janbu's Simplified method (1954) is similar to the Bishop's Simplified method in that it includes the normal interslice forces and ignores the interslice shear forces. The difference between the Bishop's Simplified and Janbu's Simplified methods is that the Janbu's Simplified method satisfies only horizontal force equilibrium, as opposed to moment equilibrium. Later, computers made it possible to more readily handle the iterative procedures inherent in the limit equilibrium method, and this lead to mathematically more rigorous formulations which include all interslice forces and satisfy all equations of statics. Two such methods are the Morgenstern-Price (M-P) (1965) and Spencer (1967) methods. Spencer only considered a constant *X/E* ratio for all slices in the General Limit Equilibrium (GLE) equation (Eqn. 1), which infers that the ratio of shear to normal is a constant

between all slices. The M-P method can utilize any general appropriate function and hence considered in this study.

The interslice shear forces in the GLE method are governed by the equation proposed by Morgenstern and Price (1965), which is expressed as

$$X = E\lambda f(x) \tag{3.1}$$

where, *f(x)* is a function which provides the relation between the interslice normal force (*E*) and shear force (*X*), and λ is the reduction factor.

Slope/W can accommodate a wide range of different interslice force functions, namely Constant, Half-sine, Clipped-sine, Trapezoidal and Data point fully specified. The Spencer method uses a constant interslice function which infers that the ratio of shear to normal is a constant between all slices. One does not need to select the function; it is fixed to be a constant function in the software when the Spencer method is selected. Only the Morgenstern-Price allows for user-specified interslice functions. Some of the functions available are the constant, half-sine, clipped-sine, trapezoidal and data-point specified. The most commonly used functions are the constant and half-sine functions. A Morgenstern-Price analysis with a constant function is the same as a Spencer analysis. Slope/W by default uses the half-sine function for the M-P method. The half-sine function tends to concentrate the interslice shear forces towards the middle of the sliding mass and diminishes the interslice shear in the crest and toe areas. Defaulting to the half-sine function for these methods is based primarily on experience and intuition and not on any theoretical considerations. Other functions can be selected if deemed necessary. However, in the present study an extensive analysis has not been conducted to study the influence of different functions on the

slope stability assessment and the Slope/W default Half Sine function is utilised. The GLE formulation estimates *Fm* and *Ff* for a range of lambda (λ) values. A plot similar to Fig. 3.1 can be drawn with these computed *Fm* and *Ff* values with lambda (λ). The Morgenstern-Price (M-P) FoS is the factor of safety corresponding to the point where the two curves intersects in Fig. 3.1. However, it is to be noted that since the method is purely based on the principles of statics, and there is no mention of displacement or deformations, it is not always possible to obtain realistic stress distributions from this method.

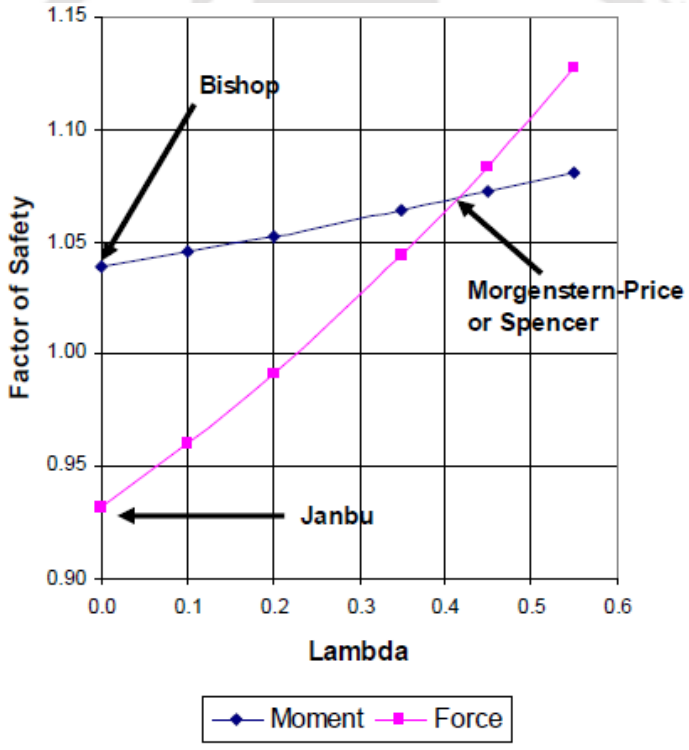

Fig. 3.1 A typical plot of factor of safety versus lambda (λ) (adopted from Slope/W v2018)

As an alternative to the limit-equilibrium (LE) stability analysis, the theory of the Finite Element Stress method is applied. This method computes the stability factor of a slope based on the stress state in the soil obtained from a finite element stress analysis. A FoS is defined as that factor by

which the shear strength of the soil must be reduced in order to bring the soil mass into a state of limiting equilibrium along a selected slip surface. For an effective stress analysis, the shear strength is defined as

$$s = c' + (\sigma_n - u)\tan\varphi' \qquad (3.2)$$

where, s is effective shear strength of the soil, c' is effective cohesion, φ' is effective angle of internal friction, σ_n is normal stress on shear plane, and u is pore-water pressure.

For a total stress analysis, the strength parameters are defined in terms of total stresses and pore-water pressures are not taken into consideration. The stability analysis involves passing a slip surface through the earth mass and dividing the inscribed portion into vertical slices. The slip surface may be circular, composite (i.e., combination of circular and linear portions) or consist of any shape defined by a series of straight lines (i.e., fully specified slip surface). Slope/W conducts a slope stability analysis as described above to estimate stress-based FoS against failure.

Slope/W accommodates a comprehensive algorithm for conducting stability analysis within a probabilistic framework. Most of the input parameters can be considered as random variable characterising the same by assigning a probability distribution function (pdf), and a Monte Carlo Simulation (MCS) scheme is then adopted to produce a pdf of the resulting FoS. Once the pdf of the FoS are known, the probability of failure and reliability index of the earth structure can be computed. Although most natural material parameters may vary statistically in a Normal distribution manner, for general purposes, Slope/W includes several probability density functions (pdf) namely Normal, Lognormal, Uniform, Triangular and Generalized Spline function for

accounting the special circumstances. The present study utilises the Lognormal pdf for characterising various input random variables.

3.2.2. Sigma/W for Stress-Deformation Modeling

This section presents the methods, equations, procedures, and techniques used in the formulation and development of the Sigma/W module. Sigma/W is formulated for either two-dimensional plane strain or axisymmetric problems using the small displacement - small strain theory. In the present study, Sigma/W is used only for the two dimensional plane strain problems.

The finite element equation used in the Sigma/W formulation for a given time increment is expressed as

$$\tau\int_V([B]^T[C][B])dV\{a\} = b\int_V\left(\langle N\rangle^T\right)dV + p\int_A\left(\langle N\rangle^T\right)dA + \{F_n\} \qquad (3.3)$$

where, [B] is the strain-displacement matrix, [C] is the constitutive matrix, {a} is the vector of nodal incremental x- and y-displacements, <N> is the row vector of interpolating functions, A is the area along the boundary of an element, V is the volume of an element, b is the unit body force intensity, p is the incremental surface pressure, and {Fn} is the concentrated nodal incremental load vector. Equation 3.3 is summed over all the elements in the discretized domain. It should be noted the Sigma/W is formulated for incremental analysis. For each time step, the incremental displacements are calculated for the incremental applied load. These incremental values are then added to the values from the previous time step. The accumulated values are reported in the output files. Using this incremental approach, the unit body force is only applied when an element is subjected to analysis for the first time. For a two-dimensional plane strain analysis, Sigma/W

considers all elements to be of unit thickness. For constant element thickness, *t*, Eqn. 3.3 is modified as

$$\tau\int_A([B]^T[C][B])dA\{a\} = bt\int_A\left(\langle N\rangle^T\right)dA + pt\int_L\left(\langle N\rangle^T\right)dL \tag{3.4}$$

In an abbreviated form, the finite element equation is written as

$$[K]\{a\} = \{F\} = \{F_b\} + \{F_s\} + \{F_n\} \tag{3.5}$$

where, [*K*] is the element characteristic (or stiffness) matrix, {*a*} is the nodal incremental displacement vector, {*F*} is the applied nodal incremental force, {*Fb*} is the incremental body force vector, {*Fs*} is the force vector due to surface boundary incremental pressures, and {*Fn*} is the vector of concentrated nodal incremental forces.

Sigma/W solves the finite element equation for each time step to obtain incremental displacements and calculates the resultant incremental stresses and strains. It then sums all these increments since the first time step and reports the summed values in the output files. It uses Gauss-Legendre numerical integration (also termed quadrature) to form the element characteristic (or stiffness) matrix [*K*]. The variables are first evaluated at specific points within an element. These points are called integration points or Gauss points. These values are then summed for all the Gauss points within an element.

In Sigma/W, the nodal forces are included in the finite element formulation (as shown in Eqn. 3.5) by two different approaches. Either the nodal forces can be specified as boundary conditions, or they can be calculated internally when the elements are first provided with a stress release. For each element, the nodal forces are computed using the following expression

$$\{F\} = \int_V [B]^T \{\sigma\} dV \tag{3.6}$$

where, $\{\sigma\}$ is the vector of element stresses, $[B]$ is the strain-displacement matrix, and V is the elemental volume. The resultant nodal forces are accumulated at each node. To simulate the removal of soils, as in an excavation, the signs on the nodal forces are reversed before these forces are incorporated into the finite element equation. In the displacement output files, Sigma/W reports the nodal forces at all nodes where displacement or boundary conditions are specified. However, in this case, the change of signs are not specified.

3.2.3. Quake/W for Non-linear Dynamic Modeling

This section presents the methods, equations, procedures, and techniques used in the formulation and development of the Quake/W module. Quake/W is formulated for either two-dimensional plane strain or axisymmetric problems using small displacement - small strain theory. In the present study, Quake/W is used only for the two dimensional plane strain problems.

The governing equation of motion for dynamic response of a system in finite element formulation can be expressed as:

$$[M]\{\ddot{a}\} + [D]\{\dot{a}\} + [K]\{a\} = \{F\} \tag{3.7}$$

where, [M] is mass matrix, [D] is damping matrix, [K]is stiffness matrix, {F} is vector of loads, { $\ddot{a}$ } is vector of nodal accelerations, { $\dot{a}$ } is vector of nodal velocities, and {a} is vector of nodal displacements.

The vector of loads could be made up by different forces:

$$\{F\} = \{F_b\} + \{F_s\} + \{F_n\} + \{F_g\} \tag{3.8}$$

where, $\{F_b\}$ is body force, $\{F_s\}$ is force due to surface boundary pressures, $\{F_n\}$ is concentrated nodal force, and $\{F_g\}$ is force due to earthquake load.

The mass matrix can be a consistent mass matrix or a lumped mass matrix. Quake/W uses a lumped mass matrix. The lumped mass matrix is given as:

$$[M] = \int_v \rho[\psi] dv \tag{3.9}$$

where, ρ is mass density, $[M]$ is mass, and $[\psi]$ is a diagonal matrix of mass distribution factors. It is common practice to assume the damping matrix to be a linear combination of mass matrix and stiffness matrix:

$$[D] = \alpha[M] + \beta[K] \tag{3.10}$$

where, α and β are scalars and called Rayleigh damping coefficients. They can be related to a damping ratio η by:

$$\eta = \frac{\alpha + \beta\omega^2}{2\omega} \tag{3.11}$$

where, ω is the particular frequency of vibration for the system.

Quake/W computes the Rayleigh damping coefficients by using the lowest (or, fundamental) and the second lowest (or, first higher mode) system frequencies and a constant damping ratio.

The stiffness matrix is expressed as:

$$[K] = \int_v [B]^T [C][B] dv \tag{3.12}$$

where, [B] is strain-displacement matrix and [C] is constitutive matrix.

Quake/W uses Gauss-Legendre numerical integration (also termed quadrature) to form the element characteristic (or stiffness) matrix [K]. The variables are first evaluated at specific points within an element. These points are called integration points or Gauss points. These values are then

summed for all the Gauss points within an element. The motion equation is a second-order propagation type of equation. This equation can be solved in either frequency domain or time domain. Solution in time domain is preferred when material property may change with time. There are many methods for advancing the solution in time domain. Quake/W uses Wilson-θ method to perform the time domain integration of the motion equation. Quake/W computes the stresses and strains at each integration point within each element once the nodal displacements have been obtained.

3.2.4. *Rslope2d* for RFEM Modeling

Rslope2d is a computer model developed by Griffiths and Fenton (2000; 2004) for random finite element method (RFEM) based probabilistic analysis of slopes. The RFEM is a powerful probabilistic method for slope stability analysis because the spatial correlation of soil properties is modelled explicitly and no assumption about the shape or location of the failure surface is required to be made in advance. Failure occurs through soil elements whose shear strength is lower than the applied shear stresses. The procedures for probabilistic slope stability analysis adopted in *Rslope2d* can be summarised as follows:

1. Simulate a 2-dimensional (2-D) spatially random soil profile based on the prescribed statistical parameters of the chosen soil properties;
2. Perform finite element slope stability analysis on the simulated soil profile to determine whether the slope 'fails' under specific convergence criteria; and
3. Repeat Steps 1 and 2 many times as part of the Monte Carlo simulation process to establish the probability of failure, *Pf*.

In *Rslope2d*, a 2-D spatially random soil profile is generated based on random field theory (Vanmarcke 1977, 1983), which makes use of three statistical properties: the mean (μ), a measure of the variance (e.g. standard deviation, σ, or coefficient of variation, CoV), and the scale of fluctuation, θ. To generate random fields for the specified soil properties (c and φ), random field theory is implemented in *Rslope2d*. The computer model uses the local average subdivision (LAS) method developed by Fenton and Vanmarcke (1990). The LAS method generates correlated local averages of the soil property based on a standard normal distribution function (i.e., having zero mean and unit variance) and a spatial correlation function. The LAS method is presented in detail by Fenton (1990) and Fenton and Vanmarcke (1990).

In this study, the two-dimensional spatial variation in the slope domain is characterized by an exponentially decaying (Markovian) correlation function (expressed in Eqn, 3.13) which implies the covariance between points decays exponentially with absolute separation distance between the points in the field.

$$\rho(k) = \exp\left(-\frac{2|k|}{\theta}\right) \tag{3.13}$$

where, ρ is the correlation coefficient for the random field values at any two points separated by a lag distance k. The field is assumed to be quadrant symmetric (i.e., correlation between points with lag (x,y) is the same as the correlation between points with lag (-x,y), (x,-y), etc.).

3.2.4.1. *Transformation of the Normal RF into Lognormal RF*

In the present study, the random variables (cohesion, c, and angle of internal friction, φ) are defined by a lognormal pdf. The slope geometry, mean and CoV values of cohesion, c, and angle of internal friction, φ, are considered same as considered in case of LEM based probabilistic study. In

Rslope2d, first, a standard normal random field [$G(x)$] is generated utilising the LAS method for a soil property (X) assigned from a lognormal distribution using a mean value (μ_X), and a standard deviation value (σ_X). Then the generated field is transformed into a lognormal distribution using the following expression:

$$X_i = \exp\{\mu_{\ln X} + \sigma_{\ln X} G(x_i)\} \tag{3.14}$$

where, x_i is the vector of the coordinates of the centre of the i^{th} element, X_i is the value of the soil property assigned to that element, $\mu_{\ln X}$ and $\sigma_{\ln X}$ are the mean and standard deviation, respectively, of the underlying normally distributed ln$X$.

$\mu_{\ln X}$ and $\sigma_{\ln X}$ can be estimated using the Eqns. (3.15) and (3.16), respectively,

$$\mu_{\ln X} = \ln X - \frac{1}{2}\sigma^2_{\ln X} \tag{3.15}$$

$$\sigma_{\ln X} = \sqrt{\ln\left(1 + CoV_X^2\right)} \tag{3.16}$$

3.2.4.2. *Local Averaging*

The statistical parameters of the input soil properties such as mean, standard deviation, and scale of fluctuation (SoF) are defined at the point level. In the LAS method, the point variance is decreased by local averaging method, which is governed by a *variance function*, Γ^2. The variance reduction is dependent on the size of the averaging domain and the scale of fluctuation (Vanmarcke 1983). The variance function for an exponentially decaying correlation function is expressed as:

$$\Gamma^2(T) = 2\left(\frac{\theta}{2T}\right)^2\left(\frac{2T}{\theta} - 1 + e^{-\frac{2T}{\theta}}\right) \tag{3.17}$$

where, *T* is the size of the averaging domain. For a square finite element *T* is the size of the element. Griffiths and Fenton (2004) shows that the variance function for a square finite element with a side length of $\alpha\theta$ can be expressed as:

$$\Gamma^2 = \frac{4}{\alpha\theta}\int_0^{\alpha\theta}\int_0^{\alpha\theta} \exp\left(-\frac{2}{\theta}\sqrt{x^2+y^2}\right)(\alpha\theta - x)(\alpha\theta - y)\,dxdy \tag{3.18}$$

The variance function for an exponentially decaying correlation function with square finite element, is shown in Fig. 3.2 (Griffiths and Fenton, 2004). This figure shows that elements that are large, as compared to the SoF, results in very significant variance reduction ($\Gamma^2 \to 0$) and elements that are small compared to the SoF ($\alpha \to 0$) results in very little reduction in variance ($\Gamma^2 \to 1$). Therefore, in case of fixed element size, a smaller SoF results in greater reduction in variance and a larger SoF results in less reduction in variance.

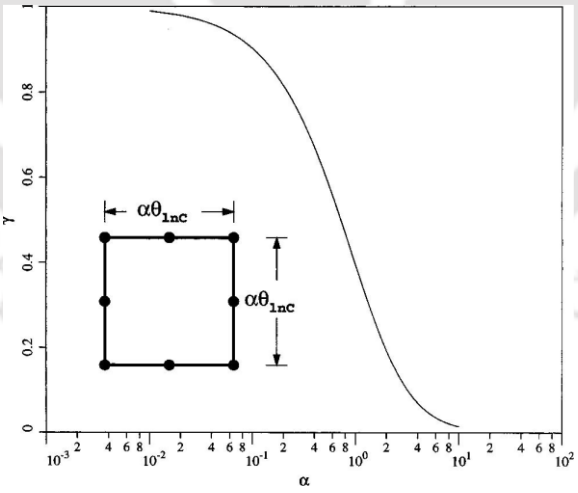

Fig. 3.2 Reduction in variance over a square finite element (Griffiths and Fenton, 2004)

Griffiths and Fenton (2004) also showed that in case of Normal distribution, local averaging leads to reduction in variance but the mean is not affected. However, local averaging reduces both the mean and the standard deviation in case of a Lognormal distribution. This is attributed to that fact that the mean and variance of a Lognormal distribution are influenced by both the mean and variance of the underlying Normal distribution (Griffiths and Fenton, 2004; Fenton and Griffiths, 2008; Chok, 2009)

3.3. GEOMETRY AND MESHING

In GeoStudio, the entire model is defined as a series of geometry objects. As shown in Fig. 3.3, these objects can be soil regions, circular openings line objects, surface regions, and point objects. In GeoStudio, the geometry of a model is totally defined in prior to the consideration of the discretization or meshing.

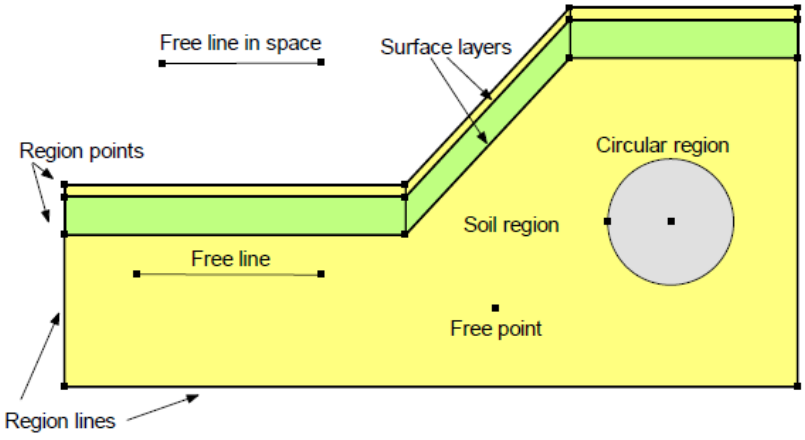

Fig. 3.3 Geometry objects in GeoStudio (adopted from Sigma/W Manual, 2018)

GeoStudio uses the concept of regions and points to define the geometry of a problem and to facilitate discretization of the problem. The utilization of regions offers all the advantages of

dividing a large domain into smaller pieces, working and analyzing the smaller pieces, and then connecting the smaller pieces together to obtain the behavior of the whole domain, similar to the fundamental concept of finite elements. The regions may be simple straight-sided shapes like quadrilaterals or triangles or a free form, multi-sided polygon.

Discretization or meshing is one of the most fundamental aspects of finite element modeling, which is used to classify any given region, surface, or line, into smaller parts to address the global response of the same from localized responses. GeoStudio has its own system and algorithms for meshing, which are designed specifically for the analysis of geotechnical and geo-environmental problems. The default scheme of meshing is fully automatic and there is no need to draw individual "finite elements" as a default mesh would be generated once the geometry regions are specified. However, the generated default mesh can be altered globally or locally according to the demand of the problem being analyzed.

One of the main features of a finite element are its constituent nodes. The nodes are used to describe the distribution of the primary unknowns within the element. All finite element equations are formed at the nodes. In a finite element formulation, it is necessary to adopt a model describing the distribution of the primary variable within the element (e.g., total head). The distribution could be linear or curved. For a linear distribution of the primary unknown, the nodes are required only at the corners of the element. With three nodes defined along an edge, a quadratic or any other higher order equation can be utilized for describing the distribution of the primary unknown within the element. The compatibility between different elements are established through their common nodes by considering the distribution of the primary unknown along the common element edge to

be utilized by both the individual elements for their local estimations. The meshing algorithms in GeoStudio ensure element compatibility within regions. A special integer-based algorithm is also included to check the compatibility between regions. This algorithm ensures that common edges between regions have the same number of elements and nodes. Even though the software is very powerful and seeks to ensure mesh compatibility, the user nonetheless needs to be careful about creating adjoining regions. The integer-programming algorithm in GeoStudio seeks to ensure that the same number of element divisions exist between points along an edge of a region. The number of element divisions are automatically adjusted in each region until this condition is satisfied. Consequently, it is often noticed that the number of divisions along the edge of a region is higher than what was specified as default.

There are different finite element mesh patterns available as default in Geostudio, namely (a) Quads and Triangles (b) Triangles only (c) Rectangular grid of Quads, and (d) Triangular grid of Quads / Triangles. In a finite element formulation, there are many integrals to be determined for achieving local scale equilibrium. For simple element shapes like 3-noded or 4-noded brick (rectangular) elements, it is possible to develop closed-formed solutions to obtain the integrals. However, for higher-order and more complex element shapes, it is necessary to conduct numerical integration. GeoStudio uses the Gauss quadrature scheme for conducting the numerical integration. This scheme is involved in sampling the element characteristics at specific points, known as Gauss points, and then adding up the sampled information. Table 3.1 lists some of the element types available in GeoStudio and their available integration points.

Table 3.1 Commonly available element types available in GeoStudio and their corresponding integration points

Element Type	Integration Points	Comments
4-noded quadrilateral	4	Default
8-noded quadrilateral	4 or 9	4 is the default
3-noded triangle	1 or 3	3 is the default
6-noded triangle	3	Default

GeoStudio presents the results for a Gauss region, but the associated data is actually computed at the exact Gauss integration sampling points. In the present study, the use of mixed 'quad and triangle' unstructured mesh with 4-noded quadrilateral and 3-noded triangle element type is utilized. Figure 3.4 shows the typical unstructured mesh of 'quad and triangle'. The total number of nodes and elements used in the models depends on the number of mesh elements used and the adopted refinements.

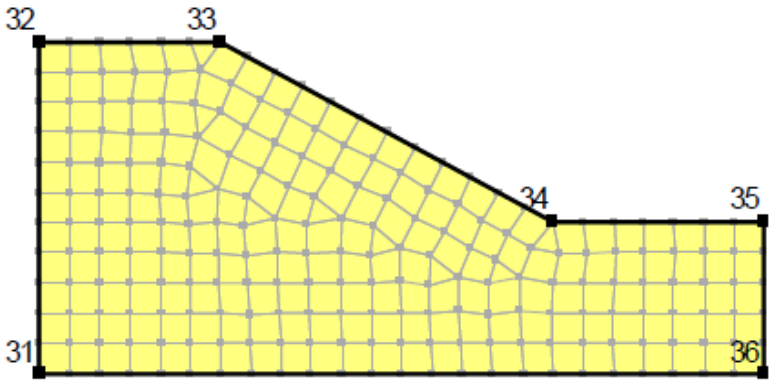

Fig. 3.4 Typical 'quad and triangle' meshing scheme adopted to represent a slope (adopted from Sigma/W Manual, 2018)

In *Rslope2d*, once the random field is transformed into the desired lognormal field, it is then mapped onto the finite element mesh, which is established according to the user-defined slope geometry. A typical finite element mesh for a 1:1 slope with a height, H = 10 m, is shown in Fig. 3.5. Each element within the slope geometry is 1 m by 1 m in size and it is assigned a random variable of the particular soil property (i.e. c or φ). The computer model uses 8-noded quadrilateral elements with reduced integration for the generation of gravity loads, stiffness matrix generation and stress redistribution phases of the algorithm (Chok, 2009).

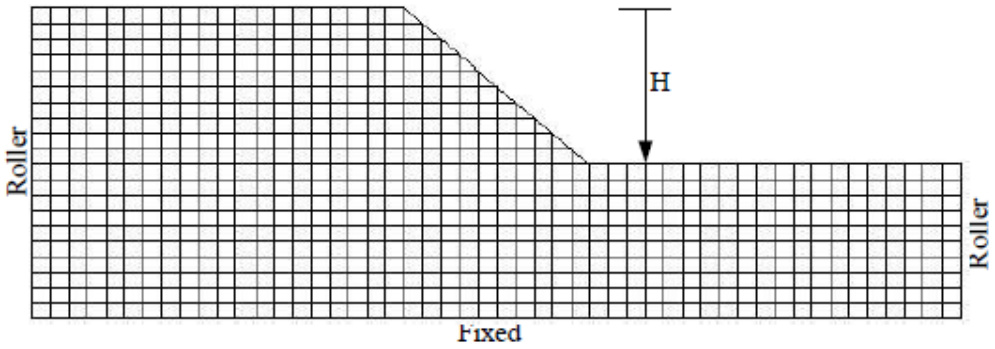

Fig. 3.5 Typical finite element mesh used in *Rslope2d* RFEM model

3.4. MATERIAL MODELS AND MATERIAL PROPERTIES

This section describes the various soil models and properties in GeoStudio and *Rslope2d*, and their influence on the generated results. Well-defined soil models and the chosen properties of the constituent materials can be critical in obtaining an efficient solution of the finite element equations and therefore it is important to have a clear understanding of them.

3.4.1. Material Models in Slope/W Analysis

The commonly available methods used to evaluate FoS in Slope/W are based on limit equilibrium formulations except for the one which uses finite element computed stresses. Many different material models are available in Slope/W that can be used to calculate the FoS of slopes. These material models include 'Mohr Coulomb model', 'Undrained model', 'High Strength model', 'Bedrock or Impenetrable model', 'Bilinear strength model', 'Anisotropic Strength model', 'Spatial Mohr Coulomb model', 'Anisotropic Function model' and 'Model for Normal/Shear Function interactions'. In the present study, the Mohr Coulomb material model and Impenetrable/Bedrock model has been used for slope material and foundation material respectively, to compute the stability of the slope.

3.4.2 Material Models in Sigma/W Analysis

Sigma/W includes six inbuilt constitutive models for soils as well as an option for inducing the user-defined constitutive model. For each of these models, the response will be different depending on the type of stress characteristics assigned to the model, namely whether it is assigned with total stress, effective stress with no pressure change, or effective stress with pore-water pressure change. The in-built models available are (a) Linear elastic model (b) Anisotropic elastic model (c) Hyperbolic model (d) Elastic Plastic model (e) Cam Clay model, and (f) Modified Cam Clay model. For the present study, the elastic-plastic model is utilized. The Elastic-Plastic model in Sigma/W describes an elastic-perfectly plastic relationship. The elastic-perfectly plastic Mohr-Coulomb (M-C) model necessitates 5 input parameters, specifically the strength parameters (cohesion c, angle of internal friction φ and dilatancy angle ψ) and the stiffness parameters (Elastic modulus E and Poisson's ratio v). A typical stress-strain curve for this model is shown in Fig. 3.6.

The generated stress is directly proportional to the corresponding strain, until the yield point is reached. Beyond the yield point, the stress-strain curve is perfectly horizontal, indicating substantial increase in strain without change in stress. In Sigma/W, soil plasticity is formulated using the theory of incremental plasticity (Hill, 1950). Sigma/W uses the Mohr-Coulomb yield criterion as the yield function for the Elastic-Plastic model. The following equation provides a common form of the Mohr-Coulomb criterion expressed in terms of principal stresses.

$$F = \sqrt{J_2}\sin\left(\theta+\frac{\pi}{3}\right)-\sqrt{\frac{J_2}{3}}\cos\left(\theta+\frac{\pi}{3}\right)\sin\phi-\frac{I_1}{3}\sin\phi-c\cos\phi \qquad (3.19)$$

The Mohr-Coulomb criterion can also be written in terms of the stress invariants I_1, I_2 and θ. The yield function, F, can then be written as follows (Chen and Zhang, 1991).

$$F = \sqrt{J_2}\sin\left(\theta+\frac{\pi}{3}\right)-\sqrt{\frac{J_2}{3}}\cos\left(\theta+\frac{\pi}{3}\right)\sin\phi-\frac{I_1}{3}\sin\phi-c\cos\phi \qquad (3.20)$$

where,

$J_2 = \frac{1}{6}\left[\left(\sigma_x-\sigma_y\right)^2+\left(\sigma_y-\sigma_z\right)^2+\left(\sigma_z-\sigma_x\right)^2\right]+\lambda_{xy}^2$ = the second deviatoric stress invariant,

$\theta = \frac{1}{3}\cos^{-1}\left(\frac{3\sqrt{3}}{2}\frac{J_3}{J_2^{3/2}}\right)$ = the load angle,

$J_3 = \sigma_x^d\sigma_y^d\sigma_z^d-\sigma_z^d\lambda_{xy}^2$ = the third deviatoric stress invariant,

$I_1 = \sigma_x+\sigma_y+\sigma_z$ = the first deviatoric stress invariant,

φ is the angle of internal friction, and c is the cohesion of the soil.

The deviatoric stress σ_i^d in the i[th]-direction can be defined as:

$$\sigma_i^d = \sigma_i - \frac{I_1}{3} \tag{3.21}$$

where, I = x, y or z.

When the angle of internal friction, φ, is equal to zero, the Mohr-Coulomb yield criterion becomes the Tresca criterion (Smith and Griffiths, 1988):

$$F = \sqrt{J_2}\sin\left(\theta + \frac{\pi}{3}\right) - c \tag{3.22}$$

The plastic potential function, G, used in Sigma/W has the same form as the yield function, F (i.e., $G = F$) except the internal friction angle, φ, is replaced by the dilation angle, ψ. Thus, the potential function is given by:

$$F = \sqrt{J_2}\sin\left(\theta + \frac{\pi}{3}\right) - \sqrt{\frac{J_2}{3}}\cos\left(\theta + \frac{\pi}{3}\right)\sin\phi - \frac{I_1}{3}\sin\phi - c\cos\phi \tag{3.23}$$

The derivatives of the yield function in terms of the stress invariants are computed using the chain rule of differentiation.

$$\left\langle \frac{dF}{d\sigma} \right\rangle = \frac{dF}{dI_1}\left\langle \frac{dI_1}{d\sigma} \right\rangle + \frac{dF}{dJ_2}\left\langle \frac{dJ_2}{d\sigma} \right\rangle + \frac{dF}{d\theta}\left\langle \frac{d\theta}{d\sigma} \right\rangle \tag{3.24}$$

Derivatives of the Mohr-Coulomb yield function, with respect to the stress invariants, can be written as follows:

$$\frac{dF}{dI_1} = -\frac{\sin\varphi}{3}$$

$$\frac{dF}{dJ_2} = \frac{1}{2\sqrt{J_2}}\left\{\sin\left(\theta + \frac{\pi}{3}\right) + \frac{1}{\sqrt{3}}\sin\varphi\cos\left(\theta + \frac{\pi}{3}\right)\right\} \tag{3.25}$$

$$\frac{dF}{d\theta} = \sqrt{J_2}\cos\left(\theta + \frac{\pi}{3}\right) + \sqrt{\frac{J_2}{3}}\sin\varphi\sin\left(\theta + \frac{\pi}{3}\right)$$

The derivatives of the stress invariants with respect to the stresses are:

$$\left\langle \frac{dI_1}{d\sigma} \right\rangle = \langle 1110 \rangle$$

$$\left\langle \frac{dJ_2}{d\sigma} \right\rangle = \left\langle \sigma_x^d \sigma_y^d \sigma_z^d 2\lambda_{xy} \right\rangle$$

$$\left\langle \frac{d\theta}{d\sigma} \right\rangle = \frac{\sqrt{3}}{2J_2 \sin 3\theta}\left(\left\langle \frac{dJ_3}{d\sigma} \right\rangle - \frac{3J_3}{2J_2}\left\langle \frac{dJ_2}{d\sigma} \right\rangle \right) \tag{3.26}$$

$$\left\langle \frac{dJ_3}{d\sigma} \right\rangle = \left\langle \sigma_y^d \sigma_z^d + \frac{J_2}{3}\sigma_x^d \sigma_z^d + \frac{J_2}{3}\sigma_x^d \sigma_y^d + \frac{J_2}{3} - \lambda_{xy}^2 \right\rangle$$

Similarly, the derivatives of the potential function can be obtained by substituting ψ for φ in Eqn. 3.25.

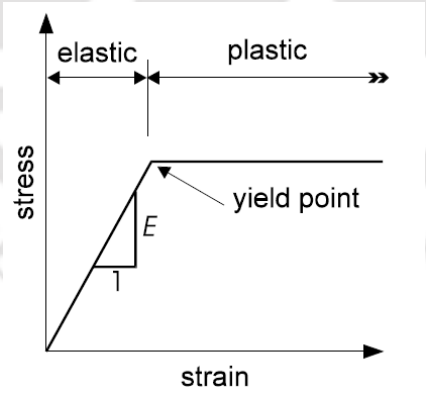

Fig. 3.6 Elastic-perfectly plastic constitutive relationship (adopted from Sigma/W Manual, 2018)

3.4.3. Material Models in Quake/W Analysis

Quake/W provides three different material models namely (a) linear elastic model, (b) equivalent linear model and (c) nonlinear model. In the present study, nonlinear material model is utilized which can be defined using unit weight (γ), Poisson's ratio (v), shear strength parameters (c and φ), damping ratio (ξ) as a constant or a function, pore-water pressure function, recoverable modulus function, maximum shear modulus (G_{max}) as a constant or a function, steady state strength and collapse surface angle (for liquefied zones).

3.4.4. Material Models in *Rslope2d*

The FE based algorithm for slope stability analysis in *Rslope2d* utilises an elastic-perfectly plastic stress-strain law with a Mohr-Coulomb failure criterion for plain strain conditions. The computer model (*Rslope2d*) used in present study uses cohesion (c), friction angle (φ), dilation angle (ψ), Young's Modulus (Es), Poisson's ratio (υ), and unit weight (γ) of soil as input parameters to conduct the elastoplastic FE slope stability analysis.

3.5. BOUNDARY CONDITIONS

This section presents the various types of boundary conditions that can be applied in GeoStudio and *Rslope2d* analyses. There are many ways to apply forces and displacements to soil and structural elements in order to replicate real world loading conditions. The boundary conditions are, in essence, the driving force in any numerical analysis, and applying them correctly on the boundaries of a problem is one of the key components of a numerical analysis. The solutions to the numerical problems are considered as a direct response to the applied boundary conditions. The determination of the correct boundary conditions might sometimes demand an iterative process, since the boundary conditions themselves are a part of the solution. Furthermore, during

a transient analysis, boundary conditions may change with time, which can substantially add to the numerical complexity. Due to the extreme importance of boundary conditions, it is essential to have a thorough understanding of this aspect of numerical modeling to obtain meaningful results. Most importantly, it is essential to have a clear understanding of the physical significance of the various types of boundary condition. This section discusses the various types of boundary conditions that are used in Sigma/W and Quake/W simulations for the present study. In GeoStudio, all the boundary conditions must be applied directly on geometry items such as region faces, region lines, free lines or free points. There is no way to apply a boundary condition directly on an element edge or node. The advantage of connecting the boundary condition with the geometry is that they become independent of the mesh and the mesh can be changed without losing the specified boundary conditions.

3.5.1. Boundary Conditions in Slope/W Modeling

As Slope/W is intended to operate on the limit equilibrium analysis to identify potential failure mechanisms through force and moment equilibrium, deformation or displacement is not involved in such analysis. Hence, through an in-built mechanism, the standard displacement boundary conditions are already imposed in the Slope/W simulation models during their creation and need not to be defined by the user. In Slope/W, the boundary conditions are also applied to the methods involved in the determination of the radius of the critical slip surface during the Limit Equilibrium (LE) based stability analysis. For defining the slip circles to be examined during the analysis, there are two different methods: (a) the Grid and Radius method, and (b) the Entry and Exit method. In the 'Entry and Exit' method in Slope/W, as shown by the demarcating red colored lines in Fig. 3.7, the number of entries and exits can be specified as the number of increments along these two

lines. This method is more popular in use amongst the two techniques, and is used in the present study.

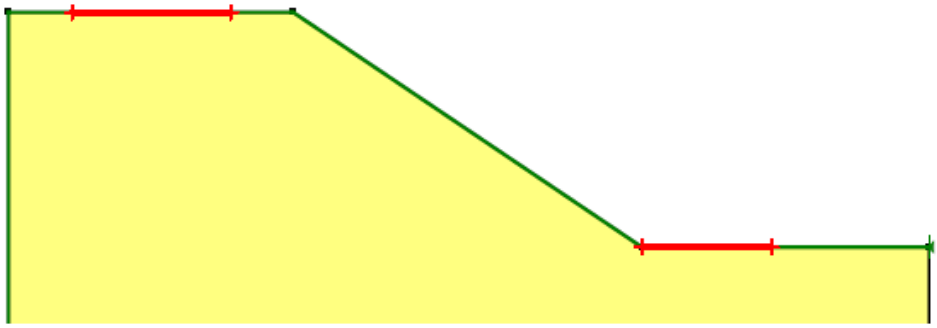

Fig. 3.7 The elements of 'Entry and Exit' method for bounding trial slip circles (adopted from Slope/W Manual, 2018)

3.5.2. Boundary Conditions in Sigma/W Modeling

In Sigma/W, multiple boundary condition types are implemented to support virtually all load-deformation modelling scenarios. Displacement, force or spring boundary conditions may be applied to points or nodes along geometry lines, while stress and fluid pressure boundary conditions may be applied to the element edges or lines. Fundamentally, there are only two types of boundary conditions that can be applied to a stress-deformation analysis; namely, 'stress' and 'force or displacement' type boundary conditions. In all stress-deformation models, it is critical to put a "bound" to the problem, which means that some parts of the geometry must be defined as 'zero displacement' boundary conditions. The base of the model is bounded in both directions, as there should not be any deformation along any direction at the base, whereas the far left and right edges are bounded in the Cartesian x-direction by specifying zero displacement. The X-Y stress boundary condition is utilized in the present study to simulate the excavation of slope toe in various stages. Figure 3.8 shows a typical representation of the boundary condition adopted for stress-

deformation analysis in Sigma/W for a toe-excavated reinforced slope with a sheet pile anchor retention system.

3.5.3. Boundary Conditions in Quake/W and *Rslope2d* Modeling

The boundary conditions utilised in Quake/W are primarily same as Sigma/W modelling. However, in Quake/W module, the base of the model is restrained from displacement in both the directions, and the far lateral boundaries are restrained from vertical displacement but are kept free from any horizontal restraint. In *Rslope2d*, fixed-base is assumed at the lower boundary and rollers are assumed at the two vertical boundaries.

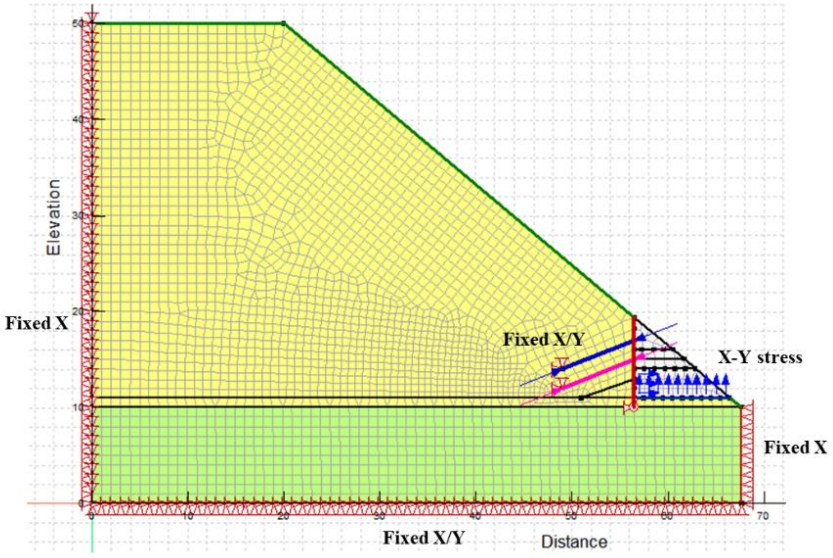

Fig. 3.8 Typical representation of the application of the boundary conditions in stress-deformation analysis of toe excavated reinforced slope with a sheet pile anchor retention system using Sigma/W

3.6. ANALYSES TYPES

The three different modules of GeoStudio is capable of solving different types of analyses and the choice of the analyses types would depend on the objective(s) of the modelling. The more common scenario is to define multiple analyses to investigate a single problem. This section gives a brief overview about the different analyses types present in the all the three modules (Slope/W, Sigma/W and Quake/W) and describes the ones which are used in the present study.

3.6.1. Available Analyses Types in Slope/W Modeling

The different types of analysis present in Slope/W are based on the General Limit Equilibrium theory (GLE) or the Finite Element (FE) computed stresses within a limit equilibrium framework, as described in Section 3.2.1. The different methods based on GLE that are available in Slope/W are (a) Ordinary or Fellenius method (b) Bishop's simplified method (c) Janbu's simplified method (d) Spencer's method (e) Morgenstern-Price method (f) Corps of Engineers method (g) Lowe-Karafiath method (h) Sarma's method, and (i) Janbu's Generalized method. In this study, the Morgenstern-Price method (the 'FE based stress' method) is used which is widely popular for the determination of the factor of safety values. The use of finite element computed stresses inside a limit equilibrium framework to assess stability has many advantages. Firstly, there is no requirement to make assumptions about the interslice forces as they evolve during the analysis itself. Secondly, the stability factor is deterministically determined once the stresses are computed, and consequently, there are no issues with convergence during iterations. Thirdly, the issue of displacement compatibility is completely satisfied, and the computed ground stresses are much closer to reality. Fourthly, the stress concentrations are indirectly considered in the stability analysis, and hence, the soil-structure interaction effects are readily handled. Finally, the dynamic stresses arising from earthquake shaking can be directly considered in the stability analysis. Thus,

FE computed stresses inside the LE framework finds more application while calculating the FoS through Slope/W modeling simulations.

3.6.2. Available Analyses Types in Sigma/W Modeling

The Sigma/W module provides a number of analyses types, namely 'in-situ analysis', 'load/deformation analysis', 'coupled stress/PWP analysis', 'stress redistribution analysis', 'volume change analysis' and 'dynamic deformation analysis'. For the present study, the in-situ and load/deformation analyses techniques are used.

3.6.2.1 *In-situ Analysis*

The initial stresses are established by applying the self-weight of soil by means of a body load. The specified unit weight when multiplied by the element volume creates a downward nodal force. The value of Poisson's ratio (for each material) will control the development of horizontal stresses. The stiffness properties (e.g. Young's Modulus) of the materials does not influence the initial stresses. The ratio of horizontal (σ'_h) to vertical effective stresses (σ'_v) in saturated soils, having a history of one-dimensional deformation (e.g. sedimentation and possibly over consolidation), is called the coefficient of earth pressure at rest, and is expressed as:

$$k_0 = \frac{\sigma'_h}{\sigma'_v} = \frac{\nu}{1-\nu} \tag{3.19}$$

For undrained scenarios, Sigma/W limits the value of Poisson's ratio (ν) to 0.495; therefore, k_0 is limited to approximately 0.98. Overconsolidated soils generally have k_0 values that exceed this value; i.e., the effective horizontal stresses exceed the vertical effective stresses. The initial stress states with $k_0 > 0.98$ cannot be established using the 'In-situ' type of analysis. The well-established 'k_0 through gravity loading' technique is used for handling such type of problem.

3.6.2.2 *Load / Deformation Analysis*

The Load/Deformation analysis is used for those problems wherein the resulting changes in stress and displacements are evaluated owing to the applied loads. Some of these problems include placement of fill and excavation or construction procedures. In the case of a fill placement analysis, the weight of the fill is added to the model on the first load step, and the resulting deformation is determined. In the case of an excavation analysis, Sigma/W calculates the resultant forces associated with the removal of the excavated elements and applies these forces as boundary loads at the nodes along the face of the excavation.

3.6.3. Available Analyses Types in Quake/W Modeling

There are basically three types of analyses available in Quake/W, namely (a) Initial Static, (b) Equivalent Linear Dynamic and (c) Nonlinear Dynamic. The present study uses the Nonlinear Dynamic analysis type for assessment of seismic response of slope. When subjected to dynamic conditions, the soil mass undergoes cycles of loading-unloading-reloading sequences, thereby resulting in a series of stress and strain reversals, which are represented by hysteresis loops. Each of the hysteresis loop, representing a complete cycle of loading-unloading-reloading, is characterized by two peak points of stress reversals, as shown in Fig. 3.9a. The initial slope of the shear stress-shear strain cycle is represented as maximum shear modulus (G_{max}), while the slope of the line joining the point of origin (i.e. the beginning of cyclic loading) and the point of stress reversal (whether in positive or negative quadrants) represent the secant shear modulus (G_{sec}). Several such cycles or successive hysteresis loops can be plotted together, and the smooth curve joining the peak points (i.e. the points of stress reversals) of the consecutive cycles is referred as

the ‘backbone curve’ or the ‘skeleton curve’, as shown in Fig. 3.9b. Any line joining the origin to a point in the backbone curve at a particular shear strain represents the secant shear stiffness that would be expected in the soil mass at that corresponding shear strain (Fig. 3.9c). It can be noted from Fig. 3.9b that with the increasing numbers of cycles, the secant shear modulus continuously decreases, thereby representing the shear softening or the stiffness degradation of the soil mass upon successive cycles of loading and unloading. This manifestation is represented through a ‘modulus degradation curve’, expressed as the variation of the ratio G_{sec}/G_{max} over the shear strain (Fig. 3.9d). This curve serves to be one of the most important dynamic property of soil controlling the behaviour of the soils subjected to dynamic or cyclic loading. Based on a known backbone curve, it is possible to regenerate the hysteresis loops for a soil sample subjected to cyclic loading. Such regeneration is governed by Masing or Non-Masing rules, the details of which are available in standard literature (Kramer, 1996).

In a dynamic analysis, it is essential to travel through the entire earthquake time history in very small steps due to very sudden changes in motion. Earthquake shaking often only lasts for a matter of seconds; thus, to capture all the characteristics of the motion, the time steps must be fractions of a second. A typical value is two hundredths (0.02) of a second. This consequently results in a large number of time steps. For example, for an acceleration time history of duration 10 seconds, a total of 500-time steps is required if the time steps are to be in increments of 0.02 seconds. This is the reason that a Quake/W analysis is so computationally intensive. The non-linear scheme in Quake/W goes through the entire earthquake record only once but uses several iterations at each time step to achieve a converged solution. With the non-linear soil model, G_{tan} is obtained from the slope of the hyperbolic stress-strain curve. As the strain increases, the slope of the hyperbolic

curve decreases which means that the soil stiffness modulus decreases. The modulus reduction indirectly is inherent in the shape of the hyperbolic stress-strain curve.

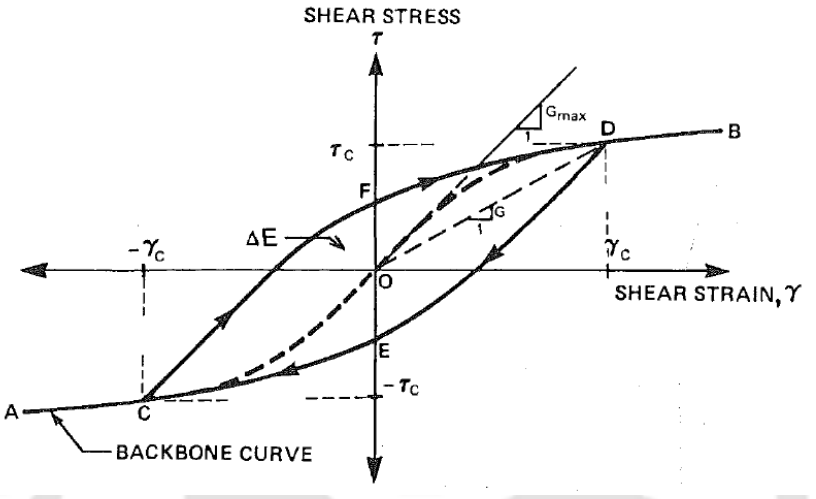

(a)

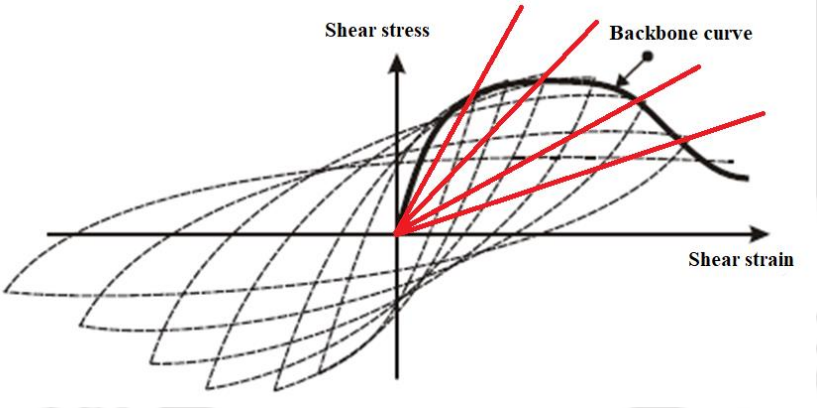

(b)

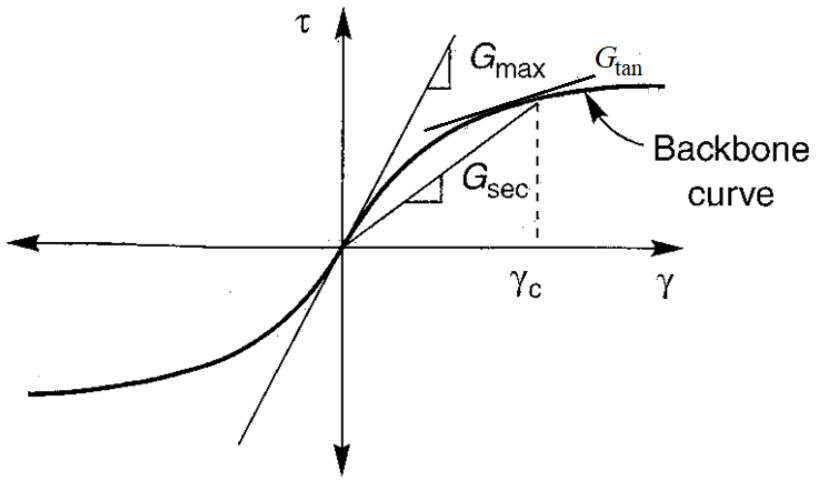

(c)

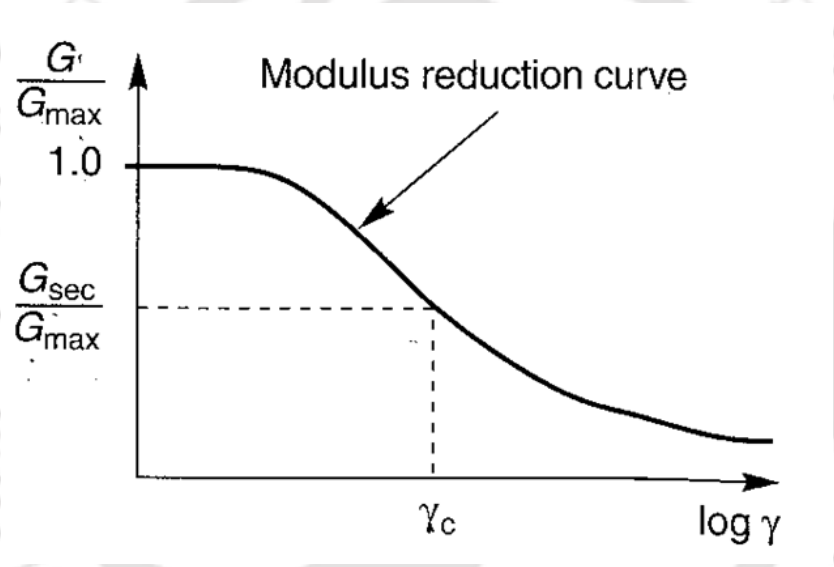

(d)

Fig. 3.9 (a) Typical hysteresis loop generated during cyclic loading of soil (b) Typical development of backbone curve from hysteresis loops (c) Typical representations of maximum and secant shear moduli (d) Typical representation of the modulus reduction curve

3.6.4. Analysis Type in *Rslope2d* based RFEM analysis

The FE based algorithm in *Rslope2d* estimates a deterministic FoS using the strength reduction method (Matsui and Sun, 1992), which is based on the mean values of the shear strength parameters. The strength reduction method is based on the concept that the FoS of a structure is

that factor by which the original shear strength parameters must be divided to bring the slope to the point of failure. The shear strength parameters at the point of failure, c_f and φ_f, are given by:

$$c_f = \frac{c}{FoS} \tag{3.20}$$

$$\phi_f = \arctan\left(\frac{\tan\varphi}{FoS}\right) \tag{3.21}$$

This definition of FoS is the same as used in the LEMs, and is expressed as the ratio of shear strength of soil to shear stress required for equilibrium (Duncan 1996). The validation studies by Griffiths and Lane (1999) indicated good agreement between the FoS estimated by the FEM and those computed from the stability charts developed by Taylor (1937) or Bishop and Morgenstern (1960).

In FE analysis using *Rslope2d*, non-convergence of the algorithm within a specified number of iterations is used as a criterion of the failure of the slope. In this algorithm, when the stress distribution cannot be found anymore that simultaneously satisfies both the Mohr-Coulomb failure criteria and global equilibrium, the slope is considered to have failed (Griffiths and Lane, 1999). This is usually accompanied by a significant increase in the nodal displacements within the mesh. Griffiths and Fenton (2004) reported that in a case study, for a 2:1 undrained clay slope, an iteration limit of 500 is sufficient to assure the convergence of solutions.

The probability of failure is estimated using MCS. The precision of the computed probability of failure (P_f) has a high dependency on the number of MCS conducted. The precision increases with an increase in the numbers of simulations. However, to generate a reliable and consistent result, it is essential to estimate the minimum number of simulations. It is due to the fact that repetitive FE

analysis is a cumbersome task and the computation of P_f generally converges within a certain number of simulations. Further increase in number of simulations does not refine the result greatly but will unfavourably increase the computational time and effort.

3.7. PROJECT AND ANALYSES TREE IN GEOSTUDIO

In GeoStudio v2018, multiple analyses can be included in a single project that allows different material properties and different boundary conditions to be specified and implemented across the model as well as spanned in time. This facilitates sequential modeling of staged construction or excavation in which the soil material over a geometrical location is added or removed over time and/or the boundary conditions, or the material properties could be changed with time. Including multiple analyses in a single project could be used for a variety of reasons such as: (a) conducting sensitivity analyses for variations in material properties and boundary conditions; (b) analyzing staged construction; (c) establishing initial conditions for a transient analysis; (d) integrating various GeoStudio analyses modules; or, (e) linking together multiple transient analyses.

GeoStudio uses a 'Parent-Child' terminology to describe the relative position of each analysis within a project. Figure 3.10 displays a typical 'Analysis Tree' combining the in-situ and load deformation analyses (utilizing Sigma/W module), nonlinear dynamic analysis (utilizing Quake/W module), and the slope stability analysis (utilizing the Slope/W module) for simulation of toe excavated slope retained by sheet pile and anchor system.

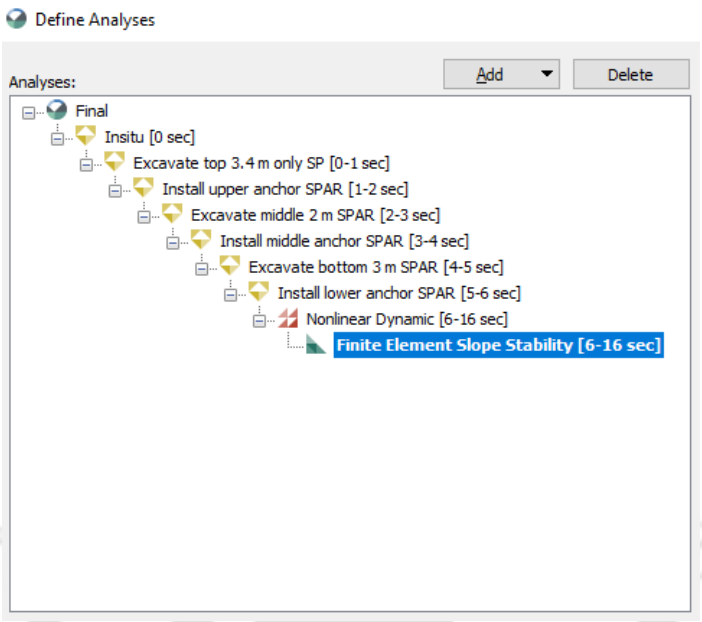

Fig. 3.10 A typical representation of an 'Analysis Tree' from a GeoStudio v2018 'Project'

The in-situ analysis in Sigma/W module is the 'Parent' that is used to define the initial stress conditions. Then, the load deformation analysis is conducted to simulate the upper layer of toe excavation considering in-situ Sigma/W analysis as 'Parent'. Hence, the 'load deformation' analysis within the Sigma/W analysis becomes the 'Child' carrying the information of the 'Parent'. In similar manner, the excavation and sheet pile anchor retention system are simulated in Sigma/W, consequently using the 'parent' and 'child' relation. Sigma/W generated stress is incorporated in Quake/W module to conduct a nonlinear dynamic analysis considering the last stage of Sigma/W analysis of anchor installation as 'parent'. Finally, a FE based slope stability analysis is carried out in the 'Project' by incorporating the Quake/W generated stress in Slope/W module as a 'child' analysis of the 'parent' Quake/W analysis. One significant benefit of the 'Analysis tree' is that all the analyses related to a specific project are contained within a single file, and are linked to each other. It would not be necessary to refer other files to establish initial conditions or integrate the various GeoStudio products.

3.8. SUMMARY

This chapter provides a background of the numerical modelling and methods adopted in the study of the dissertation work. The working principles of various important modules of GeoStudio software package, which are used in the present study (Slope/W, Sigma/W and Quake/W), and *Rslope2d* computer model are discussed. A brief discussion is also provided about the FE modelling and its intricacies related to geometry and domain definition, meshing and mesh characteristics, as well as boundary conditions. A description is provided related to various material models, along with their constitutive behaviour and input properties, which are used in the present study. Finally, a description is provided about the various types of analyses available, their solution strategies and their mathematical formulations. This chapter gives a detailed insight about the working principles of the softwares, and which is used for the rest of the study, as would be described in the subsequent chapters of the dissertation report.

CHAPTER 4

ESTIMATION OF THE VERTICAL SCALE OF FLUCTUATION OF SPATIALLY VARYING SPT DATA

4.1. GENERAL

Geotechnical variability originates from different sources of uncertainties, out of which the primary ones pertain to inherent soil variation, error in measurement and transformation model uncertainty. The inherent variation of soil properties results mainly from the natural geological phenomenon that continuously modify the in-situ or residual soil mass. The error in measurement is primarily due to operation, equipment and other testing effects. These first two sources together can be reported as 'data scatter' (Kulhawy, 1992). In-situ measurements are also affected by statistical uncertainty or sampling error resulting from the lack of information and are commonly included within the measurement error (Kulhawy, 1992). This type of uncertainty can be reduced by collecting more data. The next source of uncertainty is related to correlation models or empirical relations used to obtain design soil properties from in-situ or laboratory measurements. The relative contribution of these sources to the overall uncertainty in any of the design soil properties entirely depends on the site conditions, equipment used, operational error and the accuracy of the correlation model used. Therefore, soil property statistics, which are solely derived depending on a total variability analyses, is applicable only to the specific set of circumstances (site conditions, measurement methods, and correlation models) based on which the design soil properties are determined (Phoon and Kulhawy, 1999).

As mentioned in Chapter 2, to characterize inherent variation, second moment statistics (i.e., mean and standard deviation) are not enough, regardless of whether the measurement has been conducted in the laboratory (controlled tests) or in the field (ambience-guided tests). Two sets of measurements having similar second moment statistics and statistical distributions may have noticeable differences in their spatial distribution. Assessment of inherent spatial variation of soil properties from in-situ or laboratory data by statistical stochastic process has attracted a lot of researcher attention for last three decades. Among the various techniques of subsurface investigations, Standard penetration test (SPT) and Cone penetration test (CPT) are the most appreciated in-situ tests in geotechnical engineering for the characterisation of inherent soil variability. Several researchers have modelled the inherent soil variation using the SPT and CPT data (Alonso and Krizek, 1975; Tang, 1979; Nadim, 1986; Campanella et al., 1987; Wu et al., 1987; Reyna and Chameau, 1991; Kulhawy et al., 1992; Fenton, 1999; Phoon et al., 2003; Elkateb et al., 2003; Uzielli et al., 2005; RaghuKanth and Dash, 2008). Nadim (1986) has provided a method to characterize the inherent geotechnical variability and anisotropy using random field theory. Fenton (1999) developed one-dimensional stochastic soil model to characterize CPT data at the New Airport site, north of Oslo, Norway. Uzielli et al. (2005) developed a finite-scale weakly stationary random field model to characterize normalized cone tip resistance and friction ratio (FR). Raghukanth and Dash (2008) proposed a stochastic model for spatial variation in SPT data for assessment of liquefaction probability in Guwahati City, India. Stuedlein et al. (2012) applied random field modelling to characterize Beaumont clay at a field test site near Houston, Texas. Recently, Bayes' theorem is being applied to determine the most probable correlation function of the spatial data by weighting of their posterior probabilities (Cao and Wang, 2013, 2014; Wang et al., 2010b, 2013, 2014, 2015, 2016a).

In this chapter, to characterise inherent spatial variation of soil, vertical scale of fluctuation (SoF) is estimated for Standard Penetration Test (SPT)-*N* dataset obtained during the geotechnical site investigation conducted before construction of the GNRC multispecialty hospital in Amingaon, North Guwahati (26.2026° N, 91.6935° E), Assam, India. In this regard, the successive procedures involving decomposing and detrending of the collected data to obtain stationary residuals, and the subsequent development of one-dimensional random field model for the residuals has been attempted and the mean SoF is reported for all the borehole data. The mean SoF so estimated, depending on a particular in-situ test dataset, is not recommended for direct application to other geotechnical sites and properties without proper engineering judgement. However, data reported in the present work can be used as preliminary indication of the correlation distance. This approach would enable the sample spacing and correlation model to be chosen for a future geotechnical site investigation or any simulation-based geotechnical reliability analysis, where no a-priori knowledge of the spatial variation of the site is available.

4.2. INHERENT SPATIAL VARIABILITY IN SOIL AND RANDOM FIELD

Soils are complex engineering material that varies spatially owing to their way of formation and the continuous processes of environment that alter them. Because of these natural phenomena, in-situ soils properties vary along both vertical and horizontal directions, thus leading to spatial variability. In an idealistic situation where the soil properties could be known at every possible locations of a site, there would be no reason of modelling soil property as random field. However, in reality, due to limited data and finite analytical capacity, considering the variation in soil properties as random is often a convenient hypothesis. Therefore, it is necessary to model the inherent spatial variability of soil properties with the aid of random fields (Uzielli et al., 2005;

Stuedlein et al., 2012). Priestley (1981) explained the statistical techniques used for spatial variability investigation and provided a comprehensive insight into the time series analysis. Baecher and Christian (2003) discussed the applications of such statistical techniques in geotechnical engineering.

The variation of soil properties can be precisely described by three parameters: mean, coefficient of variation (CoV) and the scale of fluctuation (SoF), as mentioned in Chapter 2. Since the advent of the concept of correlation and scale of fluctuation by Vanmarcke (1977), different methods have been developed by researchers for the assessment of the correlation structure of geotechnical data. The scale of fluctuation (SoF) or 'correlation length' is a concise indicator of the spatial extent within which a soil property has a high correlation. Various techniques are available in the literature to estimate SoF. Vanmarcke's expeditive method (Vanmarcke, 1977), direct integration of sample autocorrelation function (Vanmarcke, 1983), autocorrelation model fitting (Spry et al., 1988), variance reduction function (Cafaro and Cherubini, 2002) and Bartlett's limit methods (Jaksa, 1995) are the suggested methods in literature, although there is no bias to any of the specific methods.

As shown in Fig. 4.1, any geotechnical property [$\xi(z)$] can be disintegrated into a trend function [$t(z)$] and a set of fluctuating residuals around the mean [$w(z)$] by a decomposition technique. In one-dimensional case, the decomposition can be expressed, as shown in Eq. 4.1, considering the depth (z) as the single spatial coordinate (Phoon and Kulhawy, 1999; Degroot and Baecher, 1993).

$$\xi(z) = t(z) + w(z) \tag{4.1}$$

The fluctuating component in Eq. 4.1 corresponds to the inherent variation in soil properties and does not consider the measurement error. This can be explained by the assumption that the aleatory uncertainty due to inherent variation in soil properties and the epistemic uncertainty resulting from error in measurement are not correlated and should be encountered individually (Uzielli et al., 2006). A conventional technique to quantify inherent variation in soil properties is to model the fluctuating residual part as a random field (Vanmarcke, 1983). For random field modelling of soil properties, stationarity is a prerequisite, as the principle forms the basis of the applied statistical methods. In case of strictly stationary dataset, all the statistical properties (e.g., mean, variance, skewness, kurtosis, etc.) are invariant to translation. Strict stationarity is mostly of conceptual importance and a severe requirement. Practically, it is convenient to relax the restraint of strict stationarity and refer to weak stationarity. In geotechnical engineering, due to limited sample size of soil properties estimated from laboratory or in-situ tests, only weak stationarity may be identified. A weakly stationary random field, which can be described using first two moments i.e. mean and variance, calls for the following: (a) its mean is spatially invariant (i.e., there exists no trend in the data), (b) its variance is constant in space, and (c) the correlation is a function of only the spatial distance, i.e., the correlation between any two data, at any two locations, depends only on their separation distance, and not on the absolute locations of the points.

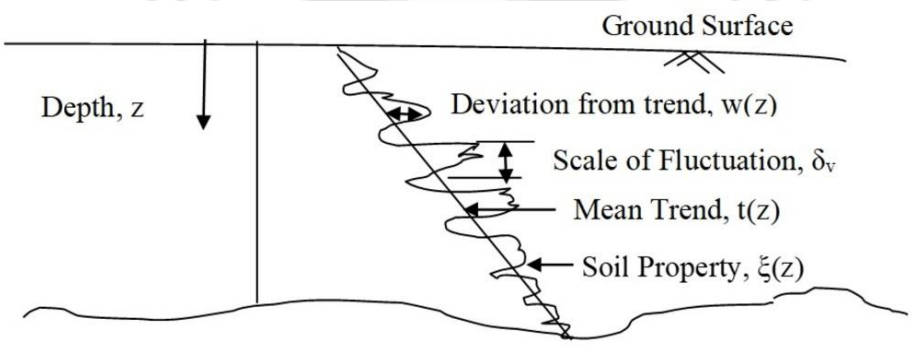

Fig. 4.1 A typical representation of the inherent variability of soil property

4.3. ONE-DIMENSIONAL RANDOM FIELD MODELLING OF FIELD SPT-*N* VALUES

In the standard penetration test, a standard split spoon sampler is driven into the soil by dropping a standard impact hammer of weight 0.63 kN from a standard height of 0.75 m. Neglecting the blows required to generate a seating penetration of 0.15 m, the number of blows (*N*) required to achieve the subsequent standard penetration of 0.3 m is measured (IS 2131: 2002). A soil having low shear strength gives less penetration value, while, for a soil having relatively higher shear strength, the penetration value would also be relatively higher. It is noticed that SPT values are substantially erratic in nature. The spatial variability in SPT data can be attributed to the inherent soil variability or measurement errors due to an imprecise equipment condition. Moreover, SPT-*N* values are non-stationary, i.e., there is a general increasing trend in the data with increasing depth. Hence, spatial variation in SPT values should be modelled as random field. In this chapter, spatial variation in SPT-*N* value is modelled as a one-dimensional random field. Figure 4.2 shows the location of the study area, in which focus has been given to the extensive SPT conducted at the Gauhati Neurological Research Centre (GNRC) campus, a super-speciality hospital located at North Guwahati, India. Fourteen numbers of 150 mm diameter boreholes were drilled in the proposed campus area, and the work was commissioned and completed in January 2011. Shell Auger and Wash boring was adopted in the site, and the SPT values (*N*-values) were recorded at a vertical interval of 1.5 m, mostly up to a depth of 20 m. The soil obtained was mostly clayey and silty sand, brownish in colour. The ground water table was mostly obtained at 2.0-2.5 m below the existing ground level. Undisturbed samples were collected at every 1.5 m interval, and were subjected to standard laboratory tests to ascertain their particle size distribution, unconfined compression strength, and their shear strength properties (cohesion and friction angle). Based on the laboratory tests conducted, the unconfined compression strength was found to lie between 0.41

to 3.69 kg/cm^2. The cohesion and angle of internal friction were found to lie between 0.09 to 1.84 kg/cm^2 and 5° to 40°, respectively. Further details about the geotechnical investigation are provided in the Appendix-I.

(a) **(b)**

Fig. 4.2 (a) Location of the study area at GNRC Hospital, North Guwahati, Assam (b) Borehole locations in study area

Figure 4.3 shows the SPT-*N* value profiles obtained from the 14 boreholes at the stated study location. It can be noted that there is an increasing trend in SPT data with depth in all the borehole data (Fig. 4.3), except BH 7. In BH 7, no significant increasing mean trend is observed. This spatial variation in *N*-value can be decomposed into a deterministic part (increasing mean trend) and an oscillating component (residuals after detrending). The deterministic part of the data is estimated by linear regression analysis. The fluctuating component (residual part) is modelled as a one-dimensional random field by a correlation function. It is worth mentioning that the determined inherent variability in soil properties is a representation of the variability of the mechanical resistance of the soil offered during the execution of field SPT. It also must be emphasized that soil property is modelled as random field to compensate the lack of data availability to simulate the soil domain perfectly, not always the soil property being actually random in nature.

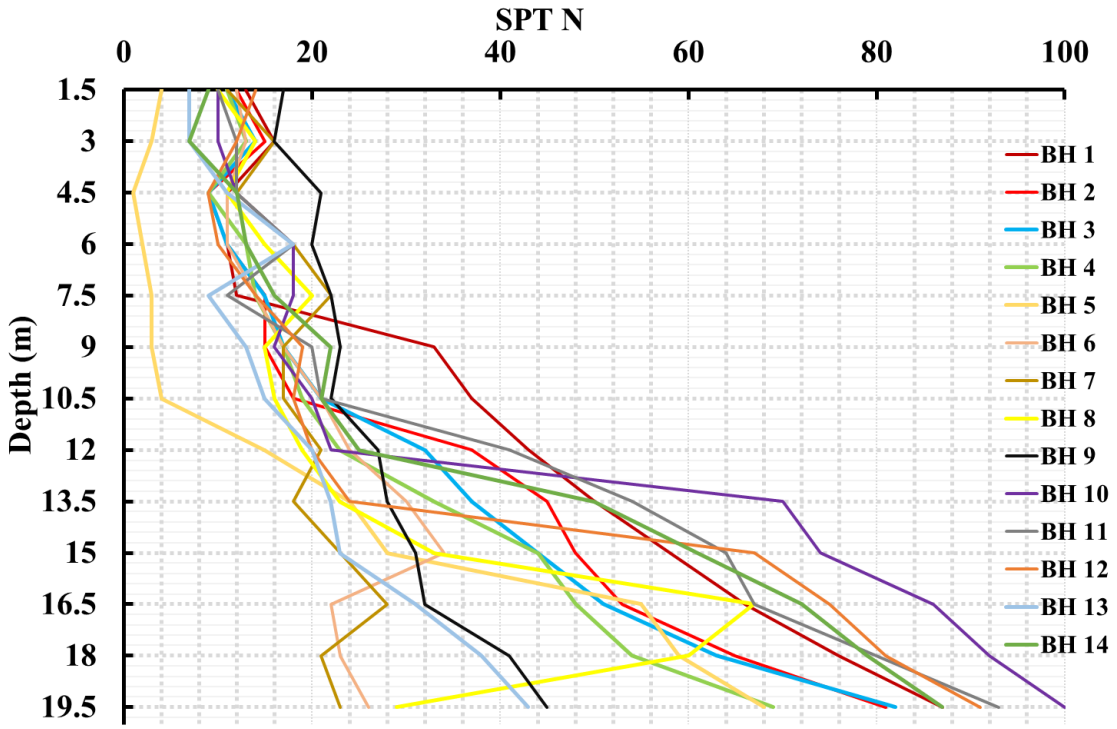

Fig. 4.3 SPT-*N* profiles from 14 boreholes at the study location

4.3.1. Decomposition and Detrending of Data

Figures 4.3 shows that the variation of *N*-value data with depth has a highly irregular increasing trend. At all the borehole locations, this non-stationarity in data is observed (except BH 7, where no significant mean trend is noticed). However, statistical modelling of spatial variation largely depends on the assumption of stationary data. All classical statistical methods for random field modelling are based on the assumption of data stationarity. Hence, data transformation is imperative. Data transformation, in general, refers to a number of methods (mainly from time series analysis), with the aim of producing a stationary dataset from a non-stationary dataset. Data transformation can be done by trend removal, differencing and variance transformation (Jaksa, 1995). Trend removal by decomposition of data is most commonly used to achieve stationary

dataset in geotechnical engineering (Fenton, 1999). A review of the other two transformation techniques is provided by Jaksa (2006). For detrending the data, the measured *N*-values are decomposed as the summation of deterministic mean trend (N_{avg}) and residuals (w) with respect to depth (z), and is expressed as:

$$N(z) = N_{avg}(z) + w(z) \tag{4.2}$$

Data transformation by decomposition technique is arbitrary to some extent, as the trend removal to produce necessary stationary dataset is established by the user. Moreover, there is no unambiguously accurate trend to be selected, rather a best suitable one is chosen. However, the trend chosen must rely on geotechnical expertise and, most importantly, should be capable of producing a stationary dataset for further statistical analysis of soil variability. Literature suggests removing the spatial trend in data using a low order polynomial function, no higher than a quadratic function (Cafaro and Cherubini, 2002). Several researchers have utilized trend removal by least-squares regression in the geotechnical literature (Phoon et al., 2003; Jaksa, 1995). Baecher and Christian (2003) suggested the trend to be selected as simple as possible without doing injustice to dataset or ignoring geologic setting. In this study as well, the spatial trend is modelled by linear least squares regression analysis for all the 14-borehole profile. For illustration purpose, three typical borehole profiles (BH 1, BH 2, BH 6) are taken in consideration. Figure 4.4 shows the trend removal in the three typical borehole profiles (BH 1, BH 2, BH 6). It is observed that a single trend function cannot be fitted for borehole profile BH 1, as a change in stratification at a depth of 11 m is encountered. Up to 11 m of depth brownish grey clay with some trace of silt is observed, beyond this depth presence of sand increased the SPT-*N* value. Hence, two separate trend function is fitted in this case. A quadratic function is found to be best fitted for initial part of BH 1, whereas, the tail

part is best fitted with a linear trend function as shown in Fig. 4.4a. No significant improvement in the regression is noticed by characterizing the tail part as quadratic function, hence for simplicity linear function is chosen. On the other hand, it is seen that the mean trend in BH 2 can be characterized using a single trend function, which comes out to be quadratic in this case. However, in BH 6, it is observed that two separate trend functions are required to characterize the mean trend. In BH 6, both the parts are best fitted with quadratic function. BH 7 shows no increasing mean trend in data (Fig. 4.3), hence the residuals can be simply estimated by removing the constant mean from the data. All the best fitted mean trend functions for 14-borehole profiles are listed in Table 4.1.

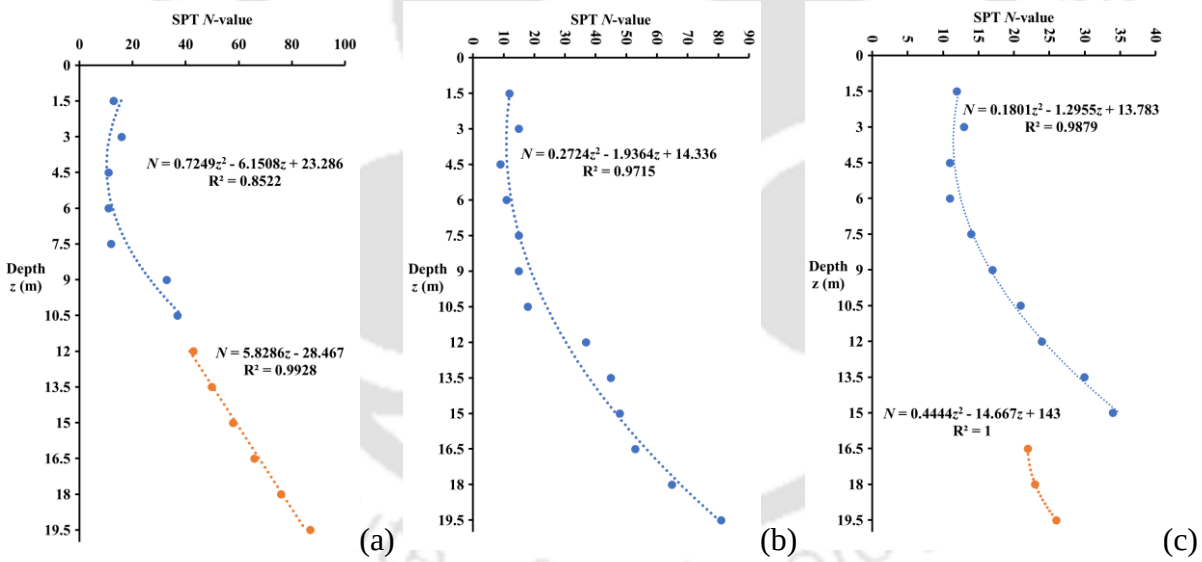

Fig. 4.4 Typical detrending of SPT-*N* data for (a) BH1 (b) BH2 (c) BH6

As mentioned earlier, the significance of decomposition of field data into deterministic and fluctuating component has been recognized by several researchers. However, it has been pointed out that inappropriate trend removal from a field measurement profile may result in biased

estimation of correlation. The set of residuals that are used for assessment of correlation structure and other statistical parameters describing the random field solely depends on the model used for trend removal. For illustration purpose, the spatial variation of residuals with depth after detrending the data for BH 2 is shown in Fig. 4.5. Alonso and Krizek (1975) recommended inspecting the dataset visually to identify the any existing trend. For the present dataset, the visual examination of the residuals after detrending shows no appreciable spatial trend (well distributed around the mean value). Therefore, the residual dataset is considered to be stationary.

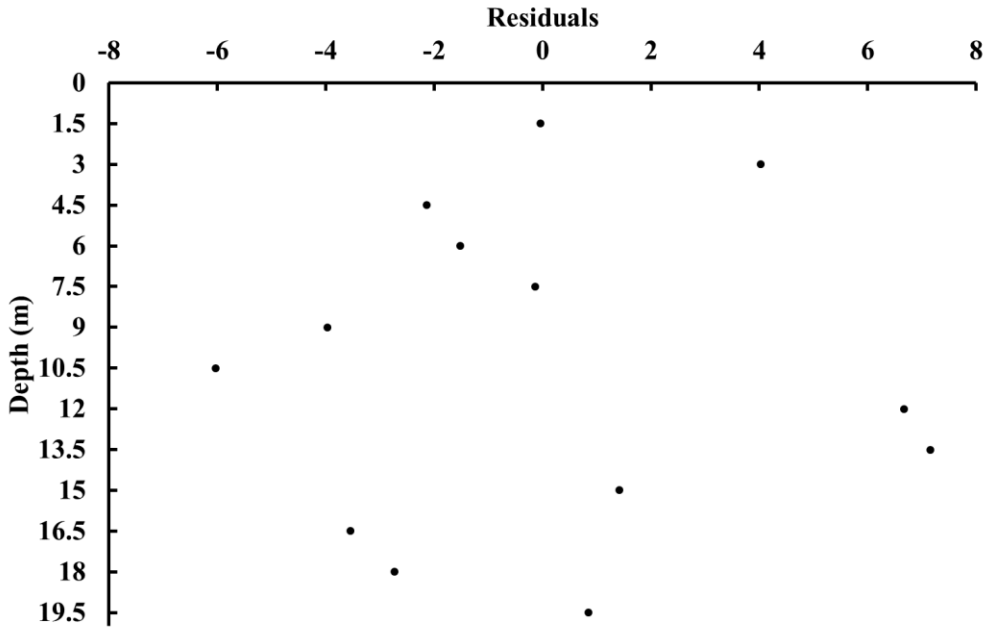

Fig. 4.5 Variation of residuals (N-N_{avg}) with depth after detrending for BH 2

Table 4.1 Detrending function for 14-borehole profiles

BH No.	Depth (m)	Detrending Function	Coefficient of Regression, R^2
1	0-10.5	$y = 0.7249x^2 - 6.1508x + 23.286$	0.8522
	10.5-19.5	$y = 5.8286x - 28.467$	0.9928
2	0-19.5	$y = 0.2724x^2 - 1.9364x + 14.336$	0.9715
3	0-19.5	$y = 0.2857x^2 - 2.348x + 15.462$	0.9896
4	0-19.5	$y = 0.2375x^2 - 1.8894x + 14.399$	0.9877
5	0-19.5	$y = 0.3699x^2 - 4.0453x + 10.664$	0.9731
6	0-15	$y = 0.1801x^2 - 1.2955x + 13.783$	0.9879
	15-19.5	$y = 0.4444x^2 - 14.667x + 143$	1
7	0-19.5	No detrending function	----
8	0-19.5	$y = 0.1162x^2 - 0.6722x + 13.083$	0.8
9	0-19.5	$y = 0.0852x^2 - 0.3763x + 18.406$	0.9582
10	0-12	$y = 1.1587x + 7.9286$	0.8602
	12-19.5	$y = 5.2x - 1.4$	0.9826
11	0-19.5	$y = 0.2862x^2 - 1.2364x + 11.112$	0.9728
12	0-13.5	$y = 0.1438x^2 - 1.1462x + 13.905$	0.8504
	13.5-19.5	$y = 5.2x - 11.2$	0.9909
13	0-19.5	$y = 0.1166x^2 - 0.6197x + 9.7552$	0.9386
14	0-19.5	$y = 0.2866x^2 - 1.319x + 9.6853$	0.9701

4.3.2. Random Field Model for Residuals

The residual of decomposition of any geotechnical property is the segment of spatial variation that is not possible to express by a simple function with respect to a reference spatial coordinate. The residual '*w*' is generated by subtracting the N_{avg} value (Eq. 4.2) from the recorded SPT-*N* value. After detrending the data, the remaining part (i.e., *w*) is considered stationary. Residuals are generally a zero-mean set that fluctuates around the mean value with respect to the reference spatial

coordinate. The stationary residuals are modelled as a random field by an auto-correlation function described by the scale of fluctuation.

The autocorrelation function represents the variation of spatial correlation as a function of spatial separation length between two locations at which data are available. The autocorrelation function is most commonly used for investigation of spatial variation of soil properties in the context of geotechnical engineering. The popularly used approach is to estimate the sample autocorrelation function (ACF) and fit a probable theoretical autocorrelation model (ACM) to the estimated ACF. As there is no reliable physical resemblance between the type of soil and nature of correlation model, a numerical approach is acceptable (Uzielli et al., 2006). For a given dataset, the choice of the correlation structure can be made depending on the comparative assessment of goodness-of-fit of the empirical ACF of the dataset to one or more theoretical ACMs. This is achieved by optimization of the characteristic parameter of model for each ACM (e.g., by least-squares regression or any other optimization techniques) and the subsequent estimation of the goodness-of-fit parameter for each ACM. The ACM with the maximum fitness can be chosen as best-fit function. Knowing the correlation model, SoF can be easily evaluated from the model parameter of the ACM.

The sample ACF for the residual random field can be estimated as (Fenton and Griffiths, 2008):

$$\rho(\tau_j) = \frac{\sum_{i=1}^{n-j+1} (X_i - \mu_X)(X_{i+j-1} - \mu_X)}{\sum_{i=1}^{n} (X_i - \mu_X)^2} \qquad j = 1, 2, ..., n \tag{4.3}$$

where, $\tau_j = (j-1)\Delta z$ is the lag distance, n is the total number of data in set, Δz is the sampling interval and μ_X is the average of the sample and is estimated as

$$\mu_X = \frac{1}{n}\sum_{i=1}^{n} X_i \tag{4.4}$$

Several theoretical 1-D ACMs are available in the literature. Table 4.2 lists four such correlation models commonly used in geotechnical engineering, namely the Single exponential, Squared exponential, Second-order Markov and Cosine exponential ACMs. The sample auto-correlation function is first estimated for all the borehole profiles and then fitted to the theoretical ACMs. The unknown parameters of the ACMs are estimated from the normalized residuals by minimizing the mean square error between the computed ACF and the theoretical ACM. To illustrate the procedure, Fig. 4.6 shows the autocorrelation function estimated for the BH 2 and the corresponding fitted ACMs. The auto-correlation value is equal to 1.0 (its maximum value) at zero correlation distance, which tends to zero with the increase in separation distance, and can take intermediate negative values. It is well known from the literature that at higher lag distances, the sample auto-correlation function computed from the data becomes noisy (Uzielli et al., 2006). At large lags, there is practically no correlation between two random quantities under consideration. The presence of such correlations coefficients at large lags obscures the interpretation about the actual decay of correlation function with spatial distance, and hence, considered as noise. Thus, correlation coefficients at large lags are ignored, and only the initial part of the correlation function (defined by the correlation function within the spatial lags until which the correlation coefficients are greater than or just reached zero values) is fitted to the ACMs. The exercise is conducted for all the 14 borehole profiles considered in this study (BH 1-14). Table 4.3 summarizes the best fitted ACMs for all the borehole profiles indicating correlation coefficient value (R^2), along with

the least root mean square error (RMSE) and sum of squares of errors (SSE) for the fitted curve. It is seen that SoF varies from 0.27 m to 0.92 m, with a mean value of 0.6 m and a CoV of 38.75%. Phoon and Kulhawy (1996) reported a mean SoF of SPT-*N* data as 2.4 m in sandy soil. The geotechnical site investigation conducted in present study area mostly encountered clayey soil with presence of sand and silt in some locations. Therefore, a comparatively smaller SoF value than in sand is expected. Moreover, the present study found that cosine exponential function is best suited for all the 14 borehole residual profiles. Vanmarcke (1978) also reported the cosine exponential function to be the best fit function for geotechnical properties. Hence, the cosine exponential function can be recommended to be used as characterizing correlation model for SPT-*N* data. However, it is to be noted that the distinction between trend in dataset and stochastic variation of residuals is not inherent to the geotechnical property, rather is dependent on the judgment of the modeler. Moreover, the mean SoF so estimated, depending on a particular in-situ test dataset, is not recommended of direct application to other geotechnical sites and properties without proper engineering judgement. However, data reported in present work can be used as preliminary indication of correlation distance, which will enable the sample spacing and correlation model to be chosen for a geotechnical site investigation or simulation based geotechnical reliability analysis with no prior knowledge of the site.

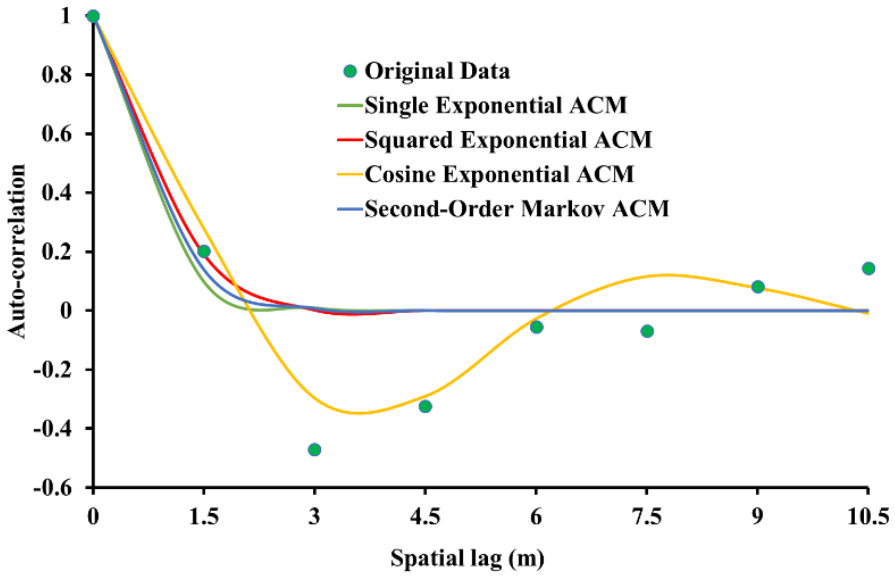

Fig. 4.6 Auto correlation model fitted to the estimated auto correlation function for BH 2

Table 4.2: 1-D correlation functions and their characteristics as typically determined for BH 2 in the present study

ACM	Function	Model Parameter	Correlation length (m)	RMSE	SSE	R^2
Single exponential	$y = e^{-ax}$	a = 1.549	1.29	0.2338	0.3827	0.7208
Squared exponential	$y = e^{-(ax)^2}$	a = 0.8595	2.06	0.2279	0.3634	0.7348
Second-order Markov	$y = e^{-ax}(1+ax)$	a = 2.313	1.73	0.1276	0.3736	0.7274
Cosine exponential	$y = e^{-ax}\cos(2\pi bx)$	a = 0.2653 b = 0.1214	0.8135	0.1261	0.09546	0.9187

Table 4.3: Summary of the soil variability analyses on the borehole data

BH No.	Fitted ACM	Unknown parameter	RMSE	SSE	R^2	SoF (m)
1	Cosine exponential	a = 0.637 b = 0.3332	0.1919	0.2209	0.8005	0.27
2	Cosine exponential	a = 0.2653 b = 0.1214	0.1261	0.09546	0.9187	0.81
3	Cosine exponential	a=0.4346 b=0.1653	0.1126	0.07601	0.9227	0.69
4	Cosine exponential	a = 0.2375 b = 0.1572	0.08515	0.07975	0.9361	0.46
5	Cosine exponential	a = 0.2684 b = 0.216	0.1046	0.1204	0.8993	0.28
6	Cosine exponential	a = 0.5372 b = 0.1593	0.138	0.2094	0.8146	0.83
7	Cosine exponential	a = 0.5304 b = 0.1591	0.1659	0.1652	0.8325	0.83
8	Cosine exponential	a = 0.2487 b = 0.1148	0.1968	0.2325	0.7975	0.85
9	Cosine exponential	a = 0.7638 b = 0.1656	0.1308	0.1026	0.8917	0.92
10	Cosine exponential	a = 0.185 b = 0.1775	0.1374	0.1132	0.9089	0.29
11	Cosine exponential	a = 0.1428 b = 0.101	0.1477	0.131	0.9103	0.68
12	Cosine exponential	a = 0.1662 b = 0.1363	0.0975	0.05704	0.9601	0.44
13	Cosine exponential	a = 0.2288 b = 0.1534	0.1273	0.0972	0.9145	0.47
14	Cosine exponential	a = 0.1602 b = 0.1134	0.08648	0.04488	0.9655	0.6

4.4. SUMMARY

This chapter reports the soil variability analysis using random field theory conducted for SPT-*N* data considering 14 borehole profiles. To obtain data stationarity for random field modeling, the SPT*N* value is decomposed as the summation of a mean trend and a set of residuals fluctuating around the mean. The deterministic mean trend is characterized using linear least-square regression analysis. The fluctuating component in the SPT data is modelled as a homogeneous random field. It is seen that cosine exponential function is best suited for all the 14 borehole residual profiles and the estimated SoF varies from 0.27 m to 0.92 m. The SoF so estimated based on particular in-situ test dataset need to be updated if a different dataset for some other regional site is to be considered. However, SoF estimated in present work can be used as preliminary indication of spatial variation, which may be used for choosing sample spacing and correlation model for similar geotechnical site investigation or simulation-based reliability analysis with no prior knowledge of the site.

CHAPTER 5

PARAMETRIC INFLUENCE ON THE PROBABILISTIC SLOPE STABILITY ASSESSMENT

5.1. GENERAL

In this chapter, a detailed stability analysis of a typical model slope is conducted through a probabilistic framework to investigate the effect of various parameters on slope stability. As discussed in Chapter 2, the incorporation of uncertainty in slope models necessarily requires the implementation of probability concepts and principles. The aim is to estimate the probability of slope failure as opposed to the ubiquitous FoS used in conventional deterministic analysis. In a probabilistic analysis, soil properties are considered as random variables and the probability of failure (P_f) is computed. In this chapter, initially, the uncertainty in soil properties is incorporated by characterizing soil shear strength parameters (cohesion, c and angle of internal friction, φ) as random variables using suitable probability distribution functions (pdf). Eventually, one-dimensional random fields are assigned to the model slope, thereby characterizing the soil shear strength parameters over a spatial extent. In this case, Monte Carlo Simulation (MCS) is adopted for the computation of the probability of slope failure.

5.2. EFFECT OF THE COEFFICIENTS OF VARIATION AND CROSS-CORRELATION

In this section, a typical 1H:1V slope section having 15 m height and 50 m length, as shown in Figure 5.1, is analysed using Slope/W module of GeoStudio v2018 by the means of MCS for estimating the probability of slope failure. In such an exercise, the soil parameters that are required

to be treated as random variables for probabilistic analysis are to be decided first. The soil properties that are used in the Limit Equilibrium Method (LEM)-based slope stability analysis in Slope/W while incorporating the elastic-perfectly plastic constitutive behaviour (i.e. following the Mohr-Coulomb behavior) are cohesion (c), angle of internal friction angle (φ) and the unit weight (γ). Alonso (1976) stated that the effect of the soil unit weight on the probability of failure of a cohesive slope is relatively less as compared to the shear strength parameters. Furthermore, it is found in several research literatures that the variability of soil unit weight is usually small (Lee et al. 1983; Phoon and Kulhawy 1999; Duncan 2000; Baecher and Christian 2003). Therefore, in the present study, only the shear strength parameters c and φ are modelled as random variables, while the unit weight is considered deterministically constant. In this section, the soil shear strength parameters are treated as random variables characterized by a lognormal distribution with no spatial variation of soil properties. Such an approach signifies that at each MCS iteration, a homogeneous slope would be considered without assigning any spatial variation of strength properties in the soil domain; however, the soil properties would take different values at each different MCS iteration that is decided as per the pdf assigned to the corresponding property.

Depending on whether a 'total' or 'effective' stress analysis is considered, the parameters c and φ can be considered under two stress states. A total stress analysis is applicable for short-term stability of slopes where the dissipation of excess pore-water pressure has not occurred, e.g., a newly cut or newly constructed cohesive slope under fully saturated condition. An effective stress analysis is applicable for problems where changes in excess pore-water pressures have occurred, e.g., an existing embankment under long-term stability scenario. In the total stress analysis, the cohesion is represented by the undrained shear strength, s_u, or undrained cohesion, c_u, (i.e., $\varphi_u = 0$)

of the soil. In the effective stress analysis, the drained cohesion, c, and drained friction angle, φ are used in the slope stability analysis and assessment. In this section, probabilistic analysis is carried out considering both undrained and drained condition for the chosen slope section, considering different coefficient of variation (CoV) and cross-correlation coefficient of soil shear strength parameters (c and φ).

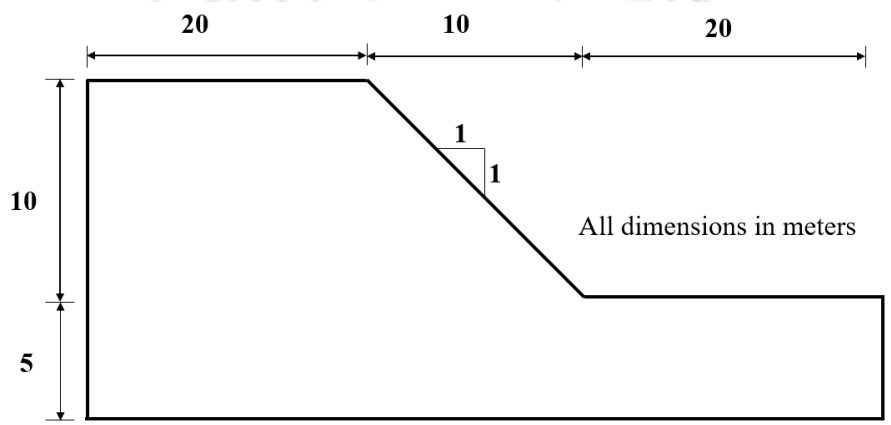

Fig. 5.1 Schematic of the typical slope geometry considered for present study

5.2.1. Stability of Monte Carlo Simulations

The accuracy of the computed probability of failure (P_f) depends on the numbers of iterations in the MCS. Generally, the accuracy increases as the number of realisations increases. However, it is necessary to find out the minimum number of MCS iterations to generate a reliable and consistent result. As the repetitive analysis is time consuming and the computation of P_f usually converges within a certain number of iterations, any further increase in the number of iterations beyond more than that required does not necessarily improve the computational outcome, rather adversely affects the computational time and effort. As mentioned in Section 2.2.2 of Chapter 2, to ensure accuracy in the value of failure probability, the direct MCS technique requires a sample number

of at least 10 times greater than the reciprocal of the desired probability level (Roberts and Casella, 1999). Hahn and Shapiro (1967) suggested that the minimum number of realisations required is dependent on the number of component random variables and the desired level of confidence, which is expressed as

$$n_{min} = m\left(\frac{100d}{\varepsilon}\right)\frac{(1-P_f)}{P_f} \tag{5.1}$$

where, n_{min} is the minimum number of iterations for the MCS, m is the number of random variables, ε is the relative percentage error in computing P_f; and d is the normal standard deviate corresponding to the desired confidence levels as presented in Table 5.1.

Table 5.1 Normal standard deviates for different confidence levels

Confidence Level	Normal Standard Deviate, d
80%	1.282
90%	1.645
95%	1.96
100%	2.576

To estimate the minimum number of MCS iterations using Eqn. 5.1, an a-priori value of P_f is needed to initiate the simulation, which might not be always available. Hahn and Shapiro (1967) suggested to consider P_f = 0.5 as initial estimate of the n_{min}. Considering P_f = 0.5, Table 5.2 lists the minimum number of simulations (n_{min}) needed for different magnitudes of relative errors (ε ranging from 0.5%-50%), confidence levels (90% and 95%) and numbers of random variables (m = 1 and 2). It is found that to attain a relative error of less than 5%, for a 95% confidence level, the number of simulations should be more than 1500 in case of single random variable and more than 3000 in case of two random variables. Considering Table 5.2 as a reference, the numbers of MCS required is further investigated and reported in subsequent sections in this chapter.

Table 5.2 Minimum number of realisations required for achieving desired accuracy

Relative error	m = 1		m = 2	
ε (%)	95%	90%	95%	90%
0.5	153664	108241	307328	216482
1	38416	27060	76832	54121
5	1537	1082	3073	2165
10	384	271	768	541
50	15	11	31	22

5.2.2. Undrained Condition

A mean undrained cohesion (c_u) of 45 kPa is taken for the present study and the coefficient of variation (CoV) for c_u is considered to be varying in the range 0.05-1. The unit weight (γ) is considered to be constant at 20 kN/m^3. The analysis is carried out in Slope/W module of GeoStudio v2018 using the Morgenstern-Price LEM method and MCS is used to evaluate the probability of failure (or reliability index). A deterministic analysis of the identical slope resulted in a stable slope having a FoS value of 1.3. Figure 5.2 indicates the influence of the number of MCS iterations on the estimated P_f value. It is found that 2000 numbers of MCS iterations is adequate for the current slope stability analysis problem, indicated by the presence of insignificant fluctuations in the estimated P_f value on further increment in iterations. Therefore, it is decided to adopt 2000 number of MCS iterations in present study.

The probabilistic results are presented in terms of Reliability Index (RI) as shown in Fig. 5.3. It is noticed that a slope predicted as safe by a deterministic analysis may have very low reliability index (or high probability of failure) value depending on the CoV of the soil shear strength parameters. In this case, depending on the values of CoV, the RI varies from 0.333 to 3.49. It is seen that as the CoV for c_u increases, the Reliability Index decreases leading to an increase in probability of failure (P_f). This is because with the increase in CoV, the deviation of the undrained

cohesion from its mean value increases for different Monte Carlo Simulation (MCS) realizations. This leads to more uncertainty in the cohesion value, thereby resulting in a decrease in Reliability Index.

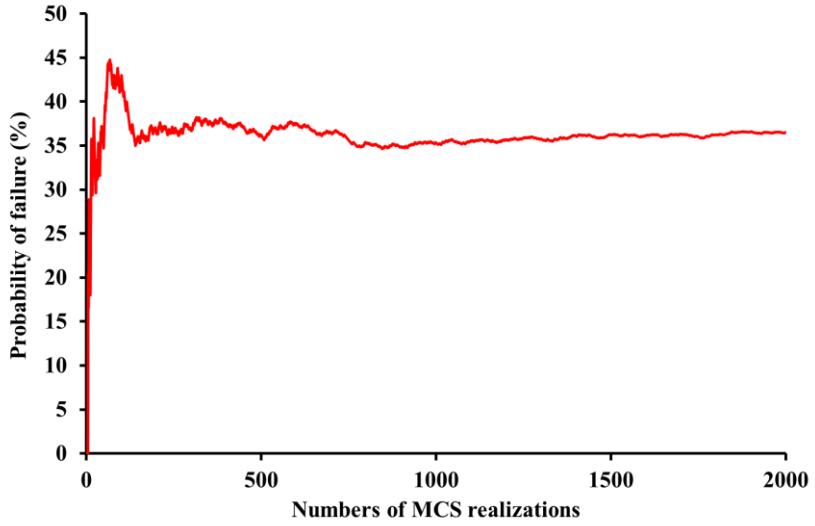

Fig. 5.2 Typical variation in the probability of failure with the numbers of MCS iterations

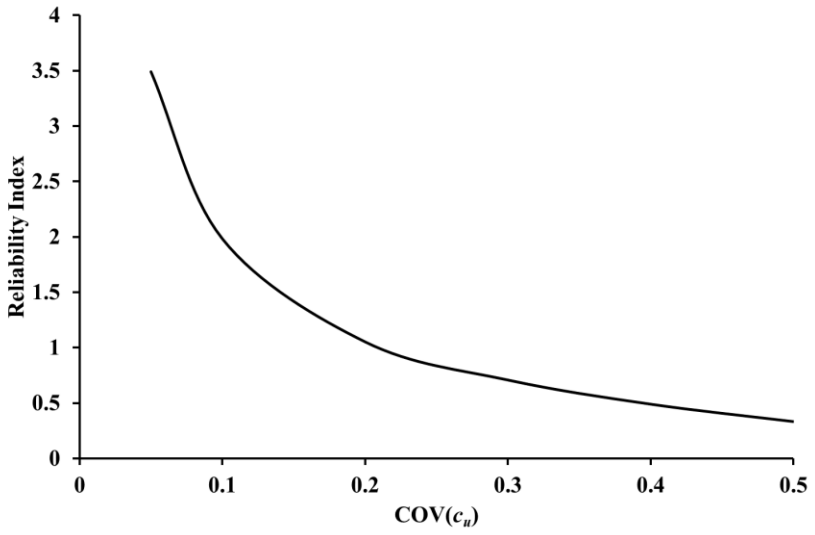

Fig. 5.3 Variation of reliability index (RI) with CoV(c_u) under undrained condition

5.2.3. Drained Condition

For drained condition, the mean cohesion (c) and angle of internal friction (φ) are taken as 45 kPa and 20^o respectively. The unit weight is assumed to be 20 kN/m^3. In this case as well, 2000 number of MCS is found to be adequate to produce a consistent outcome. A deterministic analysis of the slope using Morgenstern-Price LEM results in a stable slope having a FoS value of 2.1. The probabilistic results are shown in Fig. 5.4-5.8. Figure 5.4 shows the variation of Reliability Index with CoV(c) and cross-correlation coefficient of c and φ (i.e. $\rho_{c\varphi}$) for CoV(φ) = 0.1. It is seen that the as the variability of c increases from its mean value, i.e. with the increase in CoV(c), the RI decreases for all magnitudes of $\rho_{c\varphi}$. Moreover, it is also noticed that the RI increases as the soil properties c and φ becomes more negatively correlated. As c and φ are more negatively correlated, the chances of one soil property taking higher value with a lower value of the other property increases, hence the slope becomes more stable leading to high RI. Therefore, the cross-correlation coefficient of soil properties plays an important role in deciding the stability of slope in terms of probability of failure or Reliability Index, which is further explained with the help of Fig. 5.5-5.7.

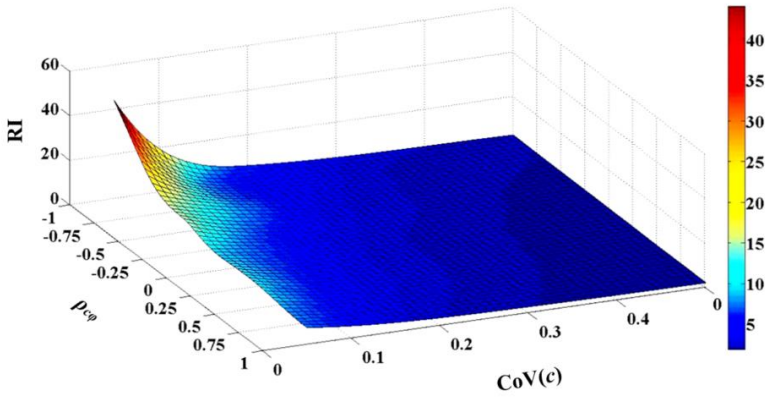

Fig. 5.4 Variation of RI with CoV(c) and $\rho_{c\varphi}$, given CoV(φ) = 0.1

Figure 5.5 to 5.7 shows variation of Reliability Index with CoV(c) and CoV(φ) for different correlation coefficients ($\rho_{c\varphi}$ = 0, 0.5 and -0.5, respectively). The RI values vary from 1.59 to 18.13 depending on CoV and cross-correlation coefficient. It is noticed that with no correlation or positive correlation between c and φ, the variation of RI shows a common pattern as discussed earlier. On the other hand, when the c and φ are negatively correlated, the variation of Reliability Index shows a different pattern based on CoVs of c and φ (Fig 5.7), which is more evidently represented in Fig. 5.8.

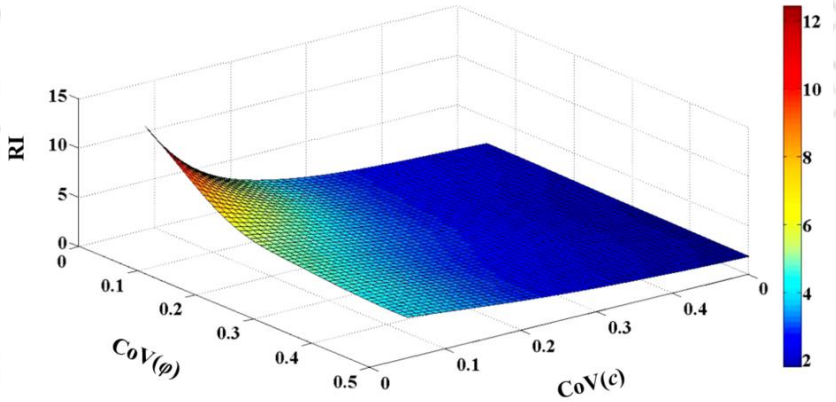

Fig. 5.5 Variation of RI with CoV(c) and CoV(φ) for $\rho_{c\varphi}$ = 0

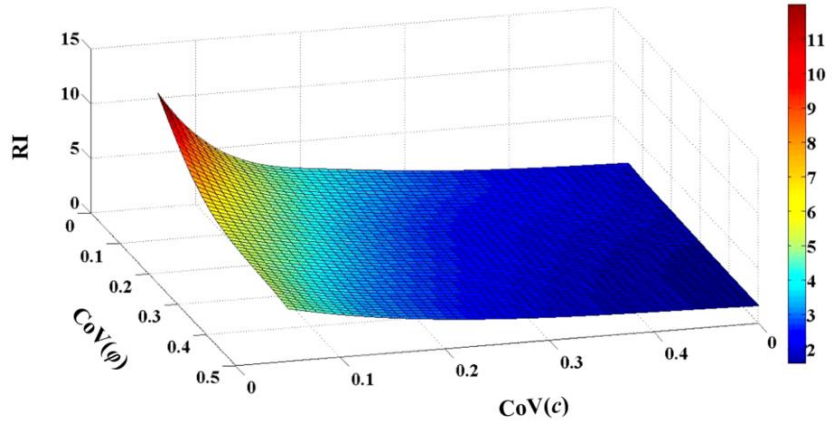

Fig. 5.6 Variation of RI with CoV(c) and CoV(φ) for (a) $\rho_{c\varphi}$ = 0.5

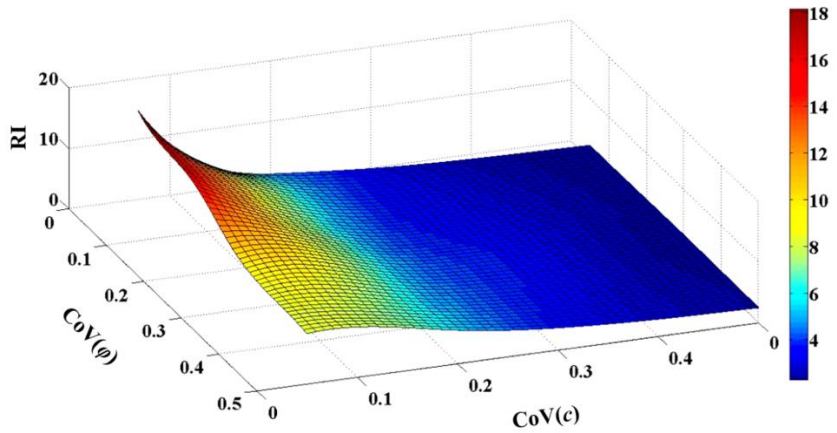

Fig. 5.7 Variation of RI with CoV(c) and CoV(φ) for (a) $\rho_{c\varphi}$ = -0.5

Figure 5.8 shows variation of Reliability Index with CoVs of c and φ. It is seen that when c and φ are negatively correlated, RI shows a random variation with CoV(c) and CoV(φ). When CoV(c) is very small, c tends to take its mean value or a value very near to its mean. Since c and φ are negatively correlated, as c value tends to take high value, φ tends to take lower value. Hence, with the increase of CoV(φ), φ will further decrease in most of the cases, leading to a lower reliability index. On the other hand, when CoV(c) is high, c will deviate more from its mean value. In this case, if c is taking very less value, φ will have to take high value from its characterizing probability distribution function (pdf). Hence, whatever is the CoV of φ, there will be more probability for φ to take a value very near to its mean value or even greater than mean value; thereby, the RI slightly increases or mostly remains the same. It is noted that CoV(φ) has less influence on RI in comparison to that imparted by CoV(c).

It is clear from the study that, cross-correlation coefficient of c and φ (i.e. $\rho_{c\varphi}$) has very significant influence on the RI, especially when they are negatively correlated. In all practical cases, in-situ soil shows negative correlation between c and φ. Hence, the correlation coefficient between soil

shear strength properties must be intricately determined with the help of statistical analysis of the field data before proceeding to the slope stability analysis. This would aid in more realistic estimate of the failure probability of the slope for practical purposes.

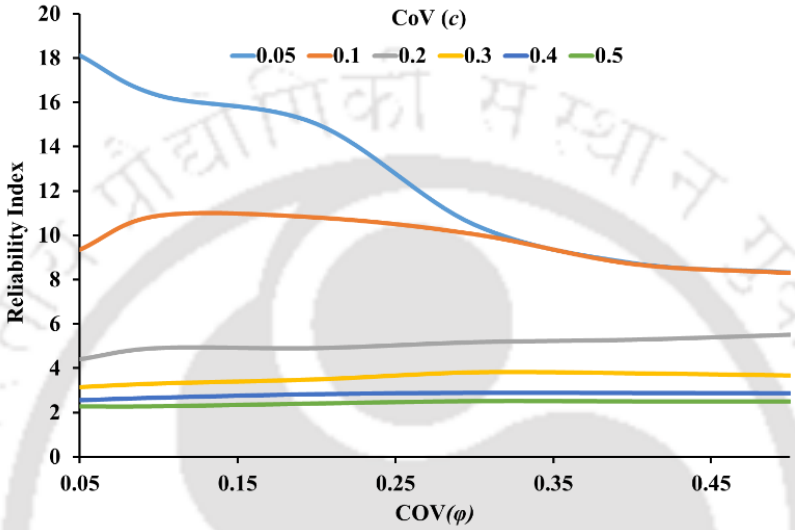

Fig. 5.8 Variation of RI with CoV(c) and CoV(φ) for $\rho_{c\varphi}$ = -0.5

5.3. EFFECT OF VARIATION OF SLOPE INCLINATION

5.3.1. Undrained Condition

For the same typical model slope as described in Fig. 5.1, the mean undrained cohesion (c_u) is considered as 45 kPa for the study, and the CoV(c) is assumed to be 0.1. Figure 5.9 shows the variation of RI with slope inclination. It is expectedly observed that an increase in the slope inclination leads to a less stable slope, which is manifested by a reduction in the reliability index. In the present scenario, the RI is observed to vary from 0.657 to 2.979 depending on the slope inclination.

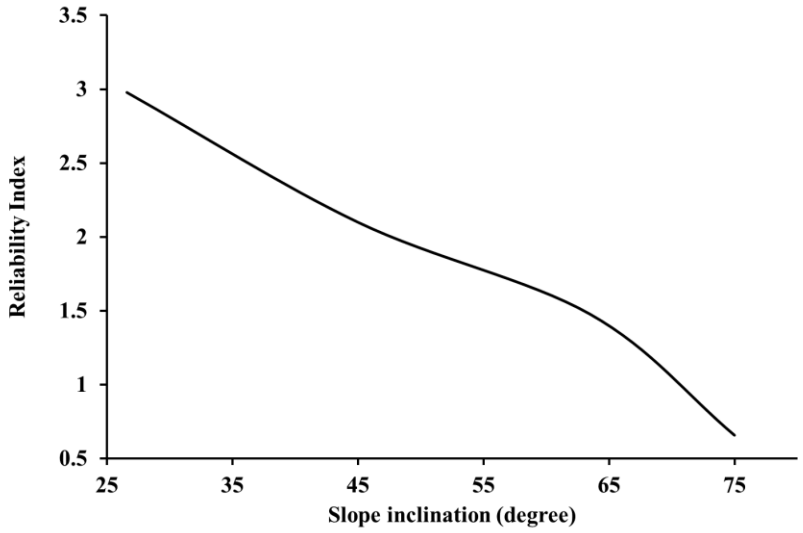

Fig. 5.9 Variation of reliability index with slope inclination under undrained condition

5.3.2. Drained Condition

For drained condition, the mean cohesion (c) and angle of internal friction (φ) considered for this study are 45 kPa and 20^o respectively. CoV is assumed to be 0.1 for both the shear strength parameters c and φ. Figure 5.10 shows the variation of RI with slope inclination for different cross-correlation coefficient between c and φ. It is seen that as the slope inclination increases leading to a less stable slope, the corresponding RI decreases. Moreover, RI increases with the increase in the magnitude of the negative cross-correlation coefficient between c and φ, the reason of which has already been discussed in Section 5.2. The value of RI varies from 4.294 to 13.353 depending on the slope inclination and the cross-correlation coefficient.

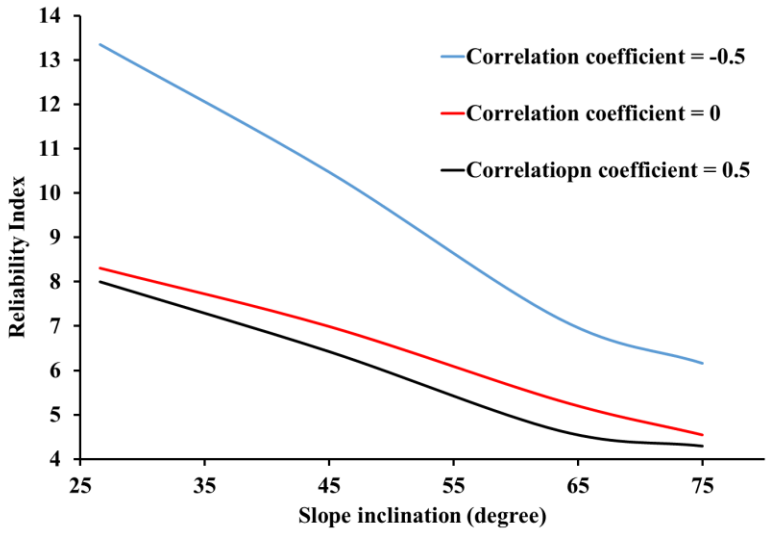

Fig. 5.10 Variation of reliability index with slope inclination and cross-correlation coefficient between the shear strength parameters under drained conditions

5.4. EFFECT OF SPATIAL VARIABILITY OF SOIL PROPERTIES

A reasonable criticism of the method utilized in the previous sections is that the method considers the soil properties to be random variables. However, the inherent spatial variation of the shear strength in a soil domain is not captured in the MCS iterations. The shear strength properties are considered as random variables defined by a Lognormal distribution on the mean strength estimates. Hence, each iteration considers a homogeneous slope without assigning any spatial variation of strength properties in the soil domain.

Moving beyond the deficiencies in the LEM-based probabilistic method utilized in previous sections, this section reports the influence of spatial variation of soil properties on the slope stability. In this section, a typical slope model of 2H:1V grade having 60 m length and 15 m height is considered. The slope materials are assumed having a mean cohesion (c) of 5 kPa and a mean angle of internal friction (φ) of 20º. The standard deviations of c and φ considered are 1.5 kPa and

6.22º, respectively. Considering 1D spatial variation in the soil shear strength parameters, the stated slope section is analysed with the aid of Slope/W module of GeoStudio v2018. The slope stability is assessed using Morgenstern-Price LEM coupled with MCS for evaluation of the probability of failure.

In this study, to generate 1D random field in horizontal direction, the chosen soil properties are sampled for specified distances to estimate the failure probability for different correlation lengths. In the Slope/W module, the properties are sampled only once if the specified sampling distance is greater than the actual length of the slip surface within that soil. Slope/W tracks the distance along the slip surface and when the distance exceeds the specified sampling distance, the properties are sampled further. When the last sampling segment along the slip surface within a particular soil stratum is shorter than the specified distance, the strength is correlated with the previous segment as described by Krahn (2004). The procedure involves local averaging as described by El-Ramly et al. (2002). For example, when a soil domain of 60 m length is sampled for specified distance, for example 25 m, there will be two complete sampling distances of 25 m and a partial sampling distance of 10 m. A partial sampling distance is considered to be correlated with the immediate preceding sampling distance. The coefficient of correlation between the two soil sections can be computed with the aid of the expression as proposed by Vanmarcke (1983):

$$\rho(\Delta Z,\Delta Z^{'})=\frac{Z_0^2\Gamma(Z_0)-Z_1^2\Gamma(Z_1)+Z_2^2\Gamma(Z_2)-Z_3^2\Gamma(Z_3)}{2\Delta Z\Delta Z[\Gamma(\Delta Z)\Gamma(\Delta Z^{'})]^{0.5}} \tag{5.2}$$

$$\begin{aligned} Z_1 &= \Delta Z + Z_0 \\ Z_2 &= \Delta Z + Z_0 + \Delta Z' \\ Z_3 &= \Delta Z' + Z_0 \end{aligned} \tag{5.2a}$$

where, $\Delta Z, \Delta Z'$ are the length of the two sections, Z_0 is the distance between the two sections, and $\Gamma(.)$ is a dimensionless variance function that is approximated as

$$\Gamma(Z) = \begin{cases} 1.0 \text{ when } Z \le \theta \\ \dfrac{\theta}{Z}, \text{ when } Z > \theta \end{cases} \tag{5.3}$$

The failure probabilities are computed using MCS for different dimensionless correlation lengths ($\Theta = \theta / L$, where L is the length of slope in the horizontal direction). Figure 5.11 illustrates the influence of the dimensionless correlation length on the probability of failure of the stated slope. It is observed that P_f varies from zero to 15.6% depending on the magnitude of Θ. The failure probability increases rapidly (i.e. reliability index decreases) with the increase in the correlation length. The failure probability is negligible when the correlation length is very small. This is attributed to the fact that for small correlation lengths, the local averaging is maximum and, thus, the soil properties tend to take their mean values. Now, as the chosen virgin slope has been safe for its mean value of shear strength parameters, the failure probability is very less (or negligible). The failure probability is highest when dimensionless correlation length approaches unity, thereby indicating the entire soil domain as homogeneous for all the MCS iterations, with different values of shear strength for different iterations. It is also noticed that for large values of Θ, the probability of failure becomes either constant or exhibits negligible fluctuation in its magnitude. Hence, it is seen that depending on the chosen correlation length, ignoring the spatial variability of soil properties may result in underestimation or overestimation of failure probability of the slope. Very small or large correlation lengths are of mere numerical interest. Under practical considerations, the correlation lengths are of intermediate range, over which the P_f shows a significant variation. Hence, geotechnical engineers should be aware of the best possible spatial variability prevalent in

the site and develop a realistic random field model for a practical probabilistic slope stability analysis.

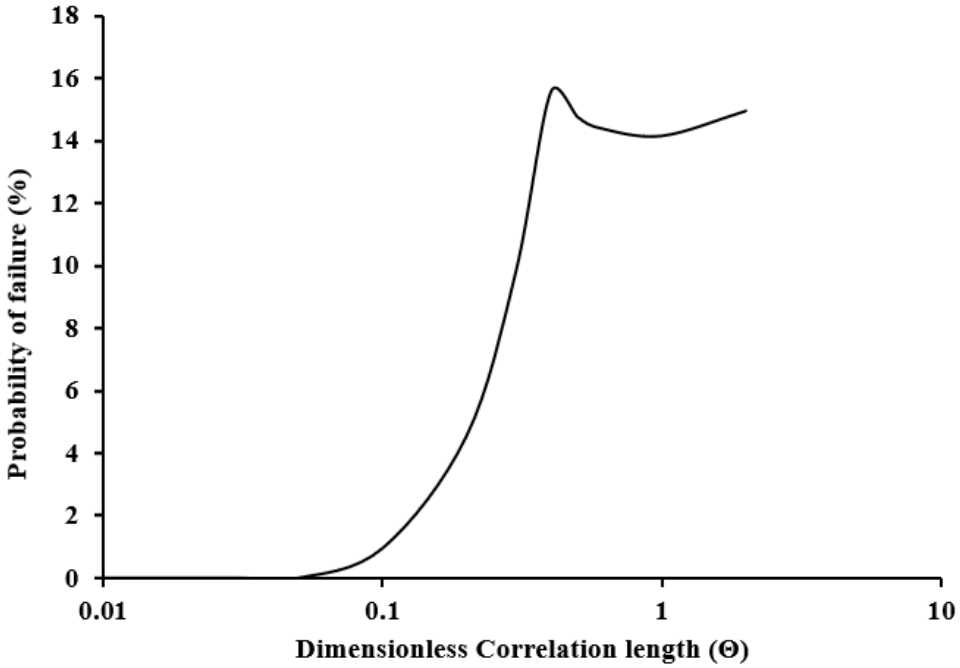

Fig. 5.11 Effect of 1D spatial variation of soil shear strength parameters on the probability of failure of a typical slope

5.5. SUMMARY

This chapter reports the outcome of the parametric study to assess the influence of various parameters on probabilistic slope stability study conducted using Slope/W module of GeoStudio v2018. Initially, an LEM-based probabilistic stability study is conducted for a chosen slope section considering the soil shear strength parameters as random variable. The effects of CoV and cross-correlation coefficient ($\rho_{c\varphi}$) between shear strength parameters (c and φ), and slope inclination on estimation of slope failure probability are investigated. It is found that the CoV of shear strength parameters and their cross-correlation governs the estimation of failure probability. The reliability

index (RI) decreases with an increase in CoV when the shear strength parameters are either not correlated or they are positively correlated. In case of negative cross-correlation, RI shows a random variation with the variation in CoV(c) and C(φ). When CoV(c) is very small, with the increase of CoV(φ), reliability index decreases. On the other hand, when CoV(c) is high, whatever is the CoV(φ), the RI either slightly increases or practically remains same. It is noted that CoV(φ) has less influence on RI in comparison to that imparted by CoV(c). Eventually one-dimensional random field is also incorporated in the study to simulate the inherent spatial variation of soil shear strength in the horizontal direction and the influence of the same on failure probability estimation is investigated. The study shows that the probability of failure varies rapidly with the variation in correlation length up to a certain magnitude, while the same shows negligible fluctuation in value when dimensionless correlation length approaches unity. The intermediate range of the dimensionless correlation length is of practical importance to the geotechnical engineers, and that the best possible spatial variability prevalent in the site should be ascertained to conduct a practical probabilistic slope stability analysis.

CHAPTER 6

HILLSLOPE INSTABILITY INDUCED BY TOE EXCAVATION: A COMPARATIVE STUDY OF LEM-BASED DETERMINISTIC AND PROBABILISTIC APPROACHES

6.1. GENERAL

Roadways constructed by excavating the toe of hill slopes are foremost means of transportation and communication in most of the hilly regions in India. Failure of such cut slopes may result in loss of life and property and also creates hindrance in communication in such hilly regions (Huang and Chan, 2004; Borgatti and Soldati, 2005; Zhang et al., 2009, 2012). Although geotechnical profession shows an ample progress in subsuming probabilistic concepts to encounter various geotechnical uncertainties, there is a lack of using such advance techniques in geotechnical practices such as to assess the safety of toe excavated hill slopes, as mentioned in Section 2.6 of Chapter 2. Therefore, in this chapter, the stability of a cut slope in the hilly region is addressed through a probabilistic framework and the influence of considering such uncertainties on the stability is reported. First, a detailed report on the deterministic assessment of the stability of hillslope subjected to toe cutting is presented. Thereafter, a probabilistic LEM-based study of slope instability due to vertical toe excavation and the corresponding estimation of the probability of failure (or reliability) is conducted. The effect of the coefficient of variation (CoV) on the probability of failure (or reliability) of slope due to toe excavation is examined. The study of probabilistic slope instability is extended for investigating the effect of correlation between the soil shear strength properties. Further, a one-dimensional (1D) spatial variation of soil strength

properties in the horizontal direction is considered to simulate inherent spatial variation of soil as observed in the field and P_f is estimated for the same test slope.

6.2. DETERMINISTIC LEM STUDY

Generally, for achieving more carriageway of roadways, vertical or inclined cuts on natural slopes are commonly practiced in the hilly terrains. In the north-eastern and many other regions of India, the existence of lateritic soils make the slopes eligible to sustain near-vertical cuts (80º-90º) during the dry periods of the year when the roadway extension projects are mainly mobilized. Therefore, this report deals with only vertical toe excavation for achieving more carriageway. To study the effect of vertical toe cutting on hill slopes, a typical slope overlying a hardrock foundation is analyzed using different modules of GeoStudio. The shear strength properties of the soil (cohesion, c and angle of internal friction, φ) are assigned that are supposed to follow the Mohr-Coulomb failure criterion. Figure 6.1 shows the schematic diagram of the slope geometry adopted which highlights the possible width of toe cut (b_t).

First, a complete deterministic study on the slope sections is conducted for a wide range of c and φ values (c and φ values are varied from 0-70 kPa and 15°-40°, respectively) for a slope height (H) of 20 m, 30 m and 40 m and for different slope inclinations (such as, i = 30°, 40°, 50°, 60°). The range of parameters considered for this exercise typically represents the commonly encountered hillslope materials in the north-eastern region of India (Das, 1992; Saikia et al., 1996; Kalita, 2001; Saikia, 2002; Das, 2003; Das and Saikia, 2010; Saikia et al., 2014; Acharyya and Dey, 2015; Kumar et al., 2015; Talukdar et al., 2018; Acharyya and Dey, 2019; Sarma et al., 2019;2020; Dey and Murali, 2021). A typical monograph (comprising a set of tables) illustrating the stability of the

dry slope sections is presented in Table 6.1, in which the failed slopes are marked in **red** color. The sub-tables provide a treatise about the extent of toe cut which can be operated on slopes of various characteristics. It is clearly depicted that the steeper inclination and increasing height of the slope results in a significant reduction of the inherent stability even under significant magnitudes of shear strength parameters. It is to be noted that for the low height slope (H = 20 m) with steeper inclinations (50º and 60º in particular), increasing the width of toe excavation would also lead to larger height of vertical cut. Depending on the particular slope geometry, the larger excavation width might lead to a significant removal of the slope face, thereby leading to a vertical standing slope face and forming a nearly rectangular section. For such slopes, the stability is guided by the shear strength parameters and the corresponding depth if unsupported excavation. In case the depth of unsupported excavation becomes approximately equal to or exceeds the height of the chosen slope section, the resulting excavated section shows higher stability, and a higher factor of safety as shown in Table 6.1(C and D).

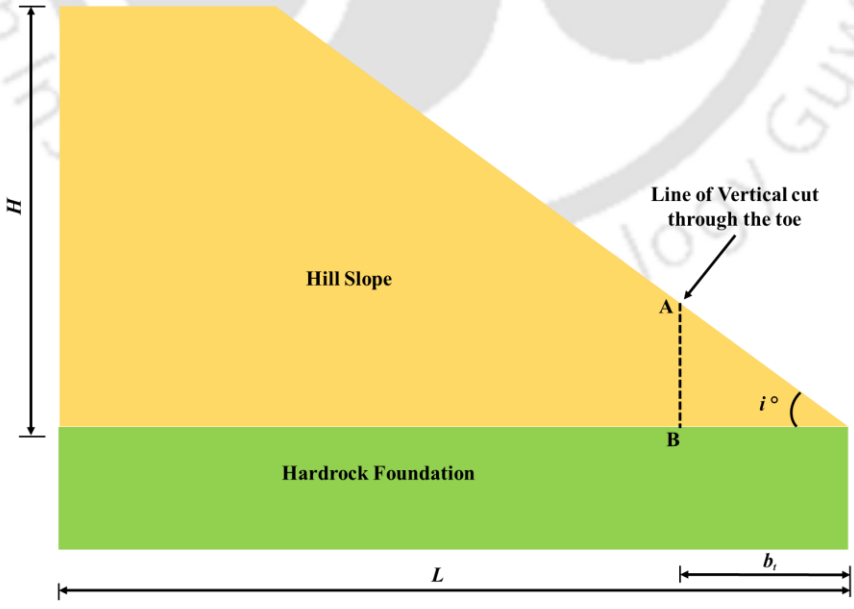

Fig. 6.1 Schematic diagram of slope geometry adopted showing vertical toe excavation

Table 6.1: Stability of dry slopes of varying height, angle of inclination, shear strength parameter of hillslope material and varying extent of toe excavation

(A) Height of slope section, H = 20 m, Angle of inclination, i - 30°										
	b_t = 0					b_t = 2.5 m				
φ (deg)	15	20	25	30	35	15	20	25	30	35
c (kPa)										
10	0.842	1.046	1.264	1.49	1.731	0.819	1.023	1.217	1.427	1.66
30	1.326	1.551	1.782	2.033	2.305	1.282	1.506	1.734	1.972	2.236
50	1.775	2.01	2.257	2.519	2.796	1.719	1.944	2.183	2.441	2.725
70	2.209	2.457	2.71	2.977	3.274	2.131	2.377	2.621	2.879	3.166
	b_t = 5 m					b_t = 7.5 m				
c (kPa)										
10	0.777	0.955	1.139	1.338	1.558	0.721	0.883	1.055	1.236	1.43
30	1.228	1.437	1.659	1.887	2.135	1.163	1.361	1.56	1.766	1.987
50	1.638	1.862	2.09	2.331	2.598	1.559	1.769	1.979	2.208	2.453
70	2.042	2.268	2.505	2.763	3.028	1.947	2.158	2.385	2.616	2.868
	b_t = 10 m									
c (kPa)										
10	0.649	0.79	0.938	1.091	1.247					
30	1.081	1.249	1.42	1.592	1.784					
50	1.458	1.644	1.837	2.032	2.239					
70	1.824	2.019	2.217	2.433	2.657					

(B) Height of slope section, H = 20 m, Angle of inclination, i - 40°										
	b_t = 0					b_t = 2.5 m				
φ (deg)	15	20	25	30	35	15	20	25	30	35
c (kPa)										
10	0.659	0.81	0.959	1.121	1.301	0.622	0.758	0.904	1.05	1.207
30	1.088	1.257	1.435	1.617	1.813	1.027	1.191	1.35	1.523	1.714
50	1.474	1.656	1.85	2.044	2.258	1.399	1.572	1.747	1.937	2.13
70	1.858	2.043	2.237	2.448	2.673	1.759	1.939	2.127	2.317	2.527
	b_t = 5 m					b_t = 7.5 m				
c (kPa)										
10	0.563	0.68	0.8	0.931	1.074	0.492	0.593	0.695	0.798	0.912
30	0.951	1.09	1.24	1.391	1.552	0.873	0.984	1.121	1.234	1.379
50	1.3	1.456	1.612	1.775	1.954	1.21	1.329	1.484	1.601	1.766
70	1.642	1.802	1.968	2.148	2.326	1.697	1.78	1.85	1.964	2.15

	b_t = 10 m				
***c* (kPa)**					
10	0.427	0.509	0.589	0.676	0.765
30	0.77	0.87	0.975	1.075	1.187
50	1.08	1.194	1.303	1.419	1.548
70	1.475	1.499	1.62	1.752	1.874

(C) Height of slope section, *H* = 20 m, Angle of inclination, *i* - 50°

	b_t = 0					b_t = 2.5 m				
***φ* (deg)**	**15**	**20**	**25**	**30**	**35**	**15**	**20**	**25**	**30**	**35**
***c* (kPa)**										
10	0.543	0.657	0.776	0.892	1.021	0.491	0.586	0.688	0.797	0.907
30	0.928	1.066	1.204	1.353	1.504	0.849	0.974	1.091	1.216	1.356
50	1.277	1.42	1.577	1.738	1.902	1.398	1.318	1.44	1.584	1.73
70	1.643	1.768	1.921	2.091	2.28	1.826	1.943	1.841	1.946	2.079
	b_t = 5 m					b_t = 7.5 m				
***c* (kPa)**										
10	0.426	0.504	0.583	0.669	0.766	0.363	0.425	0.491	0.563	0.637
30	0.768	0.916	0.994	1.12	1.197	0.678	0.763	0.839	0.925	1.022
50	1.08	1.266	1.379	1.489	1.617	0.946	1.06	1.17	1.244	1.358
70	1.507	1.498	1.725	1.847	1.909	1.294	1.388	1.438	1.557	1.689
	b_t = 10 m									
***c* (kPa)**										
10	0.321	0.365	0.418	0.474	0.532					
30	0.618	0.679	0.76	0.814	0.893					
50	0.863	0.953	1.049	1.129	1.205					
70	1.153	1.234	1.294	1.397	1.502					

(D) Height of slope section, *H* = 20 m, Angle of inclination, *i* - 60°

	b_t = 0					b_t = 2.5 m				
***φ* (deg)**	**15**	**20**	**25**	**30**	**35**	**15**	**20**	**25**	**30**	**35**
***c* (kPa)**										
10	0.456	0.543	0.643	0.727	0.827	0.393	0.468	0.543	0.609	0.69
30	0.889	0.921	1.031	1.139	1.263	0.728	0.863	0.961	1.054	1.108
50	1.419	1.522	1.5	1.504	1.636	1.113	1.205	1.241	1.41	1.528
70	1.87	1.974	2.084	2.027	1.985	1.331	1.547	1.645	1.67	1.87

	b_t = 5 m					b_t = 7.5 m				
***c* (kPa)**										
10	0.333	0.391	0.442	0.497	0.558	0.29	0.338	0.387	0.438	0.469
30	0.635	0.723	0.783	0.869	0.961	0.578	0.644	0.703	0.769	0.841
50	0.937	0.983	1.077	1.193	1.281	0.904	0.905	0.977	1.056	1.127
70	1.221	1.302	1.388	1.481	1.551	1.461	1.554	1.624	1.315	1.402
	b_t = 10 m									
***c* (kPa)**										
10	0.272	0.317	0.344	0.384	0.426					
30	0.678	0.599	0.659	0.725	0.768					
50	1.028	1.064	1.145	1.233	1.253					
70	1.898	1.952	1.456	1.543	1.64					

(E) Height of slope section, *H* = 30 m, Angle of inclination, *i* - 30°

	b_t = 0					b_t = 2.5 m				
***φ* (deg)**	**15**	**20**	**25**	**30**	**35**	**15**	**20**	**25**	**30**	**35**
***c* (kPa)**										
10	0.752	0.952	1.153	1.363	1.595	0.74	0.93	1.122	1.33	1.561
30	1.091	1.309	1.536	1.772	2.034	1.069	1.284	1.507	1.742	2.002
50	1.401	1.633	1.863	2.114	2.392	1.371	1.596	1.826	2.075	2.349
70	1.704	1.935	2.182	2.438	2.716	1.663	1.892	2.137	2.387	2.662
	b_t = 5 m					b_t = 7.5 m				
***c* (kPa)**										
10	0.716	0.895	1.083	1.288	1.515	0.683	0.855	1.038	1.232	1.442
30	1.043	1.256	1.471	1.703	1.945	1.013	1.215	1.423	1.634	1.862
50	1.337	1.556	1.783	2.029	2.29	1.3	1.508	1.731	1.966	2.216
70	1.619	1.846	2.082	2.328	2.6	1.571	1.794	2.018	2.259	2.526
	b_t = 10 m									
***c* (kPa)**										
10	0.646	0.812	0.978	1.16	1.36					
30	0.978	1.165	1.353	1.548	1.76					
50	1.253	1.456	1.668	1.887	2.113					
70	1.519	1.731	1.947	2.181	2.418					

(F) Height of slope section, H = 30 m, Angle of inclination, i - 40°										
	b_t = 0					b_t = 2.5 m				
φ (deg)	15	20	25	30	35	15	20	25	30	35
c (kPa)										
10	0.578	0.718	0.867	1.029	1.2	0.556	0.695	0.834	0.979	1.139
30	0.883	1.046	1.209	1.386	1.581	0.855	1.007	1.168	1.339	1.517
50	1.154	1.327	1.505	1.697	1.892	1.116	1.282	1.456	1.632	1.825
70	1.41	1.593	1.782	1.976	2.191	1.366	1.544	1.72	1.912	2.113
	b_t = 5 m					b_t = 7.5 m				
c (kPa)										
10	0.527	0.648	0.776	0.915	1.069	0.483	0.597	0.716	0.836	0.968
30	0.811	0.959	1.11	1.265	1.436	0.764	0.9	1.035	1.182	1.328
50	1.066	1.227	1.383	1.553	1.742	1.012	1.153	1.303	1.462	1.624
70	1.313	1.474	1.647	1.821	2.009	1.243	1.399	1.552	1.714	1.894
	b_t = 10 m									
c (kPa)										
10	0.442	0.543	0.643	0.751	0.864					
30	0.715	0.832	0.958	1.077	1.211					
50	0.955	1.078	1.219	1.351	1.502					
70	1.193	1.319	1.449	1.603	1.757					

(G) Height of slope section, H = 30 m, Angle of inclination, i - 50°										
	b_t = 0					b_t = 2.5 m				
φ (deg)	15	20	25	30	35	15	20	25	30	35
c (kPa)										
10	0.468	0.574	0.681	0.798	0.927	0.436	0.534	0.638	0.743	0.857
30	0.745	0.874	1.003	1.135	1.282	0.705	0.82	0.938	1.068	1.201
50	0.986	1.131	1.268	1.418	1.579	0.939	1.066	1.2	1.332	1.474
70	1.224	1.363	1.52	1.674	1.839	1.161	1.3	1.435	1.582	1.739
	b_t = 5 m					b_t = 7.5 m				
c (kPa)										
10	0.398	0.484	0.572	0.668	0.774	0.356	0.43	0.511	0.587	0.668
30	0.659	0.756	0.869	0.975	1.092	0.607	0.695	0.798	0.889	0.985
50	0.889	0.993	1.123	1.227	1.363	0.872	0.964	1.079	1.167	1.251
70	1.242	1.289	1.377	1.477	1.599	1.103	1.209	1.322	1.437	1.518
	b_t = 10 m									
c (kPa)										
10	0.317	0.384	0.445	0.508	0.578					
30	0.55	0.63	0.715	0.793	0.907					
50	0.763	0.845	0.933	1.053	1.127					
70	0.949	1.056	1.142	1.249	1.369					

(H) Height of slope section, H = 30 m, Angle of inclination, i - 60°										
	b_t = 0					b_t = 2.5 m				
φ (deg)	15	20	25	30	35	15	20	25	30	35
c (kPa)										
10	0.385	0.467	0.55	0.635	0.727	0.349	0.418	0.491	0.569	0.649
30	0.641	0.738	0.841	0.949	1.06	0.639	0.686	0.777	0.86	0.962
50	0.958	0.983	1.09	1.199	1.324	0.886	0.982	1.037	1.154	1.239
70	1.342	1.33	1.323	1.444	1.575	1.133	1.229	1.331	1.434	1.51
	b_t = 5 m					b_t = 7.5 m				
c (kPa)										
10	0.312	0.367	0.427	0.491	0.562	0.274	0.321	0.371	0.426	0.484
30	0.539	0.621	0.693	0.803	0.86	0.489	0.557	0.621	0.691	0.777
50	0.741	0.827	0.915	1.009	1.142	0.678	0.766	0.853	0.915	1.01
70	0.989	1.026	1.128	1.21	1.377	0.852	0.969	1.033	1.135	1.198
	b_t = 10 m									
c (kPa)										
10	0.25	0.285	0.327	0.372	0.418					
30	0.45	0.515	0.579	0.635	0.697					
50	0.642	0.708	0.763	0.848	0.923					
70	0.818	0.89	0.968	1.042	1.119					

(I) Height of slope section, H = 40 m, Angle of inclination, i - 30°										
	b_t = 0					b_t = 2.5 m				
φ (deg)	15	20	25	30	35	15	20	25	30	35
c (kPa)										
10	0.704	0.892	1.085	1.295	1.526	0.692	0.875	1.067	1.277	1.508
30	0.97	1.182	1.4	1.636	1.898	0.957	1.166	1.384	1.62	1.871
50	1.213	1.43	1.661	1.908	2.169	1.193	1.409	1.639	1.883	2.143
70	1.439	1.671	1.904	2.154	2.432	1.415	1.646	1.875	2.125	2.402
	b_t = 5 m					b_t = 7.5 m				
c (kPa)										
10	0.675	0.854	1.045	1.252	1.479	0.655	0.831	1.018	1.216	1.432
30	0.942	1.147	1.363	1.588	1.83	0.925	1.124	1.33	1.546	1.772
50	1.172	1.386	1.615	1.851	2.11	1.147	1.359	1.582	1.813	2.068
70	1.39	1.615	1.843	2.091	2.364	1.363	1.581	1.807	2.052	2.313
	b_t = 10 m									
c (kPa)										
10	0.632	0.805	0.981	1.17	1.381					
30	0.901	1.094	1.288	1.489	1.709					
50	1.121	1.329	1.542	1.767	2.001					
70	1.333	1.544	1.767	2.005	2.256					

(J) Height of slope section, H = 40 m, Angle of inclination, i - 40°										
	b_t = 0					b_t = 2.5 m				
φ (deg)	15	20	25	30	35	15	20	25	30	35
c (kPa)										
10	0.53	0.671	0.82	0.969	1.132	0.518	0.655	0.789	0.934	1.095
30	0.776	0.929	1.092	1.261	1.441	0.755	0.907	1.065	1.226	1.404
50	0.986	1.154	1.325	1.502	1.697	0.962	1.127	1.289	1.465	1.66
70	1.185	1.361	1.539	1.734	1.93	1.16	1.327	1.505	1.685	1.88
	b_t = 5 m					b_t = 7.5 m				
c (kPa)										
10	0.499	0.622	0.753	0.895	1.052	0.47	0.588	0.715	0.842	0.981
30	0.73	0.879	1.025	1.182	1.358	0.702	0.838	0.979	1.13	1.281
50	0.933	1.087	1.246	1.42	1.598	0.899	1.044	1.199	1.357	1.526
70	1.124	1.287	1.455	1.628	1.819	1.083	1.241	1.396	1.564	1.751
	b_t = 10 m									
c (kPa)										
10	0.441	0.553	0.663	0.782	0.914					
30	0.668	0.795	0.927	1.058	1.202					
50	0.857	0.998	1.14	1.286	1.449					
70	1.04	1.185	1.334	1.497	1.659					

(K) Height of slope section, H = 40 m, Angle of inclination, i - 50°										
	b_t = 0					b_t = 2.5 m				
φ (deg)	15	20	25	30	35	15	20	25	30	35
c (kPa)										
10	0.425	0.526	0.633	0.75	0.877	0.403	0.503	0.604	0.708	0.824
30	0.649	0.769	0.891	1.024	1.165	0.62	0.733	0.854	0.975	1.102
50	0.842	0.97	1.108	1.247	1.393	0.806	0.933	1.057	1.187	1.331
70	1.015	1.162	1.3	1.45	1.616	0.981	1.114	1.249	1.392	1.535
	b_t = 5 m					b_t = 7.5 m				
c (kPa)										
10	0.379	0.467	0.559	0.658	0.769	0.348	0.429	0.516	0.6	0.69
30	0.585	0.694	0.802	0.912	1.033	0.549	0.652	0.744	0.848	0.956
50	0.766	0.882	0.998	1.123	1.26	0.752	0.845	0.937	1.058	1.168
70	0.943	1.058	1.185	1.311	1.45	0.945	1.037	1.122	1.23	1.364
	b_t = 10 m									
c (kPa)										
10	0.319	0.394	0.463	0.536	0.618					
30	0.517	0.605	0.693	0.78	0.876					
50	0.688	0.786	0.917	0.992	1.096					
70	0.902	0.939	1.11	1.201	1.339					

(L) Height of slope section, H = 40 m, Angle of inclination, i - 60°										
	b_t = 0					b_t = 2.5 m				
φ (deg)	15	20	25	30	35	15	20	25	30	35
c (kPa)										
10	0.346	0.425	0.502	0.586	0.679	0.32	0.39	0.465	0.541	0.623
30	0.548	0.646	0.743	0.843	0.951	0.519	0.601	0.692	0.786	0.883
50	0.731	0.833	0.933	1.046	1.168	0.758	0.81	0.887	0.977	1.085
70	0.993	1.01	1.119	1.23	1.356	0.952	1.05	1.082	1.199	1.292
	b_t = 5 m					b_t = 7.5 m				
c (kPa)										
10	0.29	0.353	0.417	0.486	0.561	0.264	0.318	0.375	0.436	0.493
30	0.486	0.564	0.641	0.724	0.815	0.449	0.515	0.587	0.663	0.749
50	0.652	0.777	0.834	0.943	1.038	0.608	0.681	0.762	0.859	0.955
70	0.816	0.948	1.046	1.148	1.25	0.748	0.841	0.917	1.042	1.137
	b_t = 10 m									
c (kPa)										
10	0.239	0.286	0.337	0.384	0.429					
30	0.415	0.475	0.539	0.609	0.686					
50	0.56	0.633	0.712	0.797	0.869					
70	0.708	0.788	0.879	0.939	1.046					

It is important to mention that deterministic LEM analyses have some inherent limitations. Such methods cannot encounter the uncertainties in geotechnical properties or the inherent spatial variation of soil properties, which may lead to erroneous cut slope designs resulting in failure of such slopes. To overcome the limitations of deterministic approach and gain more realistic understanding into the chances of failure of the cut slopes, a simplistic LEM based probabilistic approach is presented in the subsequent sections.

6.3. PROBABILISTIC LEM STUDY

In this study the minimum number of MCS required are investigated and it is found that 2000 number of MCS is sufficient for producing reliable and consistent results for all the slope geometry considered for the study. For example, the typical variation of probability of failure with number

of MCS realizations is shown in Fig. 6.2. It is observed that for a typical slope geometry (40 m height, 20 m crest width, and comprising horizontal width of toe excavation of 5 m), having a CoV of 0.4 for both the shear strength parameters (c and φ), 2000 number of MCS realizations are found to provide a convergent failure probability. Similar magnitude is obtained for other slope sections as well (not presented here for the sake of brevity), and hence, the same is adopted in present study.

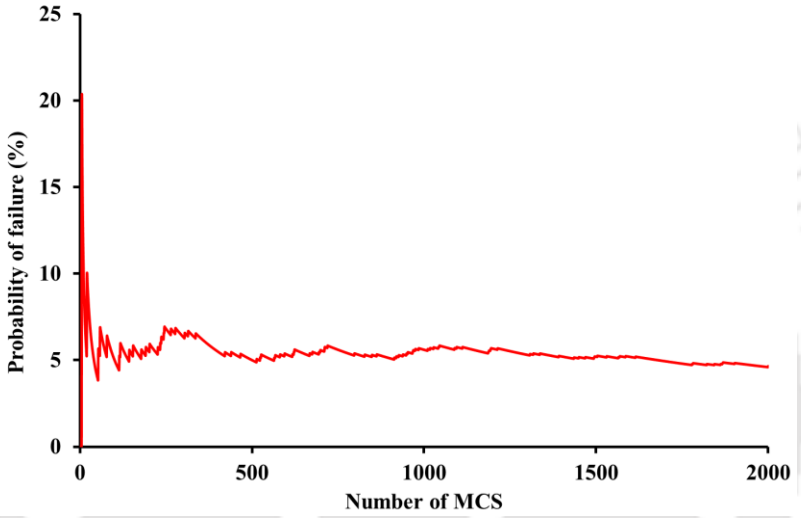

Fig. 6.2 Typical variation of the probability of failure with numbers of MCS realizations

The ranges of the soil shear strength parameters commonly encountered in the north-eastern hilly regions of India are already specified in Section 6.2. For the probabilistic analyses conducted in this section, a suitable mean value of cohesion, c, and angle of internal friction, φ, were considered as 40 kPa and 27.5º, respectively, which are well within the specified ranges of the corresponding parameters. For the chosen parameters, the different magnitudes of coefficient of variation (CoV) considered are 0.2, 0.3 and 0.4, respectively. The probability of failure (P_f) and corresponding reliability index (RI), along with deterministic factor of safety (FoS), are reported in Table 6.2. The table highlights that slopes which are considered perfectly safe from a deterministic analysis

can also be subjected to failure, as indicated by their probability of failure and reliability indices. For example, for the test slope having height (H) of 20 m, an inclination of 40º and a CoV of 0.4 for the shear strength parameters, a horizontal extent of toe cutting (b_t) of 5 m results in a high probability of failure of 8.74%, whereas the deterministic study predicts a safe cut slope with a FoS of 1.505.

The probability of failure (P_f) of any geotechnical system and their desired performance levels are presented in Table 2.1. Geotechnical designs prefer a Reliability Index (β) value of at least 2 (i.e., P_f <0.023) for desired performance level better than 'poor'. Considering the performance level of the cut slopes as per Table 2.1, the cut slopes having performance level 'below average' are marked red in Table 6.2.

Table 6.2: Comparison of the deterministic and probabilistic stability analyses of slopes with varying geometry and toe-excavation widths

Coefficient of Variation (CoV)	Slope inclination i (º)	Width of toe-excavation b_t (m)	Probability of failure P_f (%)	Reliability index RI	Deterministic FoS
		Height of slope section (H) = 20 m			
0.2	30	0	0	3.496	2.147
0.2	30	2.5	0	3.371	2.09
0.2	30	5	0.05	3.235	1.992
0.2	30	7.5	0.1	3.087	1.886
0.2	30	10	0.151	2.768	1.725
0.2	40	0	0.15	2.789	1.737
0.2	40	2.5	0.25	2.582	1.643
0.2	40	5	0.6	2.211	1.505
0.2	40	7.5	2.6	1.741	1.359
0.2	40	10	14.66	0.98	1.197
0.2	50	0	0.823	2.104	1.468
0.2	50	2.5	3.62	1.628	1.34
0.2	50	5	8	1.325	1.255

Coefficient of Variation (CoV)	Slope inclination i (°)	Width of toe-excavation b_t (m)	Probability of failure P_f (%)	Reliability index RI	Deterministic FoS
0.2	50	7.5	43.1	0.235	1.05
0.2	50	10	71.14	-0.563	0.933
0.2	60	0	7.31	1.405	1.265
0.2	60	2.5	14.5	1.015	1.184
0.2	60	5	55.81	-0.075	0.996
0.2	60	7.5	82.79	-0.975	0.886
0.2	60	10	93.92	-1.629	0.819
0.3	30	0	0.05	2.619	2.147
0.3	30	2.5	0.05	2.546	2.09
0.3	30	5	0.1	2.431	1.992
0.3	30	7.5	0.3	2.289	1.886
0.3	30	10	0.727	2.008	1.725
0.3	40	0	0.65	2.056	1.737
0.3	40	2.5	1.35	1.88	1.643
0.3	40	5	3.6	1.585	1.505
0.3	40	7.5	10.62	1.199	1.359
0.3	40	10	29.89	0.599	1.197
0.3	50	0	5.39	1.472	1.468
0.3	50	2.5	14.48	1.067	1.34
0.3	50	5	18.08	0.905	1.255
0.3	50	7.5	53.87	0.005	1.05
0.3	50	10	74.33	-0.685	0.933
0.3	60	0	19.85	0.92	1.265
0.3	60	2.5	26.25	0.676	1.184
0.3	60	5	62.11	-0.226	0.996
0.3	60	7.5	82.78	-0.989	0.886
0.3	60	10	92.62	-1.502	0.819
0.4	30	0	0.2	2.21	2.147
0.4	30	2.5	0.2	2.164	2.09
0.4	30	5	0.45	2.054	1.992
0.4	30	7.5	0.95	1.911	1.886
0.4	30	10	2.65	1.633	1.725
0.4	40	0	2.3	1.703	1.737
0.4	40	2.5	4.15	1.539	1.643
0.4	40	5	8.74	1.263	1.505
0.4	40	7.5	21.03	0.871	1.359
0.4	40	10	37.98	0.388	1.197
0.4	50	0	11.87	1.141	1.468
0.4	50	2.5	25.42	0.732	1.34
0.4	50	5	26.84	0.676	1.255

Coefficient of Variation (CoV)	Slope inclination i (°)	Width of toe-excavation b_t (m)	Probability of failure P_f (%)	Reliability index RI	Deterministic FoS
0.4	50	7.5	60.04	-0.16	1.05
0.4	50	10	80.17	-0.845	0.933
0.4	60	0	30.13	0.594	1.265
0.4	60	2.5	34.07	0.481	1.184
0.4	60	5	68.49	-0.372	0.996
0.4	60	7.5	84.87	-1.107	0.886
0.4	60	10	93.09	-1.571	0.819
Height of slope section (H) = 30 m					
0.2	30	0	0.05	2.826	1.824
0.2	30	2.5	0.05	2.751	1.791
0.2	30	5	0.1	2.716	1.75
0.2	30	7.5	0.15	2.585	1.692
0.2	30	10	0.3	2.453	1.618
0.2	40	0	1.1	2.011	1.45
0.2	40	2.5	1.95	1.829	1.397
0.2	40	5	3.9	1.595	1.333
0.2	40	7.5	8.42	1.282	1.246
0.2	40	10	19.5	0.884	1.153
0.2	50	0	11.76	1.129	1.213
0.2	50	2.5	23.23	0.76	1.133
0.2	50	5	40.79	0.305	1.047
0.2	50	7.5	47.95	0.141	1.005
0.2	50	10	89.12	-1.263	0.869
0.2	60	0	46.85	0.135	1.019
0.2	60	2.5	60.55	-0.22	0.949
0.2	60	5	95.4	-1.781	0.858
0.2	60	7.5	97.04	-1.982	0.777
0.2	60	10	99.27	-2.677	0.715
0.3	30	0	0.35	2.253	1.824
0.3	30	2.5	0.4	2.096	1.791
0.3	30	5	0.55	2.053	1.75
0.3	30	7.5	0.85	1.951	1.692
0.3	30	10	1.6	1.83	1.618
0.3	40	0	5.35	1.473	1.45
0.3	40	2.5	7.9	1.337	1.397
0.3	40	5	11.35	1.157	1.333
0.3	40	7.5	20.31	0.879	1.246
0.3	40	10	31.38	0.55	1.153
0.3	50	0	23.72	0.781	1.213
0.3	50	2.5	34.12	0.479	1.133

Coefficient of Variation (CoV)	Slope inclination i (°)	Width of toe-excavation b_t (m)	Probability of failure P_f (%)	Reliability index RI	Deterministic FoS
0.3	50	5	48.74	0.105	1.047
0.3	50	7.5	52.89	-0.022	1.005
0.3	50	10	88.45	-1.245	0.869
0.3	60	0	54.31	-0.049	1.019
0.3	60	2.5	63.77	-0.344	0.949
0.3	60	5	94.47	-1.687	0.858
0.3	60	7.5	94.36	-1.715	0.777
0.3	60	10	97.38	-2.157	0.715
0.4	30	0	1	1.84	1.824
0.4	30	2.5	1.25	1.792	1.791
0.4	30	5	1.8	1.739	1.75
0.4	30	7.5	2.65	1.651	1.692
0.4	30	10	4.3	1.529	1.618
0.4	40	0	10.55	1.204	1.45
0.4	40	2.5	13.5	1.087	1.397
0.4	40	5	19.15	0.929	1.333
0.4	40	7.5	28.49	0.652	1.246
0.4	40	10	40.37	0.328	1.153
0.4	50	0	30.76	0.584	1.213
0.4	50	2.5	41.97	0.302	1.133
0.4	50	5	55.59	-0.071	1.047
0.4	50	7.5	58.69	-0.181	1.005
0.4	50	10	91.35	-1.405	0.869
0.4	60	0	61.74	-0.239	1.019
0.4	60	2.5	68.46	-0.508	0.949
0.4	60	5	95.1	-1.713	0.858
0.4	60	7.5	94.13	-1.712	0.777
0.4	60	10	95.9	-2.021	0.715
Height of slope section (H) = 40 m					
0.2	30	0	0.2	2.426	1.651
0.2	30	2.5	0.25	2.367	1.63
0.2	30	5	0.4	2.296	1.604
0.2	30	7.5	0.5	2.21	1.572
0.2	30	10	0.65	2.146	1.525
0.2	40	0	5.9	1.422	1.295
0.2	40	2.5	8	1.298	1.265
0.2	40	5	11.3	1.156	1.222
0.2	40	7.5	18.6	0.897	1.17
0.2	40	10	29.74	0.602	1.107
0.2	50	0	36.7	0.397	1.067

Coefficient of Variation (CoV)	Slope inclination i (°)	Width of toe-excavation b_t (m)	Probability of failure P_f (%)	Reliability index RI	Deterministic FoS
0.2	50	2.5	49.85	0.106	1.019
0.2	50	5	62.7	-0.241	0.965
0.2	50	7.5	74.39	-0.681	0.897
0.2	50	10	90.22	-1.355	0.845
0.2	60	0	77.37	-0.738	0.897
0.2	60	2.5	88.77	-0.1278	0.833
0.2	60	5	98.42	-2.427	0.778
0.2	60	7.5	99.94	-2.798	0.736
0.2	60	10	100	-4.778	0.655
0.3	30	0	1.25	1.843	1.651
0.3	30	2.5	1.5	1.798	1.63
0.3	30	5	1.95	1.743	1.604
0.3	30	7.5	2.35	1.676	1.572
0.3	30	10	3.35	1.601	1.525
0.3	40	0	15.1	1.029	1.295
0.3	40	2.5	18.2	0.932	1.265
0.3	40	5	22.65	0.81	1.222
0.3	40	7.5	30.42	0.61	1.17
0.3	40	10	38.97	0.37	1.107
0.3	50	0	45.6	0.209	1.067
0.3	50	2.5	54.58	-0.02	1.019
0.3	50	5	64.19	-0.297	0.965
0.3	50	7.5	74.84	-0.71	0.897
0.3	50	10	89.63	-1.31	0.845
0.3	60	0	75.13	-0.678	0.897
0.3	60	2.5	86.45	-1.131	0.833
0.3	60	5	97.28	-2.151	0.778
0.3	60	7.5	99.24	-2.411	0.736
0.3	60	10	100	-4.102	0.655
0.4	30	0	3.35	1.57	1.651
0.4	30	2.5	3.95	1.531	1.63
0.4	30	5	4.65	1.483	1.604
0.4	30	7.5	5.5	1.424	1.572
0.4	30	10	7.2	1.351	1.525
0.4	40	0	22.7	0.822	1.295
0.4	40	2.5	26.2	0.738	1.265
0.4	40	5	29.6	0.62	1.222
0.4	40	7.5	36.29	0.439	1.17
0.4	40	10	45.78	0.222	1.107
0.4	50	0	50.6	0.081	1.067

Coefficient of Variation (CoV)	Slope inclination i (º)	Width of toe-excavation b_t (m)	Probability of failure P_f (%)	Reliability index RI	Deterministic FoS
0.4	50	2.5	58.24	-0.124	1.019
0.4	50	5	66.44	-0.372	0.965
0.4	50	7.5	79.35	-0.856	0.897
0.4	50	10	91.36	-1.461	0.845
0.4	60	0	76.36	-0.734	0.897
0.4	60	2.5	87.76	-1.204	0.833
0.4	60	5	98.24	-2.356	0.778
0.4	60	7.5	98.94	-2.375	0.736
0.4	60	10	100	-4.014	0.655

6.4. EFFECT OF COEFFICIENT OF VARIATION (CoV)

A typical slope section of 40 m height and 40° inclination is adopted for the study. The mean value of cohesion, c, and angle of internal friction, φ, considered are 40 kPa and 27.5º, respectively. Figure 6.3 exhibits the results obtained from present study, in terms of reliability index (β) and probability of slope failure (P_f), for different CoV of soil shear strength parameters and horizontal extent of toe cutting (b_t). It is noticed that failure probability largely depends on the CoV of shear strength parameters for all the cases of toe excavations. Analyses with maximum CoV result in higher probability of failure and lower reliability index. This is because with the increase in CoV, the c and φ values become more scattered from their mean value over the analysis domain, and, hence, the P_f increases. Based on the results obtained, it is seen that the virgin slope itself has very high probability of failure (P_f) varies from approximately 6-23% for CoV range of 0.2-0.4). Therefore, toe cutting is not at all recommended for the chosen slope section under aforementioned conditions based on the probabilistic LEM study. On the other hand, the deterministic study indicated the cut slope to fail for low values of soil shear strength parameters, while for higher values of soil shear strength parameters, a toe cutting of maximum horizontal extent of 10 m with proper safety measures was recommended. Hence, comparing the results from deterministic and

probabilistic studies, it is well understood that the simplifying assumption of soil to be homogeneous in deterministic study may result in erroneous cut slope design.

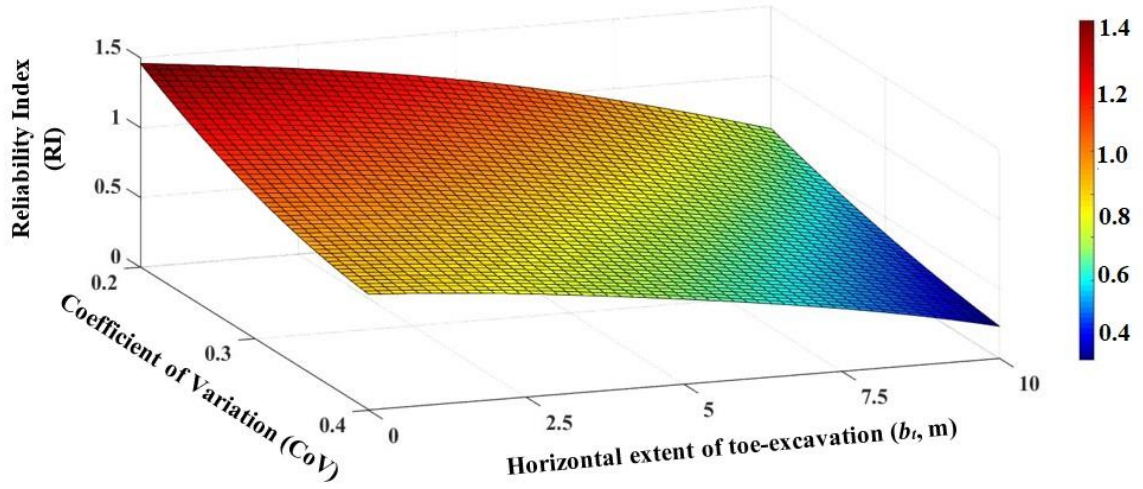

(a)

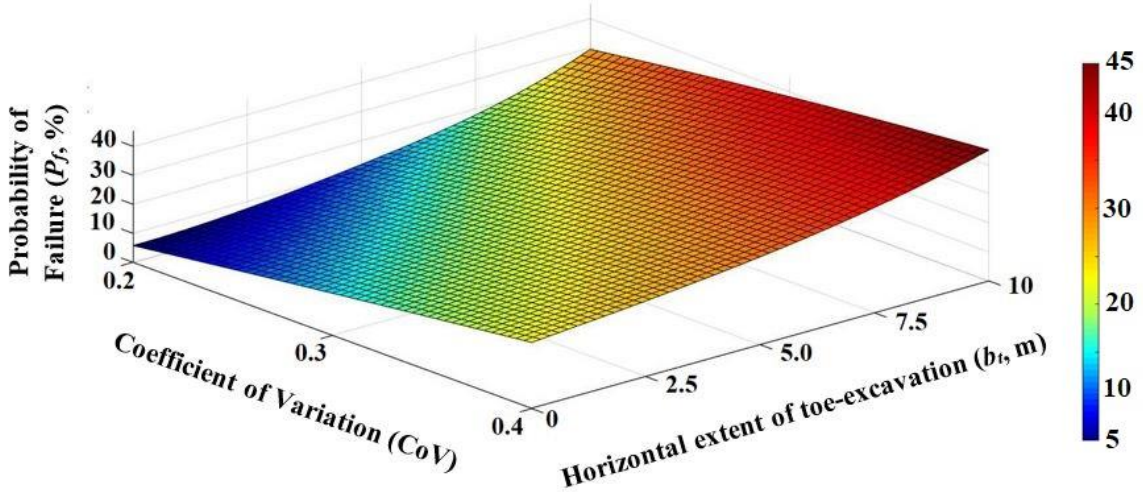

(b)

Fig. 6.3 Variation of (a) reliability index and (b) probability of failure with the horizontal extent of toe excavation and CoV of shear strength parameters

6.5. EFFECT OF SLOPE INCLINATION

To study the effect of slope inclination, a few analyses were carried out with the same mean values for cohesion, c, and angle of internal friction, φ, for a typical slope section having height of 40 m

with CoV value of 0.2. Figure 6.4 exhibits the results obtained from these analyses. It is seen that the inclination of the virgin slope (i) has high impact on the horizontal extent of vertical toe cutting (b_t) that can be adopted in hill slopes. For slope inclination (i) of 30°, a horizontal extent of toe cutting of 10 m can be carried out with very low probability of failure (0.8%); whereas, for higher slope inclinations (i > 30°), the virgin slopes tend to fail (Fig. 6.4) under aforementioned condition. Hence, toe cutting in such conditions (i > 30°) are not at all recommended without adequate safety measures.

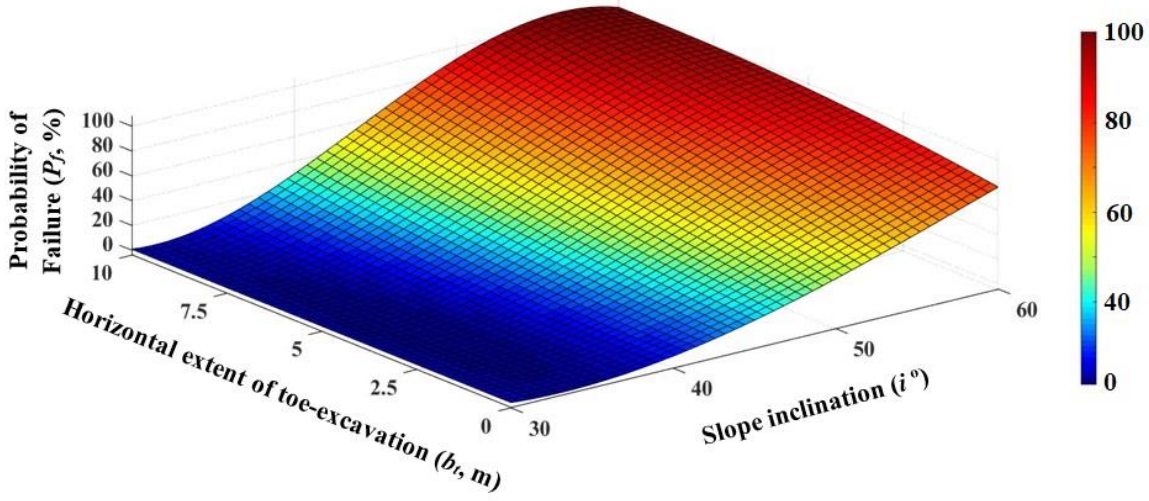

Fig. 6.4 Variation of probability of failure with horizontal extent of vertical toe cutting and slope inclination for CoV = 0.2 against the mean shear strength parameters

6.6. EFFECT OF CORRELATION COEFFICIENT

A thorough knowledge of the actual correlations between the shear strength parameters of the hill-slope soils are extremely important for conducting a practical probabilistic slope stability analysis.

This attempt would provide a clear picture about the realistic stability of the slope and indicating the possible requirement of a retention system. Such realistic stability results are not exhibited through deterministic analysis of approximated homogeneous slopes, which in many cases lead to either a failed slope or an uneconomical and massive retention system.

Based on the above discussion, the influence of the correlation coefficient on the stability of the earlier described slope section (H = 40 m, i = 40°) is assessed. In this case, only a CoV of 0.2 is considered for the shear strength parameters with their mean values as considered in previous sections. The same chosen section is analyzed for different correlation coefficients (ranging from -0.5 to +0.5) relating c and φ. Figure 6.5 shows the variation in the probability of failure and reliability index with the correlation coefficient and horizontal extent of toe cutting (b_t). It is found that as the soil properties become more negatively correlated, the probability of failure decreases (reliability index increases), which is in consent with the findings by the previous researches (Griffiths et al., 2009; Griffiths et al., 2011). For better clarity, the variation in the probability of failure with the horizontal extent of toe cutting has been explicitly highlighted for specific values of correlation coefficient (Fig. 6.6). It can be clearly noted that the choice of correlation coefficient has noticeable influence on the slope stability in a probabilistic framework. The actual choice of the correlation coefficient for a practical slope stability problem is governed by the spatial distribution of the shear strength properties of the slope soil. The results indicate the requirement of utmost importance of good field investigation to assess the correlation between soil parameters in the slope. It is inadvertent that based on the assessed correlation, the estimated failure probability of a specific slope would be meaningful which can pave a scientific design of such cut slopes in the hilly terrain.

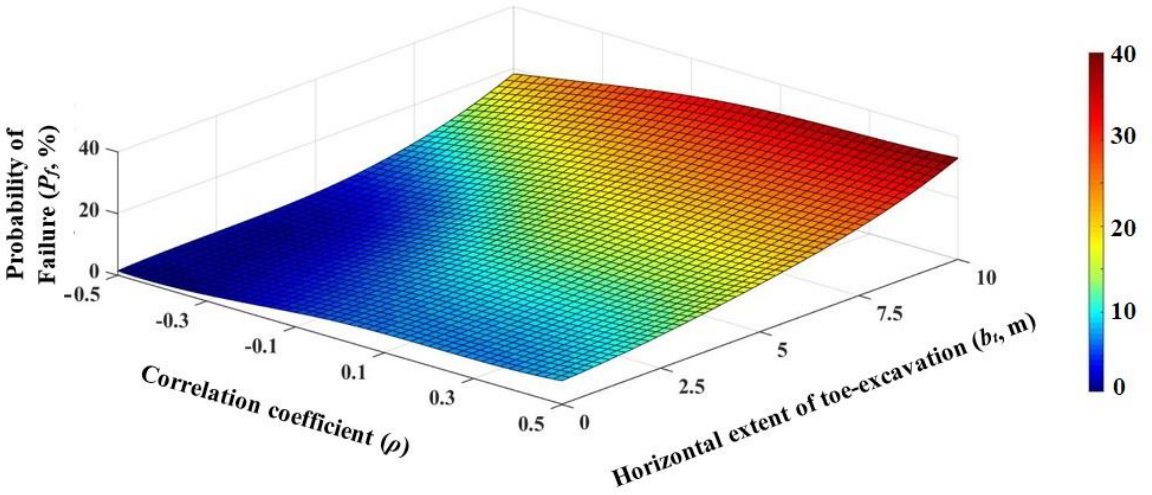

(a)

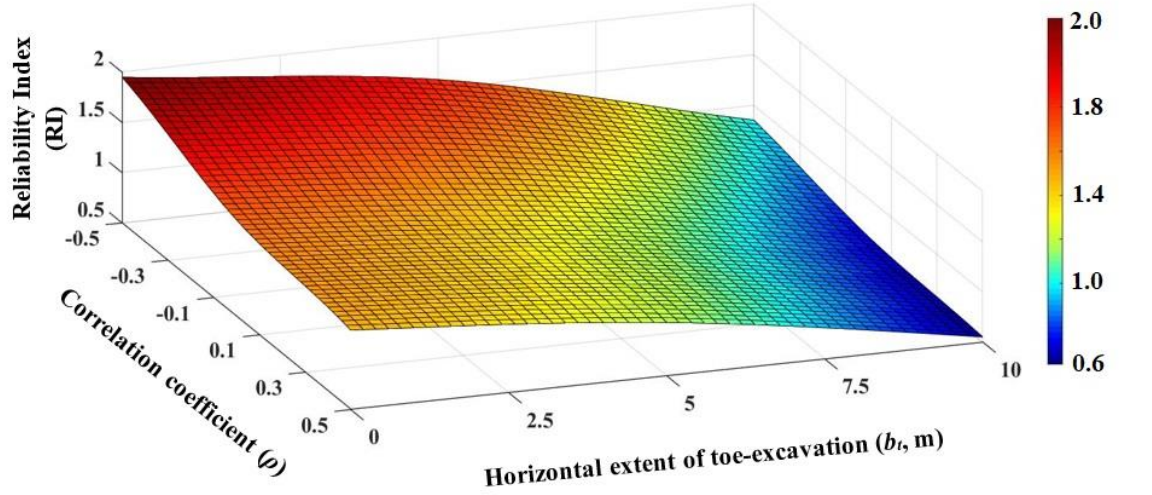

(b)

Fig. 6.5 Variation in the (a) probability of failure (b) reliability index with correlation coefficient for varying extent of toe excavation

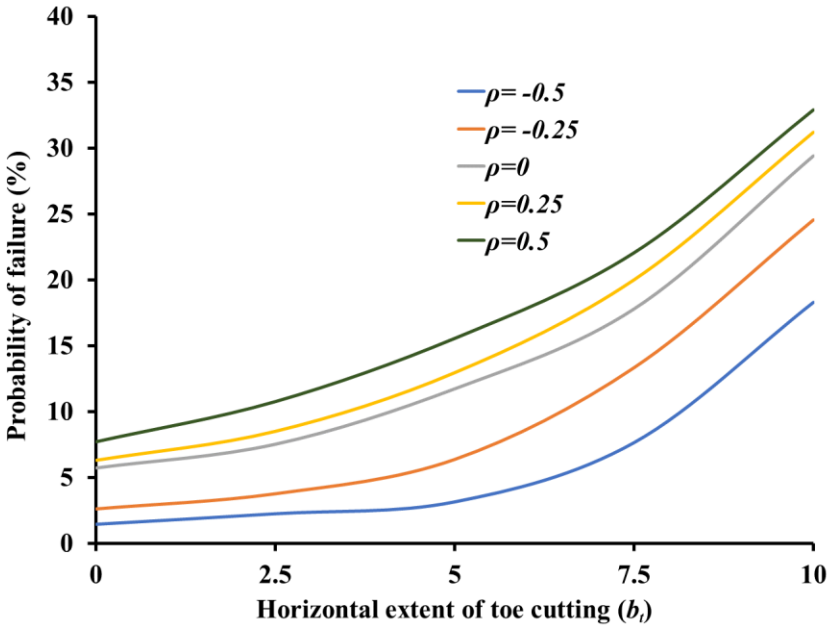

Fig. 6.6 Line diagram showing the variation of probability of failure with correlation coefficient (ρ) for varying extent of toe cutting

6.7. INFLUENCE OF CORRELATION LENGTH AND SPATIAL VARIATION OF SOIL SHEAR STRENGTH PARAMETERS

The application of 1D spatial variation of soil properties in horizontal direction can be found in geotechnical problems such as braced excavations in soft clays considering spatial variation of soil shear strength parameters (Luo et al., 2018), rainfall-induced landslides considering spatial variation of hydraulic conductivity and shear strength parameters (Cho, 2014; Dou et al., 2015; Nguyen et al., 2014), stability of tailing dyke on pre-sheared clay-shale considering spatial variability of shear strength and pore-pressure parameters (El-Ramly et al., 2003), and dynamic response of zoned earthen dam considering spatial variability of shear strength parameters (DeWolfe et al., 2010). In the present study, the incorporation of one-dimensional spatial variation in horizontal direction for slope stability analysis has been carried out based on the concepts

presented by Vanmarcke (1983) and El-Ramly et al. (2002, 2005), as discussed in Section 5.4 of Chapter 5. Although few studies, as mentioned above, has been carried out incorporating 1-D spatial variability of soil properties (mostly on hydraulic conductivity) for rainfall-induced landslide analysis, yet no such studies incorporating 1D spatial variability are reported in the context of hillslope instability induced by toe-excavations.

Therefore, this section reports the influence of one dimensional spatial variation of soil properties on the cut slope stability. For different horizontal extent of vertical toe cutting, Fig. 6.7 shows the three-dimensional (3D) variation of the probability of failure and reliability index in terms of the dimensionless correlation length ($\Theta = \theta / L$, where L is the length of slope in the horizontal direction as shown in Fig. 6.1). Very small correlation length (represent extremely erratic random field) and very large correlation length (representing sufficiently homogeneous field) have lesser practical significance, while the intermediate range of correlation length is of prime interest to the geotechnical engineers (Griffiths et al., 2007). Therefore, in this section, a one-dimensional random field is generated for each MCS by incorporating spatial variation of soil properties in the horizontal direction using correlation length. In this study, the dimensionless correlation length (Θ) is varied from 0.1 to 1. For better clarity, for the virgin slope, the variation of probability of failure with dimensionless correlation length has been explicitly highlighted for specific values of the horizontal extent of toe cutting (Fig. 6.8) for various magnitudes of CoV (0.2, 0.3 and 0.4). It is observed that the failure probability increases rapidly (reliability index decreases) with increase in correlation length. The failure probability is negligible when the correlation length is very small. This is because, for small correlation lengths, the soil properties tend to take their mean values. Now, as the virgin slope is safe for its mean value of shear strength parameters, the failure

probability is very less (negligible). The failure probability is highest when dimensionless correlation length is equal to unity, indicating the entire soil domain as homogeneous for all the MCS iterations, with different values of shear strength in different iteration. Hence, it is seen that ignoring spatial variability may result in underestimation or overestimation of failure probability depending on its correlation length. This trend is observed for all the cut slopes as shown in Fig. 6.7.

Based on the results from several analyses, the following can be stated regarding toe excavation for the slope considered in the present study:

(a) For CoV = 0.2, a maximum horizontal extent of 7 m can be excavated without leading to slope failure if $\Theta \leq 0.2$, beyond which toe excavation is not recommended (for $\Theta > 0.2$).

(b) For CoV = 0.3, a maximum horizontal extent of 5 m can be excavated without leading to slope failure if $\Theta \leq 0.1$, beyond which toe excavation is not recommended ($\Theta > 0.1$).

(c) For, CoV = 0.4, toe excavation is not recommended at all, as the virgin slope itself has a high probability of failure.

The observed results clearly indicate that depending upon the actual CoV and correlation length, the stability analysis of the same slope would yield different outcomes. Hence, the outcomes clearly highlight that it is extremely important to conduct elaborate field investigation to ascertain the spatial variation of the soil shear strength parameters. This would be useful for specific cases of assessment of slope stability on a probabilistic framework, in which a meaningful site-specific correlation length can be considered for the practical purpose.

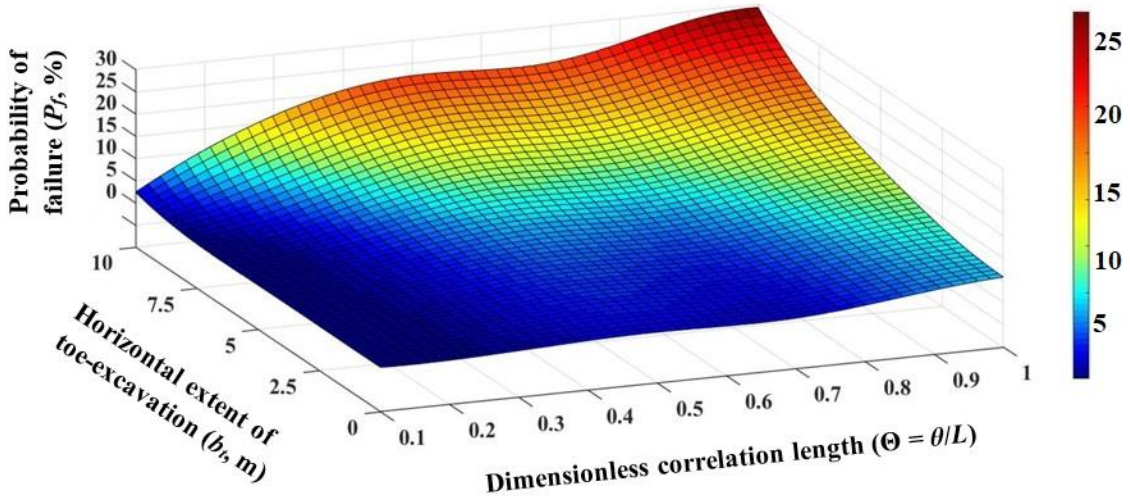

(a1)

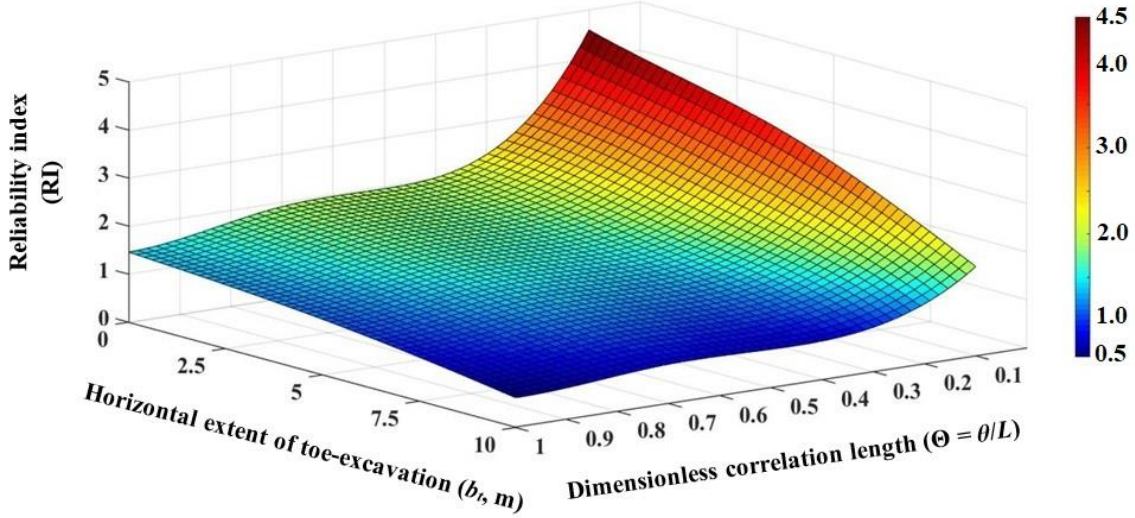

(a2)

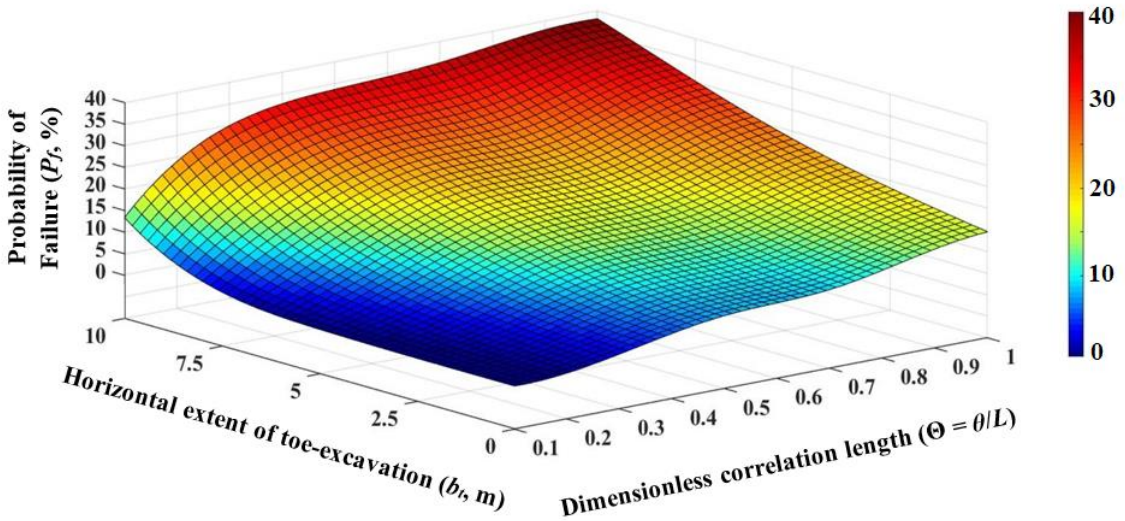

(b1)

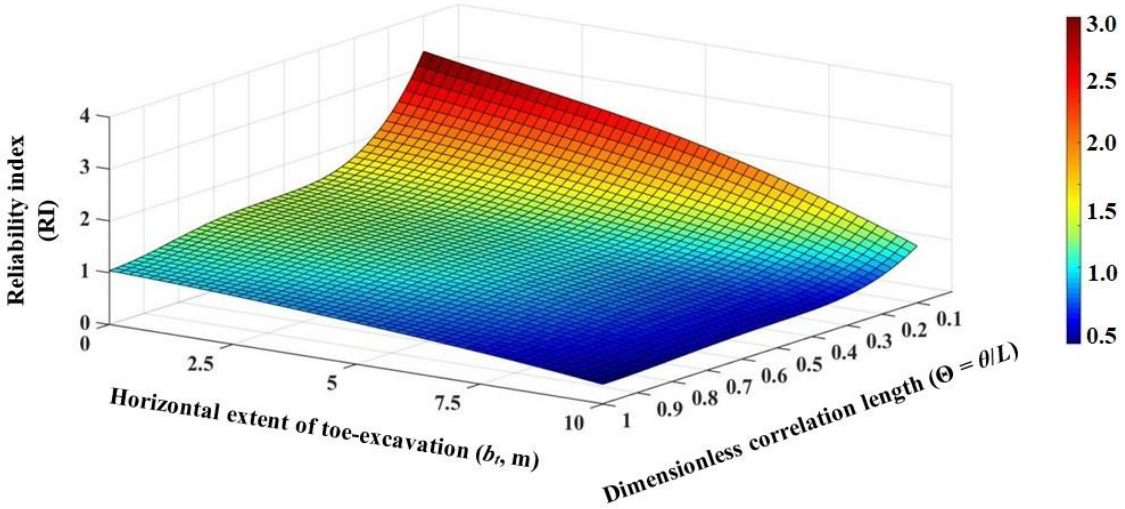

(b2)

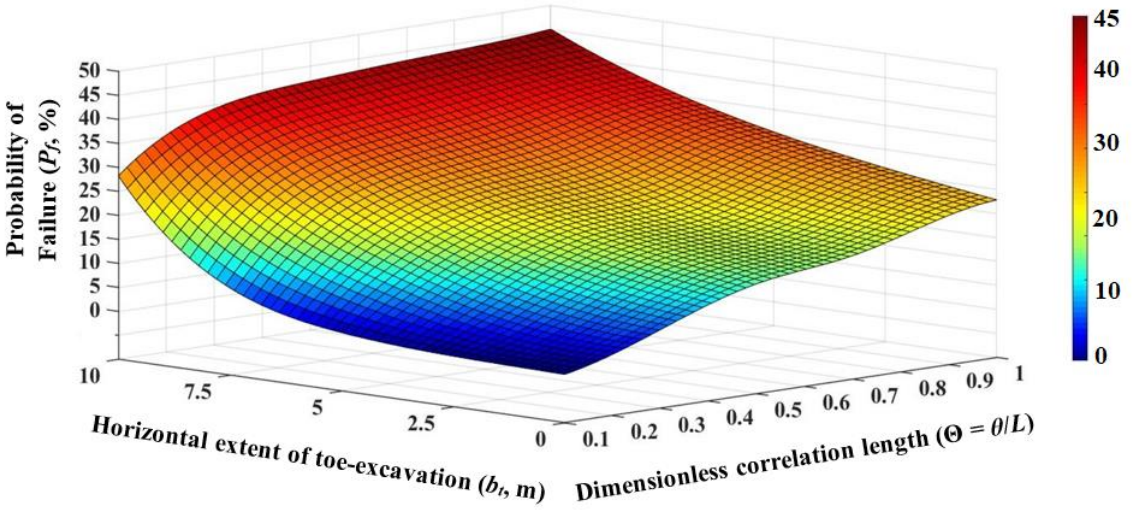

(c1)

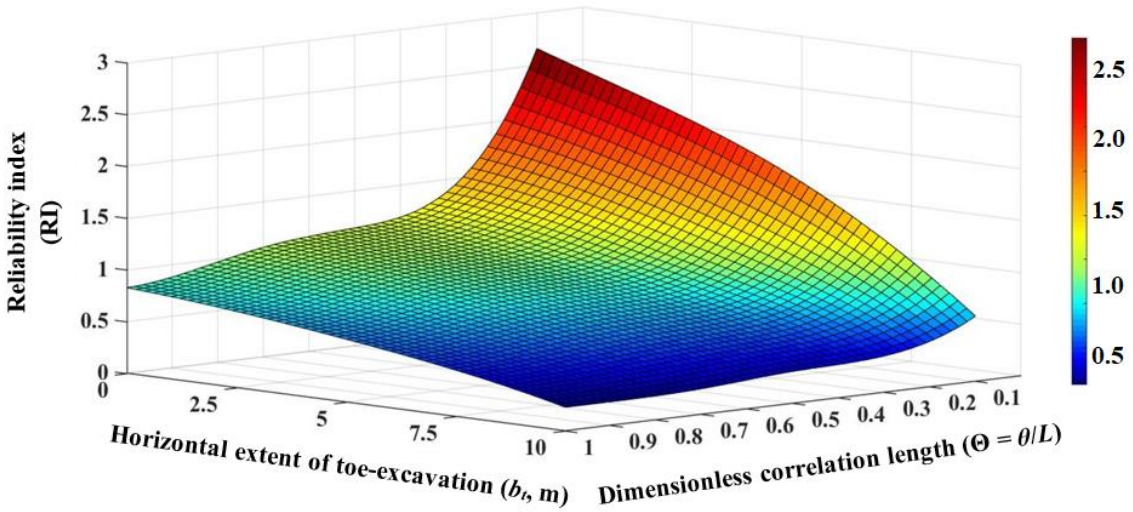

(c2)

Fig. 6.7 Variation in the probability of failure and reliability index with dimensionless correlation length ($\Theta = \theta/L$) for various horizontal extent of vertical toe cutting (a1, a2) CoV = 0.2 (b1, b2) CoV = 0.3 (c1, c2) CoV=0.4

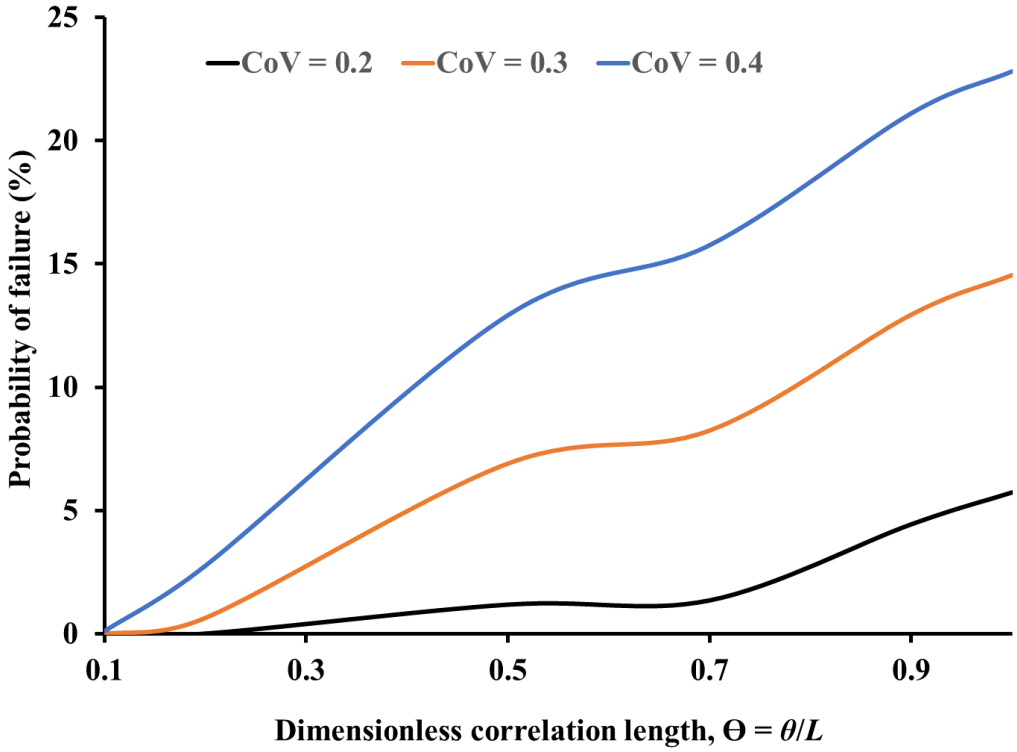

Fig. 6.8 Variation in the probability of failure with dimensionless correlation length ($\Theta = \theta/L$) for the virgin slope section chosen for the present study

It is worth mentioning that the present study is limited to only assigning 1D random field by sampling the soil domain for a specific distance in horizontal direction. However, it is well known that soil exhibits inherent variation in both the horizontal and vertical direction. Therefore, characterizing soil domain with 1D spatial variation may not simulate the actual field condition appropriately. Nonetheless, this approach can be essentially considered applicable for those residual hill-slopes that are mostly characterized by predominantly single soil layer with spatially distributed properties in horizontal direction and insignificant spatial variation in the vertical direction. To cater the probabilistic study of effect of toe excavation of hill slopes comprising variation of soil properties in both horizontal and vertical, a 2D random field can be generated to simulate the field condition better using more advanced methods by the means of random field

theory. A detailed study of the effect of toe cutting on hill slope stability using RFEM is further presented in Chapter 8 of this thesis.

Although probabilistic analysis in various fields of geotechnical engineering have taken huge leaps, yet it is very much necessary that simplistic methods are adopted to gain knowledge and understanding to the application of the same in design practices. The work presented here is simplified enough to get a good understanding of the outcomes of toe excavation of hill-slopes form a probabilistic framework. Deterministic analysis of assumed homogeneous slopes might bring misfortune in real cases of expansion of transportation networks in hilly terrains. Hence, this study provides a good insight into the chances of failure of toe-excavated hillslopes even when the deterministic analysis may adjudge them to be complete safe. Such scenarios are quite common in the hillslopes of north-eastern India, and such studies give a sense of caution and necessitate the requirement for better design practices.

Furthermore, although the present study has primarily addressed the hilly terrains of north-eastern India, given the range of parameters considered in the present study, the developed methodology for assessing the instability due to the excavation of the hillslope toe is equally applicable for any residual and lateritic soil slope situated anywhere in India or even around the world. It is to be noted that in the present study, the considered slope geometry is much simplified representation of the complex geometries of soil slope commonly encountered in practice. Most of the slopes in practice will comprise undulating geometry with noticeable changes in the slope inclinations, formations of concave, straight or convex curvatures, and presence of convergent, parallel or divergent plan shapes (Sabzevari and Noroozpour, 2014). It is worth mentioning that the

fundamental methodology and the proposition of the LEM-based probabilistic approach presented in this chapter for slopes with simplified geometry yet remains valid for the slopes with complex geometries as long as the geometry is properly represented in the numerical model. The presence of complex geometries might yield stability outcomes of different magnitude based on the toe-excavations, but nonetheless the proposed concept and methodology remains effective for natural slopes having undulating curvatures and plan shapes.

It is also worth mentioning that along with the uncertainties involved with the shear strength parameters, the uncertainties in slope geometry and water table location should also be considered as important factors affecting the cut slope instability in hilly terrains. The uncertainty in slope geometry primarily encompasses the uncertainty in slope inclination and presence of complex slope profiles. Based on the fundamentals of slope stability, given the interdependency of the soil shear strength parameters and slope inclination, a steeper slope is always expected to develop instability. In this study, although the uncertainties in the slope inclination is not directly incorporated, the effect of the slope inclination on both deterministic and probabilistic studies are presented with expected outcomes. The presence of water table in a hillslope leads to the saturation of soil below the phreatic line. Further, the inclination of the water table governs the severity of the seepage forces which the hillslopes may experience. Hence, given that both the stated factors are detrimental to the stability of a hillslope, the uncertainties associated with the location of intersection of the water table with the slope face and the inclination of the water table are supposed to influence the probability of failure of a hillslope. On a deterministic basis, the influence of the above two factors are well illustrated in earlier literature (Chakraborty and Dey, 2016 a,b,c). Thus, the uncertainties associated with the slope geometry and the location of water table are supposed

to influence the probability of slope failure. However, the present study presumed the slope geometry to be deterministic and the slope to be dry and devoid of the presence of water table. Accordingly, the uncertainties involved only with the shear strength parameters are considered in the present study, leaving behind the future scopes to incorporate the uncertainties in complex slope geometries and hydraulic conditions commonly encountered in the hillslopes.

6.8. SUMMARY

This chapter reports the influence of toe excavation on the stability of hill slopes in a probabilistic framework. Initially, a deterministic LEM-based study is conducted, using Slope/W module of GeoStudio v2018, for a wide range of soil shear strength parameters for various slope sections. Next, an LEM based probabilistic study is conducted in Slope/W considering the soil shear strength parameters as random variable to address the uncertainty related to soil shear strength. This chapter also presents a comparative study between the LEM based deterministic and probabilistic analysis for slope sections subjected to toe excavation operation. The effect of CoV of the soil shear strength parameters, and their cross-correlation ($\rho_{c\varphi}$) on the computation of failure probability of toe excavated slope section having various inclinations are also investigated. The influence of spatial variation of soil shear strength parameters on failure probability of toe excavated slope sections are also reported in this chapter.

CHAPTER 7

PROBABILISTIC ASSESSMENT OF TOE-EXCAVATED HILL SLOPE SUPPORTED BY SHEET PILE WALL OR SHEET-PILE-ANCHOR RETENTION SYSTEM

7.1. GENERAL

This chapter illustrates and highlights the adoption of a probabilistic framework for incorporating a Sheet-Pile (SP) and Sheet-Pile-Anchor retention (SPAR) system adopted as a measure of mitigating the movement and failure of a toe-excavated slope. The probabilistic method adopted in the study is effective in assessing the response of the retention system while considering the uncertainties in the soil shear-strength parameters and their spatial distribution in the hill-slope. The virgin slope is first investigated for its natural in-situ stability using Finite Element (FE) analysis using coupled Sigma/W-Slope/W analysis. Further, the SPAR system is introduced as a mitigation measure along with stage-wise excavation of the toe, and the response of the same is investigated through FE analysis. At each stage, the probability of failure of the virgin or the toe-excavated retained slope is estimated while considering uncertainty in soil shear-strength parameters. It is found that with detailed analysis and prediction of failure probability, a stable toe excavation in slope can be designed with proper mitigation system. However, most of the literatures available on effect of toe cutting on hill slope stability till now deals with the slope stability problem deterministically. Very few literatures are available in geotechnical engineering which encounter probabilistic study of reinforced slopes. A brief literature survey is presented in Chapter 2 under Section 2.5 of this thesis.

This chapter is an extension of the LEM based probabilistic study of the excavated slopes in Chapter 6, where the methodology of incorporating probabilistic concepts to study the effect of toe cutting on hill slopes is developed. In this chapter, investigation is carried out for safe design of cut slopes with the help of sheet pile anchor system. The analysis is first carried out for unreinforced slope using FE method in Sigma/W module of the GeoStudio and the stress generated in Sigma/W is incorporated in Slope/W for estimation of failure probability. In the next phase, a sheet pile anchor system is introduced as a retention for the cut slope in Sigma/W and then coupled with Slope/W for computation of failure probability at different stages of slope toe excavation and reinforcement installation. Analysis shows that with the correct prediction of failure probability, a safe cut slope can be designed with proper retention system.

7.2. NUMERICAL MODELLING

Generally, for achieving more carriageway of roadways, vertical or inclined cuts on natural slopes are commonly practiced in the hilly terrains, as mentioned in Section 6.2 of Chapter 6. In the north-eastern and many other regions of the country, the existence of lateritic soils make the slopes eligible to sustain near-vertical cuts during the dry periods of the year, during which the roadway extension projects are mainly mobilized. Therefore, this chapter deals with only vertical toe excavation for achieving more carriageway. To study the effect of vertical toe cutting on hill slopes, a slope of 40 m height is considered (common in the northeastern region of India) that is inclined at 40° to the horizontal and overlying a hard rocky foundation. The shear strength properties of the soil (cohesion, c and angle of internal friction, φ) are considered, which follows a Mohr-Coulomb failure criterion. Figure 7.1 shows the schematic diagram of the adopted slope geometry.

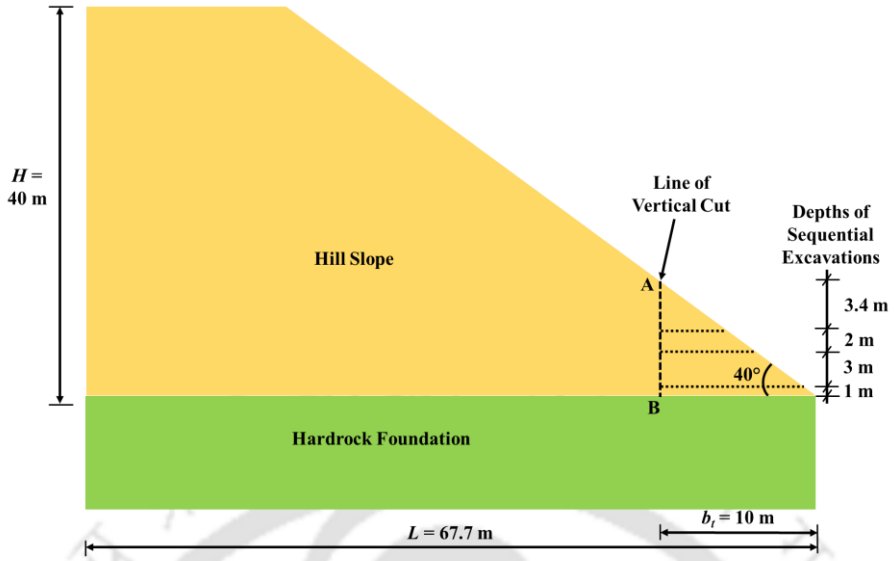

Fig. 7.1 Schematic diagram of chosen slope geometry showing the line of vertical cut through the toe and depths of sequential excavations

Deterministic study on the chosen slope, using Slope/W module of GeoStudio (v2018), is reported in Section 6.2 of Chapter 6 for a wide range of *c* and *φ* values (*c*: 0-80 kPa, *φ*: 15°-40°). The study summarized that the chosen slope is not at all suitable for toe excavation even in the dry condition for low *c* and *φ* values of hillslope material. For example, for *c* and *φ* value of 30 kPa and 15° respectively, the FoS of the virgin slope is 0.776. For slightly higher values of *c* and *φ,* toe excavation may be conducted subjected to proper retention for providing required safety against failure. For example, for *c* and *φ* value of 50 kPa and 20° respectively, the FoS of the cut slope for a vertical toe excavation of horizontal width of 5 m is 1.087. However, as mentioned earlier, deterministic LEM analyses cannot accommodate the uncertainties in geotechnical properties or inherent spatial variation of soil properties, which may lead to erroneous cut slope designs resulting in unwanted failure of such slopes. Therefore, to overcome such limitations, probabilistic concepts are entailed for proper assessment of geotechnical uncertainty resulting in reliable cut slope

designs. To consider the uncertainty, soil shear strength parameters (cohesion, c and angle of internal friction, φ) are assigned random values based on Lognormal Distribution function. The mean value of cohesion, c and angle of internal friction, φ, considered are 40 kPa and 27.5º respectively. The unit weight of soil is considered as deterministic and a value of 18 kN/m^3 is assigned. It is observed that probabilistic assessment of cut slope stability largely depends on coefficient of variation (CoV) of the shear strength parameters. The FEM based stability analyses of the virgin slope estimated a deterministic FoS of 1.472 against the critical failure surface (Fig. 7.2). However, for a relatively high CoV value of 0.4, toe cutting is not at all recommended as the virgin slope itself shows a high probability of failure (9.45%), and is best left undisturbed. However, keeping in mind the variability of material parameters encountered in the natural hillslopes of the northeastern region, many practical circumstances demand excavation even in those slopes that are potentially unstable. Hence, this study emphasizes on the aspect of unavoidable toe excavation in weaker slopes, sufficed by a proper retention measure and analyzed from a probabilistic perspective. In this chapter, the chosen slope with a CoV value of 0.4 and having the above-mentioned shear strength properties are considered for an excavation width (b_t) of 10 m. The aim of this study is to assess the failure probability of excavated slopes, while seeking a proper retention measure to reduce the probability of failure of the same, and appreciate a safer operational condition.

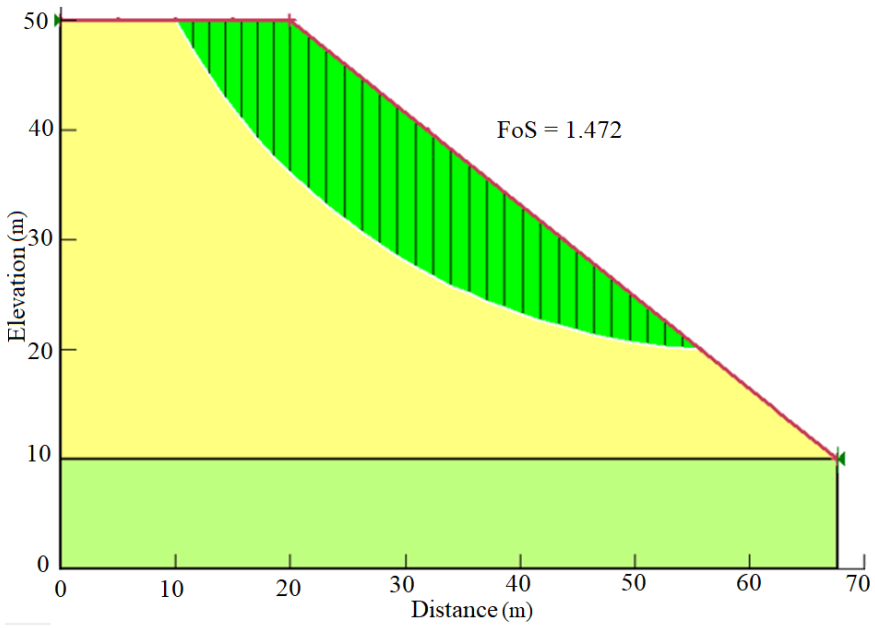

Fig. 7.2 Critical stability of the virgin slope

7.3. PROBABILISTIC ANALYSIS OF UNREINFORCED TOE-EXCAVATED SLOPE

In this regard, as mentioned, first a FEM-based probabilistic analysis is carried out for the unreinforced toe-excavated slope with a vertical cut having a horizontal extent of 10 m. GeoStudio (v2018) is used for conducting the various analyses and drawing the inferences. Firstly, an in-situ FEM-based slope stability analysis is conducted in Sigma/W (stress-deformation module). The generated stresses are subsequently incorporated in LEM-based Slope/W (slope stability module) for the computation of failure probability using MCS. For the present problem, the stability assessment for the toe excavation scenario is conducted in four consecutive stages as outlined:

S-I. Stability of the chosen virgin slope section

S-II. Stability of the section after a vertical cut of depth 3.4 m is carried out.

S-III. Stability of the section after vertical excavation is carried out for next 2 m.

S-IV. Stability assessment of the section after further 3 m of vertical excavation.

In Sigma/W analysis, the simulation of excavation stages involves the removal of in-situ stresses, which eventually results in an outward pull on the vertical face of the cut and an upward heaving at the horizontal excavation level. Thus, proper stress boundary conditions need to be specified on the excavated faces with proper directions. The applied stress boundary conditions should be so directed that its summation with the originally estimated in-situ stress should be zero (Sigma/W 2018). Figure 7.3 shows a typical application of such stress boundary conditions upon 1st stage excavation. Based on the S-I analysis, the stated boundary stresses are identified. Figures 7.4 and 7.5 shows the lateral stress distribution along the vertical cut and the vertical stress distribution along different levels of excavations made in the chosen slope. Accordingly, the corresponding estimated boundary stresses are judiciously used while conducting the stress-deformation analyses for different excavation sequences.

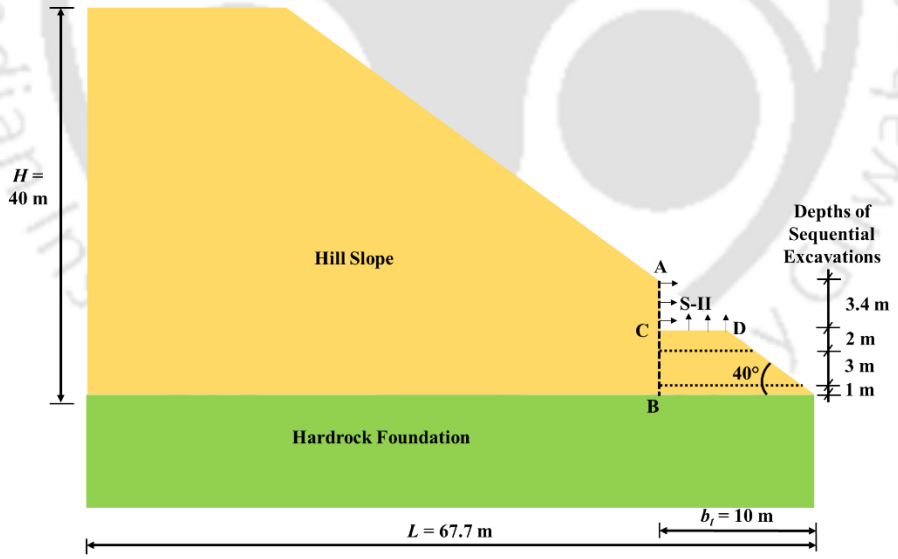

Fig. 7.3 Typical application of stress boundary conditions for simulation of excavation stages

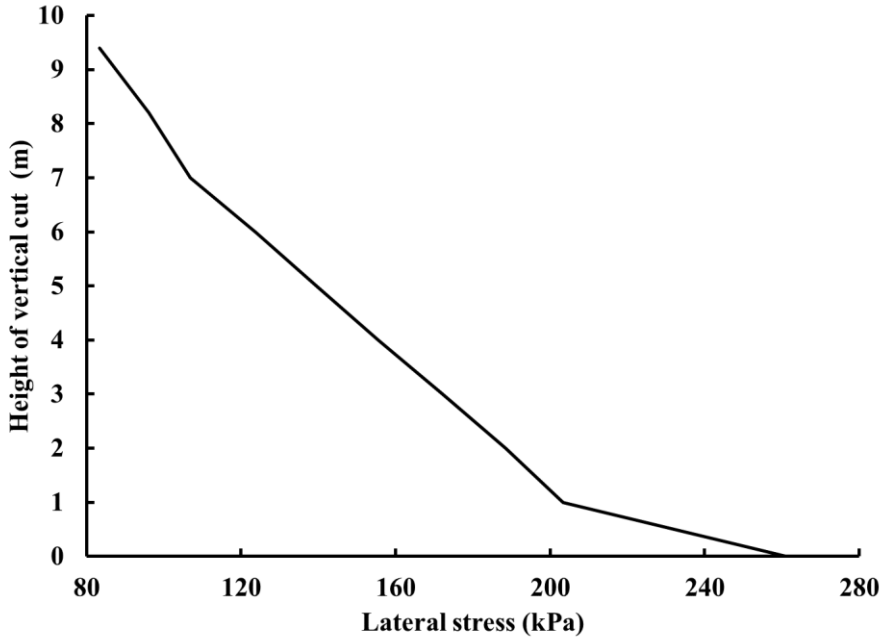

Fig. 7.4 In-situ lateral stress along the line of vertical cut AB of the chosen slope

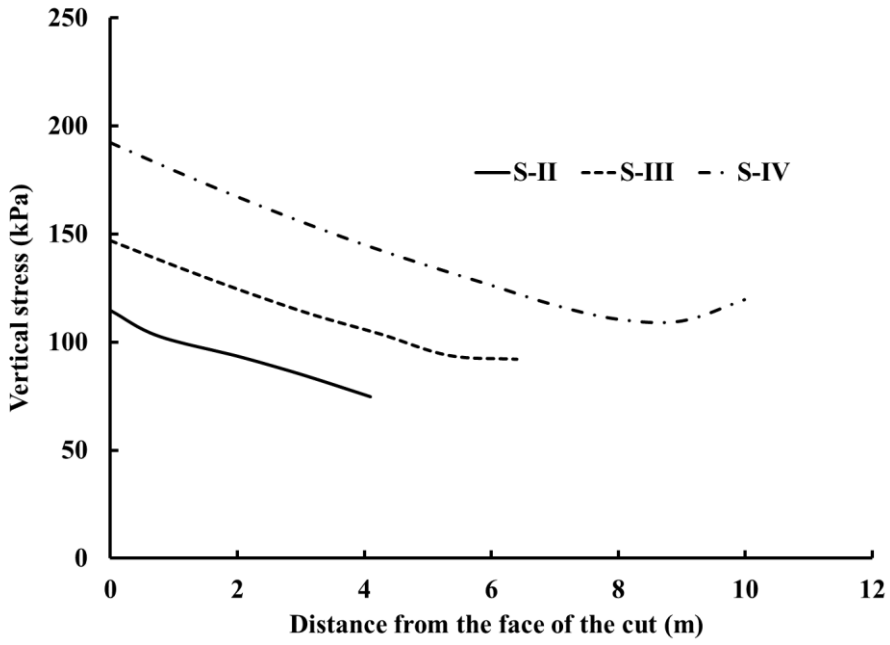

Fig. 7.5 In-situ vertical stress along the horizontal base of excavations at different levels

The FEM-based analysis indicated a deterministic FoS value of 1.101 and a failure probability of 45.5% for the cut slope (Fig. 7.6). The figure also highlights the probabilistic FoS and its distribution over the realizations of the MCS. As can be observed, for this part of the study, 2000 realizations of MCS are conducted. The number of realizations were decided based on achieving a convergent probability of failure, as shown in Fig. 7.7. The obtained safety predictors (FoS and P_f) indicate that toe excavation up to a horizontal width of 10 m is not safe in the chosen slope, and would potentially trigger slope failure. However, in practice, a two-lane extension of existing roadway through the hilly terrains of the north-eastern region of India (or even in other places of the world) demands such excavation width. Hence, in this context, the next section elaborates the application of a retention system and its safety analyses based on a probabilistic approach.

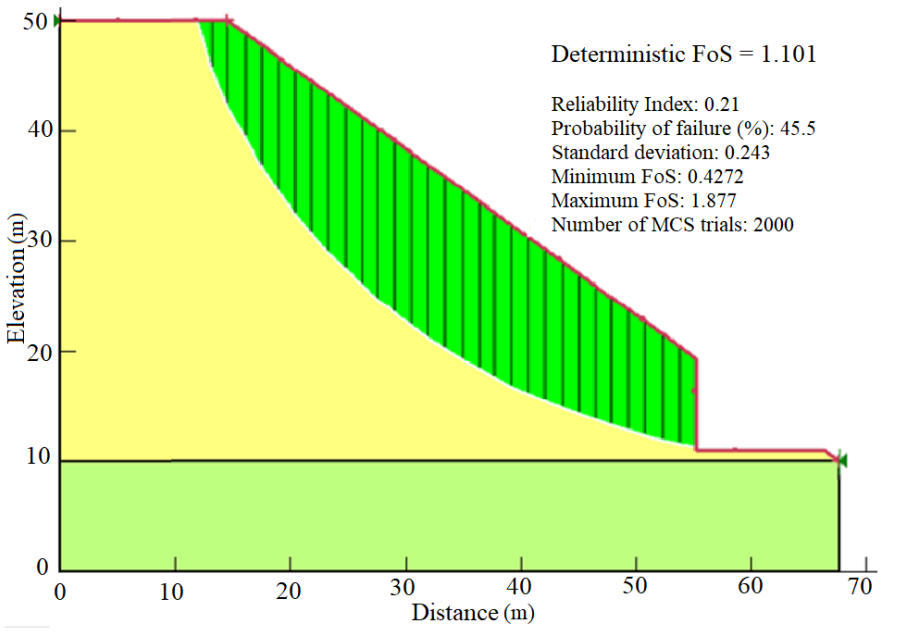

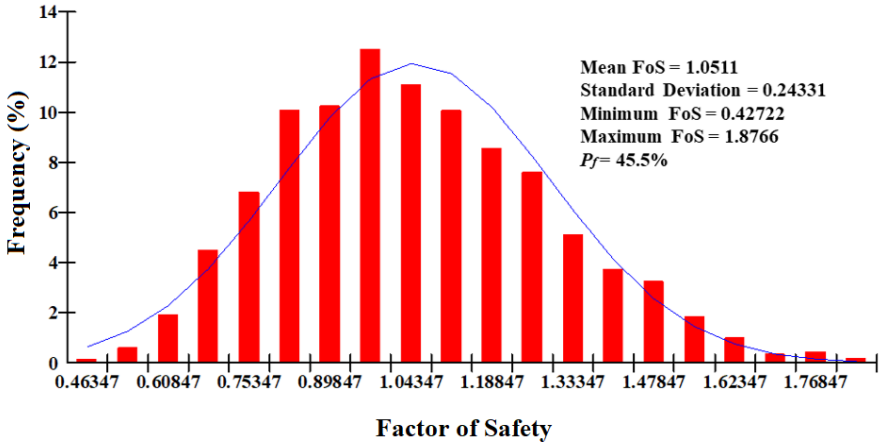

Fig. 7.6 (a) Critical stability of unreinforced slope with vertical toe excavation (b) Distribution of the FoS for 2000 MCS realizations in the probabilistic approach

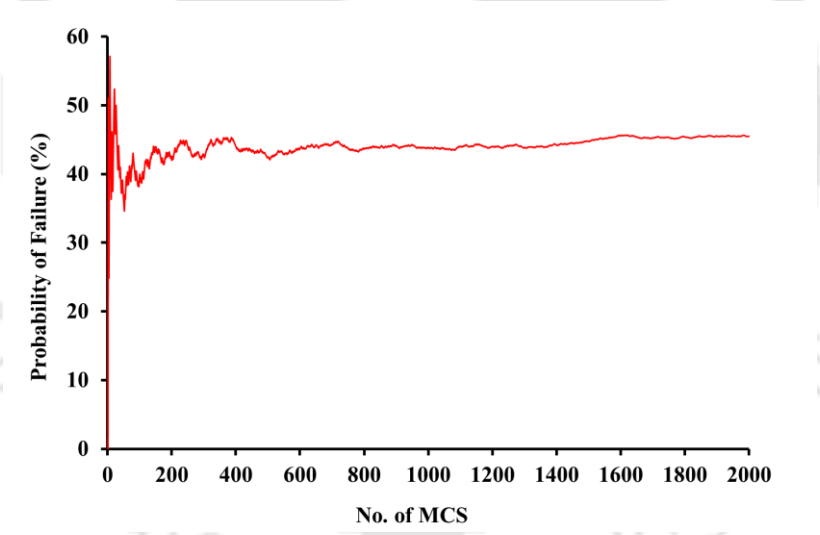

Fig. 7.7 Estimation of minimum number of MCS realizations to obtain convergent solution

7.4. PROBABILISTIC ANALYSIS OF TOE EXCAVATED SLOPE WITH RETENTION SYSTEMS

In this section, the chosen slope is considered with a vertical cutting at a horizontal extent of 10 m from the toe and is supported by retention systems. As mentioned, the aim is to probabilistically

analyze the retention measure and assess the improvement in the failure probability in comparison to the unreinforced cut slope. It has been suggested in the literature that sheet pile walls (cantilever or anchored) can be adopted conveniently and economically as retention measure when the height of the retained backfill exceeds 6 m (Das, 1999; Tsinker, 1983).

Sheet pile walls are generally used as earth retaining structures along shorelines or slopes. A sheet pile wall is essentially a row of interlocking, vertical pile segments installed to form a straight wall to provide stability with sufficient safety margin. Sheet piles can be made of different type of materials such as wooden sheet piles, pre-cast concrete sheet piles and steel sheet piles. However, steel sheet piles are commonly used because of their lightweight and resistance to high driving stress developed when being driven into hard soils. There are two primary types of sheet piles, cantilever sheet piles and anchored sheet piles. A cantilever sheet pile wall acquires its support through interaction with the surrounding soil only, whereas an anchored sheet pile wall acquires its support through a combination of interactions between the surrounding soil and mechanical anchors. For both the cases, the support from surrounding soil is mainly acquired through passive pressure exerted on the embedded section of the sheet pile wall below the dredge line or bottom of the excavation. The use of anchored sheet pile wall (anchor system made of prestressed cables) tends to reduce the lateral deflection, bending moment and depth of penetration of the sheet pile wall, thereby providing better control on the deformation of the retained system. For the chosen slope, the horizontal extent of 10 m resulted in an unsupported vertical cut of 8.4 m. Hence, in this regard, in an initial attempt, only a sheet pile (SP) is incorporated in the cut slope as a retention system. In the next phase, an anchored sheet-pile retention system is incorporated in the chosen cut slope.

7.4.1. Sheet Pile Wall as Retention System for the Stability of Cut Slope

In the present study, as mentioned, the process of sequential toe excavation and reinforcement of the excavated part using a SP wall is modeled using the FE-based stress-deformation analysis, while the probability of failure of the excavation and reinforcement is assessed with the aid of LE-based slope stability analysis. In the numerical modeling for the stress-deformation analysis, the sheet pile wall is represented by structural beam element, the properties of which are listed in Table 7.2. The boundary conditions are computed and applied on the excavation face and base for all the stages as discussed earlier in Section 7.3. Other steps adopted in the numerical modeling and simulation also remain same as discussed earlier. For the present problem, the stability assessment for the toe excavation scenario and the sequential reinforcing is carried out in four consecutive stages as outlined:

SP-I. Stability of the virgin slope section

SP-II. Stability of the section after a steel sheet pile is driven along the section A-B (Fig. 7.8), and a vertical cut of depth 3.4 m is carried out outside the sheet pile wall from its upper end.

SP-III. Stability of the section after vertical excavation is carried out for the next 2 m on the outer side of the sheet pile wall.

SP-IV. Stability of the section after the last 3 m of vertical excavation is carried out while leaving an embedment depth of 1 m.

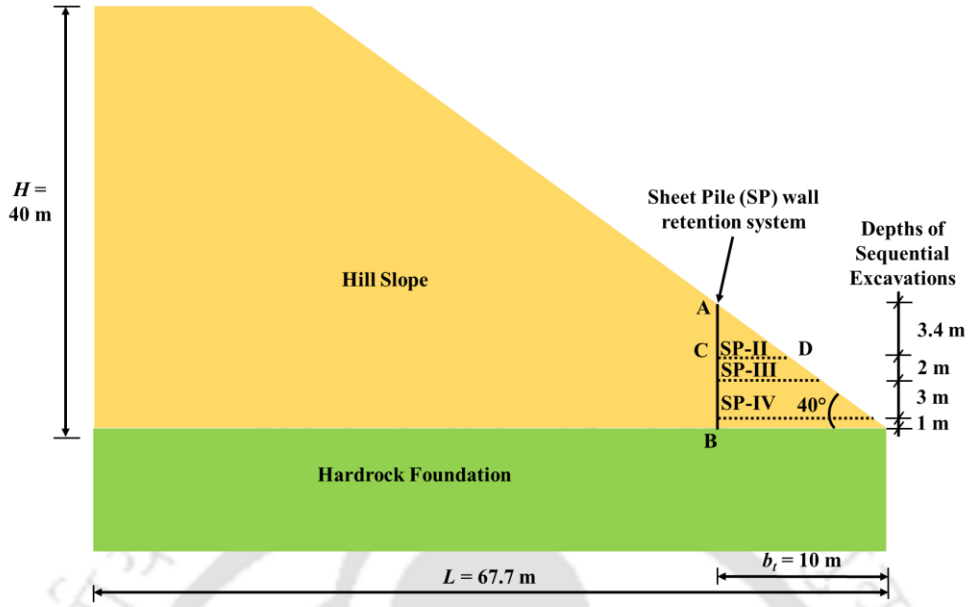

Fig. 7.8 Schematic diagram of sheet pile (SP) wall used as retention measure against the sequential toe excavation of the hill slope

Figure 7.9 shows the deflection of the SP wall along its height (Section AB: zero at bottom and 9.4 m at top) at different stages of the excavation. It is seen that in SP-I, before the commencement of excavation, the deflection at Section AB is zero, which is used as the benchmark. In the next stages, the SP wall is installed, and excavation is conducted stagewise. The wall deflection increases with subsequent excavation and shows an excessive lateral movement of the SP wall of around 178 mm at top of the wall after completion of desired excavation. Figure 7.10 shows the distributions of bending moments and shear forces along the height of the sheet pile at different stages of construction. As obvious, the bending moment is zero at the top of the sheet pile which is free to deform laterally. It is observed that the magnitude of positive bending moment increases with the stages of the excavation, while the location of maximum bending moment approximately remains constant. The fixed-end moment and shear force at the embedded base of the SP wall increases with the successive excavations.

In the next stage, stress generated in the Sigma/W stress-deformation analysis is incorporated in Slope/W module to assess the deterministic and probabilistic-based stability of the slope. The FEM based study results in a deterministic FoS of 1.163. In the probabilistic study, as earlier, 2000 number of MCS realizations are considered to compute the probability of cut slope considering the soil shear strength parameters as random variable. The probabilistic study reveals that the cut slope with SP wall results in a probability of failure of 36.8%. Therefore, in comparison to the the unreinforced slope, it can be noted that with the provision of a SP wall retention measure, there is marginal increase in the deterministic FoS and a meagre decrease in the failure probability. Hence, it can be ascertained that the SP wall retention system is not providing desirable resistance to the soil movement for an excavation width of 10 m. Hence, in this regard, as a next attempt, the sheet pile anchor retention system is analyzed to test its efficacy.

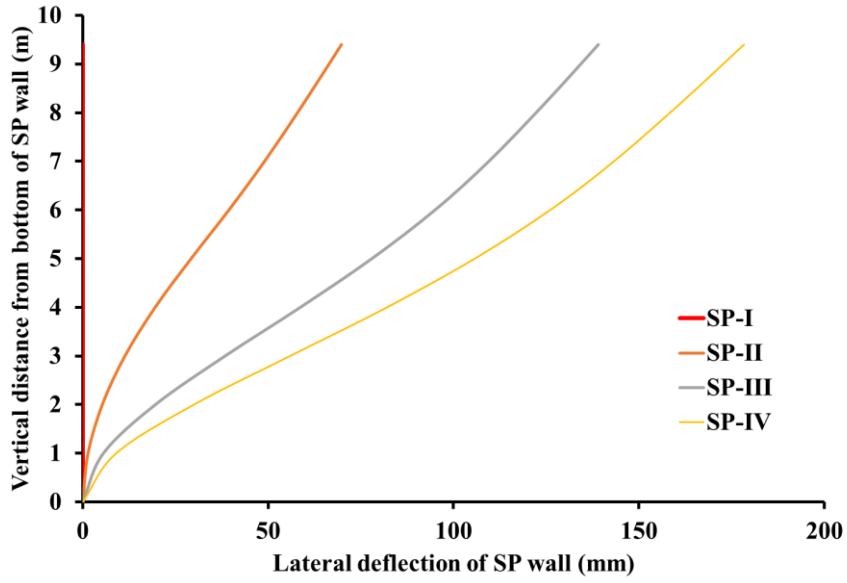

Fig. 7.9 Lateral deflection of sheet pile wall at different stages of excavation

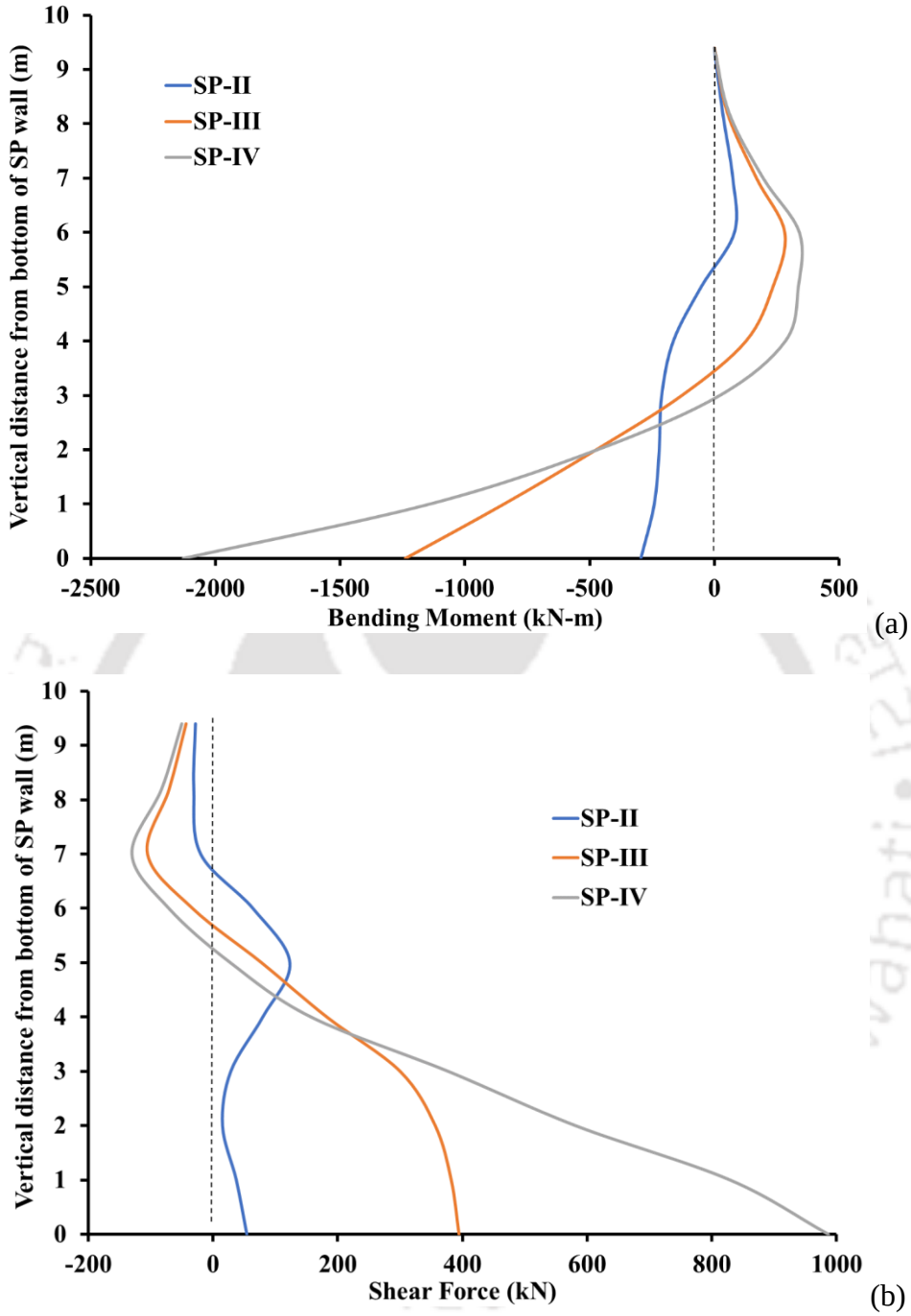

Fig. 7.10 (a) Bending moment and (b) shear force distribution along the height of the sheet pile wall at different stages of excavation

7.4.2. Sheet Pile Anchor Retention (SPAR) System for the Stability of Cut Slope

In this part of the study, the stability assessment for the toe excavation scenario and the sequential reinforcing with SPAR is carried out in seven consecutive stages as outlined:

SPAR-I. Stability of the virgin slope section

SPAR-II. Stability of the section after a steel sheet pile is driven along the section A-B (Fig. 7.11, and a vertical cut of depth 3.4 m is carried out outside the sheet pile wall from its upper end.

SPAR-III. Stability of the section after the first layer of prestressed anchor of length 8.1 m is installed at an inclination of 20° with the horizontal. The anchor is prestressed with an axial force of 800 kN, and is installed at a depth of 2.4 m from the top.

SPAR-IV. Stability of the section after vertical excavation is carried out for the next 2 m on the outer side of the anchored sheet pile wall.

SPAR-V. Stability of the section after the second layer of prestressed anchor are installed with same length and inclination as the first layer. The second layer of anchors are inserted at the mid-height of the second layer of excavation, and are pre-stressed using an axial force of 600 kN.

SPAR-VI. Stability of the section after the last 3 m of vertical excavation is carried out, thereby leaving an embedment depth of 1 m.

SPAR-VII. Stability of the section after the third layer of prestressed anchor of length 5.9 m are installed at an inclination of 20° with the horizontal. The third layer of anchors are installed at the mid-height of the excavation, and are presetressed using an axial force of 500 kN.

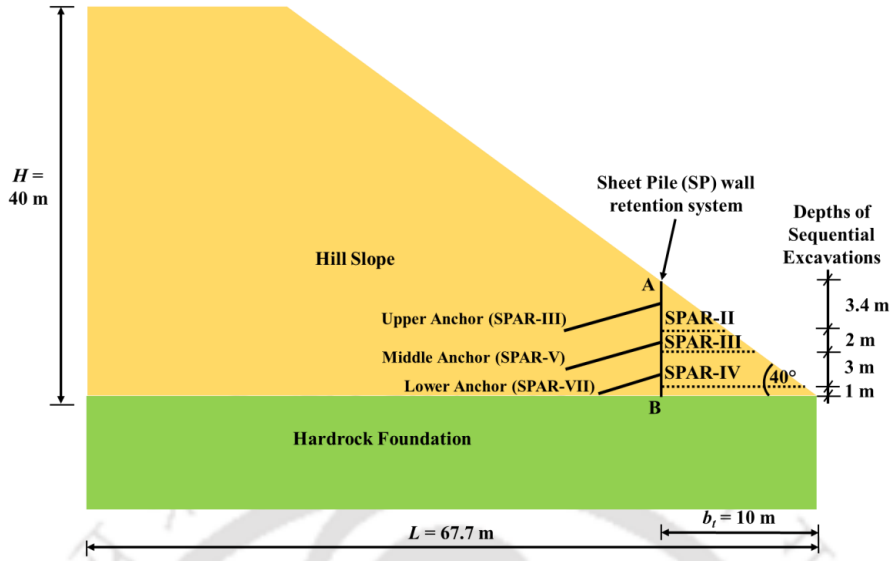

Fig. 7.11 Schematic diagram of sheet-pile-anchor retention (SPAR) system used as protection measure against the sequential toe excavation of the hill slope

The SPAR system adopted in the present study comprises a sheet pile wall and three layers of prestressed anchors. In the modeling for the stress-deformation analysis, the sheet pile wall is represented by structural beam element, the properties of which are listed in Table 7.1. The anchor is modeled by a structural bar element, the properties of which are given in Table 7.1. The lengths of the anchors are chosen based on the FEM based slope stability study conducted for the unreinforced excavation case. It is worth noticing here that for the unreinforced slope, the critical slip surface passes way above the toe of the slope (Fig 7.2). However, after excavation of the slope up to the desired depth, removal of passive confinement drags the critical slip surface to pass through the toe of the excavated slope (Fig 7.6). Therefore, based on the location of the critical slip surface, the lengths of the anchors are so chosen that they can be prolonged beyond the probable critical slip plane to the passive soil mass that can provide the resistance against failure. However, it is acknowledged that this choice of nail length and inclination of anchors might not

be the optimum one, yet as the results later suggest, they are capable of providing the required safety. As earlier, the FE-based stress-deformation analysis of reinforced slope is conducted in Sigma/W module of GeoStudio v2018. Firstly, an in-situ analysis is carried out for the virgin soil slope, and the generated stresses are further incorporated in the stress-deformation analysis of the slope for its successive stages. The stress-deformation analysis involving the toe excavation and installation of SPAR is carried out in the similar manner as discussed in Section 7.4.1 of this chapter.

Table 7.1: Material properties of various components of anchored sheet pile wall

Retention Component	Material Model	Axial modulus (kPa)	Cross-sectional area (m^2)	Moment of inertia (m^4)
Sheet pile wall	Structural beam element	$2x10^8$	0.002	0.0005
Anchor	Structural bar element	$2x10^8$	0.00126	-

Figure 7.12 shows the wall deflection along the wall height (zero at bottom and 9.4 m at top) at different stages of the excavation and anchor installation. Expectedly, the in-situ stage SPAR-I, i.e., before the excavation is commenced, the deflection along the Section AB is zero; the same is considered as a benchmark for the successive stages. After removal of top 3.4 m soil layer (SPAR-II), wall shows a significant deflection with depth. In the next step (SPAR-III), the upper anchor is installed with such a prestress value (800 kN in this case) such that the wall deflection is significantly reduced at the anchor connection level. In the step SPAR-IV, the excavation of middle layer (2 m) again leads to the increment in the wall deflection, which is followed by a decrease due to installation of middle anchor with a prestressing force of 600 kN (SPAR-V).

Subsequently, the excavation of the bottom most 3 m soil layer (SPAR-VI) and subsequent installation of the lowest level of anchors with a prestressing force of 500 kN (SPAR-VII) leads to the expected changes in the wall deflection. The prestressing forces in the anchors are so chosen that the sheet pile wall deflection can be reduced to minimum, thereby leading to generation of enough restraint to lateral movement, and the improvement in the retention and stability characteristics. Based on the present exercise, it is noticed that a nominal deflection of 14.3 mm is observed at the top of the anchored SP wall after completion of the reinforced toe excavation.

Figure 7.13 shows the tensile axial force (represented by –ve values) in the upper, middle, and lower anchors for various stages of analyses. It is noted that the maximum anchor forces are generated at the subsequent excavation after it is installed. At the respective stage of their installation, the anchor forces are equal to the prestress forces provided on the anchors during their installation. The immediately successive excavation releases the passive confinement from the wall face, and the sheet pile wall tries to move outwards, which is ably resisted by the installed anchors, thereby increasing the axial force in the anchor. Further, due to the installation of the successive lower level anchor, the axial force in the upper level anchor decreases. It can be noted that the third level anchor used in the present study does not have any successive excavation stage, and hence, only the prestress force is represented as the axial force. Figure 7.14 presents the distributions of bending moments and shear forces along the height of the SPAR system at different stages of construction. It is observed that the magnitude of positive bending moment increases with the stages of the excavation, while the same gets reduced at the successive stages of anchor installation. The location of maximum bending moment is gradually pushed towards the base of the SPAR system with the subsequent stages of construction. The fixed-end moment and shear

force at the embedded base of the SPAR system increases with the excavation sequences, while they reduce with the immediate and successive stages of anchor installation. It is also noted that the application of SPAR substantially reduces the fixed-ended bending moments and shear forces in the comparison to that obtained for SP wall retention system, thereby indicating the superiority of the SPAR system over the conventional SP retention system.

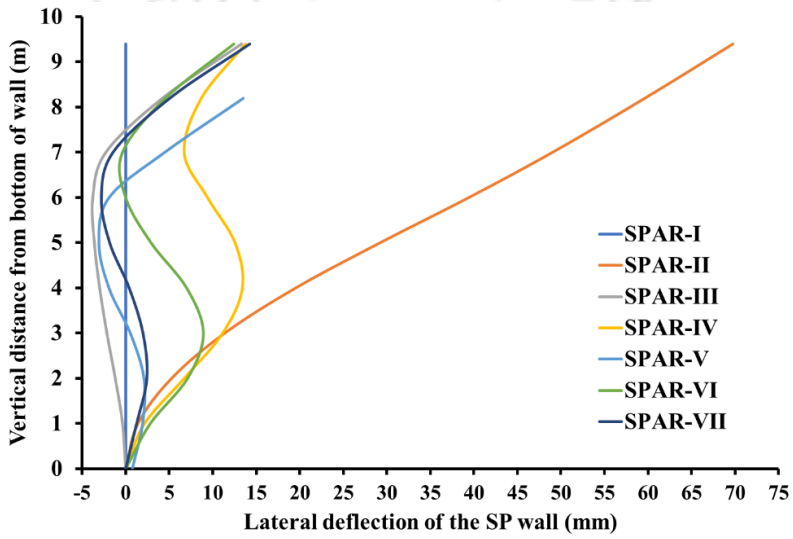

Fig. 7.12 Lateral deflection of sheet pile of the SPAR system at different stages of excavation

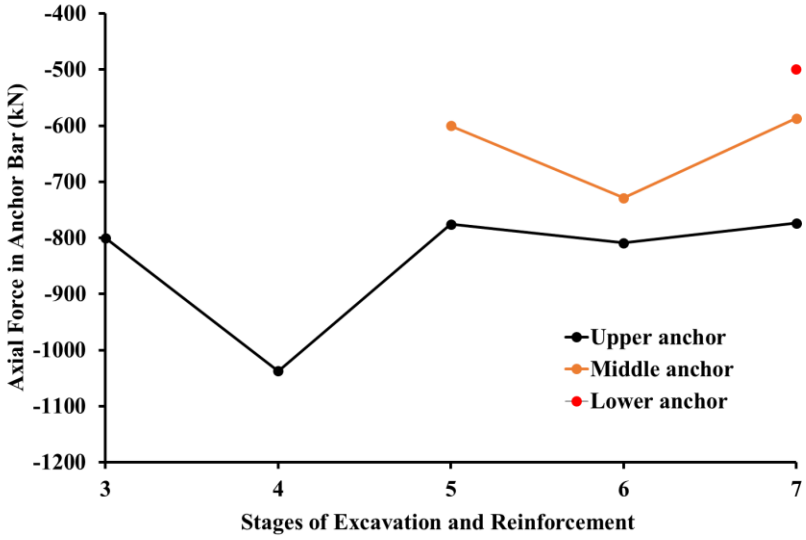

Fig. 7.13 Variation of axial forces in various anchor layers during different stages of excavation and reinforcement while using SPAR as retention system

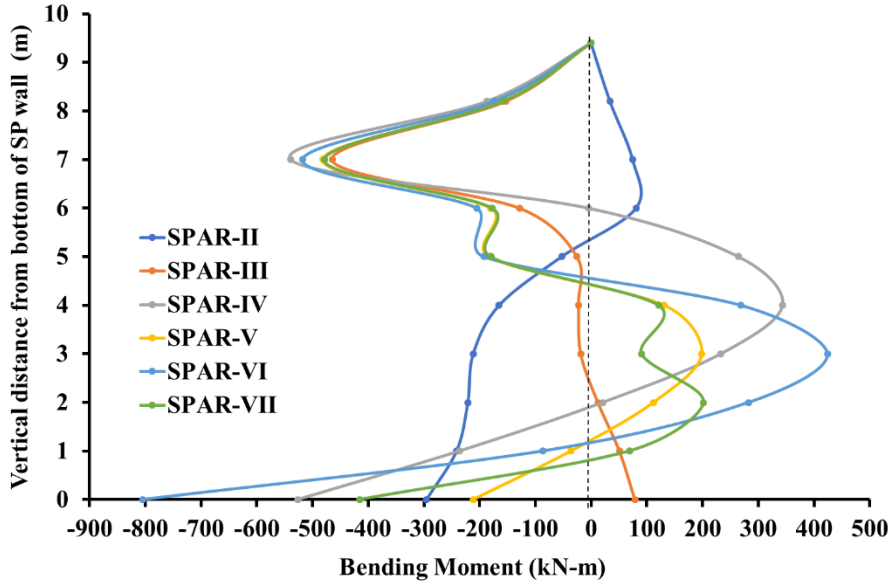

(a)

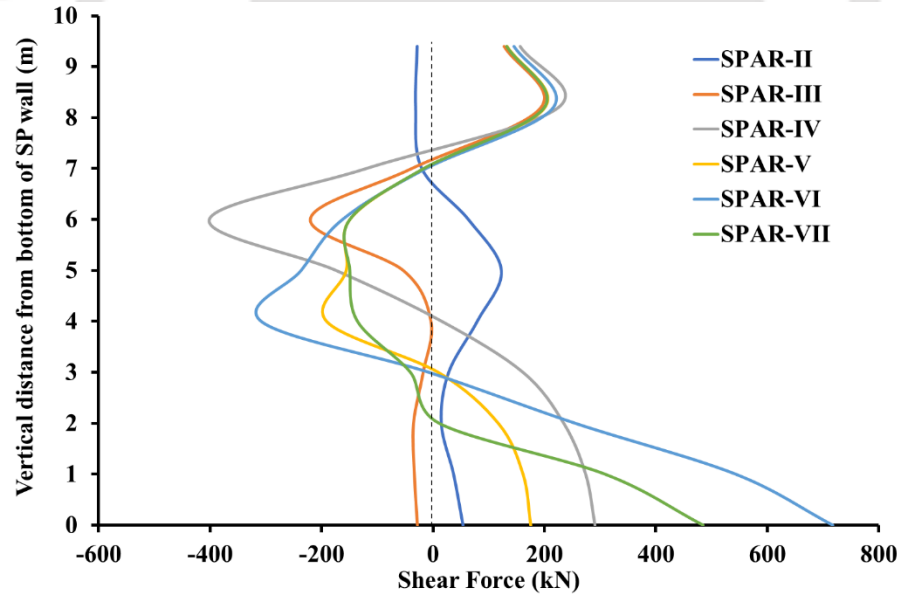

(b)

Fig. 7.14 (a) Bending moment and (b) shear force distribution along the height of the sheet pile wall in SPAR system at different stages of excavation and reinforcement

On completion of FE analysis of the cut slope retained by SPAR system, the stress generated in Sigma/W in the final stage (SPAR-VII) is incorporated in Slope/W module of GeoStudio for FE based slope stability analysis for the consequent estimation of failure probability of the reinforced cut slope. A critical state may occur in an unstable cut slope during stabilization and reinforcement stages as well. Hence, it is extremely important to assess the stability during the successive excavation and reinforcement installation phases.

The FEM based deterministic approach exhibited a high FoS of 1.414 when SPAR system is used as a retention measure for the cut slope. For the probabilistic analyses, the shear strength parameters and other geotechnical parameters are taken same as in the case of unreinforced slope. In this case as well, 2000 numbers of Monte Carlo simulations are conducted for estimation of failure probability of the reinforced cut slope. Figure 7.15 shows the failure mechanism developed for a typical MCS iteration during SPAR-VII analysis, highlighting the critical slip surface and the failure slope mass. Figure 7.16 shows the variation of probability of failure at different stages of the SPAR installation. The failure probability of the virgin slope (SPAR-I) is estimated to be 9.45%. At each subsequent stages of excavation, there is an expected increase of the failure probability due to the removal of the passive confinement outside the sheet pile wall. For the stages SPAR-II, SPAR-IV, and SPAR-VI, the P_f is found to be increased to 21.4%, 14.5% and 13.6%, respectively. In the intermediate stages of anchor installation, i.e. SPAR-III, SPAR-V and SPAR-VII, the P_f respectively decreases to the values of 9.35%, 9.25% and 12.9%, which are lesser than their corresponding preceding stages. Hence, the conducted stage analysis reveals that the chosen slope has a 12.9% probability of failure when it is retained by a SPAR system. It is also experienced that incorporation of SPAR system is successful in substantially reducing the failure probability in

comparison to the same obtained with the application SP wall retention system (for which the probability of failure was 36.8%). Hence, it is imperative that SPAR system proves to be a better retention system to be adopted for the stabilization of toe-excavated hill-slopes, which are sometimes unavoidable for the expansion of transportation networks.

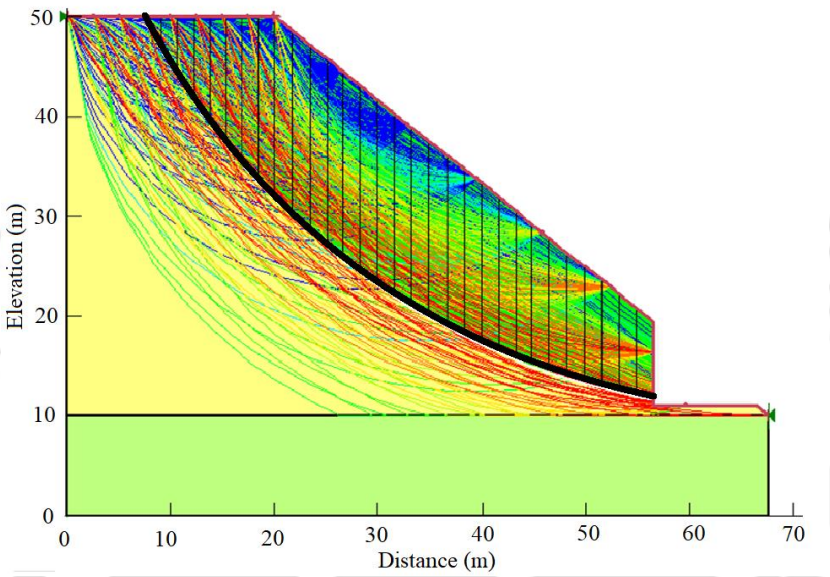

Fig. 7.15 Stability of the cut slope retained by SPAR system obtained for a typical MCS iteration conducted for the stage SPAR-VII

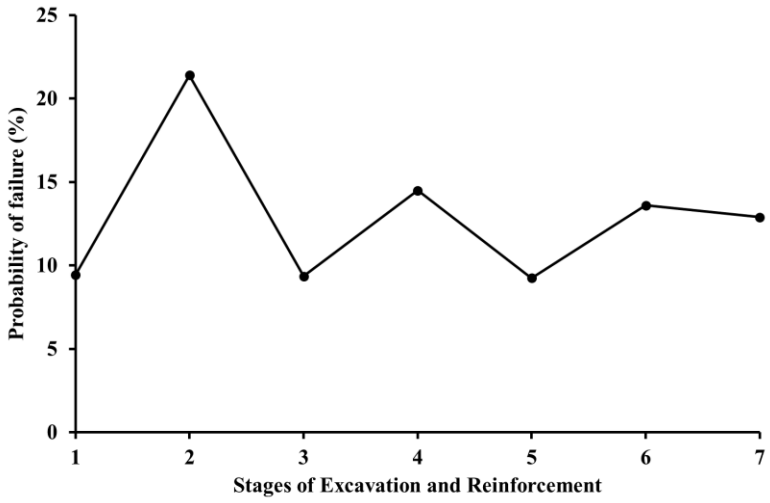

Fig. 7.16 Variation in the probability of failure of the cut slope retained by SPAR system for different stages of excavation and reinforcement

7.5. EFFECT OF SPATIAL VARIATION OF SOIL SHEAR STRENGTH

In this section, a one-dimensional spatial variation of soil shear strength properties along the horizontal direction is considered by using varying correlation lengths, as described in Section 5.4 of chapter 5. Figure 7.17 shows the variation of failure probability with the dimensionless correlation length, $\Theta = \theta / L$ (where, L is the base width of the chosen slope geometry) for retained cut slope for different stages of construction activity. It is exhibited that the failure probability highly depends on the correlation length. The failure probability increases rapidly with increase in correlation length, which is an alternative indication of the decrease in the reliability index. The failure probability is highest when dimensionless correlation length is equal to unity, indicating the entire soil domain as homogeneous for all the MCS iterations. Hence, the exercise clearly indicates that ignoring spatial variability may result in erroneous cut slope design leading to slope failure even after adopting proper cut slope retention measures.

Figure 7.18 shows a comparison of the failure probabilities of the unreinforced and retained cut slopes (using SP wall and SPAR retention systems) for different dimensionless correlation lengths. Firstly, the plots are indicative of the efficacy of the SPAR retention measure in substantially reducing the failure probability of the cut slope. Further, it is seen that for all the cases, P_f is substantially influenced by the correlation length. For the cut slope retained by the SPAR system, depending on Θ, P_f varies from zero to 12.9%. The results indicate that the cut slope retained by SPAR has negligible probability of failure for a large range of Θ. This illustration exhibits that the SPAR system is quite effective in stabilizing the cut slope and keeps it safe whether from a

deterministic or probabilistic perspective, including the scenarios that incorporates spatial variability. Up to a value of Θ = 0.2, the chosen slope geometry is absolutely stable without any chance of failure. However, it is to be appreciated that the understanding of the spatial variability of soil shear strength parameters in the field demands for investigations, so that for specific cases of assessment of slope stability on a probabilistic framework, a meaningful site-specific correlation length can be considered for the practical purpose. With realistic assessment of spatial variation of soil strength properties and proper mitigation measure, a cut slope can be designed with far more reliability.

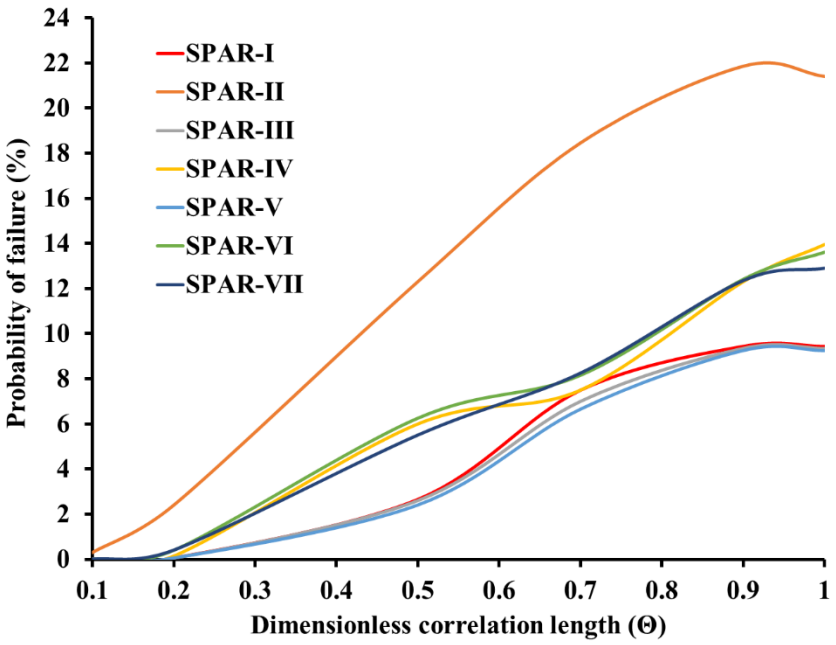

Fig. 7.17 Variation of probability of failure with dimensionless correlation length for different stages of excavation and reinforcement in the SPAR retained cut slope

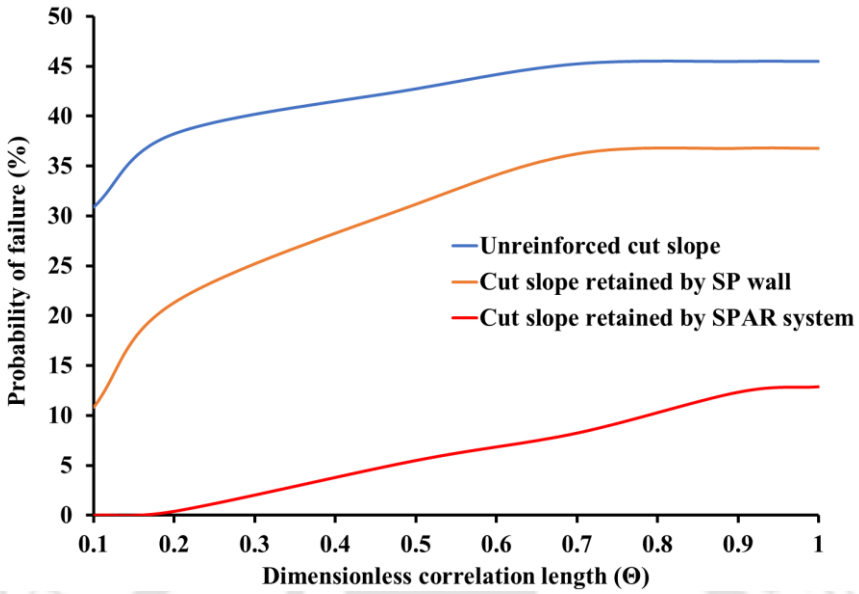

Fig. 7.18 Variation in the probability of failure for dimensionless correlation length for unreinforced and retained cut slopes

7.6. SUMMARY

This chapter reports the adoption of a probabilistic study for incorporation of a Sheet Pile (SP) wall or a Sheet-Pile-Anchor retention (SPAR) system for mitigating instability of a toe-excavated slope, while incorporating the uncertainties in the soil shear-strength parameters and their spatial variation. The representative toe excavated unsupported slope is first investigated. Further, the SP wall or the SPAR system, incorporated as a mitigation measure, are analyzed for their stability in each stage of sequential activities of excavation and anchor installation within probabilistic framework. It is found that with detailed analysis and prediction of failure probability, a stable toe excavation in slope can be designed with proper mitigation system.

CHAPTER 8

RANDOM FINITE ELEMENT ANALYSIS FOR TOE EXCAVATION INDUCED SLOPE INSTABILITY

8.1. GENERAL

A detailed LEM based probabilistic analysis, using Slope/W module of GeoStudio v2018, is presented in Chapter 6 of the thesis to assess the influence of various parameters on cut slope failure probability. Although the LEM based probabilistic analyses presented in Chapter 6 for prediction cut slope safety is simple and less time consuming, however, the method has some inherent limitations. As mentioned earlier, the LEM presumes the location and shape of the failure plane for slope stability analysis and is capable of simulating spatial variability of the soil shear strength parameters only in the horizontal direction for probabilistic stability analysis. Therefore, to overcome such limitations related to LEM based probabilistic analysis using Slope/W, literature suggests incorporating random finite element method (RFEM) utilising random field theory. In this chapter, the study of cut slope instability, presented in Chapter 6, is extended using a two-dimensional (2D) spatial variation of soil strength properties to simulate inherent spatial variation of soil as observed in the field using RFEM with the help of a computer model *Rslope2d* (Griffiths and Fenton, 2000; 2004). The basic principles of RFEM and development of the random field theory in geotechnical engineering field is discussed in detail in the Section 2.3.1.2 of the Chapter 2. The RFEM is a more pragmatic probabilistic approach for cut slope stability analysis. In this method, the spatial variation of soil properties is modelled both in horizontal and vertical direction, and the shape or location of the failure plane is not presumed. Rather, the failure plane is allowed

to develop through the soil elements in which the shear strength is exceeded by the applied shear stresses. A detailed comparison of the two approaches, namely LEM based probabilistic slope stability approach using Slope/W module of GeoStudio and RFEM using *Rslope2d*, is presented in this chapter for better understanding of the aptness of the techniques for precise cut slope design in practise.

8.2. NUMERICAL MODEL FOR PRESENT STUDY

In the present study, a typical 2H:1V slope section, having a height (*H*) of 40 m and a crest length (*H*/2) of 20 m, is adopted (Fig. 8.1). The vertical cut of horizontal width (b_t) 10 m is considered in this study. The probability of failure for the cut slope is first estimated by LEM based probabilistic method, as presented in Chapter 6, for the chosen slope section using Slope/W module of GeoStudio v2018. In the next phase, the cut slope stability is evaluated by RFEM for the same slope section using *Rslope2d* computer model. In both the probabilistic approaches, soil shear strength parameters cohesion, *c*, and angle of internal friction, φ, are assigned as random variables characterized by a Log-normal probability distribution function (pdf).

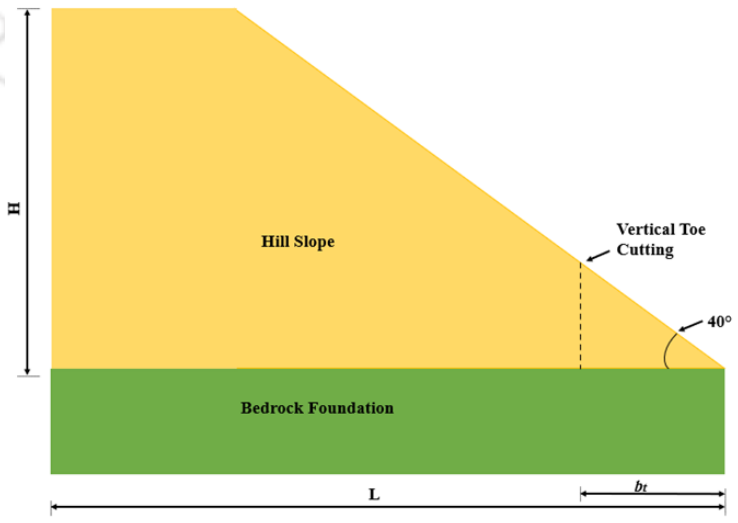

Fig. 8.1 Schematic diagram of adopted slope geometry showing line of vertical toe excavation

8.3. LEM BASED PROBABILISTIC ANALYSIS FOR CUT SLOPE STABILITY

This section presents the LEM based probabilistic approach for estimating the probability of failure for the chosen slope section. In this approach, spatial variation of soil strength properties (cohesion, *c*, and angle of internal friction, φ) variation is considered only in horizontal direction (one-dimensional random field) and the analyses are conducted in Slope/W module of GeoStudio. Further explanation of the LEM based probabilistic method for cut slope analysis are furnished in Chapter 5 and 6. The mean value of cohesion, *c*, and angle of internal friction, φ, considered are 40 kPa and 27.5° respectively. The coefficient of variation (CoV) is considered as 0.4 for both cohesion and angle of internal friction. Soil unit weight (γ) is considered as deterministic in this study and assigned a value of 20 kN/m^2. 2000 number of MCS is found adequate to produce consistent estimation of failure probability and hence adopted in this section (Fig. 8.2). The probabilities of failure of the test slope for different correlation lengths are estimated in this study. For generalization, the correlation length is presented with a dimensionless parameter, dividing the absolute correlation length by the width of the excavated cut slope [$\Theta = \theta/(L\text{-}b_t)$]. The results are presented in Section 8.5 of this chapter.

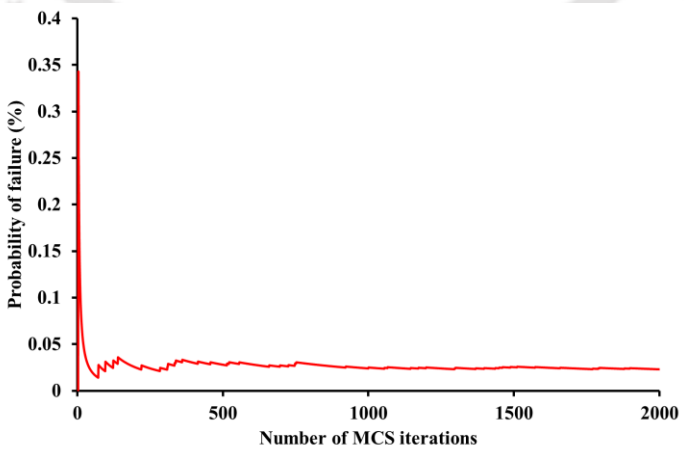

Fig. 8.2 Variation in the probability of failure with numbers of MCS iterations for $\Theta = 1$

8.4. RFEM BASED PROBABILISTIC ANALYSIS FOR CUT SLOPE USING *Rslope2D*

A more advanced and appropriate tool for probabilistic analysis in geotechnical engineering, to incorporate spatial variation of soil shear strength parameters, was developed in 1990's, commonly known as 'Random Finite Element Method' (RFEM) (Paice, 1997; Griffiths and Fenton, 2000). However, the current practice of toe excavation for road constructions in hilly regions in India still lacks the usage of such advanced techniques. This chapter utilizes the computer model *Rslope2d* for RFEM analysis of the chosen cut slope section. The numerical background of the computer model is discussed in detail in Chapter 3 of this thesis.

In this approach, the soil parameters that are required to be treated as random variables for generation of random field are first decided. The input parameters for the soil model used in the elastoplastic finite element slope stability analysis algorithm in *Rslope2d* are cohesion, c; angle of internal friction, φ; dilation angle, ψ; Young's Modulus, E_s; Poisson's ratio, υ; and unit weight, γ. The dilation angle, ψ, affects the volume change of the soil during yielding and the elastic parameters (i.e. Young's modulus, E_s, and Poisson's ratio, υ) affects the computed deformations prior to the failure while conducting the slope stability analysis. However, Griffiths and Lane (1999) stated that the elastic parameters have little influence on the predicted factor of safety. Griffiths and Lane (1999) also stated that the most important parameters in finite element slope stability analysis are the same as those used in the traditional limit equilibrium approach, namely the strength parameters c and φ, unit weight, γ, and the geometry of the slope. Hence, it is considered that only the variability of the cohesion, friction angle and unit weight influence the probability of failure of a slope. However, as discussed in Section 5.2 of Chapter 5, the effect of the soil unit weight on the probability of failure of a clay slope is relatively less as compared to

the shear strength parameters (Alonso, 1976). Therefore, only the shear strength parameters *c* and φ are modelled as random fields in *Rslope2d*.

The mean value of cohesion, *c*, and angle of internal friction, φ, considered are 40 kPa and 27.5°, respectively, same as considered in LEM based probabilistic study in Section 8.3 of this chapter. The shear strength parameters cohesion, *c*, and angle of internal friction, φ, are characterised using Log-normal pdf with a coefficient of variation (CoV) of 0.4 for both the parameters. Other parameters are held constant at their deterministic values, e.g., unit weight, $\gamma = 20$ kN/m^3; Young's modulus, $E_s = 1\times10^5$ kPa; Poisson's ratio, $\upsilon = 0.3$; and dilation angle, $\psi = 0°$. In this stage, for simplicity of the analyses, the cross-correlation between cohesion, *c*, and angle of internal friction, φ, is considered as zero, which means there is no correlation between the parameters. The effect of CoV and cross-correlation between cohesion, *c*, and angle of internal friction, φ, on probability of failure of the cut slopes is reported in Section 8.6 in this chapter.

To simulate the spatial variation in slope domain for the specified soil properties (*c* and φ), *Rslope2d* uses the random field theory developed by Vanmarcke (1977, 1983). The computer model uses the local average subdivision (LAS) method developed by Fenton and Vanmarcke (1990). In this chapter, the 2D spatial variation of the shear strength parameters in the slope domain is characterized by an exponentially decaying (Markovian) correlation function, expressed in Eqn. 8.1. The correlation function implies that the covariance between the points in the field decays exponentially with absolute distance between the points.

$$\rho(k) = \exp\left(-\frac{2|k|}{\theta}\right) \tag{8.1}$$

where, ρ = correlation coefficient between the underlying random field values at any two points separated by a lag distance *k.* The field is assumed to be quadrant symmetric, i.e., the correlation between the points with lag (x,y) is the same as the correlation between points with lag (-x,y), (x,-y), and (-x,-y).

In the FE analysis using *Rslope2d,* non-convergence of the iterative solver algorithm within a specified number of iterations is used as a criterion of the failure of the slope. In this algorithm, when the stress state distribution cannot be found anymore that simultaneously satisfies both the Mohr-Coulomb failure criteria and global equilibrium, the slope is considered to have failed (Griffiths and Lane, 1999). This is usually accompanied by a significant increase in the nodal displacements within the mesh. Griffiths and Fenton (2004) reported that in a case study for a 2:1 undrained clay slope, an iteration limit of 500 was found sufficient to assure the convergence of solutions.

Griffiths and Fenton (2004) reported that 1000 number of the MCS is sufficient for a 2:1 undrained clay slope to generate converged estimations of the P_f. It is seen that the number of MCS required to generate a consistent result is partly relying on the number of random variables under consideration. Therefore, it is logical to assume that number of realisations required in MCS for *c*-φ soil will be double that of a cohesive soil problem (Chok, 2009). However, Chok (2009) recommended to adopt 1000 iteration limit and 4000 number of MCS for a drained slope (*c*-φ soil) in *Rslope2d* computer model. Therefore, in present study the same is adopted as per the suggestion of Chok (2009) to estimate the probability of cut slope failure. The probability of failure of the chosen slope section is estimated for various correlation lengths and reported in Section 8.5 of this

chapter. Figure 8.3 shows typical meshes corresponding to different correlation lengths considered for the analysis for the shear strength parameter cohesion (*c*), where light greyish regions represent relatively weaker sections of the slope. The dark blackish cells represent the strongest element while the whitish cells represents the weakest in the realization. Figure 8.3a represents a comparatively smaller correlation length ($\Theta = 0.05$) while Fig. 8.3b represents a larger correlation length ($\Theta = 1$). It should be noted that both these cohesion distributions are taken from the same Log-normal distribution assigned to the property, and only the spatial correlation length is different.

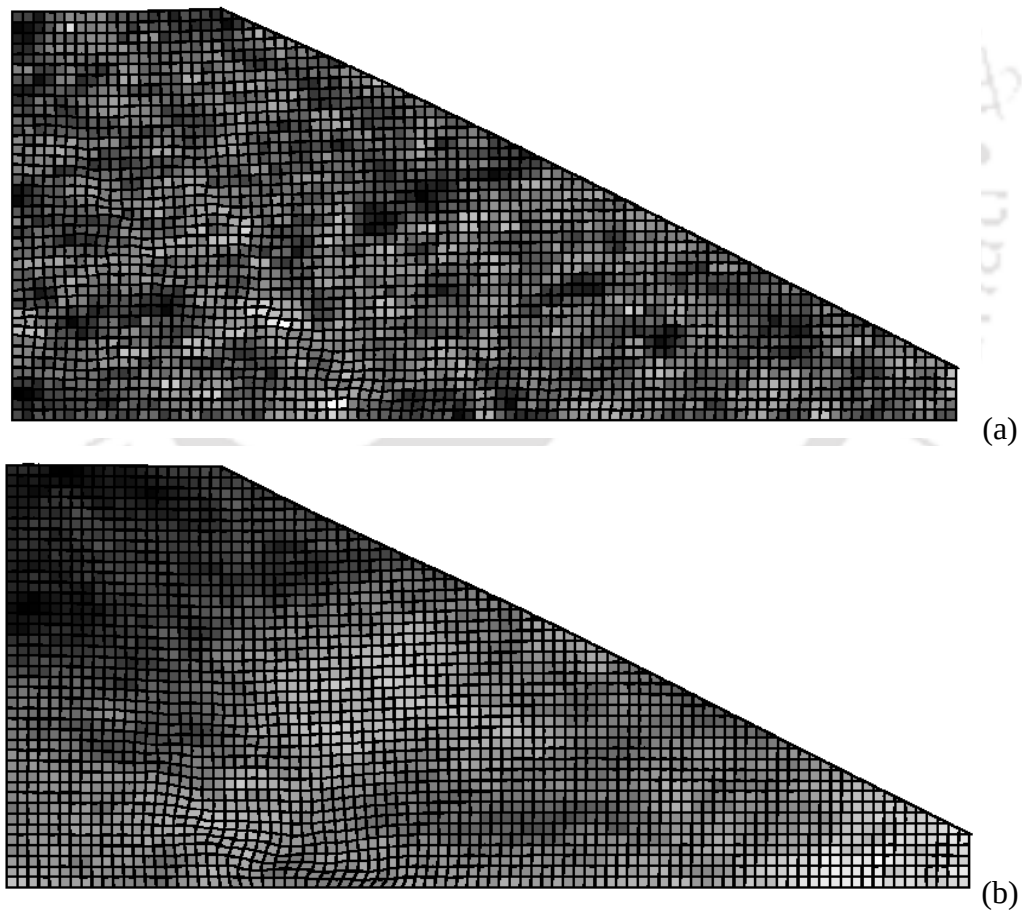

Fig. 8.3 Two dimensional random field for dimensionless correlation length of (a) $\Theta = 0.05$ and (b) $\Theta = 1$

8.5. COMPARISON OF LEM AND RFEM BASED ANALYSIS

The deterministic study conducted on the slope section using LEM in Slope/W and FEM in *Rslope2d* results in a FoS value of 1.63 and 2, respectively. Therefore, according to a deterministic analysis, for the chosen slope section, a safe horizontal width of 10 m cut for road construction operation can be recommended. Figure 8.4 presents the comparison of failure probabilities of the chosen slope section (b_t = 10 m) considering 1D random field (based on LEM based probabilistic approach) with the probabilities of failure considering 2D random field in RFEM analyses for different correlation lengths. The study shows that the LEM based probabilistic study predicts the chosen slope section to be safe, with a low value of probability of failure having a performance level 'above average', for a dimensionless correlation length (Θ) up to 0.7. On the contrary, RFEM analysis shows that the chosen slope section is safe, having a low value of failure probability with a performance level 'above average', for a dimensionless correlation length (Θ) up to 0.5.

Therefore, it is observed that combining LEM with one-dimensional random fields underestimates failure probabilities of slope section as compared to RFEM. The 2D random field in *Rslope2d* can simulate the field uncertainty much more realistically than the 1D spatial variation, thereby increasing the probability of failure. Moreover, LEM method presumes the failure mechanism using deterministic methods (using Morgenstern-Price method in present study), whereas, the RFEM allows the failure surface to originate through the weakest path in the soil layers in a particular realization. RFEM is able to search out the weakest path through the soil mass and hence, the local anomalies generating from the locations of weak areas govern the failure probability.

It is also noticed that estimation of probability of cut slope failure, in both the methods, are highly influenced by the spatial variability of the soil domain. When the correlation length is small, the failure probability is essentially zero; the failure probability increases rapidly for intermediate correlation lengths. The local averaging gets maximized for very small value of correlation length. Therefore, for small correlation lengths, the soil properties tend to take their mean values and, for each realization, the soil domain become essentially homogeneous. Considering the mean values provide a safe slope (having FoS greater than unity for this particular slope geometry under specified soil properties), the failure probability is always zero. When the correlation length is large (dimensionless correlation length approaches to 1), the entire soil domain becomes strongly correlated. Hence, within each realization the slope becomes essentially homogeneous, but different from one realization to the next. As a result, the probability of failure values for both the approaches considered in present study coincides for large correlation lengths (Fig. 8.4). However, for intermediate values of correlation lengths, the slope is not homogeneous and the estimation of failure probability is governed by the spatial variation in soil that is characterized using correlation length.

The study reveals that probability of cut slope failure is very sensitive to the choice of correlation length characterizing the spatial correlation model (in both the approaches) to simulate the in-situ spatial variation of the soil shear strength parameters. Very small correlation lengths or large correlation lengths are of mere mathematical interest, which have very little practical importance. Geotechnical engineers are most likely to encounter intermediate correlation lengths, and the study shows that P_f changes rapidly in this intermediate range. It is also noteworthy that in this intermediate range of dimensionless correlation length, the two different approaches presented in

this chapter predict noticeably different probabilities of failure. Hence, it highlights the importance of ascertaining a proper and reliable spatial variation model for a particular site before designing an engineered cut slope. This realization calls for the necessity to conduct reasonable numbers of field investigations to ideate the in-situ spatial variation of the desired properties that can be suitably transpired to the realistic slope stability analysis of cut-slopes.

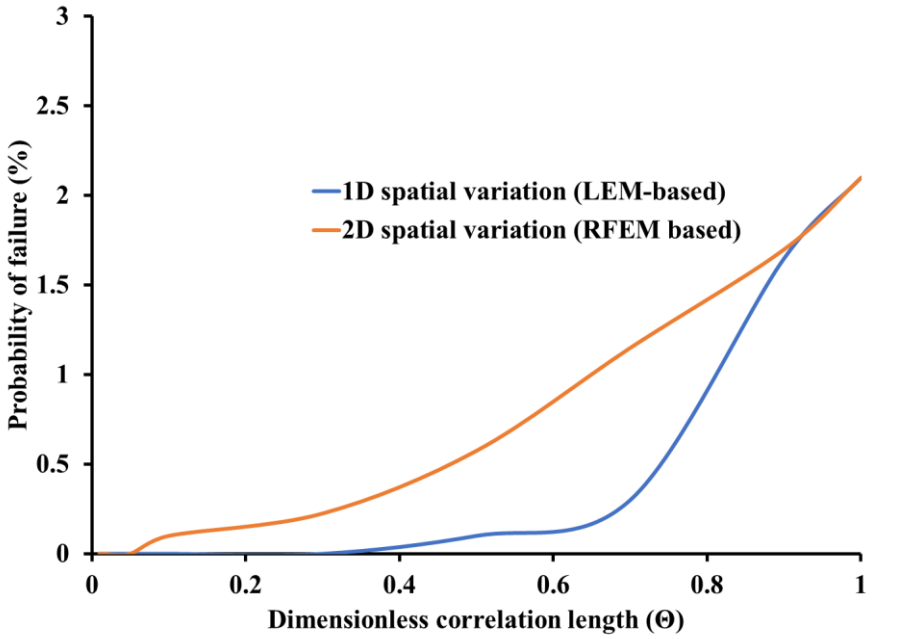

Fig. 8.4 Comparison of the probability of failure for various dimensionless correlation length (Θ) for the slope section chosen in the present study

8.6. EFFECT OF COEFFICIENT OF VARIATION (CoV) AND CORRELATION COEFFICIENT IN RFEM ANALYSIS

In this section, the effect of the coefficient of variation (CoV) and cross-correlation between the soil shear strength properties (cohesion, c, and angle of internal friction, φ) are studied for the chosen slope section (b_t = 10 m) using RFEM in *Rslope2d*. In *Rslope2d* program, the cross-

correlation ($\rho_{c\varphi}$) between c and φ is implemented by 'covariance matrix decomposition' method (Fenton 1994) as follows:

1. Specify the cross-correlation coefficient, $\rho_{c\phi}$ ($-1 < \rho_{c\phi} < 1$)
2. Form the correlation matrix between $G_{\ln c}(x)$ and $G_{\ln \varphi}(x)$, which is assumed to be stationary (i.e., same at all points x in the random field)

$$\rho = \begin{bmatrix} 1.0 & \rho_{c\phi} \\ \rho_{c\phi} & 1.0 \end{bmatrix} \tag{8.2}$$

3. Compute the Cholesky decomposition of ρ, i.e. find the lower triangular matrix L, such that

$$LL^T = \rho \tag{8.3}$$

4. Generate two independent standard normally distributed random fields, $G_1(x)$ and $G_2(x)$, each having a scale of fluctuation of θ
5. At each spatial point, x, form the underlying point-wise correlated random fields

$$\begin{bmatrix} G_{\ln c}(x_1) \\ G_{\ln \phi}(x_2) \end{bmatrix} = \begin{bmatrix} L_{11} & 0.0 \\ L_{21} & L_{22} \end{bmatrix} \begin{bmatrix} G_1(x_1) \\ G_2(x_2) \end{bmatrix} \tag{8.4}$$

6. Transform the standard normal random field of c and φ to the final lognormal random field using the following equation:

$$X_i = \exp\{\mu_{\ln X} + \sigma_{\ln X} G(x_i)\} \tag{8.5}$$

where, x_i is the vector of the coordinates of the centre of the i^{th} element, X_i is the value of the soil property assigned to the specified element, $\mu_{\ln X}$ and $\sigma_{\ln X}$ are the mean and standard deviation, respectively, of the underlying normally distributed ln$X$. $\mu_{\ln X}$ and $\sigma_{\ln X}$ can be estimated using the Eqns. 8.6 and 8.7, respectively,

$$\mu_{\ln X} = \ln X - \frac{1}{2}\sigma^2_{\ln X} \tag{8.6}$$

$$\sigma_{\ln X} = \sqrt{\ln\left(1 + CoV_X^2\right)} \tag{8.7}$$

In this section, the different values of CoV considered are as 0.2, 0.3 and 0.4. The different magnitudes of the cross-correlation coefficient between the shear strength parameters of soil (c and φ) is considered as -0.5, 0 and 0.5. The probability of failure of chosen slope section (b_t = 10 m) is estimated using *Rslope2d* for a dimensionless correlation length Θ = 1, while considering the aforementioned CoV and cross-correlation values between c and φ. The results are presented in Fig. 8.5. The probabilities of failure (P_f) of the cut slope (b_t = 10 m), considering a dimensionless correlation length Θ = 1 and cross-correlation coefficient of 0.5, are zero, 0.73% and 5.83% for CoV values of 0.2, 0.3 and 0.4, respectively. Hence, it is seen that the probability of failure is increasing due to increase in CoV value. As with the increase of CoV, the c and φ values become more scattered from their mean value, hence the P_f increases.

The probabilities of failure (P_f) of the cut slope (b_t = 10 m), considering a dimensionless correlation length Θ = 1 and CoV of 0.4, are 0.23%, 2.1% and 5.83% for cross-correlation coefficient values of -0.5, 0 and 0.5, respectively. It is seen that the probability of failure of the cut slope decreases when the c and φ are not correlated or becomes more negatively correlated, which is in consent with the findings of the LEM based probabilistic analysis presented in Chapter 5 and 6. Therefore, a slope with negative or no correlation between c and φ is likely to be more stable compared to a slope with positive correlation. Therefore, the RFEM analysis conducted on the chosen cut slope section (b_t = 10) in this study shows that the probability of failure is highly sensitive to the selection of CoV and cross-correlation coefficient value of the random variables (cohesion, c, and angle of internal friction, φ). Hence, it can be realised that the proper selection of CoV and cross-correlation

coefficient value is required for estimation of probability of failure of cut slope failure using RFEM.

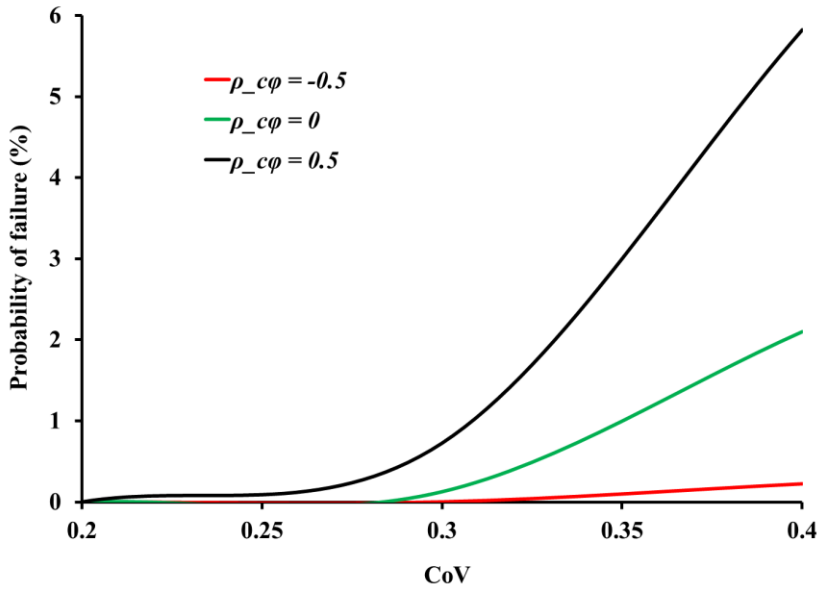

Fig. 8.5 Variation of probability of failure with CoV for various cross-correlation coefficients

8.7. SUMMARY

This chapter reports the contrast between the LEM based probabilistic slope stability analysis using Slope/W module of GeoStudio with RFEM based analysis using *Rslope2d*. The study shows that the estimated failure probability is highly governed by the spatial correlation length. Moreover, LEM based study underestimates the probability of failure in the intermediate range of dimensionless correlation length (Θ), as it ignores the spatial variation of slope in vertical direction and presumes the critical slope surface. On the other hand, RFEM is capable of simulating spatial variation in both the directions and also allows the slip surface to generate along the weakest path. The RFEM based analysis for the chosen slope section is also extended to investigate the effect of CoV and cross-correlation coefficients of shear strength parameters on estimation of slope failure

probability. The study shows that the proper selection of CoV and cross-correlation coefficient have high impact on computed failure probability. However, the major drawback of the RFEM is that the method is computationally intensive and requires ample knowledge of probabilistic theories related to random field modelling for geotechnical structures. Moreover, the computer model *Rslope2d* is not readily available and the RFEM is not widely used in commercially available geotechnical softwares for practise. Hence, it makes it a bit difficult for practising engineers to make use of such advanced techniques for practical design purpose. In such cases, the LEM based probabilistic slope stability studies comes handy and can be utilised with proper engineering judgement of the site under consideration for better assessment of slope stability over the conventional deterministic study.

CHAPTER 9

PROBABILISTIC ASSESMENT OF SEISMIC RESPONSE OF CUT SLOPES

9.1. GENERAL

In seismically active regions of India, earthquake is one of the most crucial factors leading to catastrophic failure of natural or toe-cut hill slopes. Hence, investigations on the stability of slopes under earthquake conditions is imperative in such earthquake prone zones. The stereotypical approach for the assessment of seismic response of hill slopes in geotechnical engineering practise is to predict the safety of the slope structure using deterministic FoS value under assigned earthquake condition. However, it is established in the previous chapters of this thesis that a deterministic analysis becomes inappropriate for predicting the stability of a slope where a wide variation in geotechnical properties is expected to be present at the site. In this regard, a few literatures are available that address the incorporation of probabilistic concepts in dynamic slope stability analysis (Tsompanakis et al., 2010; Xiao et al., 2016; Burgess et al., 2019). A brief literature regarding probabilistic seismic slope stability study is presented in Chapter 2 under Section 2.4 of this thesis. It is noticed that the slope stability practise desperately lacks inclusion of advanced probabilistic analysis for prediction of hill slope stability in more pragmatic way under earthquake condition. Therefore, in this chapter, the LEM based probabilistic slope stability study is extended for hill slopes under earthquake condition in a simplistic manner. Initially, the earthquake is simulated by pseudo-static earthquake approach. Eventually non-linear dynamic analysis is incorporated for the chosen slope section for better understanding of the seismic

response of hill slopes under earthquake condition. The concepts of LEM based probabilistic slope stability analysis for hill slopes under earthquake condition hence developed is then extended further for the assessment of toe excavation induced slope instability. Investigation is also conducted for cut slope reinforced with a sheet pile anchor retention (SPAR) system for stability assessment of the retained system against failure upon excavation under seismic condition. The effect of the spatial variation of soil shear strength parameters is also reported for the same.

9.2. PROBABILISTIC ANALYSIS OF HILL SLOPE STABILITY UNDER EARTHQUAKE CONDITION

In this section, the LEM based probabilistic study for hill slopes is carried out for a chosen slope section under earthquake condition for the prediction of seismic response of hill slopes in a more realistic way. Initially earthquake force is incorporated by pseudo-static approach and the LEM based slope stability analysis is conducted using Slope/W module of GeoStudio v2018 for the estimation of failure probability. In the next phase, a non-linear dynamic analysis for the same slope section is carried out by coupling the Quake/W and Slope/W modules in GeoStudio v2018, for the computation of time dependent probability of failure of the slope. A 1H:1V slope having 15 m height and 50 m length, as shown in Fig. 9.1, is analysed in this section. The mean cohesion (c) of 45 kPa characterised using a log-normal pdf with a CoV value of 0.1 is considered. The unit weight of soil (γ) is considered as deterministic with a value of 20 kN/m^3.

9.2.1. Pseudo-static Approach

In a pseudo-static approach for slope stability analysis, the effects of earthquake motion are represented using accelerations that create an equivalent inertial force, which act at the centroid of

each slice in the sliding mass in the horizontal and vertical directions. The pseudo-static forces can be expressed as:

Horizontal pseudo-static force, $F_h = \frac{a_h W}{g} = k_h W$ (9.1)

Vertical pseudo-static force, $F_v = \frac{a_v W}{g} = k_v W$ (9.2)

where, a_h and a_v are the horizontal and vertical pseudo-static accelerations, g is the acceleration due to gravity, and W is the weight of the slice in the sliding mass.

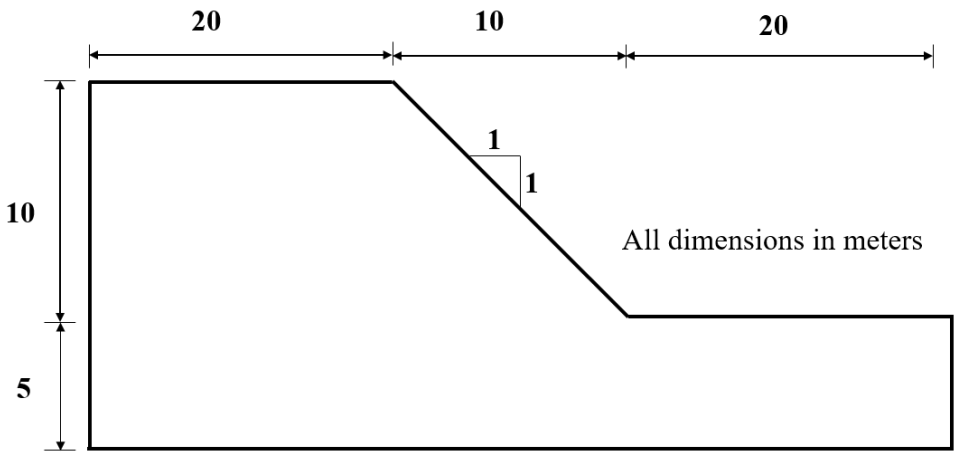

Fig. 9.1 Schematic of the slope geometry chosen for the present study

The ratio of *a/g* is represented by a dimensionless coefficient called pseudo-static acceleration coefficient and denoted by *k*. In Slope/W, the horizontal and vertical inertial force is specified using horizontal and vertical pseudo-static acceleration coefficients k_h and k_v respectively. These coefficients can be considered as a percentage of *g*. For example, a k_h value of 0.1 implies the horizontal pseudo-static acceleration is 0.1g.

Horizontal seismic coefficient values often range from 0.1 to 0.2 (Seed and Martin, 1966; Seed et al., 1978; Seed, 1979; Seed, 1981; Seed, 1983). In this study, the horizontal and vertical pseudo-static acceleration coefficients are varied for a range of 0.10 – 0.18 and 0.05 – 0.09 as shown in Table 9.1. Initially, uncertainties related to only shear strength of soil is considered by characterizing the shear strength parameters as random variables using a log-normal pdf. In a further attempt, the uncertainties in the pseudo-static acceleration coefficients are also incorporated by characterizing them with a log-normal pdf within a range of 0-0.2g and 0-0.1g for the pseudo-static acceleration coefficients in the horizontal (k_h) and vertical (k_v) direction, respectively. The standard deviation of 0.02 is considered for the pseudo-static acceleration coefficients in every case. The aim of this section is to find out the effect of pseudo-static acceleration coefficients on the failure probability computation of hill slopes.

It is found that 2000 number of MCS iteration is adequate to generate consistent and reliable results for all the cases presented in this section. Fig. 9.2 shows the variation of probability of failure with number of MCS iteration for the case with deterministic constant $k_h = 0.12$, $k_v = 0.06$. The analysis of the slope section using Morgenstern-Price LEM under static condition (i.e., $k_h = 0$, $k_v = 0$) results in a deterministic FoS of 1.263 and a probability of failure of 1.25%. Therefore, the slope is safe under static condition. The results of the pseudo-static analysis on the same test slope are shown in Table 9.1. It is seen that the probability of slope failure increases with increase in pseudo-static forces. Moreover, it is observed that considering pseudo-static acceleration coefficients as random variable shows a slight decrease in failure probability in the study, compared to the case when pseudo-static earthquake coefficients are considered as deterministic constant. This is because when pseudo-static acceleration coefficients are considered as random variable, there are

possibilities that the random variable taking values less than its mean value in some of the MCS iterations, leading to a decrease in failure probability. For example, in case of the probabilistic study where the pseudo-static coefficients were considered with mean values k_h = 0.12, k_v = 0.06, the coefficients were chosen from the range of 0-0.2g and 0-0.1g, respectively. In such a scenario, for few MCS iterations, the pseudo-static coefficients attained the magnitude that is less than their mean values, thereby resulting in lesser failure probability. From the results, it is noticed that a slope predicted safe under static condition may fail under earthquake condition, which is a clear manifestation of the necessity of appropriate assessment of the hill slope stability in seismic prone areas. The results also show that ignoring uncertainty in pseudo-static earthquake coefficients may result in over estimation of slope failure probability, which can lead to conservative designs.

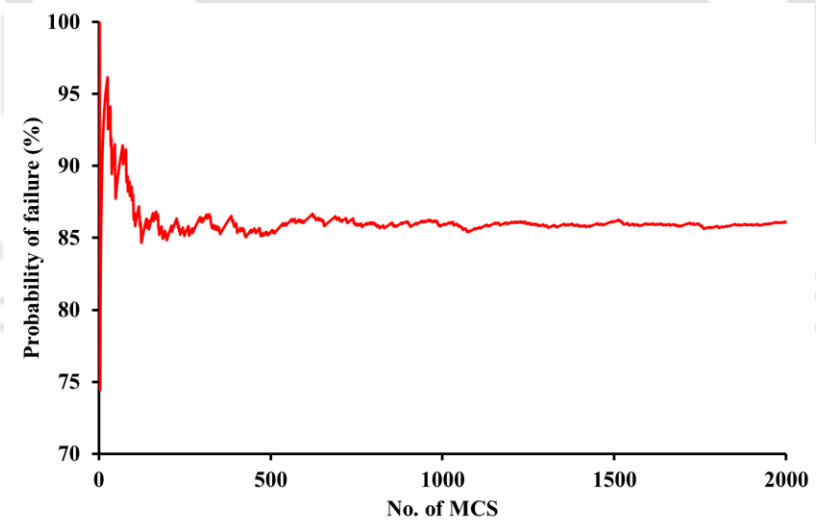

Fig. 9.2 Variation in the probability of failure with numbers of MCS iterations for constant k_h = 0.12, k_v= 0.06

9.2.2. Non-linear Dynamic Approach

In this section, a non-linear dynamic analysis is conducted for the same test slope (Fig. 9.1) in the Quake/W module of GeoStudio v2018 and the stress generated is incorporated in Slope/W module to determine the FE based FoS and maximum probability of failure for the entire duration of applied earthquake. For dynamic analysis, the Poisson's ratio (ν), damping ratio (ξ) and maximum shear modulus (G_{max}) for the slope material is considered as 0.334, 0.1 and 5 MPa, respectively. In the present study, the scaled-down strong motion (with a peak horizontal acceleration value of 0.12g) of the 1971 San Fernando earthquake time history (Morrison et al., 1977), recorded at the abutment of concrete Pacoima Dam (located 5 km east of San Fernando dam), is assigned, which is represented in Fig. 9.3.

Table 9.1: Variation in the deterministic factor of safety, reliability index and probability of failure with pseudo-static acceleration coefficients

Pseudo-static acceleration coefficients	**k_h = 0.18, k_v = 0.09**		**k_h = 0.16, k_v = 0.08**		**k_h = 0.12, k_v = 0.06**	
	Constant	**Random**	**Constant**	**Random**	**Constant**	**Random**
Deterministic FoS	0.791	0.791	0.826	0.826	0.905	0.905
RI	-2.475	-2.128	-1.983	-1.777	-1.013	-0.899
P_f(%)	99.25	98.15	97.2	96.4	86.1	83.55
Pseudo-static acceleration coefficients	**k_h = 0.10, k_v = 0.05**		**k_h = 0, k_v = 0**			
	Constant	**Random**	**Constant**	**Random**		
Deterministic FoS	0.947	0.947	1.263	1.263		
RI	-0.523	-0.449	1.916	1.916		
P_f(%)	72.35	69.65	1.25	1.25		

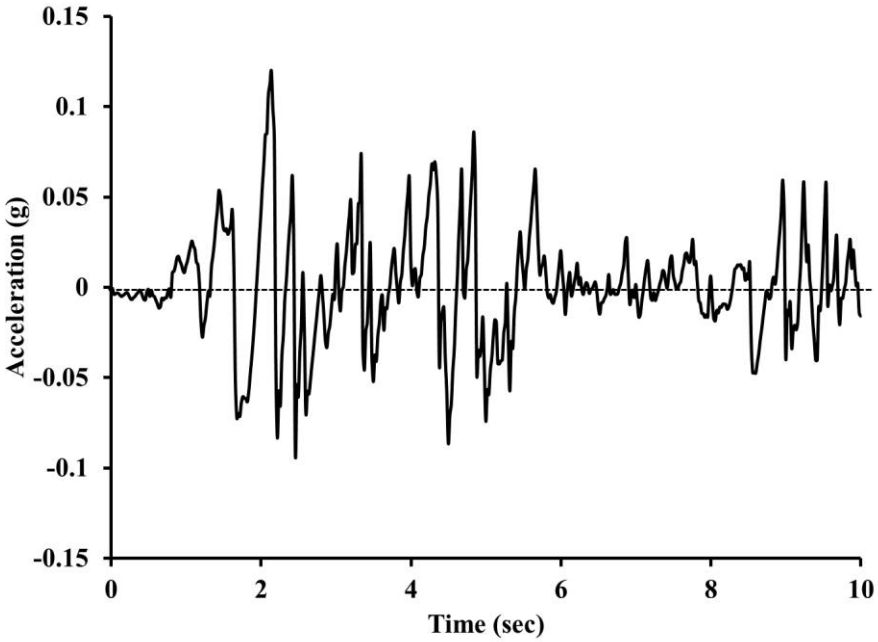

Fig. 9.3 A typical earthquake time history recorded during the 1971 San Fernando earthquake

The stress generated in non-linear dynamic Quake/W analysis are incorporated in Slope/W module to compute the time-dependent failure probability for the chosen slope section during the entire duration of the earthquake. The results obtained from dynamic analyses are shown in Fig. 9.4. It is noticed that the maximum P_f is approximately 1.17%. It can be recalled from Table 9.1 that a pseudo-static analysis of the same slope section (for k_h = 0.12, k_v = 0.06) gave a high P_f value of 86.1%. Under the assigned earthquake time history having 0.12g peak horizontal acceleration, the slope shows a probability of failure much less than what is found in pseudo-static analysis during the entire duration of earthquake history. Therefore, it can be said that a pseudo-static analysis highly overestimates P_f, which can lead to highly uneconomical design. This signifies the limitation of the pseudo-static approach where it considers the seismic acceleration to be acting for an indefinite time in contrast to the actual time-history response of the acceleration records. It

is also worth noting that the P_f is largely dependent on the seismic region in which the slope is situated and the earthquake time history that is governed by the local site effects as well.

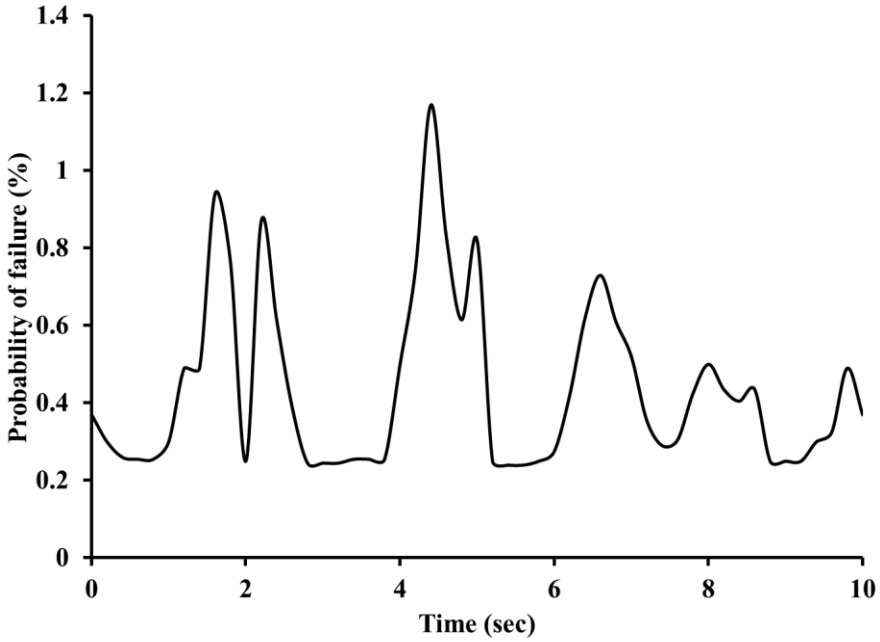

Fig. 9.4 Variation of probability of failure with time during earthquake occurrence

9.3. PROBABILISTIC ANALYSIS OF TOE EXCAVATION INDUCED SLOPE INSTABILITY UNDER EARTHQUAKE CONDITION

In this section, the probabilistic stability study as developed in Section 9.2 is extended for the assessment of seismic response of cut slopes. Seismic response of toe excavated hill slopes are accounted for both the pseudo-static and nonlinear dynamic approaches, in a similar manner as discussed in Section 9.2. The slope section considered in analysis is shown in Fig. 9.5. Here, the slope height (H) is adopted as 40 m with a crest length of 20 m and an inclination of 40°. A vertical toe cut of horizontal width of 10 m (b_t) is considered for the present study. The mean value of cohesion, c, and angle of internal friction, φ, are considered 40 kPa and 27.5° respectively,

characterized by Log-normal pdf for the shear strength parameters. In this study, the CoV is considered as 0.4 for both c and φ. The unit weight of soil is considered as deterministic and a value of 18 kN/m^3 is assigned in this regard.

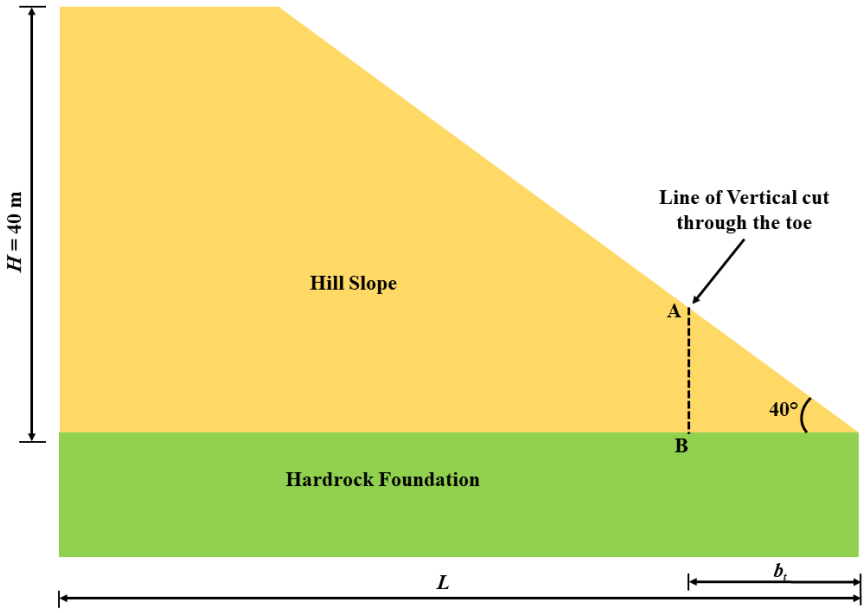

Fig. 9.5 Schematic diagram of chosen slope geometry showing vertical toe cutting

9.3.1. Dynamic Analysis of Cut Slopes by Pseudo-static Approach

The horizontal and vertical pseudo-static acceleration coefficients is considered in this section as 0.12g and 0.06g, respectively; corresponding to Zone-IV (IS 1893 Part 1: 2002). The aim of this study is to investigate the effect of seismic actions on the cut slope within probabilistic framework rather than assessing the severity of the earthquake zones. The analysis can be extended for other seismic zones as well in a similar manner to assess the severity of different zones. In this case as well, 2000 number of MCS iteration is found to be adequate for producing consistent results. The pseudo-static analysis using LE-based Morgenstern-Price method in Slope/W module results in a deterministic FoS of 0.956 and a probability of failure of 68.2% for the cut slope section as shown

in Fig. 9.6. The same cut slope section shows a FE-based deterministic FoS of 1.101 and a failure probability of 45.5% at the end of sequential excavation under static condition, as illustrated in Chapter 7.

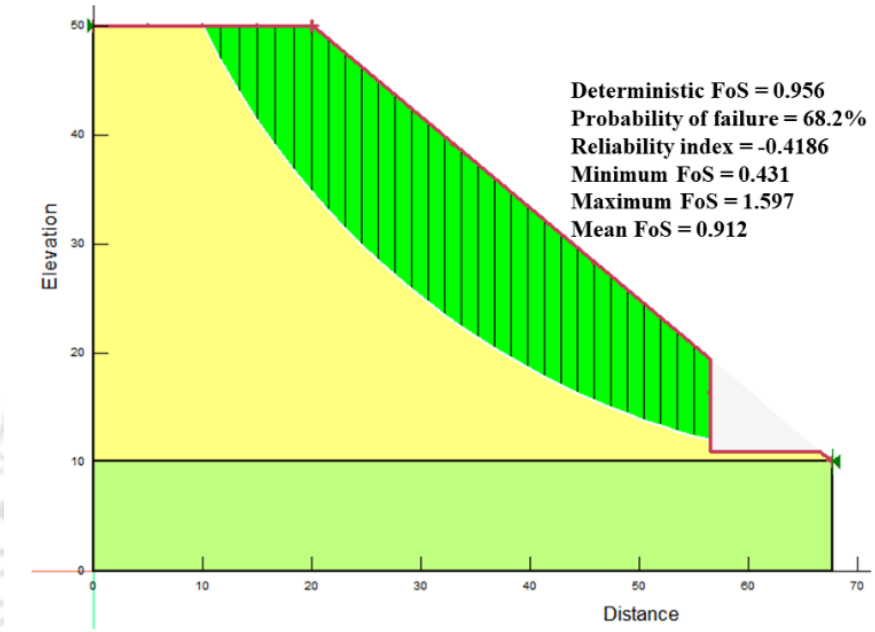

(a)

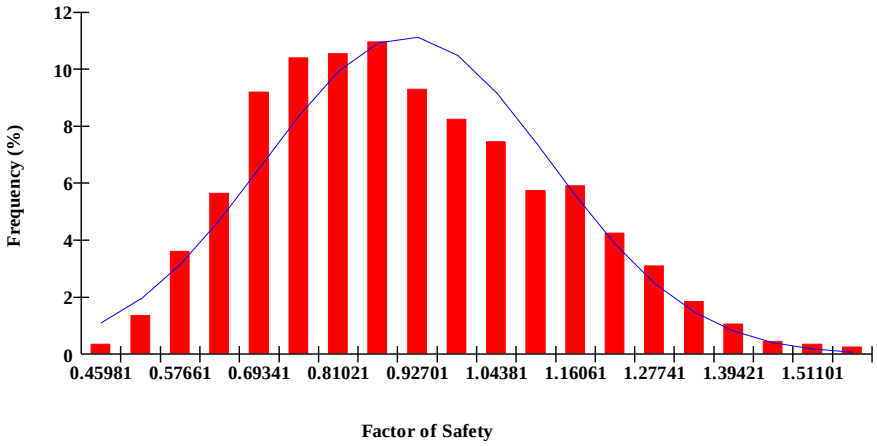

(b)

Fig. 9.6 (a) Critical stability of cut slope with vertical toe excavation (b) Distribution of the FoS for 2000 MCS realizations in the probabilistic approach

9.3.2. Dynamic Analysis of Cut Slopes by Non-linear Dynamic Approach

9.3.2.1. *Stability of the Toe-Excavated Unreinforced Slope*

A non-linear dynamic analysis is conducted in this section to study the effect of vertical toe cutting on hill slopes under dynamic condition. Firstly, an in-situ FEM-based slope stability analysis is conducted in Sigma/W (stress-deformation module). The detail of the FEM based slope stability analysis of the test slope under consideration is discussed in Section 7.3 of Chapter 7. The generated stresses are subsequently incorporated in Quake/W module for non-linear dynamic analysis of the cut slope for the earthquake motion as shown in Fig. 9.3. The Quake/W generated stresses are then incorporated in Slope/W (slope stability module) for the computation of time-dependent failure probability using MCS. In this case as well, 2000 numbers of MCS is conducted for computation of probability of failure. The results are shown in Fig. 9.7. It is seen that a maximum probability of failure of 51.2% occurred during the entire duration of earthquake motion.

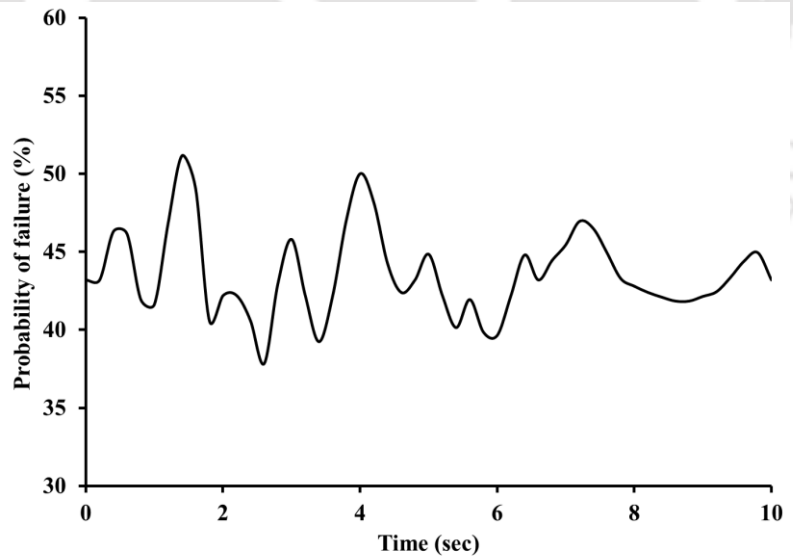

Fig. 9.7 Variation in the probability of failure of the unreinforced toe-excavated slope during the earthquake duration

9.3.2.2. *Stability of the Toe-Excavated Reinforced Slope*

In this section, the seismic response of toe excavated slope retained by SPAR, as considered in Section 7.4.2 of Chapter 7, is evaluated using FEM based probabilistic slope stability analysis by coupling different modules of GeoStudio v2018. A non-linear dynamic analysis is conducted for the evaluation of time-dependent failure probability of the reinforced cut slope. The slope geometry and soil properties considered are same as in Section 7.4.2 of Chapter 7 (also shown in Fig. 9.8). Figure 9.3 shows the hypothetical earthquake time history assigned for the excitation of the cut slope. First, using Sigma/W module of GeoStudio v2018, a FEM analysis in carried out for stage-wise simulation of the installation of SPAR system and excavation of the toe, as discussed in Section 7.4.2 of Chapter 7. The stress generated at the last stage is incorporated in Quake/W analysis for non-linear dynamic analysis of the retained cut slope. Next, the stresses generated in Quake/W analysis is incorporated in the Slope/W module for the estimation of failure probability of the retained cut slope during the entire time duration of motion. The results obtained from the study is presented in Fig. 9.9. The analyses show that the reinforced cut slope structure shows a P_f value of as high as 15.1% during the assigned earthquake time history, whereas, for the same reinforced slope under consideration, a P_f value of 12.9% was predicted under static condition (as highlighted in Chapter 7). Hence, the addition of seismic force makes the slope more vulnerable to failure. It is also worth noticing that incorporation of retention measure by means of SPAR reduces the P_f value significantly (from 51.2% to 15.1%) as compared to the unreinforced cut slope excited by the same earthquake motion.

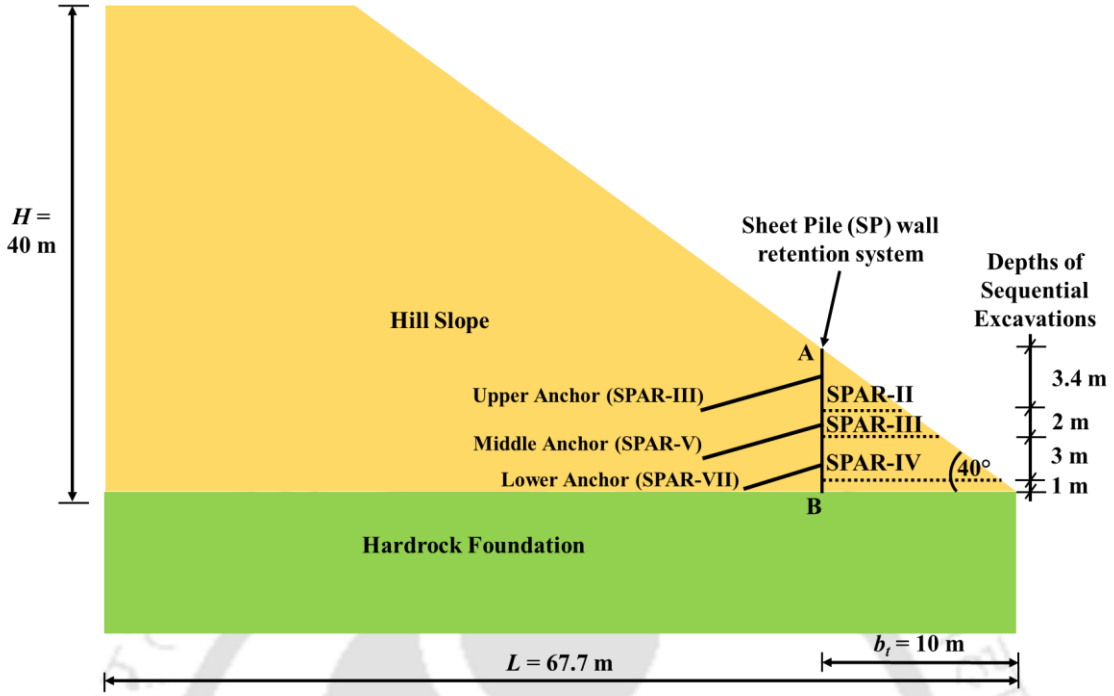

Fig. 9.8 Schematic diagram of sheet-pile-anchor retention (SPAR) system used as protection measure against the sequential toe excavation of the hill slope

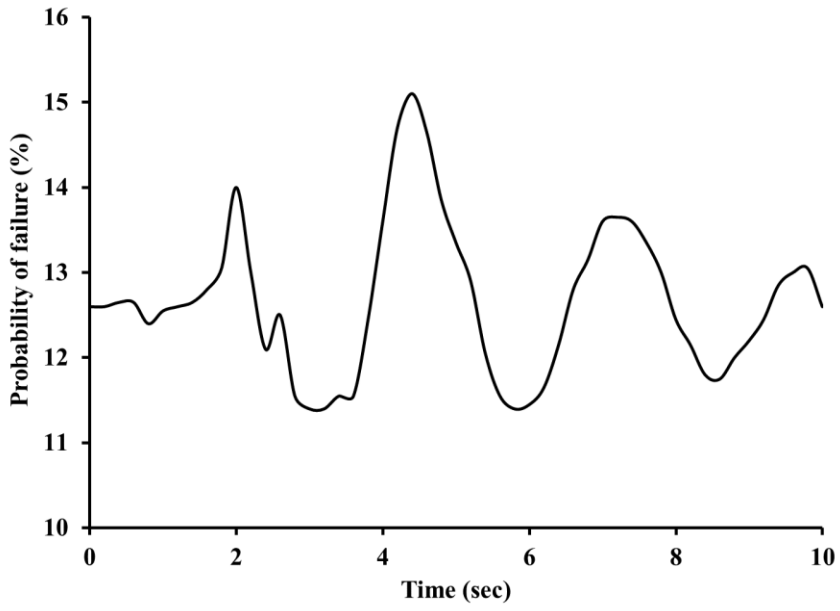

Fig. 9.9 Variation in the probability of failure of the reinforced toe-excavated slope during the earthquake duration

9.3.2.3. *Effect of Spatial Variability on Seismic Response of Reinforced Cut Slope*

In this section, the effect of the spatial variation in the soil shear strength parameters are assessed on seismic response of reinforced cut slope. The chosen reinforced toe-excavated slope section is considered for dynamic analysis and the probability of failure is estimated for various correlation lengths. A one-dimensional random field for soil shear strength parameters, as described in Section 5.3 of Chapter 5 of the thesis, are assigned in the horizontal direction to model the spatial variation in Slope/W module of GeoStudio v2018. The results are shown in Fig. 9.10 as the variability in the temporal probability of failure for various correlation lengths assumed in the present study. The result reveals that the probability of slope failure under earthquake condition highly depends on the correlation length of the random field characterizing the spatial variability of soil shear strength parameters. The same slope may exhibit different seismic response based on the existing spatial variability. It is seen that the chosen slope section shows a low probability of failure for a dimensionless correlation length value (Θ) up to 0.2 under dynamic excitation, and hence safe upon excavation under static as well as dynamic condition. Therefore, to anticipate seismic response of a cut slope, utmost attention needs to be paid in modeling soil spatial variation. It is also largely important to ascertain the spatial variability actually present in the field, and make a realistic modeling of the same so that proper understanding of the failure of slope can be developed in a probabilistic framework.

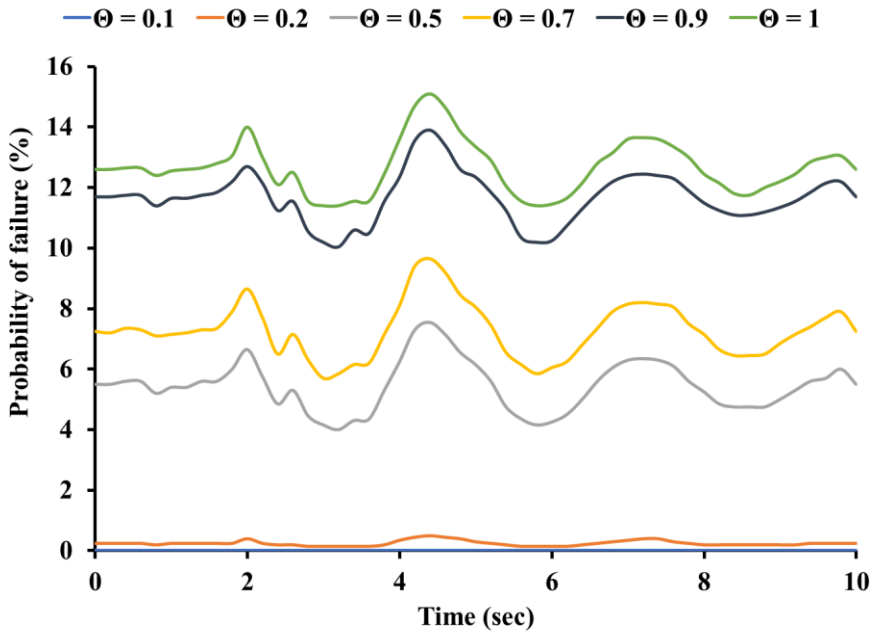

Fig. 9.10 Variation in the probability of failure with time during earthquake duration for various dimensionless correlation length value (Θ) for the cut slope retained with SPAR

9.4. SUMMARY

This chapter presents an overview of the LEM-based probabilistic assessment of the seismic response of natural and toe-excavated hillslopes. Both pseudo-static and nonlinear dynamic analyses are conducted to exhibit the seismic behaviour of the natural and unreinforced cut slope. The influence of the variation of pseudo-static acceleration coefficients (considered either constant or randomly varying over a log-normal distribution) on the deterministic and probabilistic stability of a cut slope is investigated. The nonlinear dynamic analysis successfully elucidated the temporal variation of the safety factor during the entire duration of the earthquake. It is noted that by considering the same peak ground acceleration, the probability of failure obtained from probabilistic analysis are substantially lower than that obtained from the pseudo-static analysis, thereby indicating the exhibition of realistic response through a nonlinear dynamic analysis.

Further, nonlinear dynamic analysis is conducted for cut slope reinforced with SPAR system and the influence of spatial variability of soil shear strength parameters on the seismic response of the cut slope retained by SPAR system is exhibited. The obtained results elucidated that the probability of failure of such systems is largely influenced by the correlation length, thereby indicating the absolute necessity to investigate the same for a specific to avoid overestimated or underestimated design of retention systems.

CHAPTER 10

SUMMARY, CONCLUSIONS, RECOMMENDATIONS AND FUTURE SCOPES

10.1. SUMMARY

This dissertation reports the probabilistic assessment of toe excavation induced slope instability while considering uncertainty in soil shear strength parameters, cross-correlation between them and their spatial variation in slope domain. A stochastic model of spatially varying Standard Penetration Test (SPT) N data is developed using random field theory. The influence of various parameters on probabilistic slope stability study using a simplistic LEM based probabilistic approach is established. A schematic approach to incorporate the LEM based probabilistic method for toe excavation induced slope stability study is presented. The study is extended to ascertain the performance of a sheet pile wall (SP) and a sheet pile anchor retention (SPAR) system in mitigating the slope failure through probabilistic cut slope stability analysis. Further, the study incorporated Random Finite Element Method (RFEM) for probabilistic cut slope analysis to assess the efficacy of the advanced RFEM over the traditional LEM based probabilistic approach for cut slope stability analysis. The seismic response of cut slope within a probabilistic framework is also investigated.

10.2. CONCLUSIONS FROM THE PRESENT STUDY

Based on the investigations and numerical simulations conducted for the present study, the following remarks and conclusions are drawn:

- The spatial variability in the SPT-*N* values, characterised using random field theory, is best represented by the 'Cosine Exponential' ACM. For modelling the spatial variability in *N*-value, a mean SoF of the residual field is obtained as 0.6 m with a CoV of 38.75%.

- Depending on the uncertainty of soil shear strength parameters, slopes assessed safe through deterministic analysis might be adjudged unsafe with varying failure probability. Overall, out of several slope sections judged safe by deterministic analysis, nearly 79% of them exhibit high probabilities of failure with different performance levels (hazardous - 51.9%, unsatisfactory - 15.7%, poor - 17.6% and below average - 14.7% of the unstable cases).

- As the shear strength parameters of soil become more negatively correlated, the probability of failure for the toe-excavated slope decreases, consequently allowing larger permissible horizontal extent of toe excavation. With the decrease of the cross-correlation coefficient from +0.5 to -0.5, on an average, the failure probability of a cut slope decreases by 70%.

- Spatial variation in shear strength parameters significantly impact the probability of failure for unsupported or retained slopes. P_f rapidly increases with an increase in correlation length up to a certain extent, and becomes nearly constant as Θ approaches unity.

- An increase in slope inclination, expectedly, leads to less stable slope and noticeable increase in P_f. For the slope section considered in this study, depending on slope inclination

(26.6° to 75°) and $\rho_{c\varphi}$ (-0.5 to +0.5), the Reliability Index shows a significant variation from 0.657 to 2.979 for the undrained condition and 4.294 to 13.353 for the drained condition.

- The permissible extent of toe excavation and the failure probability highly depends on the coefficient of variation (CoV) of the shear strength parameters and spatial variation of soil shear strength. For the typical hillslope having an inclination of 40º, Θ ranging in 0.1-0.2 and CoV value ranging in 0.2-0.3, a maximum horizontal extent of 5-7 m can be excavated in the toe without leading to slope failure. However, for the same slope with CoV value of 0.4, the virgin slope itself would have a high probability of failure and toe-excavation is not recommended at all in such case. The specified ranges would vary for other typical hillslope inclinations.

- Probabilistic approach aided in successful assessment of the efficacy of the retention measures applied to support cut slopes. The SP and SPAR systems helped in improving the deterministic FoS of cut slope from 1.101 (unsupported slope) to the safety factors of 1.163 and 1.414, respectively. However, the probabilistic approach clearly revealed that application of SP wall could reduce the failure probability only marginally from 45.5% (unsupported slope) to 36.8%, while the application of SPAR systems reduced it significantly to 12.9%, thus establishing the suitability of the latter retention measure.

- The variation of in-situ spatial variability may lead to significant variation in the failure probability of cut slopes, and even under that circumstances, the SPAR system exhibited substantial retention capacity. Based on a 1-D horizontal spatial variability, the SPAR system could indicate successful retention of cut slope without any chance of failure for Θ < 0.2.

- Considering 2-D spatial variability in soil shear strength parameters using RFEM approach proves better and realistic in comparison to the conventional LEM based probabilistic approach incorporating 1-D spatial variability. Ignoring spatial variation in vertical direction in LEM based probabilistic study under-estimates the slope failure probability, resulting in selection of an unsafe toe excavation width for road construction or widening operation in hill slopes.

- The probabilistic pseudo-static slope stability analysis indicates that ignoring uncertainty in pseudo-static earthquake coefficients over-estimates the hillslope failure probability (in the tune of 2-5%) in comparison to the cases when acceleration coefficients are considered constant.

- Pseudo-static earthquake analysis for cut slope largely overestimates the slope failure probability, resulting in designing a lesser width of toe excavation or an uneconomical retention system for larger cut widths. Depending on the magnitude of the pseudo-static coefficients based on the location of project site, the probability of failure of a virgin slope (1.17%) can be largely overestimated approximately in the tune of 85%. Nonlinear dynamic analysis of unsupported or retained cut slopes provide a more realistic magnitude of the maximum failure probability during a seismic motion.

- Probabilistic seismic stability of a retained slope is largely dependent on the spatial variation of shear strength of soil. Under dynamic excitation, a cut slope reinforced with SPAR system exhibits a very low probability of failure with a performance level 'above average' for $\Theta < 0.2$, while the probability of failure is very high with a 'poor' performance level beyond $\Theta = 0.2$.

10.3. RECOMMENDATIONS FROM THE PRESENT STUDY

Based on the findings from the present study, the following recommendations are provided:

- For important and major projects involving slope cutting activity for roadway construction or enhancement, it is extremely important to conduct thorough site investigations to ascertain the best possible representation of the soil shear strength parameters distributed over the project stretch.

- Standard penetration test being the most commonly practised in the field should be utilized to estimate the SoF in the residual fields of *N*-values obtained from a particular site. It is not recommended to directly use the estimated SoF from one site for another. However, in absence of any prior information, appropriate ranges of SoF to be used for numerical analysis can be derived from several studies available in existing literature, however with sufficient justification and engineering judgment.

- The assessed soil shear strength parameters should be thoroughly analysed to establish their randomness and spatial variability in terms of mean, coefficient of variations, cross-correlation coefficients and the correlation lengths corresponding to the identified autocorrelation models.

- For slopes located in seismic zones, it is strongly recommended that probabilistic seismic analysis be conducted to have thorough understanding of the chances of failure of the slope in its unsupported or retained state.

- For any slope retention measure, it is recommended to analyse different types of feasible retention systems for the project stretches. To assess their suitability under seismic conditions, probabilistic pseudo-static analysis should always be conducted.

- However, given the fact that pseudo-static response overestimates the slope instability and lead to uneconomical designs of retention systems, the analysis should also be sufficed with a probabilistic nonlinear dynamic analysis of retained slopes for establishing the temporal and realistic variation in the safety states of the slope and realistic performance of the retention system.

- Given the fact that LEM-based probabilistic approaches incorporating 1-D spatial variability underestimates the failure probabilities, RFEM based analyses incorporating 2-D spatial variability of the parameters are recommended. In case a 2-D spatial variability is not readily available at the site, standard literature may be referred for generating synthetic yet reasonable spatial variabilities, and use the same for various probabilistic analysis for unsupported or retained slopes.

10.4. LIMITATIONS OF THE PRESENT STUDY AND FUTURE SCOPES OF WORK

Any research work performed has its own limitations and thus paves the way and scope for further research. Some of them, as applicable for the present study, are listed as follows:

- The reported work does not incorporate the hydrological factors (water table fluctuation, seepage, and rainfall) commonly responsible in many slope failures. Incorporation of such features is important and is expected to build further understanding on the failure of cut slopes due to hydrological reasons. Further, the spatial variability of the hydrological and other related parameters can bring new insight into the problem.

- The present study incorporates only two of the conventional retention systems for the protection of the cut slope. In the present date, several advanced slope retention and

stabilization techniques are in practice, involving conventional cantilever or counterfort retaining walls, soil nailing, surficial protection covers, mechanically stabilized walls (MSEW), geotextile wrap faced walls, and gabion walls to name a few. The applicability and response of such traditional and other increasingly popular retention measures need to be assessed in a probabilistic framework while incorporating the random field modeling of spatial variability.

- The present study had only touched upon the nonlinear dynamic analysis and seismic response of toe excavated cut slopes, which must be further extensively studied for more realistic simulation of the soil spatial variability using RFEM or other advanced techniques.

- The RFEM coupled with MCS is computationally exhaustive. Performing parametric studies or sensitivity analysis is therefore a cumbersome task. Moreover, the RFEM based computer programs (such as *Rslope2d*) might not be readily available and usable. To overcome this limitation, a series of probabilistic stability charts can be developed for road construction excavating hill slopes.

- Apart from approximately 1300 simulations for deterministic analyses, the present study involved approximately 5100 probabilistic simulations conducted in GeoStudio while around 20 simulations conducted in *Rslope2d*. Each of the probabilistic analyses conducted in Geostudio comprised 2000 MCS, while each of the analyses conducted in *Rslope2d* comprised 4000 MCS. Each of the probabilistic analyses in Geostudio required a computational time of 5 minutes, while each analyses conducted in *Rslope2d* required around 100 minutes of computational time. Although the computational time would definitely vary with the computational resource used, yet it is understandable that the

computational effort required in substantial. Hence, for further improvement in computational efficiency of Monte Carlo procedures at relatively small probability levels, an advanced subset simulation method can be used in future studies. Subset simulation is a stochastic simulation technique for efficiently generating failure samples and computing probability of failure at relatively small level.

REFERENCES

- Acharyya R, Dey A **(**2015) "Site characterization and bearing capacity estimation for a school building located on hillslope" *Proceedings of the Indian Geotechnical Conference,* Pune, India, 1-10.

- Acharyya R, Dey A (2019) "Suitability of the typology of shallow foundations on hill-slopes" *Indian Geotechnical Journal*, 49(6): 635-649. https://dx.doi.org/10.1007/s40098-019-00360-y

- Allahverdizadeh P, Griffiths DV, Fenton GA (2015) "The Random Finite Element Method (RFEM) in probabilistic slope stability analysis with consideration of spatial variability of soil properties" *Proceedings of the International Foundations Congress and Equipment Expo*, 1946–1955. https://doi.org/10.1061/9780784479087.178

- Alonso EE (1976) "Risk analysis of slopes and its application to slopes in Canadian sensitive clays" *Geotechnique*, 26(3): 453-472. https://doi.org/10.1680/geot.1976.26.3.453

- Alonso EE, Krizek RJ (1975) "Stochastic formulation of soil properties" *Proceedings of the 2nd International Conference on Application of Statistics and Probability in Soil and Structural Engineering*, Aachen, 2: 9-32.

- Au SK, Beck JL (2001) "Estimation of small failure probabilities in high dimensions by Subset Simulation" *Probabilistic Engineering Mechanics*, 16(4): 263–277. https://doi.org/10.1016/S0266-8920(01)00019-4

- Au SK, Beck JL (2003) "Subset Simulation and its application to probabilistic seismic performance assessment" *Journal of Engineering Mechanics, ASCE*, 129(8): 1-17. https://doi.org/10.1061/(ASCE)0733-9399(2003)129:8(901)

- Ausilio E, Conte E, Dente G (2001) "Stability analysis of slopes reinforced with piles" *Computers and Geotechnics*, 28(8): 591-611. https://doi.org/10.1016/S0266-352X(01)00013-1.

- Ayalew L, Moeller D, Reik G (2009) "Geotechnical aspects and stability of road cuts in the Blue Nile Basin, Ethiopia" *Geotechnical and Geological Engineering*, 27(6): 713–728. https://doi.org/10.1007/s10706-009-9270-3

- Babu GD, Mukesh M (2004) "Effect of soil variability on reliability of soil slopes" *Geotechnique*, 54(5): 335-337. https://doi.org/10.1680/geot.2004.54.5.335

- Baecher GB, Christian JT (2003) *Reliability and Statistics in Geotechnical Engineering*. John Wiley and Sons, England.

- Bartier PM, Keller CP (1996) "Multivariate interpolation to incorporate thematic surface data using inverse distance weighting (IDW)" *Computers and Geosciences*, 22(7): 795-799. https://doi.org/10.1016/0098-3004(96)00021-0

- Basma AA (1990) "Reliability-based design of sheet pile structures" *Reliability Engineering and System Safety*, 33(2): 215–30. https://doi.org/10.1016/0951-8320(91)90060-K

- Bhattacharya G, Jana D, Ojha S, Chakraborty S (2003) "Direct search for minimum reliability index of earth slopes" *Computers and Geotechnics*, 30(6): 455-462. https://doi.org/10.1016/S0266-352X(03)00059-4

- Bishop AW, Morgenstern NR (1960) "Stability coefficients for earth slopes" *Geotechnique*, 10: 129-150. https://doi.org/10.1680/geot.1960.10.4.129

- Borgatti L, Soldati M (2005) "Geomorphological hazard and human impact in mountain environments: an introduction" *Geomorphology*, 66(1-4): 7-11. https://doi.org/10.1016/j.geomorph.2004.10.001

- Burgess J, Fenton GA, Griffiths DV (2019) "Probabilistic seismic slope stability analysis and design" *Canadian Geotechnical Journal*, 56(12): 1979-1998. https://doi.org/10.1139/cgj-2017-0544

- Cafaro F, Cherubini C (2002) "Large sample spacing in evaluation of vertical strength variability of clayey soil" *Journal of Geotechnical and Geoenvironmental Engineering, ASCE*, 128(7): 558-568. https://doi.org/10.1061/(ASCE)1090-0241(2002)128:7(558)

- Campanella RG, Wickremesinghe DS, Robertson PK (1987) "Statistical treatment of cone penetrometer test data" *Proceedings of the 5th International Conference on Application of Statistics and Probability in Soil and Structural Engineering*, Vancouver, 1011-1019.

- Cao Z, Wang Y (2013) "Bayesian approach for probabilistic site characterization using cone penetration tests" *Journal of Geotechnical and Geoenvironmental Engineering, ASCE*, 139(2): 267-276. https://doi.org/10.1061/(ASCE)GT.1943-5606.0000765

- Cao Z, Wang Y (2014) "Bayesian model comparison and selection of spatial correlation functions for soil parameters" *Structural Safety*, 49: 10-17. https://doi.org/10.1016/j.strusafe.2013.06.003

- Chakraborty R, Dey A **(**2016a) "Stability of hill-slope using FE and LE analyses" *Proceedings of the National Level Conference on Engineering Problems and Application of Mathematics*, Agartala, India, 1-5.

- Chakraborty R, Dey A (2016b) "Numerical investigation of slope instability induced by hydraulic and seismic actions" *Proceedings of the North-East Students Geo-Congress*, Agartala, India 237-244.

- Chakraborty R, Dey A **(**2016c) "Effect of toe cutting on hill-slope stability" *Proceedings of the Indian Geotechnical Conference*, Madras, India, 1-4.

- Chen WF, Zhang H (1991) *Structural Plasticity: Theory, Problems, and CAE Software*. Springer-Verlag.

- Chen F, Zhang R, Wang Y, Liu H, Bohlke T, Zhang W (2020) "Probabilistic stability analyses of slope reinforced with piles in spatially variable soils" *International Journal of Approximate Reasoning*, 122: 66-79. https://doi.org/10.1016/j.ijar.2020.04.006

- Chen G, Zhu J, Qiang M, Gong W (2018) "Three-dimensional site characterization with borehole data – a case study of Suzhou area" *Engineering Geology*, 234(21): 65-82. https://doi.org/10.1016/j.enggeo.2017.12.019

- Cherubini C (1997) "Data and considerations on the variability of geotechnical properties of soils" *Proceedings of the International Conference on Safety and Reliability*, Lisbon, 2: 1583-1591.

- Cherubini C (2000) "Probabilistic approach to the design of anchored sheet pile walls" *Computers and Geotechnics*, 26(3-4): 309-330. https://doi.org/10.1016/S0266-352X(99)00044-0.

- Chia CF, Jiun HL (2008) "Numerical study on the optimum layout of soil–nailed slopes" *Computers and Geotechnics*, 35(4): 585-599. https://doi.org/10.1016/j.compgeo.2007.09.002.

- Ching J, Phoon KK, Wu SH (2016) "Impact of statistical uncertainty on geotechnical reliability estimation" *Journal of Engineering Mechanics, ASCE*, 142(6): 04016027-1-13. https://doi.org/10.1061/(ASCE)EM.1943-7889.0001075

- Ching J, Wang JS, Juang CH, Ku CS (2015) "Cone penetration test (CPT)-based stratigraphic profiling using the wavelet transform modulus maxima method" *Canadian Geotechnical Journal*, 52 (12), 1993–2007. https://doi.org/10.1139/cgj-2015-0027

- Cho SE (2009) "Probabilistic assessment of slope stability that considers the spatial variability of soil properties" *Journal of Geotechnical and Geoenvironmental Engineering, ASCE*, 136(7): 975–984. https://doi.org/10.1061/(ASCE)GT.1943-5606.0000309

- Cho SE (2014) "Probabilistic stability analysis of rainfall-induced landslides considering spatial variability of permeability" *Engineering Geology*, 171: 11-20. http://dx.doi.org/10.1016/j.enggeo.2013.12.015

- Cho SE, Park HC (2009) "Effect of spatial variability of cross-correlated soil properties on bearing capacity of strip footing" *International Journal for Numerical and Analytical Methods in Geomechanics*, 34: 1-26. https://doi.org/10.1002/nag.791

- Chok YH (2009) "Modelling the effects of soil variability and vegetation on the stability of natural slopes" *Ph.D. Thesis*. University of Adelaide, Adelaide, Australia.

- Chowdhury RN, Sidi I, Tang WH (1988) "Discussion: Reliability model on progressive slope failure" *Géotechnique*, 38(4): 641-646. https://doi.org/10.1680/geot.1988.38.4.641

- Christakos G (1992) *Random Field Models in Earth Sciences*. Academic Press, Elsevier, San Diego, USA.

- Christian JT, Ladd CC, Baecher GB (1994) "Reliability applied to slope stability analysis" *Journal of Geotechnical Engineering, ASCE*, 120(12): 2180-2207. https://doi.org/10.1061/(ASCE)0733-9410(1994)120:12(2180)

- Chwała M (2021) "Upper-bound approach based on failure mechanisms in slope stability analysis of spatially variable *c-φ* soils", *Computers and Geotechnics*, 135: 104170-1-19. https://doi.org/10.1016/j.compgeo.2021.104170.

- Crisp MP, Jaksa M, Kuo YL, Fenton GA, Griffiths DV (2019) "A method for generating virtual soil profiles with complex, multi-layer stratigraphy". *Georisk: Assessment and Management of Risk for Engineered Systems and Geohazards*, 13(2): 154–163. https://doi.org/10.1080/17499518.2018.1554817

- Crisp MP, Jaksa M, Kuo YL, Fenton GA, Griffiths DV (2020) "Characterising site investigation performance in a two layer soil profile" *Canadian Journal of Civil Engineering*, 48(2): 115-123. https://doi.org/10.1139/cjce-2019-0416

- Cui L, Sheng D (2005) "Genetic algorithms in probabilistic finite element analysis of geotechnical problems" *Computers and Geotechnics*, 32(8): 555-563. https://doi.org/10.1016/j.compgeo.2005.11.005

- Das BM (1999) *Principle of Foundation Engineering*. Pacific Grove, Brooks/Cole, USA.

- Das HK (2003) "A case study of recent landslides in Greater Guwahati" *ME Thesis*. Gauhati University, Assam, India.

- Das N (1992) "An investigation of soil characteristics of the Greater Guwahati landslide areas" *ME Thesis*. Gauhati University, Assam, India.

- Das UK, Saikia BD (2010) "Shear strength of unsaturated residual soils of the hills in Guwahati" *Proceedings of the Indian Geotechnical Conf*erence *GEOtrendz*. Bombay, India, 1-4.

- De Marsily G, Delay F, Gonçalvès J, Renard P, Teles V, Violette S (2005) "Dealing with spatial heterogeneity" *Hydrogeology Journal*, 13(1): 161-183. https://doi.org/10.1007/s10040-004-0432-3

- DeGroot DJ (1996) "Analysing spatial variability of in situ soil properties". In: *Uncertainty in the Geologic Environment: From Theory to Practice*, Ed(s) Shackelford CD et al., ASCE, New York, 210-238.

- Degroot DJ, Baecher GB (1993) "Estimating autocovariance of in-situ soil properties", *Journal of Geotechnical Engineering, ASCE*, 119(1): 147-166. https://doi.org/10.1061/(ASCE)0733-9410(1993)119:1(147)

- DeWolfe GF, Griffiths DV, Huang J (2010) "Probabilistic and Deterministic Slope Stability Analysis by Random Finite Elements" *GeoTrends: The Progress of Geological and Geotechnical Engineering in Colorado at the Cusp of a New Decade*. GPP 6. https://doi.org/10.1061/41144(391)9

- Dey A, Murali Krishna A (2021) "Comprehensive rainfall induced landslide hazard analysis of 'Sunsali' and 'Noonmati' hills in Guwahati region" *Project Report.* National

Geospatial Program, Department of Science and Technology, Govt. of India, New Delhi, India, Rep. No. NRDMS/02/60/017(G).

- Dou HQ, Han TC, Gong XN, Qiu ZY, Li ZN (2015) "Effects of the spatial variability of permeability on rainfall-induced landslides" *Engineering Geol*ogy, 192: 92-100. http://dx.doi.org/10.1016/j.enggeo.2015.03.014

- Duncan JM (1996) "State of the art: Limit equilibrium and finite-element analysis of slopes" *Journal of Geotechnical Engineering, ASCE*, 122(7): 577-596. https://doi.org/10.1061/(ASCE)0733-9410(1996)122:7(577)

- Duncan JM (2000) "Factors of safety and reliability in geotechnical engineering" *Journal of Geotechnical and Geoenvironmental Engineering, ASCE*, 126(4): 307-316. https://doi.org/10.1061/(ASCE)1090-0241(2000)126:4(307)

- Dyson AP, Tolooiyan A (2019) "Prediction and classification for finite element slope stability analysis by random field comparison" *Computers and Geotechnics*, 109: 117-129. https://doi.org/10.1016/j.compgeo.2019.01.026.

- Elfeki A, Dekking M (2001) "A Markov chain model for subsurface characterization: theory and applications" *Mathematical Geology*, 33(5): 569-589. https://doi.org/10.1023/A:1011044812133

- Elkateb T, Chalaturnyk R, Robertson PK (2003) "An overview of soil heterogeneity: quantification and implications on geotechnical field problems" *Canadian Geotechnical Journal*, 40(1): 1-15. https://doi.org/10.1139/t02-090

- El-Ramly H, Morgenstern NR, Cruden DM (2003) "Probabilistic stability analysis of a tailings dyke on presheared clay-shale" *Canadian Geotechnical J*ournal, 40: 192-208. http://dx.doi.org/10.1139/T02-095

- El-Ramly H, Morgenstern NR, Cruden DM (2005) "Probabilistic assessment of stability of a cut slope in residual soil" *Geotechnique*, 55(1): 77-84. https://doi.org/10.1680/geot.55.1.77.58590

- El-Ramly H, Morgernstern NR, Cruden DM (2002) "Probabilistic slope stability analysis for practice" *Canadian Geotechnical Journal*, 39(3): 665-683. https://doi.org/10.1139/t02-034

- Erginal AE, Türkeş M, Ertek TA, Baba A, Bayrakdar C (2008) "Geomorphological investigation of the excavation-induced Dündar landslide, Bursa- Turkey". *Geografiska Annaler (Series A: Physical Geography)*, 90(2): 109-123. https://doi.org/10.1111/j.1468-0459.2008.00159.x

- Evans SG (1982) "Landslides and surficial deposits in urban areas of British Columbia: a review" *Canadian Geotechnical Journal*, 19(3), 269-288. https://doi.org/10.1139/t82-034

- Fang HW, Chen YF, Hou ZK, Xu GW, Wu JX (2020) "Probabilistic analysis of a cohesion-frictional slope using the slip-line field theory in a Monte-Carlo framework" *Computers and Geotechnics*, 120: 103398 https://doi.org/10.1016/j.compgeo.2019.103398

- Fellenius W (1936) "Calculation of the Stability of Earth Dams" *Proceedings of the Second Congress of Large Dams*, 4: 445-463.

- Feng X, Jimenez R (2014) "Bayesian prediction of elastic modulus of intact rocks using their uniaxial compressive strength" *Engineering Geology*, 173: 32-40. https://doi.org/10.1016/j.enggeo.2014.02.005

- Fenton GA (1990) "Simulation and analysis of random fields" *Ph.D. Thesis*. Department of Civil Engineering and Operations Research, Princeton University, New Jersey, USA.

- Fenton GA (1994) "Error evaluation of three random field generators" *Journal of Engineering Mechanics, ASCE*, 120(12): 2478-2497. https://doi.org/10.1061/(ASCE)0733-9399(1994)120:12(2478)

- Fenton GA (1999) "Random field modeling of CPT data" *Journal of Geotechnical and Geoenvironmental Engineering, ASCE*, 6: 486-498. https://doi.org/10.1061/(ASCE)1090-0241(1999)125:6(486)

- Fenton GA, Griffiths DV (2003) "Bearing-capacity prediction of spatially random *c-φ* soils" *Canadian Geotechnical Journal*, 40: 54-65. https://doi.org/10.1139/t02-086

- Fenton GA, Griffiths DV (2004) "Reply to discussion by R. Popescu on, Bearing capacity prediction of spatially random *c-φ* soils" *Canadian Geotechnical Journal*, 41: 368–369. https://doi.org/10.1139/t03-080

- Fenton GA, Griffiths DV (2007) "Random field generation and the local average subdivision method" In: *Probabilistic Methods in Geotechnical Engineering*, Ed(s). DV Griffiths, GA Fenton, 491: 201-223. https://doi.org/10.1007/978-3-211-73366-0_9

- Fenton GA, Griffiths DV (2008) *Risk Assessment in Geotechnical Engineering*. John Wiley & Sons, Inc, Hoboken, NJ, USA.

- Fenton GA, Vanmarcke EH (1990) "Simulation of random fields via local average subdivision" *Journal of Engineering Mechanics, ASCE*, 116(8): 1733-1749. https://doi.org/10.1061/(ASCE)0733-9399(1990)116:8(1733)

- Ferson S, Hajagos JG (2006) "Varying correlation coefficients can underestimate uncertainty in probabilistic models" *Reliability Engineering & System Safety*, 91: 1461-1467. https://doi.org/10.1016/j.ress.2005.11.043

- Forrest WS, Orr TL (2010) "Reliability of shallow foundations designed to Eurocode 7" *Georisk: Assessment and Management of Risk for Engineered Systems and Geohazards*, 4(4): 186-207. https://doi.org/10.1080/17499511003646484

- Geostudio Quake/W (2018) *Dynamic Modeling with Quake/W*. GEO- SLOPE International, Calgary, AB, Canada.

- Geostudio Sigma/W (2018). *Stress-Strain Modeling with SIGMA/W*, GEO-SLOPE International, Calgary, AB, Canada,.

- Geostudio Slope/W (2018) *Stability Modeling with Slope/W*. GEO- SLOPE International, Calgary, AB, Canada.

- Gong W, Juang CH, Martin II JR, Tang H, Wang Q, Huang H (2018) "Probabilistic analysis of tunnel longitudinal performance based upon conditional random field simulation of soil properties" *Tunnelling and Underground Space Technology*, 73: 1-14. https://doi.org/10.1016/j.tust.2017.11.026

- Gong W, Luo Z, Juang CH, Huang H, Zhang J, Wang L (2014) "Optimization of site exploration program for improved prediction of tunneling-induced ground settlement in clays" *Computers and Geotechnics*, 56: 69-79. https://doi.org/10.1016/j.compgeo.2013.10.008

- Gong W, Zhao C, Juang CH, Tang H, Wang H, Hu X (2020) "Stratigraphic uncertainty modelling with random field approach" *Computers and Geotechnics*, 125. https://doi.org/10.1016/j.compgeo.2020.103681

- Griffiths DV, Fenton GA (2000) "Influence of soil strength spatial variability on the stability of an undrained clay slope by finite elements" *Proceedings of the GeoDenver Symposium, Slope Stability 2000,* 184-193.

- Griffiths DV, Fenton GA (2004) "Probabilistic slope stability analysis by finite elements" *Journal of Geotechnical and Geoenvironmental Engineering, ASCE,* 130: 507-518. https://doi.org/10.1061/(ASCE)1090-0241(2004)130:5(507)

- Griffiths DV, Fenton GA (2007) *Probabilistic Methods in Geotechnical Engineering*. Springer, Verlag Wien, Vienna, Austria.

- Griffiths DV, Fenton GA, Denavit MD (2007) "Traditional and advanced probabilistic slope stability analysis" *Proceedings of the GeoDenver 2007 Symposium*, 1-10. https://doi.org/10.1061/40914(233)19

- Griffiths DV, Huang J, Fenton GA (2009) "Influence of Spatial Variability on Slope Reliability Using 2-D Random Fields" *Journal of Geotechnical and Geoenvironmental Engineering, ASCE,* 135(10): 1367-1378. https://doi.org/10.1061/(ASCE)GT.1943-5606.0000099

- Griffiths DV, Huang J, Fenton GA (2011) "Probabilistic infinite slope analysis" *Computers and Geotechnics*, 38(4): 577–584. https://doi.org/10.1016/j.compgeo.2011.03.006

- Griffiths DV, Huang J, Fenton GA (2015) "Probabilistic slope stability analysis using non-stationary random fields" *Proceedings of the 5th International Symposium on Geotechnical Safety and Risk*, Rotterdam, 690-695.

- Griffiths DV, Lane PA (1999) "Slope stability analysis by finite elements" *Geotechnique*, 49(3): 387-403. https://doi.org/10.1680/geot.1999.49.3.387

- Hahn GJ, Shapiro SS (1967) *Statistical Models in Engineering*. Wiley, New York.

- Halim IS (1991) "Reliability of geotechnical systems considering geological anomaly" *Ph.D. Thesis*. University of Illinois, Urbana-Champaign, USA.

- Hansen L, Eilertsen R, Solberg IL, Rokoengen K (2007) "Stratigraphic evaluation of a Holocene clay-slide in Northern Norway" *Landslides*, 4(3): 233-244. https://doi.org/10.1007/s10346-006-0078-4

- Hassan AM, Wolff TF (1999) "Search algorithm for minimum reliability index of earth slopes" *Journal of Geotechnical and Geoenvironmental Engineering, ASCE*, 125(4): 301-308. https://doi.org/10.1061/(ASCE)1090-0241(2001)127:2(194.2)

- Hata Y, Ichii K, Tokida K (2012) "A probabilistic evaluation of the size of earthquake induced slope failure for an embankment" *Georisk: Assessment and Management of Risk for Engineered Systems and Geohazards*, 6(2): 73-88. https://doi.org/10.1080/17499518.2011.604583

- Hayashi H, Tang WT (1994) "Probabilistic evaluation on progressive failure in cut slopes" *Structural Safety*, 14(1-2): 31-46. https://doi.org/10.1016/0167-4730(94)90005-1.

- Hicks MA, Chen J, Spencer WA (2008) "Influence of spatial variability on 3D slope failures" *Proceedings of the 6th International Conference on Computer Simulation in Risk Analysis and Hazard Mitigation*, 335-342.

- Hicks MA, Nuttall JD, Chen J (2014) "Influence of heterogeneity on 3D slope reliability and failure consequence" *Computers and Geotechnics*, 61: 198-208. https://doi.org/10.1016/j.compgeo.2014.05.004

- Hicks MA, Samy K (2002) "Reliability-based characteristic values: a stochastic approach to Eurocode 7" *Ground Engineering*, 35(12): 30-34. http://worldcat.org/issn/00174653

- Hicks MA, Spencer WA (2008) "3D finite element modelling of slope reliability", *Proceedings of the 8th WCCM and 5th ECCOMAS*, Venice, Italy.

- Hicks MA, Spencer WA (2010) "Influence of heterogeneity on the reliability and failure of a long 3D slope" *Computers and Geotechnics*, 37(7-8): 948-955. https://doi.org/10.1016/j.compgeo.2010.08.001

- Hill, R. (1950). *The Mathematical Theory of Plasticity*. Oxford University Press, Oxford, UK.

- Hu QF, Huang HW (2007) "Risk analysis of soil transition in tunnel works" *Proceedings of the 33rd ITA-AITES World Tunnel Congress - Underground Space the 4th Dimension of Metropolises*, 209-215.

- Huang J, Fenton G, Griffiths DV, Li D, Zhou C (2017) "On the efficient estimation of small failure probability in slopes" *Landslides*, 14(2): 491-498. https://doi.org/10.1007/s10346-016-0726-2

- Huang J, Griffiths DV, Fenton GA (2010) "System reliability of slopes by RFEM" *Soils and Foundations*, 50(3): 343-353. https://doi.org/10.3208/sandf.50.343

- Huang L, Cheng YM, Li L, Yu S (2021) "Reliability and failure mechanism of a slope with non-stationarity and rotated transverse anisotropy in undrained soil strength", *Computers and Geotechnics*, 132: 103970. https://doi.org/10.1016/j.compgeo.2020.103970

- Huang R, Chan L (2004) "Human-induced landslides in China: mechanism study and its implications on slope management" *Chinese Journal of Rock Mechanics and Engineering*, 23(16): 2766– 2777.

- IS 1893 Part 1 (2002). *Criteria For Earthquake Resistant Design of Structures*, Indian Standard Code of Practice, Bureau of Indian Standards..

- IS 2131 (2002) *Method for Standard Penetration Test for Soils*, Indian Standard Code of Practice, Bureau of Indian Standards.

- Jaksa MB (1995) "The influence of spatial variability on the geotechnical design properties of a stiff, overconsolidated clay" *Ph.D. Thesis*. University of Adelaide, Adelaide, Australia.

- Jaksa MB (2006) "Modeling the natural variability of an over-consolidated clay in Adelaide, South Australia" *Proceedings of the 2nd International Workshop on Characterization and Engineering Properties of Natural Soils*, Singapore, 4: 2721–2751 https://doi.org/10.1201/NOE0415426916.ch30

- Jamshidi CR, Alaie R (2015) "Effects of anisotropy in correlation structure on the stability of an undrained clay slope" *Georisk: Assessment and Management of Risk for Engineered Systems and Geohazards*, 9(2): 109-123. https://doi.org/10.1080/17499518.2015.1037844

- Janbu N (1954) "Applications of Composite Slip Surfaces for Stability Analysis" *Proceedings of the European Conference on the Stability of Earth Slopes*, Stockholm, 3: 39-43.

- Javankhoshdel S, Bathurst RJ (2014) "Simplified probabilistic slope stability design charts for cohesive and cohesive-frictional (c -ϕ) soils" *Canadian Geotechnical Journal*, 51(9): 1033-1045. https://doi.org/10.1139/cgj-2013-0385

- Javankhoshdel S, Bathurst RJ (2015) "Influence of cross correlation between soil parameters on probability of failure of simple cohesive and c-ϕ slopes" *Canadian Geotechnical Journal*, 53(5): 839-853. https://doi.org/10.1139/cgj-2015-0109

- Javankhoshdel S, Luo N, Bathurst RJ (2017) "Probabilistic analysis of simple slopes with cohesive soil strength using RLEM and RFEM" *Georisk: Assessment and Management of Risk for Engineered Systems and Geohazards*, 11(3): 231-246. https://doi.org/10.1080/17499518.2016.1235712

- Ji J, Liao HJ, Low BK (2012) "Modeling 2-D spatial variation in slope reliability analysis using interpolated autocorrelations" *Computers and Geotechnics*, 40: 135-146. https://doi.org/10.1016/j.compgeo.2011.11.002

- Jiang SH, Li DQ, Cao ZJ, Zhou CB, Phoon KK (2014) "Efficient system reliability analysis of slope stability in spatially variable soils using Monte Carlo Simulation" *Journal of Geotechnical and Geoenvironmental Engineering, ASCE*, 141(2): 1-13. https://doi.org/10.1061/(ASCE)GT.1943-5606.0001227

- Johari A, Mousavi S, Nejad AH (2015) "A seismic slope stability probabilistic model based on Bishop's method using analytical approach" *Scientica Iranica: Transactions A Civil Engineering*, 22(3): 728-741.

- Kahatadeniya K, Nanakorna P, Neaupane KM (2009) "Determination of the critical failure surface for slope stability analysis using ant colony optimisation" *Engineering Geology*, 108: 133-141. https://doi.org/10.1016/j.enggeo.2009.06.010

- Kainthola A, Singh PK, Singh TN (2015) "Stability investigation of road cut slope in basaltic rockmass, Mahabaleshwar, India" *Geoscience Frontiers*, 6(6): 837–845. https://doi.org/10.1016/j.gsf.2014.03.002

- Kainthola A, Singh PK, Wasnik AB, Sazid M, Singh TN (2012) "Finite element analysis of road cut slopes using Hoek and Brown failure criterion" *International Journal of Earth Sciences and Engineering*, 5(5): 1100–1109.

- Kalita UC (2001) "A study of landslide hazards in North-Eastern India" *Proceedings of the 11th International Conference in Soil Mechanics and Geotechnical Eng*ineering, 1-3: 1167-1170.

- Kang GC, Song YS, Kim TH (2009) "Behavior and stability of a large-scale cut slope considering reinforcement stages" *Landslides*, 6: 263-272. https://doi.org/10.1007/s10346-009-0164-5.

- Kitch WA (1994) "Deterministic and probabilistic based analyses of reinforced soil slopes" *Ph.D. Thesis*. University of Texas at Austin, USA.

- Kitch WA, Gilbert RB, Wright SG (2012) "Probabilistic Assessment of commercial design guides for steep reinforced slopes: Implications for design". In *GeoRisk 2011: Geotechnical Risk Assessment and Management,* (Eds). Juang CH et al., *ASCE,* Atlanta, 103: 1-22. https://doi.org/10.1061/41183(418)115

- Kourkoulis R, Gelagoti F, Anastasopoulos I, Gazetas D (2012) "Hybrid method for analysis and design of slope stabilizing piles" *Journal of Geotechnical and Geoenvironmental Engineering, ASCE,* 138(1): 1-14. https://doi.org/10.1061/(ASCE)GT.1943-5606.0000546

- Krahn J (2004) *Stability Modeling with SLOPE/W, An Engineering Methodology*. First Edition, GEO-SLOPE International Ltd, Calgary, Alberta, Canada.

- Kramer SL (1996) *Geotechnical Earthquake Engineering*, Prentice Hall, New Jersey, USA.

- Kulatilake PHSW, Um JG (2003) "Spatial variation of cone tip resistance for the clay site at Texas A and M University" *Geotechnical and Geological Engineering*, 21(2): 149-165. https://doi.org/10.1023/A:1023526614301

- Kulhawy FH (1992) "On the evaluation of static soil properties" *Proceedings of the Stability and Performance of Slopes and Embankments II, ASCE,* 95-115.

- Kulhawy FH, Birgisson B, Grigoriu MD (1992) "Reliability based foundation design for transmission line structures: Transformation models for in-situ tests", *Rep. No. EL-5507(4),* Electric Power Research Institute (EPRI), Palo Alto, California, USA.

- Kumar SS, Tamang DT, Timsina R, Dey A **(**2015) **"**Laboratory investigations to assess the geotechnical characteristics of soils from Sikkim hill slopes**"** *Proceedings of the Indian Geotechnical Conference*, Pune, India, 1-10.

- Lacasse S, Nadim F (1996) "Uncertainties in characterizing soil properties", In *Uncertainty in the Geologic Environment: From Theory to Practice*, Ed(s). Shackelford CD et al., *ASCE*, New York, 49-75.

- Le TMH (2014) "Reliability of heterogeneous slopes with cross-correlated shear strength parameters" *Georisk: Assessment and Management of Risk for Engineered Systems and Geohazards*, 8(4): 250-257. https://doi.org/10.1080/17499518.2014.966117

- Lee IK, White W, Ingles OG (1983) *Geotechnical Engineering*. Pitman, London.

- Lee SG, Hencher SR (2009) "The repeated failure of a cut-slope despite continuous reassessment and remedial works" *Engineering Geology*, 107(1-2): 16-41. https://doi.org/10.1016/j.enggeo.2009.03.011

- Lee SW, Ching J (2020) "Simplified risk assessment for a spatially variable undrained long slope" *Computers and Geotechnics*, 117: 103228. https://doi.org/10.1016/j.compgeo.2019.103228

- Leshchinsky D, Boedeker RH (1989) "Geosynthetic reinforced soil structures" *Journal of Geotechnical Engineering, ASCE*, 115(10): 1459-1478. https://doi.org/10.1061/(ASCE)0733-9410(1989)115:10(1459)

- Li DQ, Jiang SH, Cao ZJ, Zhou W, Zhou CB, Zhang LM (2015a) "A multiple response-surface method for slope reliability analysis considering spatial variability of soil properties" *Engineering Geology*, 187: 60-72. https://doi.org/10.1016/j.enggeo.2014.12.003

- Li DQ, Qi XH, Cao ZJ, Tang XS, Phoon KK, Zhou CB (2016c) "Evaluating slope stability uncertainty using coupled Markov chain" *Computers and Geotechnics*, 73: 72-82. https://doi.org/10.1016/j.compgeo.2015.11.021

- Li DQ, Qi XH, Phoon KK, Zhang LM, Zhou CB (2014b) "Effect of spatially variable shear strength parameters with linearly increasing mean trend on reliability of infinite slopes" *Structural Safety*, 49: 45-55. https://doi.org/10.1016/j.strusafe.2013.08.005

- Li DQ, Xiao T, Cao ZJ., Zhou CB, Zhang LM (2016a) "Enhancement of random finite element method in reliability analysis and risk assessment of soil slopes using Subset Simulation" *Landslides*, 13, 293-303. https://doi.org/10.1007/s10346-015-0569-2

- Li JH, Cassidy MJ, Huang JS, Zhang LM, Kelly R (2016d) "Probabilistic identification of soil stratification" *Géotechnique*, 66(1), 16-26. https://doi.org/10.1680/jgeot.14.P.242

- Li KS, Lumb P (1987) "Probabilistic design of slopes" *Canadian Geotechnical Journal*, 24(4): 520-535. https://doi.org/10.1139/t87-068

- Li L, Liang RY (2014) "Reliability-based design for slopes reinforced with a row of drilled shafts" *International Journal for Numerical and Analytical Methods in Geomechanics*, 38(2): 202-220. https://doi.org/10.1002/nag.2220

- Li L, Wang Y, Cao ZJ (2014a) "Probabilistic slope stability analysis by risk aggregation" *Engineering Geology*, 176: 57-65. https://doi.org/10.1016/j.enggeo.2014.04.010

- Li L, Wang Y, Cao ZJ, Chu X (2013) "Risk de-aggregation and system reliability analysis of slope stability using representative slip surfaces" *Computers and Geotechnics*, 53: 95-105. https://doi.org/10.1016/j.compgeo.2013.05.004

- Li XY, Zhang LM, Li JH (2015b) "Using conditioned random field to characterize the variability of geologic profiles" *Journal of Geotechnical and Geoenvironmental Engineering*, 142(4), 04015096. https://doi.org/10.1061/(ASCE)GT.1943-5606.0001428

- Li Z, Wang X, Wang H, Liang RY (2016b) "Quantifying stratigraphic uncertainties by stochastic simulation techniques based on Markov random field" *Engineering Geology*, 201, 106-122. https://doi.org/10.1016/j.enggeo.2015.12.017

- Liao T, Mayne PW (2007) "Stratigraphic delineation by three-dimensional clustering of piezocone data" *Georisk: Assessment and Management of Risk for Engineered Systems and Geohazards*, 1(2), 102-119. https://doi.org/10.1080/17499510701345175

- Low BK, Lacasse S, Nadim F (2007) "Slope reliability analysis accounting for spatial variation" *Georisk: Assessment and management of risk for engineered systems and geohazards,* 1(4): 177-189. https://doi.org/10.1080/17499510701772089

- Low BK, Tang WH (1997) "Reliability analysis of reinforced embankments on soft ground" *Canadian Geotechnical Journal,* 34(5): 672-685. https://doi.org/10.1139/t97-032

- Lü Q, Low BK (2011) "Probabilistic analysis of underground rock excavations using response surface method and SORM" *Computers and Geotechnics,* 38: 1008-1021. https://doi.org/10.1016/j.compgeo.2011.07.003

- Lumb P (1966) "The variability of natural soils" *Canadian Geotechnical Journal,* 3(2): 74-97. https://doi.org/10.1139/t66-009

- Lumb P (1970) "Safety factors and the probability distribution of soil strength" *Canadian Geotechnical Journal,* 7(3): 225-242. https://doi.org/10.1139/t70-032

- Luo N, Bathurst RJ (2018a) "Probabilistic analysis of reinforced slopes using RFEM and considering spatial variability of frictional soil properties due to compaction" *Georisk: Assessment and Management of Risk for Engineering Systems and Geohazards,* 12(2): 87-108. https://doi.org/10.1080/17499518.2017.1362443

- Luo N, Bathurst RJ (2018b) "Deterministic and random FEM analysis of full-scale unreinforced and reinforced embankments" *Geosynthetics International,* 25(2): 164-179. https://doi.org/10.1680/jgein.17.00040

- Luo N, Bathurst RJ, Javankhoshdel S (2016) "Probabilistic stability analysis of simple reinforced slopes by finite element method" *Computers and Geotechnics,* 77: 45-55. https://doi.org/10.1016/j.compgeo.2016.04.001

- Luo Z, Hu B, Wang Y, Di H (2018) "Effect of spatial variability of soft clays on geotechnical design of braced excavations: A case study of Formosa excavation" *Computers and Geotech*nics, 103: 242-253. https://doi.org/10.1016/j.compgeo.2018.07.020

- Mahanta B, Singh HO, Singh PK, Kainthola A, Singh TN (2016) "Stability analysis of potential failure zones along NH-305, India" *Natural Hazards*, 83(3): 1341-1357. https://doi.org/10.1007/s11069-016-2396-8

- Malekpoor P S, Chenari RJ, Javankhoshdel S (2020) "Discussion of "Probabilistic seismic slope stability analysis and design" *Canadian Geotechnical Journal*, 57(7): 1103-1108. https://doi.org/10.1139/cgj-2019-0386

- Matsui T, Sun KC (1992) "Finite element slope stability analysis by shear strength reduction technique" *Soils and Foundations*, 32(1), 59-70. https://doi.org/10.3208/sandf1972.32.59

- Matsuo M, Kuroda K (1974) "Probabilistic approach to design of embankments" *Soils and Foundations*, 14(2): 1-17. https://doi.org/10.3208/sandf1972.14.2_1

- Mbarka S, Baroth J, Ltifi M, Hassis H, Darve F (2010) "Reliability analyses of slope stability" *European Journal of Environmental and Civil Engineering*, 14(10): 1227-1257. https://doi.org/10.1080/19648189.2010.9693293

- Morgenstern NR (2000) "Performance in geotechnical practice" *HKIE Transactions*. 7(2): 2-15. https://doi.org/10.1080/1023697X.2000.10667819

- Morgenstern NR, Price VE (1965) "The analysis of the stability of general slip surfaces" *Geotechnique*, 15(1): 79 – 93. https://doi.org/10.7939/R3JS9HF63

- Morrison P, Maley R, Brady G, Porcella R (1977) "Earthquake recordings on or near dams" *Report No. PB285867*, United States Committee on Large Dams, California Institute of Technology, USA.

- Mostyn GR, Soo S (1992) "The effect of autocorrelation on the probability of failure of slopes" *Proceedings of the 6th Australia, New Zealand Conference on Geomechanics: Geotechnical Risk*, 542-546.

- Nadim F (1986) "Probabilistic site description strategy", *Rpt. 51411–4*. Norwegian Geotechnical Institute, Oslo, Norway.

- Newmark NM (1965) "Effects of earthquakes on dams and embankments" *Géotechnique*, 15(2): 139-160. https://doi.org/10.1680/geot.1965.15.2.139

- Nguyen TS, Likitlersuang S, Ohtsu H, Kitaoka T (2017) "Influence of the spatial variability of shear strength parameters on rainfall induced landslides: A case study of sandstone slope on Japan" *Arabian Journal of Geosc*iences, 10: 1-12. http://dx.doi.org/10.1007/s12517-017-3158-y

- Nguyen VU, Chowdhury RN (1984) "Probabilistic study of spoil pile stability in strip coal mines-two techniques compared" *International Journal of Rock Mechanics and Mining Sciences & Geomechanics Abstracts*, 21: 303-312. https://doi.org/10.1016/0148-9062(84)90363-2

- Nguyen VU, Chowdhury RN (1985) "Simulation for risk analysis with correlated variables" *Géotechnique*, 35: 47-58. https://doi.org/10.1680/geot.1985.35.1.47

- Norberg T, Rosén L, Baran A, Baran S (2002) "On modelling discrete geological structures as Markov random fields" *Mathematical Geology*, 34: 63-77. https://doi.org/10.1023/A:1014079411253

- Paice GM (1997) "Finite element analysis of stochastic soils" *Ph.D. Thesis*. University of Manchester, UK.

- Papaioannou I, Straub D (2017) "Learning soil parameters and updating geotechnical reliability estimates under spatial variability - Theory and application to shallow foundations" *Georisk: Assessment and Management of Risk for Engineered Systems and Geohazards*, 11(1): 116-128. https://doi.org/10.1080/17499518.2016.1250280

- Papoulis A (1991) *Probability, Random Variables, and Stochastic Processes*. McGraw-Hill, New York, USA.

- Patel MD, McMechan GA (2003) "Building 2-D stratigraphic and structure models from well log data and control horizons" *Computers and Geosciences*, 29(5): 557-567. https://doi.org/10.1016/S0098-3004(03)00039-6

- Phoon KK (2008) *Reliability-Based Design in Geotechnical Engineering.* Computations and Applications. CRC Press, London, UK.

- Phoon KK, Kulhawy FH (1996) "On quantifying inherent soil variability" *Uncertainty in the Geologic Environment: From Theory to Practice (Geotechnical Special Publication 58), ASCE*, 326-340.

- Phoon KK, Kulhawy FH (1999) "Characterization of geotechnical variability" *Canadian Geotechnical Journal*, 36(4): 612-624. https://doi.org/10.1139/t99-038

- Phoon KK, Kulhawy FH, Grigoriu M.D (1999) "Characterization of geotechnical variability" *Canadian Geotechnical Journal*, 36(4): 612-624. https://doi.org/10.1139/t99-038

- Phoon KK, Kulhawy FH, Grigoriu MD (1995) "Reliability-based design of foundations for transmission line structures" *Report TR-105000*, Electric Power Research Institute, Palo Alto, California, USA.

- Phoon KK, Quek ST, An P (2003) "Identification of statistically homogeneous soil layers using modified Bartlett statistics" *Journal of Geotechnical and Geoenvironmental Engineering*, 7: 649-659. https://doi.org/10.1061/(ASCE)1090-0241(2003)129:7(649)

- Pieczy´nska-Kozłowska J, Puła W, Griffiths DV, Fenton GA (2015) "Influence of embedment, self-weight and anisotropy on bearing capacity reliability using the random finite element method" *Computers and Geotechnics*, 67: 229-238. https://doi.org/10.1016/j.compgeo.2015.02.013

- Priestley MB (1981) *Spectral Analysis and Time Series I: Univariate series*. Academic Press, New York, USA.

- Puła W, Griffiths DV (2021) "Transformations of spatial correlation lengths in random fields" *Computers and Geotechnics*, 136: 104151. https://doi.org/10.1016/j.compgeo.2021.104151.

- Qi XH, Li DQ, Phoon KK, Cao ZJ, Tang XS (2016) "Simulation of geologic uncertainty using coupled Markov chain" *Engineering Geology*, 207: 129-140. https://doi.org/10.1016/j.enggeo.2016.04.017

- RaghuKanth STG, Dash SK (2008) "Stochastic modeling of SPT N-value and evaluation of probability of liquefaction at Guwahati city" *Journal of Earthquake and Tsunami*, 3: 175-196. https://doi.org/10.1142/S1793431108000323

- Rahman NA, Tabassum N, Islam MR (2021) "Different aspects of slope failures considering large deformation: application of smoothed particle hydrodynamics (SPH)" *Innovative Infrastructure Solutions*, 6(37): 1-15. https://doi.org/10.1007/s41062-020-00405-9

- Rao P, Zhao L, Chen O, Nimbalkar S (2019) "Three-dimensional limit analysis of slopes reinforced with piles in soils exhibiting heterogeneity and anisotropy in cohesion" *Soil Dynamics and Earthquake Engineering*, 121: 194-199, https://doi.org/10.1016/j.soildyn.2019.02.030.

- Reale C, Xue J, Pan Z, Gavin K (2015) "Deterministic and probabilistic multi-modal analysis of slope stability" *Computers and Geotechnics*, 66: 172-179. https://doi.org/10.1016/j.compgeo.2015.01.017

- Reyna F, Chameau JL (1991) "Statistical evaluation of CPT and DMT measurements at the Heber Road Site" *Proceedings of the Geotechnical Engineering Congress, Gotechnical Special Publication 27*, 14-25.

- Roberts C, Casella G (1999) *Monte Carlo Statistical Methods*. Springer, Berlin, Germany.

- Sabzevari T, Noroozpour S (2014) "Effect of hillslope geometry on surface and subsurface flows" *Hydrogeology Journal*, 22: 1593-1604. https://doi.org/10.1007/s10040-014-1149-6

- Saikia BD (2002) "Geotechnical investigation of probable landslide spots within Guwahati city area". *Progress Report*. Directorate of Science and Technology, Govt. of India.

- Saikia BD, Sarma AK, Goswami D, Deka G (1996) "Landslide hazard zonation of Guwahati area". *Progress Report*. Directorate of Science and Technology, Govt. of India.

- Saikia R, Deka P, Kalita S, Dey A **(**2014**) "**Analysis and behavior of hill slopes and their stabilization measures**"** *Proceedings of the Indian Geotechnical Conference*, Kakinada, India, 2183-2190.

- Sarma CP, Dey A, Murali Krishna A (2020) "Influence of digital elevation models on the simulation of rainfall-induced landslides in the hillslopes of Guwahati, India" *Engineering Geology*, 268: 105523. https://dx.doi.org/10.1016/j.enggeo.2020.105523

- Sarma CP, Murali Krishna A, Dey A (2014) "Probabilistic slope stability analysis considering spatial variability of soil properties: Influence of correlation length" *Proceedings of 4th International Conference of the International Association for Computational Methods and Recent Advances in Geomechanics*, Kyoto, Japan, 1125-1130.

- Sarma CP, Murali Krishna A, Dey A **(**2019) "Geotechnical characterization of hillslope soils of Guwahati region" In *Geotechnical Characterisation and Geoenvironmental Engineering. Lecture Notes in Civil Engineering*, 16: 103-110 Ed(s). Stalin VK and Muttharam M., Springer, Singapore. https://dx.doi.org/10.1007/978-981-13-0899-4_13

- Schloeder CA, Zimmerman NE, Jacobs MJ (2001) "Comparison of methods for interpolating soil properties using limited data" *Soil Science Society of America Journal*, 65(2), 470-479. https://doi.org/10.2136/sssaj2001.652470x

- Schneider HR, Holtz RD (1986) "Design of slopes reinforced with geotextiles and geogrids" *Geotextiles and Geomembranes*, 3(1): 29-51. https://doi.org/10.1016/0266-1144(86)90013-0

- Schultze E (1975) "Some aspects concerning the application of statistics and probability to foundation structures" *Proceedings of 2nd International Conference on the Application of Statistics and Probability in Soil and Structural Engineering*, Aachen, 4: 457-494.

- Seed HB (1979) "Considerations in the earthquake-resistant design of earth and rockfill dams" *Geotechnique*, 29(3): 215-263. https://doi.org/10.1680/geot.1979.29.3.215

- Seed HB (1981) "Earthquake-resistant design of earth dams" *Proceedings of International Conference on Recent Advancement in Geotechnical Earthquake Engineering and Soil Dynamics*, 17.

- Seed HB (1983) "Earthquake-resistant design of earth dams" *Symposium on Seismic Design of Embankments and Caverns, ASCE National Convention*, Philadelphia, PA, 41-64.

- Seed HB, Makdisi FI, DeAlba P (1978) "Performance of earth dams during earthquakes" *Journal of Soil Mechanics and Foundation Division, ASCE*, 104(7): 967-994.

- Seed HB, Martin GR (1966) "The seismic coefficient in earth dam design" *Journal of Soil Mechanics and Foundation Division, ASCE*, 92(3): 25-58.

- Singh TN, Gulati A, Dontha L, Bhardwaj V (2008) "Evaluating cut slope failure by numerical analysis - A case study" *Natural Hazards*, 47: 263-279. https://doi.org/10.1007/s11069-008-9219-5

- Sjöberg J (1999) "Analysis of the Aznalcollar pit slope failures - a case study". In *FLAC and Numerical Modeling in Geomechanics*, Ed(s). Detournay and Hart, Rotterdam, Balkema, 63-70. https://doi.org/10.1201/9781003078531-10

- Smith IM, Griffiths DV (1988) *Programming the Finite Element Method*, John Wiley and Sons.

- Spencer E (1967) "A Method of Analysis of Embankments assuming Parallel Inter-slice Forces" *Geotechnique*, 17 (1): 11-26.

- Spry MJ, Kulhawy FH, Grigoriu MD (1988) "Reliability-based foundation design for transmission line structures: Geotechnical site characterization strategy", *Report No. EL-5507(1)*, Electric Power Research Institute (EPRI), Palo Alto, California, USA.

- Srivastava A, Babu GLS (2009) "Effect of soil variability on the bearing capacity of clay and in slope stability problems" *Engineering Geology*, 108(1-2): 142-152. https://doi.org/10.1016/j.enggeo.2009.06.023

- Stark TD, Arellano WD, Hillman RP, Hughes RM, Joyal N, Hillebrandt D (2005) "Effect of Toe Excavation on a Deep Bedrock Landslide" *Journal of Performance of Constructed Facilities*, 19(3): 244-255. https://doi.org/10.1061/(ASCE)0887-3828(2005)19:3(244)

- Stokes A, Douglas G, Fourcaud T, Giadrossich F, Gillies C, Hubble T et al. (2014) "Ecological mitigation of hillslope instability: Ten key issues facing researchers and practitioners" *Plant and Soil*, 377: 1-23. https://doi.org/10.1007/s11104-014-2044-6

- Stuedlein AW, Kramer SL, Arduino P, Holtz RD (2012) "Geotechnical characterization and random field modeling of desiccated clay" *Journal of Geotechnical and Geoenvironmental Engineering, ASCE*, 138: 1301-1313. https://doi.org/10.1061/(ASCE)GT.1943-5606.0000723.

- Tabarroki M, Ahmad F, Banaki R, Jha SK, Ching J (2013) "Determining the factors of safety of spatially variable slopes modeled by random fields" *Journal of Geotechnical and Geoenvironmental Engineering, ASCE*, 139(12): 2082-2095. https://doi.org/10.1061/(ASCE)GT.1943-5606.0000955

- Talukdar P, Bora R, Dey A **(**2018) "Numerical investigation of hill slope instability due to seepage and anthropogenic activities" *Indian Geotechnical Journal*, 48(3): 585-594. https://dx.doi.org/10.1007/s40098-017-0272-4

- Tamimi S, Amadei B, Frangopol DM (1989) "Monte Carlo simulation of rock slope reliability" *Computers and Structures*, 33(6): 1495-1505. https://doi.org/10.1016/0045-7949(89)90489-6

- Tang WH (1979) "Probabilistic evaluation of penetration resistances" *Journal of Geotechnical Engineering, ASCE*, 105(10): 1173–1191.

- Tang WH, Gilbert RB (1989) "Average property in random two-state medium" *Journal of Engineering Mechanics*, 115(1): 131-144. https://doi.org/10.1061/(ASCE)0733-9399(1989)115:1(131)

- Tang WH, Yucemen MS, Ang AHS (1976) "Probability-based short term design of soil slopes" *Canadian Geotechnical Journal*, 13(3): 201-215. https://doi.org/10.1139/t76-024

- Taylor DW (1937) "Stability of earth slopes" *Journal of the Boston Society of Civil Engineers*, 24: 197-246.

- Tian M, Li DQ, Cao ZJ, Phoon KK, Wang Y (2016) "Bayesian identification of random field model using indirect test data" *Engineering Geology*, 210: 197-211. https://doi.org/10.1016/j.enggeo.2016.05.013

- Tobutt DC (1982) "Monte Carlo simulation methods for slope stability" *Computers and Geosciences*, 8: 199-208. https://doi.org/10.1016/0098-3004(82)90021-8

- Tsinker GP (1983) "Anchored sheet pile bulkheads: design practice" *Journal of Geotechnical Engineering, ASCE*, 109(8): 1021-1038. https://doi.org/10.1061/(ASCE)0733-9410(1983)109:8(1021)

- Tsompanakis Y, Lagaros ND, Psarropoulos PN, Georgopoulos EC (2010) "Probabilistic seismic slope stability assessment of geostructures" *Structure and Infrastructure Engineering*, 6(1-2): 179-191. https://doi.org/10.1080/15732470802664001

- Tun Y.W, Pedroso DM, Scheuermann A, Williams DJ (2016) "Probabilistic reliability analysis of multiple slopes with genetic algorithms" *Computers and Geotechnics*, 77: 68-76. https://doi.org/10.1016/j.compgeo.2016.04.006

- U.S. Army Corps of Engineers (1997) Engineering and design: introduction to probability and reliability methods for use in geotechnical engineering. *Technical Letter 1110-2-547*, Department of the Army, Washington, D.C., USA.

- Umrao RK, Singh R, Ahmad M, Singh TN (2011) "Stability analysis of cut slopes using continuous slope mass rating and Kinematic Analysis in Rudraprayag District, Uttarakhand" *Geomaterials*, 1(3), 79-87. https://doi.org/10.4236/gm.2011.13012

- Uzielli M, Lacasse S, Nadim F, Phoon KK (2006) "Soil Variability Analysis for Geotechnical Practice" *Proceedings of the 2nd International Workshop on Characterisation and Engineering Properties of Natural Soils*, Singapore.

- Uzielli M, Vannucchi G, Phoon KK (2005) "Random field characterisation of stress-normalised cone penetration testing parameters" *Geotechnique*, 68(1): 3-20. https://doi.org/10.1680/geot.2005.55.1.3

- Vanmarcke EH (1977) "Probabilistic modeling of soil profiles" *Journal of Geotechnical Engineering Division, ASCE*, 103(11): 1227-1246.

- Vanmarcke EH (1978) "Probabilistic characterization of soil profiles" *Proceedings of the ASCE Specialty Workshop on Site Characterization and Exploration*, Northwestern University, 199-219.

- Vanmarcke EH (1983) *Random Fields, Analysis and Synthesis*. MIT Press, Cambridge, Massachusetts, USA.

- Vekli M, Aytekin M, Banu IS, Calik U (2012) "Experimental and numerical investigation of slope stabilization by stone columns" *Natural Hazards*, 64: 797-820. https://doi.org/10.1007/s11069-012-0272-8

- Wang H, Wang X, Wellmann JF, Liang RY (2018c) "Bayesian stochastic soil modelling framework using Gaussian Markov random fields" *ASCE-ASME Journal of Risk and Uncertainty in Engineering Systems, Part A: Civil Engineering*, 4(2): 04018014. https://doi.org/10.1061/AJRUA6.0000965

- Wang H, Wellmann JF, Li Z, Wang X, Liang RY (2017) "A segmentation approach for stochastic geological modeling using hidden Markov random fields" *Mathematical Geosciences*, 49(2), 145-177. https://doi.org/10.1007/s11004-016-9663-9

- Wang X, Li Z, Wang H, Rong Q, Liang RY (2016b) "Probabilistic analysis of shield-driven tunnel in multiple strata considering stratigraphic uncertainty" *Structural Safety*, 62: 88-100. https://doi.org/10.1016/j.strusafe.2016.06.007

- Wang X, Wang H, Liang RY, Zhu H, Di H (2018b) "A hidden Markov random field model based approach for probabilistic site characterization using multiple cone penetration test data" *Structural Safety*, 70: 128-138. https://doi.org/10.1016/j.strusafe.2017.10.011

- Wang Y (2012) "Uncertain parameter sensitivity in Monte Carlo simulation by sample reassembling" *Computers and Geotechnics*, 46: 39-47. https://doi.org/10.1016/j.compgeo.2012.05.014

- Wang Y, Au SK, Cao Z (2010b) "Bayesian approach for probabilistic characterization of sand friction angles" *Engineering Geology*, 114(3-4): 354-363. https://doi.org/10.1016/j.enggeo.2010.05.013

- Wang Y, Cao Z, Li D (2016a) "Bayesian perspective on geotechnical variability and site characterization" *Engineering Geology*, 203: 117-125. https://doi.org/10.1016/j.enggeo.2015.08.017

- Wang Y, Cao ZJ, Au SK (2010a) "Efficient Monte Carlo Simulation of parameter sensitivity in probabilistic slope stability analysis" *Computers and Geotechnics*, 37(7-8): 1015-1022. https://doi.org/10.1016/j.compgeo.2010.08.010

- Wang Y, Cao ZJ, Au SK (2011) "Practical reliability analysis of slope stability by advanced Monte Carlo Simulations in spreadsheet" *Canadian Geotechnical Journal*, 48(1): 162-172. https://doi.org/10.1139/T10-044

- Wang Y, Huang K, Cao Z (2013) "Probabilistic identification of underground soil stratification using cone penetration tests" *Canadian Geotechnical Journal*, 50(7): 766-776. https://doi.org/10.1139/cgj-2013-0004

- Wang Y, Huang K, Cao Z (2014) "Bayesian identification of soil strata in London clay" *Géotechnique*, 64(3): 239-246. https://doi.org/10.1680/geot.13.T.018

- Wang Y, Zhao T (2016) "Interpretation of soil property profile from limited measurement data: a compressive sampling perspective" *Canadian Geotechnical Journal*, 53(9): 1547-1559. https://doi.org/10.1139/cgj-2015-0545

- Wang Y, Zhao T, Cao Z (2015) "Site-specific probability distribution of geotechnical properties" *Computers and Geotechnics*, 70: 159-168. https://doi.org/10.1016/j.compgeo.2015.08.002

- Wang Y, Zhao T, Phoon KK (2018a) "Direct simulation of random field samples from sparsely measured geotechnical data with consideration of uncertainty in interpretation" *Canadian Geotechnical Journal*, 55(6): 862-880. https://doi.org/10.1139/cgj-2017-0254

- Whitman RV (1984) "Evaluating calculated risk in geotechnical engineering" *Journal of Geotechnical Engineering, ASCE*, 110(2): 143-188. https://doi.org/10.1061/(ASCE)0733-9410(1984)110:2(143)

- Whitman RV (2000) "Organizing and evaluating uncertainty in geotechnical engineering" *Journal of Geotechnical and Geoenvironmental Engineering*, 126(7): 583-593. https://doi.org/10.1061/(ASCE)1090-0241(2000)126:7(583)

- Wolff TF (1985) "Analysis and design of embankment dam slopes: A probabilistic approach" *Ph.D. Thesis*. Purdue University, Lafayette, IN, USA.

- Wu TH, Kraft LM (1970) "Safety analysis of slopes" *Journal of the Soil Mechanics and Foundations Division, ASCE*, 96(2): 609-630.

- Wu TH, Lee IM, Potter JC, Kjekstad O (1987) "Uncertainties in evaluation of strength of marine sand" *Journal of Geotechnical Engineering, ASCE*, 7: 719-738. https://doi.org/10.1061/(ASCE)0733-9410(1987)113:7(719)

- Xiao J, Gong W, Martin JR, Shen M, Luo Z (2016) "Probabilistic seismic stability analysis of slope at a given site in a specified exposure time" *Engineering Geology*, 212: 53-62. https://doi.org/10.1016/j.enggeo.2016.08.001

- Xiao T, Li DQ, Cao ZJ, Tang XS (2017) "Full probabilistic design of slopes in spatially variable soils using simplified reliability analysis method" *Georisk: Assessment and Management of Risk for Engineered Systems and Geohazards*, 11(1): 146-159. https://doi.org/10.1080/17499518.2016.1250279

- Yang X (2014) *Nature-Inspired Optimization Algorithms*. Elsevier, Amsterdam.

- Youssef AM, Soubra AH, Low BK (2008) "Reliability-based analysis and design of strip footings against bearing capacity failure" *Journal of Geotechnical and Geoenvironmental Engineering, ASCE*, 134(7): 917-928. https://doi.org/10.1061/(ASCE)1090-0241(2008)134:7(917)

- Yuceme MS, Tang WH, Ang AS (1973) "A probabilistic study of safety and design of earth slopes" *Civil Engineering Studies, Structural Research Series 402*. University of Illinois, Urbana, 1-204.

- Zhang F, Liu G, Chen W, Han W, Liang S (2009) "The evolution mechanism of the Yuanjiawan landslide in the process of cutting slope and excavation" *Chinese Journal of Geotechnical Engineering*, 31 (8): 1248-1254.

- Zhang F, Liu G, Chen W, Liang S, Chen R, Han W (2012) "Human-induced landslide on a high cut slope: a case of repeated failures due to multi-excavation" *Journal of Rock Mechanics and Geotechnical Engineering*, 4(4): 367-374 https://doi.org/10.3724/SP.J.1235.2012.00367

- Zhang J, Wang H, Huang HW, Chen LH (2017) "System reliability analysis of soil slopes stabilized with piles" *Engineering Geology*, 229: 45-52. https://doi.org/10.1016/j.enggeo.2017.09.009

- Zhu H, Zhang LM, Zhang LL, Zhou CB (2013) "Two-dimensional probabilistic infiltration analysis with a spatially varying permeability function" *Computers and Geotechnics*, 48: 249-259. https://doi.org/10.1016/j.compgeo.2012.07.010

- https://www.bentley.com/en/products/brands/plaxis (Last accessed: 28.08.2021)

- https://www.finesoftware.eu/geotechnical-software/ (Last accessed: 28.08.2021)

LIST OF PUBLICATIONS FROM THE THESIS WORK

Book Chapters (Published)

[1] **Chakraborty R** and Dey A (2021) "Influence of Toe Cutting on Seismic Response of a Typical Hill-Slope in North-East India" *Local Site Effects and Ground Failures*, Ed. T. G. Sitharam, R. S. Jakka and L. Govindaraju, Springer Nature, Singapore, Vol. 117, Lecture Notes in Civil Engineering, pp. 167-173, ISBN No. 978-981-15-9984-2.

[2] **Chakraborty R** and Dey A (2019) "A comparison of 1D and 2D spatial variability in probabilistic slope stability analysis" *Geotechnics for Transportation Infrastructure Vol 1, Lecture Notes in Civil Engineering Vol 28*, Ed. R. Sundaram, J. T. Shahu and V. Havanagi, Springer Nature, Singapore, pp. 541-553: ISBN No. 978-981-13-6701-4.

[3] **Chakraborty R** and Dey A (2019) "Stochastic modeling of the spatial variability of soil" *Advances in Numerical Methods in Geotechnical Engineering*, Ed. H. F. Shehata and C. S. Desai, Springer Nature, Switzerland, pp. 144-155: ISBN No. 978-3-030-01925-9.

[4] **Chakraborty R** and Dey A (2019) "Effect of toe cutting on hill-slope stability" *Geotechnical Applications, Lecture Notes in Civil Engineering Vol. 13*, Ed. I. V. Anirudhan, V. B. Maji, Springer, Singapore, pp. 191-198: ISBN No. 978-981-13-0367-8.

Journal Publications (Published)

[1] **Chakraborty R** and Dey A (2021) "Hillslope instability induced by toe excavation: A comparative study of LEM-based deterministic and probabilistic approaches" ***Sadhana (Springer),*** 46: 210. https://doi.org/10.1007/s12046-021-01737-7

Journal Publications (Communicated/To be communicated)

[1] **Chakraborty R** and Dey A (2021) "Probabilistic slope stability analysis: State-of-the-art review and future prospects" ***Innovative Infrastructure Solutions (Springer)*** (*Under Revi*sion).

[2] **Chakraborty R** and Dey A (2021) "Probabilistic assessment of toe-excavated hill slope supported by sheet pile wall or sheet-pile-anchor retention systems" ***Soils and Foundations (Elsevier)*** (*Under Revision*).

[3] **Chakraborty R** and Dey A (2021) "Probabilistic assessment of seismic response of cut slopes" ***Ain Shams Engineering Journal (Elsevier)*** (*Under Revision*).

[4] **Chakraborty R** and Dey A (2021) "Estimation of the vertical scale of fluctuation of spatially varying standard penetration test data" ***Probabilistic Engineering Mechanics (Elsevier)*** (*Under Preparation*).

[5] **Chakraborty R** and Dey A (2021) "Random finite element analysis for toe excavation induced slope instability" ***Indian Geotechnical Journal (Springer)***(*Communicated*).

Conference: National/International (Published)

[1] **Chakraborty R** and Dey A (2019) "Effect of spatial variation of soil on probabilistic slope stability analysis for cut slopes" ***International Conference on Landslides and Slope Stability***, Bali, Indonesia, pp. C1-1-8.

[2] **Chakraborty R** and Dey A (2017) "Importance of spatial variability on probabilistic slope stability" ***Geotechnics for Natural and Engineered Sustainable Technologies: Indian Geotechnical Conference (GeoNEst: IGC-2017)***, Guwahati, India, pp. 1-4.

[3] **Chakraborty R** and Dey A (2016) "Stability of hill-slope using LE and FE analyses" ***National Conference on Engineering Problems and Application of Mathematics: EPAM 2016***, NIT Agartala, Tripura, India, pp. 1-5.

[4] **Chakraborty R** and Dey A (2016) "Numerical investigation of slope instability induced by hydraulic and seismic actions" ***North-East Students Geo-Congress: NESGC 2016***, Agartala, India, pp. 237-244.

[5] **Chakraborty R** and Dey A (2016) "Multiple nonlinear regression analysis for slope stability using limit equilibrium method" ***International Geotechnical Engineering Conference on Sustainability in Geotechnical Engineering Practices and Related Urban Issues***, Mumbai, India, pp. 1-3.

APPENDIX-I

NAME OF PROJECT: CONSTRUCTION OF PROPOSED RCC BUILDING AT AMINGAON

BORE LOG CUM LABORATORY TEST RESULT

Boring method: Shell& Auger & Wash Boring dia: 150mm Date Commenced:01-01-11 Date completed: 01-01-11

BH: 1 DEPTH OF WATER TABLE = 2.60 M from EGL.

Depth in meters below reference	Types of Sample	Observed N-Value	Group Symbol	Visual description of soil	% Gravel > 4.75mm	% Sand 4.75-0.075 mm	Silt 0.075-0.002	% Clay < 0.002 mm	Field density, gms/cm³	Specific Gravity	Void Ratio	Natural moisture content	Unconfined compressive Strength kg/cm² (U D)	Shear Parameter		Compression Index Cc	LL%	PL%	Passing 75 micron (%)
														Cohesion ' c' kg/cm²	Angle of shearing resistance (Φ°)				
1.50-1.95	P	13	**CI**	Brownish gray CLAY trace/some silt.															
2.00	U						15	85	2.00	2.66			1.23	0.60	5				
3.00-3.45	P	16																	
3.50	U						10	90											
4.50-4.95	P	11																	
5.00	U						15	85	1.98				1.10	0.54	5				
6.00-6.45	P	11																	
6.50	U						25	75											
7.50-7.95	P	12																	
8.00	U						20	80	1.98	2.67			1.12	0.56	6				
9.00-9.45	P	33																	
9.50	U			11.00M			20	80											
10.50-10.95	P	37																	
11.00	U						15	85	2.17				3.38	1.18	6				
12.00-12.45	P	43	**CI**	Brownish gray CLAY some silt & sand.															
12.50	U			14.00M		30	20	50											
13.50-13.95	P	50																	
14.00	U					20	30	50	2.21	2.67			2.03	1.00	16				
15.00-15.45	P	58	**CI**	Brownish gray silty CLAY.															
15.50	U			15.50M			35	65											

D: Disturbed Sample:: U: Undisturbed Sample:: P: Standard Penetration test:: DS: Direct shear :: EGL: Existing ground level.::

Depth in meters below reference	Types of Sample	Observed N-Value	Group Symbol	Visual description of soil	% Gravel > 4.75mm	% Sand 4.75-0.075 mm	Silt 0.075-0.002	% Clay < 0.002 mm	Field density, gms/cm³	Specific Gravity	Void Ratio	Natural moisture content	Unconfined compressive Strength kg/cm² (U D)	Shear Parameter		Compression Index Cc	LL%	PL%	Passing 75 micron (%)
														Cohesion ' c' kg/cm²	Angle of shearing resistance (Φ°)				
16.50-16.95	P	66	**CI**	Brownish gray CLAY some silt & sand.															
17.00	U					20	30	50	2.24	2.67			2.14	1.06	17				
18.00-18.45	P	76																	
18.50	U			20.00M		25	20	55											
19.50-19.95	P	87																	
20.00	U					15	25	60	2.27	2.66			2.43	1.21	13				

D: Disturbed Sample:: U: Undisturbed Sample:: P: Standard Penetration test:: DS: Direct shear :: EGL: Existing ground level.::

BORE LOG CUM LABORATORY TEST RESULT

Boring method: Shell& Auger & Wash Boring dia: 150mm Date Commenced:31-12-10 Date completed: 31-12-10

BH: 2 DEPTH OF WATER TABLE = 2.60 M from EGL.

Depth in meters below reference	Types of Sample	Observed N-Value	Group Symbol	Visual description of soil	% Gravel > 4.75mm	% Sand 4.75-0.075 mm	Silt 0.075-0.002	% Clay < 0.002 mm	Field density, gms/cm³	Specific Gravity	Void Ratio	Natural moisture content	Unconfined compressive Strength kg/cm² (U D)	Shear Parameter		Compression Index Cc	LL%	PL%	Passing 75 micron (%)
														Cohesion ' c' kg/cm²	Angle of shearing resistance (Φ°)				
1.50-1.95	P	12	**CI**	Brownish gray CLAY some/trace silt.															
2.00	U						15	85	1.99	2.66			1.19	0.59	5				
3.00-3.45	P	15																	
3.50	U						10	90											
4.50-4.95	P	9																	
5.00	U						15	85	1.97				0.93	0.46	5				
6.00-6.45	P	11																	
6.50	U			8.00M			15	85											
7.50-7.95	P	15																	
8.00	U						15	85	2.02	2.66			1.45	0.72	6				
9.00-9.45	P	15	**CI**	Brownish gray CLAY some silt trace															
9.50	U			sand. 9.50M		10	25	65											
10.50-10.95	P	18	**CI/ CH**	Brownish gray CLAY trace/some silt.															
11.00	U						20	80	2.04				1.71	0.85	7				
12.00-12.45	P	37																	
12.50	U			15.50M			15	85											
13.50-13.95	P	45																	
14.00	U						15	85	2.19	2.66			3.32	1.84	6				
15.00-15.45	P	48																	
15.50	U						10	90											

D: Disturbed Sample:: U: Undisturbed Sample:: P: Standard Penetration test:: DS: Direct shear :: EGL: Existing ground level.::

Depth in meters below reference	Types of Sample	Observed N-Value	Group Symbol	Visual description of soil	% Gravel > 4.75mm	% Sand 4.75-0.075 mm	Silt 0.075-0.002	% Clay < 0.002 mm	Field density, gms/cm³	Specific Gravity	Void Ratio	Natural moisture content	Unconfined compressive Strength kg/cm² (U D)	Shear Parameter		Compression Index Cc	LL%	PL%	Passing 75 micron (%)
														Cohesion ‘ c’ kg/cm²	Angle of shearing resistance (Φ˚)				
16.50-16.95	P	53	**CI/CH**	Brownish gray CLAY some silt.															
17.00	U						15	85	2.22				3.39	1.67	6				
18.00-18.45	P	65																	
18.50	U						20	80											
19.50-19.95	P	81		20.00M															
20.00	U						15	85	2.28	2.66			3.43	1.73	7				

D: Disturbed Sample:: U: Undisturbed Sample:: P: Standard Penetration test:: DS: Direct shear :: EGL: Existing ground level.::

BORE LOG CUM LABORATORY TEST RESULT

Boring method: Shell& Auger & Wash Boring dia: 150mm Date Commenced:01-01-11 Date completed: 01-01-11

BH: 3 DEPTH OF WATER TABLE = 2.70 M from EGL.

Depth in meters below reference	Types of Sample	Observed N-Value	Group Symbol	Visual description of soil	% Gravel > 4.75mm	% Sand 4.75-0.075 mm	Silt 0.075-0.002	% Clay < 0.002 mm	Field density, gms/cm³	Specific Gravity	Void Ratio	Natural moisture content	Unconfined compressive Strength kg/cm² (U D)	Shear Parameter		Compression Index Cc	LL%	PL%	Passing 75 micron (%)
														Cohesion ' c' kg/cm²	Angle of shearing resistance (Φ°)				
1.50-1.95	P	11	**CI**	Brownish gray CLAY some silt.															
2.00	U						20	80	1.98	2.67			1.03	0.52	6				
3.00-3.45	P	14																	
3.50	U						15	85											
4.50-4.95	P	9																	
5.00	U						20	80	1.97				0.87	0.44	6				
6.00-6.45	P	11																	
6.50	U						15	85											
7.50-7.95	P	15																	
8.00	U						15	85	2.04	2.66			1.43	0.72	6				
9.00-9.45	P	17																	
9.50	U						15	85											
10.50-10.95	P	21																	
11.00	U						20	80	2.09	2.67			1.99	0.99	7				
12.00-12.45	P	32		12.50M															
12.50	U						20	80											
13.50-13.95	P	37	**CI**	Brownish gray CLAY some silt some sand.															
14.00	U			14.00M		20	30	50	2.11	2.67			1.91	0.94	15				
15.00-15.45	P	44	**CH**	Brownish gray CLAY some silt.															
15.50	U			15.50M			15	85											

D: Disturbed Sample:: U: Undisturbed Sample:: P: Standard Penetration test:: DS: Direct shear :: EGL: Existing ground level.::

Depth in meters below reference	Types of Sample	Observed N-Value	Group Symbol	Visual description of soil	% Gravel > 4.75mm	% Sand 4.75-0.075 mm	Silt 0.075-0.002	% Clay < 0.002 mm	Field density, gms/cm³	Specific Gravity	Void Ratio	Natural moisture content	Unconfined compressive Strength kg/cm² (U D)	Shear Parameter		Compression Index Cc	LL%	PL%	Passing 75 micron (%)
														Cohesion ‘ c’ kg/cm²	Angle of shearing resistance (Φ°)				
16.50-16.95	P	51	**CH**	Brownish gray CLAY some/trace silt.															
17.00	U						15	85	2.18				3.39	1.68	7				
18.00-18.45	P	63																	
18.50	U						15	85											
19.50-19.95	P	82																	
20.00	U						15	85	2.21	2.66			3.53	1.75	7				
20.00-20.45	P	85																	
20.50	U			20.50M			10	90											

D: Disturbed Sample:: U: Undisturbed Sample:: P: Standard Penetration test:: DS: Direct shear :: EGL: Existing ground level.::

BORE LOG CUM LABORATORY TEST RESULT

Boring method: Shell& Auger & Wash Boring dia: 150mm Date Commenced:02-01-11 Date completed: 02-01-11

BH: 4 DEPTH OF WATER TABLE = 1.70 M from EGL.

Depth in meters below reference	Types of Sample	Observed N-Value	Group Symbol	Visual description of soil	% Gravel > 4.75mm	% Sand 4.75-0.075 mm	Silt 0.075-0.002	% Clay < 0.002 mm	Field density, gms/cm³	Specific Gravity	Void Ratio	Natural moisture content	Unconfined compressive Strength kg/cm² (U D)	Shear Parameter		Compression Index Cc	LL%	PL%	Passing 75 micron (%)
														Cohesion ' c' kg/cm²	Angle of shearing resistance (Φ°)				
1.50-1.95	P	11	**CI**	Brownish gray CLAY trace/some silt.															
2.00	U						10	90	1.99	2.66			1.17	0.58	5				
3.00-3.45	P	13																	
3.50	U						15	85											
4.50-4.95	P	9																	
5.00	U						20	80	1.97				0.87	0.44	6				
6.00-6.45	P	13																	
6.50	U						15	85											
7.50-7.95	P	14																	
8.00	U						20	80	2.01	2.67			1.27	0.63	7				
9.00-9.45	P	17																	
9.50	U						15	85											
10.50-10.95	P	19																	
11.00	U						25	75	2.05				1.71	0.66	8				
12.00-12.45	P	23																	
12.50	U						20	80											
13.50-13.95	P	33																	
14.00	U						20	80	2.15	2.67			3.03	1.50	7				
15.00-15.45	P	44																	
15.50	U			15.50M			25	75											

D: Disturbed Sample:: U: Undisturbed Sample:: P: Standard Penetration test:: DS: Direct shear :: EGL: Existing ground level.::

Depth in meters below reference	Types of Sample	Observed N-Value	Group Symbol	Visual description of soil	% Gravel > 4.75mm	% Sand 4.75-0.075 mm	Silt 0.075-0.002	% Clay < 0.002 mm	Field density, gms/cm³	Specific Gravity	Void Ratio	Natural moisture content	Unconfined compressive Strength kg/cm² (U D)	Shear Parameter		Compression Index Cc	LL%	PL%	Passing 75 micron (%)
														Cohesion ‘ c’ kg/cm²	Angle of shearing resistance (Φ°)				
16.50-16.95	P	48		Brownish gray silty															
17.00	U			CLAY. 17.00M			35	65	2.19	2.67			2.60	1.29	10				
18.00-18.45	P	54		Brownish gray CLAY trace/some silt.															
18.50	U						15	85											
19.50-19.95	P	69																	
20.00	U						20	80	2.23	2.66			3.21	1.60	7				
20.00-20.45	P	84																	
20.50	U			20.50M			10	90											

D: Disturbed Sample:: U: Undisturbed Sample:: P: Standard Penetration test:: DS: Direct shear :: EGL: Existing ground level.::

BORE LOG CUM LABORATORY TEST RESULT

Boring method: Shell& Auger & Wash Boring dia: 150mm Date Commenced:03-01-11 Date completed: 03-01-11

BH: 5 DEPTH OF WATER TABLE= 0.15 M from EGL.

Depth in meters below reference	Types of Sample	Observed N-Value	Group Symbol	Visual description of soil	% Gravel > 4.75mm	% Sand 4.75-0.075 mm	Silt 0.075-0.002	% Clay < 0.002 mm	Field density, gms/cm³	Specific Gravity	Void Ratio	Natural moisture content	Unconfined compressive Strength kg/cm² (U D)	Shear Parameter		Compression Index Cc	LL%	PL%	Passing 75 micron (%)
														Cohesion ' c' kg/cm²	Angle of shearing resistance (Φ°)				
1.50-1.95	P	4	**CI/ CH**	Brownish gray CLAY trace/some silt.															
2.00	U						15	85	1.89	2.67			0.43	0.21	5				
3.00-3.45	P	3																	
3.50	U						10	90											
4.50-4.95	P	0																	
5.00	U						15	85											
6.00-6.45	P	2																	
6.50	U						20	80	1.77	2.67			0.19	0.09	5				
7.50-7.95	P	3																	
8.00	U						10	90											
9.00-9.45	P	3																	
9.50	U						10	90	1.83				0.31	0.16	4				
10.50-10.95	P	4																	
11.00	U						10	90											
12.00-12.45	P	15																	
12.50	U						30	70	2.01	2.67			1.18	0.58	9				
13.50-13.95	P	24																	
14.00	U						25	75											
15.00-15.45	P	28																	
15.50	U			15.50M			20	80	2.13				2.55	1.27	7				

D: Disturbed Sample:: U: Undisturbed Sample:: P: Standard Penetration test:: DS: Direct shear :: EGL: Existing ground level.::

Depth in meters below reference	Types of Sample	Observed N-Value	Group Symbol	Visual description of soil	% Gravel > 4.75mm	% Sand 4.75-0.075 mm	Silt 0.075-0.002	% Clay < 0.002 mm	Field density, gms/cm³	Specific Gravity	Void Ratio	Natural moisture content	Unconfined compressive Strength kg/cm² (U D)	Shear Parameter		Compression Index Cc	LL%	PL%	Passing 75 micron (%)
														Cohesion ‘ c’ kg/cm²	Angle of shearing resistance (Φ°)				
16.50-16.95	P	55	**CI/ CH**	Brownish gray CLAY trace/some silt.															
17.00	U						20	80											
18.00-18.45	P	59																	
18.50	U						15	85	2.21				3.41	1.69	6				
19.50-19.95	P	68																	
20.00	U						10	90											
20.00-20.45	P	82																	
20.50	U			20.50M			10	90	2.23				3.69	1.84	5				

D: Disturbed Sample:: U: Undisturbed Sample:: P: Standard Penetration test:: DS: Direct shear :: EGL: Existing ground level.::

BORE LOG CUM LABORATORY TEST RESULT

Boring method: Shell& Auger & Wash Boring dia: 150mm Date Commenced:26-12-10 Date completed: 26-12-10

BH: 6 DEPTH OF WATER TABLE= 1.10M from EGL.

Depth in meters below reference	Types of Sample	Observed N-Value	Group Symbol	Visual description of soil	% Gravel > 4.75mm	% Sand 4.75-0.075 mm	Silt 0.075-0.002	% Clay < 0.002 mm	Field density, gms/cm³	Specific Gravity	Void Ratio	Natural moisture content	Unconfined compressive Strength kg/cm² (U D)	Shear Parameter		Compression Index Cc	LL%	PL%	Passing 75 micron (%)
														Cohesion ' c' kg/cm²	Angle of shearing resistance (Φ°)				
1.50-1.95	P	12	**CI**	Brownish gray CLAY some silt.															
2.00	U						15	85	1.99				1.19	0.59	5				
3.00-3.45	P	13																	
3.50	U						15	85											
4.50-4.95	P	11																	
5.00	U						20	80	1.97				1.03	0.52	6				
6.00-6.45	P	11																	
6.50	U						15	85											
7.50-7.95	P	14																	
8.00	U						20	80	2.01				1.27	0.63	6				
9.00-9.45	P	17																	
9.50	U						20	80											
10.50-10.95	P	21																	
11.00	U						25	75	2.06				1.87	0.93	8				
12.00-12.45	P	24																	
12.50	U						25	85											
13.50-13.95	P	30																	
14.00	U			14.00M			15	85	2.18				2.87	1.43	6				
15.00-15.45	P	34	**CL**	Brownish gray CLAY some silt some sand. 15.50M															
15.50	U					20	30	50											

D: Disturbed Sample:: U: Undisturbed Sample:: P: Standard Penetration test:: DS: Direct shear :: EGL: Existing ground level.::

Depth in meters below reference	Types of Sample	Observed N-Value	Group Symbol	Visual description of soil	% Gravel > 4.75mm	% Sand 4.75-0.075 mm	Silt 0.075-0.002	% Clay < 0.002 mm	Field density, gms/cm³	Specific Gravity	Void Ratio	Natural moisture content	Unconfined compressive Strength kg/cm² (U D)	Shear Parameter		Compression Index Cc	LL%	PL%	Passing 75 micron (%)
														Cohesion ' c' kg/cm²	Angle of shearing resistance (Φ°)				
16.50-16.95	P	22		Brownish gray															
17.00	U			CLAY some silt.			15	85	2.08				2.20	1.09	6				
18.00-18.45	P	23																	
18.50	U						15	85											
19.50-19.95	P	26																	
20.00	U			20.00M			20	80	2.13				2.39	1.19	7				

D: Disturbed Sample:: U: Undisturbed Sample:: P: Standard Penetration test:: DS: Direct shear :: EGL: Existing ground level.::

BORE LOG CUM LABORATORY TEST RESULT

Boring method: Shell& Auger & Wash Boring dia: 150mm Date Commenced:27-12-10 Date completed: 28-12-10

BH: 7 DEPTH OF WATER TABLE= 2.30M from EGL.

Depth in meters below reference	Types of Sample	Observed N-Value	Group Symbol	Visual description of soil	% Gravel > 4.75mm	% Sand 4.75-0.075 mm	Silt 0.075-0.002	% Clay < 0.002 mm	Field density, gms/cm³	Specific Gravity	Void Ratio	Natural moisture content	Unconfined compressive Strength kg/cm² (U D)	Shear Parameter		Compression Index Cc	LL%	PL%	Passing 75 micron (%)
														Cohesion ' c' kg/cm²	Angle of shearing resistance (Φ°)				
1.50-1.95	P	11	**CI/ CH**	Brownish gray CLAY some silt.															
2.00	U						15	85	1.98	2.65			1.11	0.55	5	0.12			
3.00-3.45	P	16																	
3.50	U						15	85											
4.50-4.95	P	12																	
5.00	U						15	85	1.99				1.19	0.59	5				
6.00-6.45	P	18																	
6.50	U						20	80											
7.50-7.95	P	22																	
8.00	U						15	85	2.08	2.65			2.20	1.09	6				
9.00-9.45	P	17																	
9.50	U						15	85											
10.50-10.95	P	17																	
11.00	U						20	80	2.04				1.67	0.83	7				
12.00-12.45	P	21																	
12.50	U						15	85											
13.50-13.95	P	18																	
14.00	U						20	80	2.05	2.65			1.76	0.87	7				
15.00-15.45	P	23																	
15.50	U			15.50M			15	85											

D: Disturbed Sample:: U: Undisturbed Sample:: P: Standard Penetration test:: DS: Direct shear :: EGL: Existing ground level.::

Depth in meters below reference	Types of Sample	Observed N-Value	Group Symbol	Visual description of soil	% Gravel > 4.75mm	% Sand 4.75-0.075 mm	Silt 0.075-0.002	% Clay < 0.002 mm	Field density, gms/cm³	Specific Gravity	Void Ratio	Natural moisture content	Unconfined compressive Strength kg/cm² (U D)	Shear Parameter		Compression Index Cc	LL%	PL%	Passing 75 micron (%)
														Cohesion ‘ c’ kg/cm²	Angle of shearing resistance (Φ°)				
16.50-16.95	P	28	**CI/ CH**	Brownish gray CLAY some silt.															
17.00	U						20	80	2.15				2.55	1.27	7				
18.00-18.45	P	21																	
18.50	U						20	80											
19.50-19.95	P	23																	
20.00	U						20	80	2.11	2.67			2.16	1.07	7				

D: Disturbed Sample:: U: Undisturbed Sample:: P: Standard Penetration test:: DS: Direct shear :: EGL: Existing ground level.::

BORE LOG CUM LABORATORY TEST RESULT

Boring method: Shell& Auger & Wash Boring dia: 150mm Date Commenced:27-12-10 Date completed: 28-12-10

BH: 8 DEPTH OF WATER TABLE= 2.50M from EGL.

Depth in meters below reference	Types of Sample	Observed N-Value	Group Symbol	Visual description of soil	% Gravel > 4.75mm	% Sand 4.75-0.075 mm	Silt 0.075-0.002	% Clay < 0.002 mm	Field density, gms/cm³	Specific Gravity	Void Ratio	Natural moisture content	Unconfined compressive Strength kg/cm² (U D)	Shear Parameter		Compression Index Cc	LL%	PL%	Passing 75 micron (%)
														Cohesion ' c' kg/cm²	Angle of shearing resistance (Φ°)				
1.50-1.95	P	10	**CI**	Brownish gray CLAY some silt.															
2.00	U						10	90	1.97	2.66			1.07	0.53	5				
3.00-3.45	P	14																	
3.50	U						20	80											
4.50-4.95	P	11																	
5.00	U						20	80	1.98				1.03	0.51	6				
6.00-6.45	P	15																	
6.50	U						20	80											
7.50-7.95	P	20																	
8.00	U						15	85	2.07	2.67			2.03	1.00	5				
9.00-9.45	P	15																	
9.50	U						15	85											
10.50-10.95	P	16																	
11.00	U						15	85	2.03				1.69	0.84	6				
12.00-12.45	P	19																	
12.50	U						15	85											
13.50-13.95	P	23																	
14.00	U			14.00M			15	85	2.10	2.67			2.28	1.13	6				
15.00-15.45	P	33	**CL**	Brownish gray CLAY some silt some sand. 15.50M															
15.50	U					20	30	50											

D: Disturbed Sample:: U: Undisturbed Sample:: P: Standard Penetration test:: DS: Direct shear :: EGL: Existing ground level.::

Depth in meters below reference	Types of Sample	Observed N-Value	Group Symbol	Visual description of soil	% Gravel > 4.75mm	% Sand 4.75-0.075 mm	Silt 0.075-0.002	% Clay < 0.002 mm	Field density, gms/cm³	Specific Gravity	Void Ratio	Natural moisture content	Unconfined compressive Strength kg/cm² (U D)	Shear Parameter		Compression Index Cc	LL%	PL%	Passing 75 micron (%)
														Cohesion ' c' kg/cm²	Angle of shearing resistance (Φ°)				
16.50-16.95	P	67	**ML**	Brownish gray clayey															
17.00	U			SILT some sand. 17.00M		25	40	35	2.20				1.39	0.70	20				
18.00-18.45	P	60	**ML**	Brownish gray SILT															
18.50	U			some clay some sand. 18.50M		20	60	20											
19.50-19.95	P	29	**CH**	Brownish gray															
20.00	U			CLAY some silt. 20.00M			15	85	2.16				2.75	1.37	6				
21.00-21.45	P	38	**CI**	Brownish gray CLAY															
21.50	U			some silt trace sand. 21.50M		10	20	70											
22.50-22.95	P	93	**SP**	Whitish gray fine															
23.00	D			SAND. 23.00M		100			2.36	2.65					38-DS				
24.00-24.45	P	96	**SP**	Whitish gray medium															
24.50	D			to fine SAND.		100													
25.50-25.95	P	R																	
26.00	D					100			2.31						39-DS				
27.00-27.45	P	R																	
27.50	D					100													
28.50-28.95	P	R																	
29.00	D					100			2.34	2.65					40-DS				
30.00-30.45	P	R		30.50M															
30.50	D					100													

D: Disturbed Sample:: U: Undisturbed Sample:: P: Standard Penetration test:: DS: Direct shear :: EGL: Existing ground level.::

BORE LOG CUM LABORATORY TEST RESULT

Boring method: Shell& Auger & Wash Boring dia: 150mm Date Commenced:28-12-10 Date completed: 28-12-10

BH: 9 DEPTH OF WATER TABLE= 2.50M from EGL.

Depth in meters below reference	Types of Sample	Observed N-Value	Group Symbol	Visual description of soil	% Gravel > 4.75mm	% Sand 4.75-0.075 mm	Silt 0.075-0.002	% Clay < 0.002 mm	Field density, gms/cm³	Specific Gravity	Void Ratio	Natural moisture content	Unconfined compressive Strength kg/cm² (U D)	Shear Parameter		Compression Index Cc	LL%	PL%	Passing 75 micron (%)
														Cohesion ' c' kg/cm²	Angle of shearing resistance (Φ°)				
1.50-1.95	P	17	**CI/ CH**	Brownish gray CLAY some silt.															
2.00	U						15	85	2.04	2.67			1.71	0.84	5	0.12			
3.00-3.45	P	16																	
3.50	U						20	80											
4.50-4.95	P	21																	
5.00	U						15	85	208				2.11	1.04	6				
6.00-6.45	P	20																	
6.50	U						15	85											
7.50-7.95	P	22																	
8.00	U						15	85	2.09	2.66			2.19	1.09	6				
9.00-9.45	P	23																	
9.50	U						15	85											
10.50-10.95	P	22																	
11.00	U						20	80	2.08				2.07	1.03	7				
12.00-12.45	P	27																	
12.50	U						15	85											
13.50-13.95	P	28																	
14.00	U						15	85	2.14	2.66			2.69	1.34	7				
15.00-15.45	P	31																	
15.50	U			15.50M			15	85											

D: Disturbed Sample:: U: Undisturbed Sample:: P: Standard Penetration test:: DS: Direct shear :: EGL: Existing ground level.::

Depth in meters below reference	Types of Sample	Observed N-Value	Group Symbol	Visual description of soil	% Gravel > 4.75mm	% Sand 4.75-0.075 mm	Silt 0.075-0.002	% Clay < 0.002 mm	Field density, gms/cm³	Specific Gravity	Void Ratio	Natural moisture content	Unconfined compressive Strength kg/cm² (U D)	Shear Parameter		Compression Index Cc	LL%	PL%	Passing 75 micron (%)
														Cohesion ' c' kg/cm²	Angle of shearing resistance (Φ°)				
16.50-16.95	P	32	**CH**	Brownish gray CLAY															
17.00	U			some silt trace sand. 17.00M		5	30	65	2.18	2.67			2.32	1.15	10				
18.00-18.45	P	41	**ML**	Brownish gray SILT															
18.50	U			some clay trace sand. 18.50M		10	60	30											
19.50-19.95	P	45	**CH**	Brownish gray silty															
20.00	U			CLAY. 20.00M			35	65	2.20	2.67			2.63	1.31	11				

D: Disturbed Sample:: U: Undisturbed Sample:: P: Standard Penetration test:: DS: Direct shear :: EGL: Existing ground level.::

BORE LOG CUM LABORATORY TEST RESULT

Boring method: Shell& Auger & Wash Boring dia: 150mm Date Commenced:29-12-10 Date completed: 29-12-10

BH: 10 DEPTH OF WATER TABLE = 0.80M from EGL.

Depth in meters below reference	Types of Sample	Observed N-Value	Group Symbol	Visual description of soil	% Gravel > 4.75mm	% Sand 4.75-0.075 mm	Silt 0.075-0.002	% Clay < 0.002 mm	Field density, gms/cm³	Specific Gravity	Void Ratio	Natural moisture content	Unconfined compressive Strength kg/cm² (U D)	Shear Parameter		Compression Index Cc	LL%	PL%	Passing 75 micron (%)
														Cohesion ' c' kg/cm²	Angle of shearing resistance (Φ°)				
1.50-1.95	P	10	**CI**	Brownish gray CLAY some silt.															
2.00	U						15	85	1.97	2.67			1.02	0.50	5				
3.00-3.45	P	10																	
3.50	U						20	80											
4.50-4.95	P	12																	
5.00	U						15	85	1.99				1.19	0.59	5				
6.00-6.45	P	18																	
6.50	U						20	80											
7.50-7.95	P	18																	
8.00	U						15	85	2.05	2.67			1.85	0.92	6				
9.00-9.45	P	16																	
9.50	U			9.50M			15	85											
10.50-10.95	P	20	**CI**	Brownish gray silty CLAY.															
11.00	U						35	65	2.06	2.67			1.55	0.76	10				
12.00-12.45	P	22																	
12.50	U			12.50M			35	65											
13.50-13.95	P	70	**SP**	Whitish gray medium to fine SAND.															
14.00	D					100			2.19	2.65					38-DS				
15.00-15.45	P	74																	
15.50	D			15.50M		100													

D: Disturbed Sample:: U: Undisturbed Sample:: P: Standard Penetration test:: DS: Direct shear :: EGL: Existing ground level.::

Depth in meters below reference	Types of Sample	Observed N-Value	Group Symbol	Visual description of soil	% Gravel > 4.75mm	% Sand 4.75-0.075 mm	Silt 0.075-0.002	% Clay < 0.002 mm	Field density, gms/cm³	Specific Gravity	Void Ratio	Natural moisture content	Unconfined compressive Strength kg/cm² (U D)	Shear Parameter		Compression Index Cc	LL%	PL%	Passing 75 micron (%)
														Cohesion ' c' kg/cm²	Angle of shearing resistance (Φ°)				
16.50-16.95	P	86	**SP**	Whitish gray medium SAND.															
17.00	D					100			2.25	2.65					39-DS				
18.00-18.45	P	92																	
18.50	D			18.50M		100													
19.50-19.95	P	R	**SP**	Whitish gray medium to fine SAND.															
20.00	D			20.00M		100			2.31	2.65					40-DS				

D: Disturbed Sample:: U: Undisturbed Sample:: P: Standard Penetration test:: DS: Direct shear :: EGL: Existing ground level.::

BORE LOG CUM LABORATORY TEST RESULT

Boring method: Shell& Auger & Wash Boring dia: 150mm Date Commenced:30-12-10 Date completed: 30-12-10

BH: 11 DEPTH OF WATER TABLE = 0.20M from EGL.

Depth in meters below reference	Types of Sample	Observed N-Value	Group Symbol	Visual description of soil	% Gravel > 4.75mm	% Sand 4.75-0.075 mm	Silt 0.075-0.002	% Clay < 0.002 mm	Field density, gms/cm³	Specific Gravity	Void Ratio	Natural moisture content	Unconfined compressive Strength kg/cm² (U D)	Shear Parameter		Compression Index Cc	LL%	PL%	Passing 75 micron (%)
														Cohesion ' c' kg/cm²	Angle of shearing resistance (Φ°)				
1.50-1.95	P	10	**CI**	Brownish gray CLAY some silt.															
2.00	U						15	85	1.97	2.66			1.01	0.50	5				
3.00-3.45	P	12																	
3.50	U						15	85											
4.50-4.95	P	12																	
5.00	U						20	80	1.99				1.12	0.55	6				
6.00-6.45	P	18																	
6.50	U						20	80											
7.50-7.95	P	11																	
8.00	U						20	80	1.98				1.03	0.52	6				
9.00-9.45	P	20		9.50M															
9.50	U						15	85											
10.50-10.95	P	21	**SC**	Brownish gray															
11.00	D			SAND some clay some silt. 11.00M		60	15	25	1.92	2.67			0.61	0.31	0.23				
12.00-12.45	P	41	**CI**	Brownish gray															
12.50	U			CLAY some silt trace sand. 12.50M		10	30	60											
13.50-13.95	P	54	**CL**	Brownish gray sandy															
14.00	D			CLAY some silt. 14.00M		35	20	45	2.15	2.66			1.79	0.89	19				
15.00-15.45	P	64	**CL**	Brownish gray silty															
15.50	U			CLAY some sand.		15	40	45											

D: Disturbed Sample:: U: Undisturbed Sample:: P: Standard Penetration test:: DS: Direct shear :: EGL: Existing ground level.::

Depth in meters below reference	Types of Sample	Observed N-Value	Group Symbol	Visual description of soil	% Gravel > 4.75mm	% Sand 4.75-0.075 mm	Silt 0.075-0.002	% Clay < 0.002 mm	Field density, gms/cm³	Specific Gravity	Void Ratio	Natural moisture content	Unconfined compressive Strength kg/cm² (U D)	Shear Parameter		Compression Index Cc	LL%	PL%	Passing 75 micron (%)
														Cohesion ' c' kg/cm²	Angle of shearing resistance (Φ°)				
16.50-16.95	P	67		Brownish gray															
17.00	D			SAND some clay trace silt. 17.00M		75	10	15	2.20	2.67			0.59	0.30	31				
18.00-18.45	P	80		Brownish gray sandy CLAY some silt.															
18.50	D					35	25	40											
19.50-19.95	P	93																	
20.00	D			20.00M		35	20	45	2.27	2.67			1.81	0.89	19				

D: Disturbed Sample:: U: Undisturbed Sample:: P: Standard Penetration test:: DS: Direct shear :: EGL: Existing ground level.::

BORE LOG CUM LABORATORY TEST RESULT

Boring method: Shell& Auger & Wash Boring dia: 150mm Date Commenced:31-12-10 Date completed: 31-12-10

BH: 12 DEPTH OF WATER TABLE= 2.90M from EGL.

Depth in meters below reference	Types of Sample	Observed N-Value	Group Symbol	Visual description of soil	% Gravel > 4.75mm	% Sand 4.75-0.075 mm	Silt 0.075-0.002	% Clay < 0.002 mm	Field density, gms/cm³	Specific Gravity	Void Ratio	Natural moisture content	Unconfined compressive Strength kg/cm² (U D)	Shear Parameter		Compression Index Cc	LL%	PL%	Passing 75 micron (%)
														Cohesion ' c' kg/cm²	Angle of shearing resistance (Φ°)				
1.50-1.95	P	14	**CI**	Brownish gray CLAY some silt.															
2.00	U						15	85	2.02	2.66			1.35	0.67	6				
3.00-3.45	P	12																	
3.50	U						15	85											
4.50-4.95	P	9																	
5.00	U						20	80	1.95				0.87	0.44	6				
6.00-6.45	P	10																	
6.50	U						25	75											
7.50-7.95	P	14																	
8.00	U						20	80	2.01	2.67			1.27	0.64	6				
9.00-9.45	P	19																	
9.50	U						25	75											
10.50-10.95	P	18																	
11.00	U						15	85	2.05				1.85	0.93	6				
12.00-12.45	P	20																	
12.50	U			12.50M			15	85											
13.50-13.95	P	24	**CH**	Brownish gray CLAY some silt trace sand..															
14.00	U					10	20	70	2.09	2.66			1.95	0.97	9				
15.00-15.45	P	67																	
15.50	U			15.50M		10	15	75											

D: Disturbed Sample:: U: Undisturbed Sample:: P: Standard Penetration test:: DS: Direct shear :: EGL: Existing ground level.::

Depth in meters below reference	Types of Sample	Observed N-Value	Group Symbol	Visual description of soil	% Gravel > 4.75mm	% Sand 4.75-0.075 mm	Silt 0.075-0.002	% Clay < 0.002 mm	Field density, gms/cm³	Specific Gravity	Void Ratio	Natural moisture content	Unconfined compressive Strength kg/cm² (U D)	Shear Parameter		Compression Index Cc	LL%	PL%	Passing 75 micron (%)
														Cohesion ' c' kg/cm²	Angle of shearing resistance (Φ°)				
16.50-16.95	P	75	**SM**	Brownish gray															
17.00	D			SAND some silt trace clay. 17.00M		75	15	10	2.20	2.65			0.41	0.20	31				
18.00-18.45	P	81	**CH**	Brownish gray															
18.50	U			CLAY some silt trace sand.. 18.50M		10	15	75	2.22	2.66			3.02	1.50	9				
19.50-19.95	P	91	**CH**	Brownish gray															
20.00	U			CLAY some silt. 20.00M			20	80											

D: Disturbed Sample:: U: Undisturbed Sample:: P: Standard Penetration test:: DS: Direct shear :: EGL: Existing ground level.::

BORE LOG CUM LABORATORY TEST RESULT

Boring method: Shell& Auger & Wash Boring dia: 150mm Date Commenced:04-01-11 Date completed: 04-01-11

BH: 13 DEPTH OF WATER TABLE = 0.60M from EGL.

Depth in meters below reference	Types of Sample	Observed N-Value	Group Symbol	Visual description of soil	% Gravel > 4.75mm	% Sand 4.75-0.075 mm	Silt 0.075-0.002	% Clay < 0.002 mm	Field density, gms/cm³	Specific Gravity	Void Ratio	Natural moisture content	Unconfined compressive Strength kg/cm² (U D)	Shear Parameter		Compression Index Cc	LL%	PL%	Passing 75 micron (%)
														Cohesion ' c' kg/cm²	Angle of shearing resistance (Φ°)				
1.50-1.95	P	7	**CI**	Brownish gray CLAY some silt.															
2.00	U						10	90	1.94	2.66			0.71	0.36	5				
3.00-3.45	P	7																	
3.50	U						15	85											
4.50-4.95	P	11																	
5.00	U						15	85	1.98				1.11	0.54	6				
6.00-6.45	P	18																	
6.50	U						15	85											
7.50-7.95	P	9																	
8.00	U			8.00M			15	85	1.95	2.66			0.93	0.47	6				
9.00-9.45	P	13	**CI**	Brownish gray silty															
9.50	U			CLAY. 9.50M			35	65											
10.50-10.95	P	15	**CI/ CH**	Brownish gray CLAY some silt.															
11.00	U						15	85	2.02	2.67			1.45	0.72	6				
12.00-12.45	P	20																	
12.50	U						20	80											
13.50-13.95	P	22																	
14.00	U			14.00M			30	70	2.08	2.67			1.82	0.90	8				
15.00-15.45	P	23	**ML**	Brownish gray SILT															
15.50	U			some clay. 15.50M			80	20											

D: Disturbed Sample:: U: Undisturbed Sample:: P: Standard Penetration test:: DS: Direct shear :: EGL: Existing ground level.::

Depth in meters below reference	Types of Sample	Observed N-Value	Group Symbol	Visual description of soil	% Gravel > 4.75mm	% Sand 4.75-0.075 mm	Silt 0.075-0.002	% Clay < 0.002 mm	Field density, gms/cm³	Specific Gravity	Void Ratio	Natural moisture content	Unconfined compressive Strength kg/cm² (U D)	Shear Parameter		Compression Index Cc	LL%	PL%	Passing 75 micron (%)
														Cohesion ' c' kg/cm²	Angle of shearing resistance (Φ°)				
16.50-16.95	P	31	**CI**	Brownish gray silty															
17.00	U			CLAY. 17.00M			35	65	2.14				2.27	1.13	10				
18.00-18.45	P	38	**ML**	Brownish gray SILT															
18.50	U			some clay.			75	25											
19.50-19.95	P	43																	
20.00	U			20.00M			75	25	2.15				0.99	0.50	22				

D: Disturbed Sample:: U: Undisturbed Sample:: P: Standard Penetration test:: DS: Direct shear :: EGL: Existing ground level.::

BORE LOG CUM LABORATORY TEST RESULT

Boring method: Shell& Auger & Wash Boring dia: 150mm Date Commenced:02-01-11 Date completed: 03-01-11

BH: 14 DEPTH OF WATER TABLE= 0.80M from EGL.

Depth in meters below reference	Types of Sample	Observed N-Value	Group Symbol	Visual description of soil	% Gravel > 4.75mm	% Sand 4.75-0.075 mm	Silt 0.075-0.002	% Clay < 0.002 mm	Field density, gms/cm³	Specific Gravity	Void Ratio	Natural moisture content	Unconfined compressive Strength kg/cm² (U D)	Shear Parameter		Compression Index Cc	LL%	PL%	Passing 75 micron (%)
														Cohesion ' c' kg/cm²	Angle of shearing resistance (Φ°)				
1.50-1.95	P	9	**CI**	Brownish gray CLAY some silt.															
2.00	U						15	85	1.97	2.66			0.93	0.46	5				
3.00-3.45	P	7																	
3.50	U						15	85											
4.50-4.95	P	12																	
5.00	U						15	85	1.44				1.19	0.59	5				
6.00-6.45	P	13																	
6.50	U			6.50M			25	75											
7.50-7.95	P	16	**CI**	Brownish gray															
8.00	U			CLAY some silt trace sand. 8.00M		5	15	80	2.01	2.67			1.59	0.79	6				
9.00-9.45	P	22	**CH**	Brownish gray															
9.50	U			CLAY some silt.			20	80											
10.50-10.95	P	21																	
11.00	U			11.00M			15	85	2.18	2.66			2.13	1.05	6				
12.00-12.45	P	25	**CI**	Brownish gray silty															
12.50	U			CLAY. 12.50M			35	65											
13.50-13.95	P	50	**SP**	Whitish gray medium															
14.00	D			to fine SAND.		100			2.09	2.65					37-DS				
15.00-15.45	P	61																	
15.50	D			15.50M		100													

D: Disturbed Sample:: U: Undisturbed Sample:: P: Standard Penetration test:: DS: Direct shear :: EGL: Existing ground level.::

Depth in meters below reference	Types of Sample	Observed N-Value	Group Symbol	Visual description of soil	% Gravel > 4.75mm	% Sand 4.75-0.075 mm	Silt 0.075-0.002	% Clay < 0.002 mm	Field density, gms/cm³	Specific Gravity	Void Ratio	Natural moisture content	Unconfined compressive Strength kg/cm² (U D)	Shear Parameter		Compression Index Cc	LL%	PL%	Passing 75 micron (%)
														Cohesion ' c' kg/cm²	Angle of shearing resistance (Φ°)				
16.50-16.95	P	72	**SP**	Brownish gray medium to fine SAND.															
17.00	D					100			2.20	2.65					38-DS				
18.00-18.45	P	79																	
18.50	D					100													
19.50-19.95	P	87		20.00M															
20.00	D					100			2.28						39-DS				
21.00-21.45	P	32	**CH**	Brownish gray CLAY some silt.															
21.50	U			21.50M			20	80											
22.50-22.95	P	73	**SP**	Brownish gray medium to fine SAND.															
23.00	D					100			2.21	2.65					38-DS				
24.00-24.45	P	64																	
24.50	D					100													
25.50-25.95	P	72																	
26.00	D					100			2.20						38-DS				
27.00-27.45	P	80																	
27.50	D					100													
28.50-28.95	P	95																	
29.00	D					100			2.31	2.65					40-DS				
30.00-30.45	P	R		30.50M															
30.50	D					100													

D: Disturbed Sample:: U: Undisturbed Sample:: P: Standard Penetration test:: DS: Direct shear :: EGL: Existing ground level.::